Year : 2023

Characterization of the mechanisms driving DDI2-mediated NRF1 activation

Chavarria Claire

Chavarria Claire, 2023, Characterization of the mechanisms driving DDI2-mediated NRF1 activation

Originally published at : Thesis, University of Lausanne

Posted at the University of Lausanne Open Archive http://serval.unil.ch
Document URN : urn:nbn:ch:serval-BIB_F6C648DBFA518

UNIL | Université de Lausanne
Faculté de biologie et de médecine

Département d'Immunobiologie

Characterization of the mechanisms driving DDI2-mediated NRF1 activation

Thèse de doctorat ès sciences de la vie (PhD)

présentée à la

Faculté de biologie et de médecine
de l'Université de Lausanne

par

Claire CHAVARRIA

Master of Science UNIL Lausanne

Jury

Prof. Thierry Roger, Président
Prof. Fabio Martinon, Directeur de thèse
Prof. Sophie Janssens, Experte
Prof. David Gatfield, Expert
Prof. Maurizio Molinari, Expert

Lausanne
(2023)

UNIL | Université de Lausanne
Faculté de biologie
et de médecine

Ecole Doctorale
Doctorat ès sciences de la vie

Imprimatur

Vu le rapport présenté par le jury d'examen, composé de

Président·e	Monsieur	Prof.	Thierry	**Roger**
Directeur·trice de thèse	Monsieur	Prof.	Fabio	**Martinon**
Expert·e·s	Madame	Prof.	Sophie	**Janssens**
	Monsieur	Prof.	David	**Gatfield**
	Monsieur	Prof.	Maurizio	**Molinari**

le Conseil de Faculté autorise l'impression de la thèse de

Claire Hélène Marie Sylvie Chavarria

Maîtrise universitaire ès Sciences en biologie médicale, Université de Lausanne

intitulée

Characterization of the mechanisms driving DDI2-mediated NRF1 activation

Lausanne, le 23 juin 2023

pour le Doyen
de la Faculté de biologie et de médecine

Prof. Thierry Roger

SUMMARY

Proteostasis refers to the biological mechanisms that orchestrate synthesis, folding, trafficking and degradation of proteins in cells. Alteration of proteostasis responses can lead to the accumulation of misfolded proteins, perturbation in protein degradation and is associated with several diseases, including aging, inflammation, and cancer. One important component of proteostasis is the ubiquitin-proteasome system (UPS). The UPS is the major proteolytic pathway responsible for the degradation of intracellular proteins. Deficiency of the proteasome is associated with the accumulation of misfolded proteins and may trigger endoplasmic reticulum stress pathways. Understanding the mechanisms regulating proteasome function holds the potential to identify new therapeutic targets for the treatment of these diseases.

In this project, we investigated the biological mechanisms induced by proteasomal dysfunction, leading to the activation of the DDI2 and NRF1 adaptation pathway. Under homeostatic conditions, ER-localized NRF1 is retrotranslocated through the ERAD (ER-associated degradation) pathway and promptly degraded by the proteasome machinery. However, when the proteasome machinery is compromised, NRF1 escapes degradation and is processed into its transcriptionally active form by the aspartyl protease DDI2. The mechanistic understanding of NRF1 processing and the role of DDI2 therein was poorly understood.

In this work, we unraveled the importance of ER trafficking in mediating NRF1 ubiquitination and subsequent cleavage by DDI2. Then, we demonstrated that N-glycosylation of NRF1 in the ER, followed by deglycosylation in the cytosol, controlled the fate of the cell. Finally, we established a model in which the mechanisms responsible for NRF1 stability are also controlling its susceptibility to DDI2 proteolytic activity.

In summary, my thesis revealed a unique signal transduction mechanism involved in activating NRF1, an ER protein destined for cytosolic regulation and eventually, a nuclear function.

RÉSUMÉ

La protéostase représente l'ensemble des mécanismes biologiques qui orchestrent la synthèse, le repliement, le trafic et la dégradation des protéines dans les cellules. L'altération des réponses induites par la protéostase peut entraîner l'accumulation de protéines mal repliées, des perturbations dans la dégradation des protéines et est associée à plusieurs maladies, notamment le vieillissement, les maladies inflammatoires et le cancer. Un des acteurs principaux de la protéostase est le système ubiquitine-protéasome. Ce système est la principale voie protéolytique responsable de la dégradation des protéines intracellulaires. Les déficiences du protéasome sont associées à l'accumulation de protéines mal repliées et peuvent engendrer l'activation des voies de stress du réticulum endoplasmique. La compréhension des mécanismes régulant la fonction du protéasome est essentielle afin d'identifier de nouvelles cibles thérapeutiques pour le traitement de ces maladies.

Dans ce projet, nous avons étudié les mécanismes biologiques induits par le dysfonctionnement du protéasome, conduisant à l'activation de la voie d'adaptation de DDI2 et NRF1. Dans des conditions physiologiques, la protéine NRF1, localisée dans le réticulum endoplasmique, est rétrotransloquée par la voie ERAD (dégradation associée au réticulum endoplasmique) et rapidement dégradée par le protéasome. Cependant, lorsque l'intégrité du protéasome est compromise, NRF1 échappe à la dégradation et est clivé en sa forme transcriptionnellement active par la protéase DDI2. Jusqu'à récemment, les mécanismes d'activation de NRF1 et le rôle de DDI2 dans ceux-ci étaient peu renseignés.

Au travers de ce travail, nous avons mis en avant l'importance du trafic de NRF1 dans le réticulum endoplasmique afin d'assurer son ubiquitination et ultérieurement, son clivage par DDI2. Ensuite, nous avons démontré que la N-glycosylation de NRF1 dans le réticulum endoplasmique, suivie d'une dé-glycosylation dans le cytosol, contrôle le destin de la cellule. Enfin, nous avons établi un modèle dans lequel les mécanismes responsables de la stabilité de NRF1 contrôlent également sa sensibilité à l'activité protéolytique de DDI2.

En résumé, ma thèse a révélé un mécanisme unique de transduction du signal impliqué dans l'activation de NRF1, une protéine du réticulum endoplasmique destinée à une régulation cytosolique et éventuellement, à une fonction nucléaire.

ACKNOWLEDGEMENTS

Before reading this thesis work, I need to acknowledge several persons because of their participation in whichever manner to this project.

To Prof. Fabio Martinon, my thesis director and mentor, thank you for inspiring me in the way you see science and approach research, as well as for giving me the opportunity to grow in your lab as a scientist and as a person. Your positivity never failed me and has inspired my own vision of science.

To my PhD committee members, Prof. Thierry Roger, Prof. David Gatfield, Prof. Sophie Janssens, Prof. Maurizio Molinari and Prof. Françoise Stutz, thank you for your insightful inputs, positive criticism, and guidance throughout this project.

To all the Professors of the Wednesday meeting, Prof. Margot Thome Miazza, Prof. Pascal Schneider, Prof. Petr Broz, Prof. Alexis Jourdain, and Prof. Manuele Rebsamen, thank you for your fruitful suggestions, discussion, and constructive criticism during my progress reports.

To my lab collaborators, thank you – **Léa** for your patience and guidance from the first day until the end. You have been much more than a collaborator and was essential throughout my PhD journey. – **Lotte** for believing and supporting me throughout the difficult times. You have a been a key partner of my successes and I feel incredibly lucky to have shared my time in the lab with you. – **Katerina** for being the best lab neighbour. You brought warmth and support to my daily life and well-being. – **Sérgio** and **Mélanie** for sharing the failures and successes of the DDI2 project, and for the insightful scientific and non-scientific discussions. – **Cyrielle** for your presence, your fun and for the mental health support throughout the exhausting end of the thesis. – **Kalvin** and **Zhuo** for their encouragements throughout the last year of my thesis. – **Coline**, **Maria Sofia**, **Maéva,** and **Chloé** for the small steps you participated in but of big impact in my overall thesis work.

To all the 4th floor colleagues, Montserrat, Chantal, Daniela, Laurence, Laure, Silvia, Mélanie, Julie, Daniela, Marcus, Manhui, and Harun, thank you for enriching my working place with an incredible atmosphere, endless coffee breaks, continuous help, and joy on a daily basis.

To my friends, my roommates, my sisters from another mother, Inès, Lisa, Valentine, Laura, Bianca, Olivia, Radiana, Amélie, Antoine, Dorian, and Yoann, thank you for enlightening my life in every way possible throughout these years in my now Swiss home – for endless (feminist) conversations, for waking-up very early on week-ends to go ski touring, for the drinks at La Grenette, for paddling afterwork at the lake, for Caprices, for couch-potatoing at home (not as much as I would have liked though…), for supporting my bad decisions, for the week-ends at Le Chalet, for being mad at me for not watering my plants enough, for Paléofestival and Festin'euch, for making fun of my French accent again and again, for hiking in the Alps, for gardening on the rooftop (but not too much), for home-working together while bleaching our moustaches, for the doggos (yes I am not forgetting Lemmy, nor Charlie, how would I dare), for scooti gang, for making Covid times more bearable, for travelling through Tanzania and Corsica together, for running during ice-cold

winter to train for Sierre-Zinal while I was not even participating in the race, for road biking because somehow I got enrolled in this sport that I ~~hate~~ love, for belaying you while never climbing, for our blackouts, for our laughs, for our cries, and so on… for making my life an exceptionally exciting journey.

À ma famille, Hélène, José, Maïté, Laure, Simon, Philippe, Marie, Joseph, Joachim et Sylvie, merci de votre présence depuis les débuts et à travers les années, et de vos encouragements tout au long de ma thèse malgré la distance.

Aan Milo, bedankt voor je oneindige geloof in mij en om samen met mij dit avontuur aan te gaan. Dat er nog vele mogen volgen.

À mes parents, **Marie** et **Claude**, merci pour tout. Vous avez supporté mes échecs mais également rendu possible mes succès grâce à vos encouragements et votre confiance en moi.

À ma sœur, merci au Dr. **Sophie** Chavarria, à qui je dédie ce travail pour avoir inspiré mon envie de poursuivre une thèse, pour m'avoir épaulé à travers les années et qui continue à m'inspirer jour après jour.

Finally, to all of you, thank you for making these last years a game-changing and memorable experience in every aspect.

LIST OF ABBREVIATIONS

Å	Angstrom (unit)
AD	Alzheimer's diseases
ARE	Antioxidant response element
ATF 4/6	Activating transcription factor 4/6
ATG 5/12	Autophagy-related gene 5/12
A. thaliana	*Arabidopsis thaliana*
ATP	Adenosine triphosphate
BiP	Binding immunoglobulin protein
Btz	Bortezomib
bZIP	Basic leucine zipper
Cd	Cadmium
Cam-K2	Calmodulin-dependent protein kinase 2
CANDLE	Chronic atypical neutrophilic dermatosis with lipodystrophy and elevated temperature
C. elegans	*Caenorhabditis elegans*
ChIP	Chromatin immunoprecipitation
CHOP	C/EBP homologous protein
CLU	Clusterin
CnC	Cap'n'Collar
Crispr	Clustered regularly interspaced short palindromic repeats
CTLs	Cytotoxic T cells
Ddi1	DNA-damage inducible 1
DDI2	DNA-damage inducible 1 homolog 2
D. melanogaster	*Drosophila melanogaster*
DMEM	Dulbecco's Modified Eagle's medium
DNA	Deoxyribonucleic acid
DRIPs	Defective ribosomal products
DSK2	Dominant suppressor of kar1 protein 2
DTT	Dithiothreitol
DUBs	De-ubiquitinating enzymes
EDEM	ER-degradation enhancing α-mannosidase-like protein
eGFP	Green fluorescent protein
eIF2α	Eukaryotic translation initiation factor 2α
ER	Endoplasmic reticulum
ERAD	Endoplasmic reticulum-associated degradation
ERmanI	Endoplasmic reticulum class I α-mannosidase
FCS	Foetal calf serum
GABARAPL1	Gamma-aminobutyric acid receptor associated protein like 1
GWAS	Genome-wide association study
HDD	Helical domain
HEK	Human embryonic kidney cells
HeLa	Henrietta Lacks immortalized cells
HERP	Homocysteine-induced endoplasmic reticulum protein
HIV	Human immunodeficiency virus
HIV-1	Human immunodeficiency virus type 1
HIV-PIs	Human immunodeficiency virus protease inhibitors
HRD1	HMG-coA reductase degradation protein 1
HSC70	Heat shock cognate 71
Hsf1	Heat shock transcription factor 1
HSP	Heat shock protein

IFNγ	Interferon gamma
IRE1	Inositol-requiring enzyme 1
ISR	Integrated stress response
Itch	Itchy E3 ubiquitin protein ligase
kDa	kilodalton
LAMP-2A	Lysosomal-associated membrane protein 2A
LC3	Microtubule associated protein 1 light chain 3
MHCs	Major histocompatibility complexes
miR-101	microRNA-101
mRNA	Messenger RNA
MT	Metallothionein
mTORC1	Mammalian target of Rapamycin complex 1
NAC 53/78	NAC-domain containing protein 53/78
NFE2L1/NRF1	Nuclear factor erythroid 2-related factor 1
NFE2L2/NRF2	Nuclear factor erythroid 2-related factor 2
NF-κB	Nuclear factor kappa B
NFV	Nelfinavir
NGLY1/PNG-1	N-glycanase 1 / Peptide:N-glycanase 1
NST	Asparagine/serine/threonine-rich domain
NTD	N-terminal domain
OGT	O-linked N-acetylglucosamine (GlcNAc) transferase
o/n	Overnight
OST	Oligosaccharyl transferase
OS-9	Osteosarcoma amplified 9, endoplasmic reticulum lectin
PACE	Proteasome-associated control element
PAGE	Polyacrylamide gel electrophoresis
PCPS	Proteasome catalysed peptide splicing
PEI	Polyethyleneimine
Pen/Strep	Penicillin / Streptomycin
PERK	Protein kinase RNA-like ER kinase
PK	Proteinase K
PN	Proteostasis network
POMP	Proteasome maturation protein
PRAAS	Proteasome associated autoinflammatory syndrome
PTMs	Post-translational modifications
qPCR	Quantitative Polymerase Chain Reaction
RACs	Ras family small GTPases
RAD23A/B	UV excision repair protein 23 homolog A/B
RNA	Ribonucleic acid
ROS	Reactive oxygen species
RPMI	Roswell Park Memorial Institute
Rpn4	Regulatory particle non-ATPase 4
RT	Room temperature
RVP	Retroviral protease-like
SDS	Sodium dodecyl sulphate
SEL1L	Suppressor of Lin-12-like protein 1
SKN-1A	Skinhead-1A protein
SNPs	Single nucleotide polymorphisms
sHSP	Small HSP
S. cerevisiae	*Saccharomyces cerevisiae*
S. Pombe	*Schizosaccharomyces pombe*
STYK1	Serine threonine tyrosine kinase 1
TAP	Transporter associated with antigen processing
TCRs	T-cell receptors
TM	Tunicamycin
tRNA	Transfer RNA

UBA	Ubiquitin-associated
UBA1	Ubiquitin-like modifier-activating enzyme 1
UBL	Ubiquitin-like
UBQLNs	Ubiquilins
UIM	Ubiquitin-interacting motif
UPR	Unfolded protein response
UPS	Ubiquitin Proteasome system
VCP/p97	Valosin containing protein
WT	Wild type
XTP3-B	XTP3-transactivated protein B
Yap1	Yes-associated protein 1

TABLE OF CONTENT

LIST OF FIGURES

LIST OF TABLES

I. INTRODUCTION

Molecular Mechanism of Proteostasis

The ability of organisms to maintain the integrity of the proteome is vital for their survival. Broadly speaking, proteins are subjected to constant surveillance through the proteostasis network (PN) that monitors closely the synthesis, folding, trafficking and degradation of the cellular proteome (Balch et al., 2008). Imbalance in protein homeostasis, caused by cell stress like accumulation of misfolded proteins or exposure to environmental stimuli, leads to the activation of transcriptional programs promoting either folding or clearance of defective proteins (Labbadia & Morimoto, 2015; Powers et al., 2009). In the case of proteostasis restoration program failure, flawed proteins accumulate in the endoplasmic reticulum (ER) prompting protein degradation pathway activation and ultimately cell death. These degradation pathways have collectively been defined as the unfolded protein response (UPR). Triggering this response aims to re-establish ER proteostasis through different molecular mechanisms including the activation of ER-associated degradation (ERAD) pathway and autophagy. However, if this adaptive program fails to restore ER proteostasis, UPR will lead to an alternative response ultimately promoting apoptosis.

In the following introduction, I will describe thoroughly the basic concepts of protein homeostasis as well as the different adaptation programs driving protein quality control in the cell.

A. Cellular homeostasis

All living cells must maintain their homeostasis as changes occur in the internal as well as external environment. Cellular homeostasis refers to the internal steady state maintained by living systems through various molecular mechanisms and regulators. This phenomenon was first described by Claude Bernard in 1865 (Bernard et al., 1927) and later called "homeostasis" by Walter Bradford Cannon after the combination of the Greek words *homois* "similar" and *stasis* "standing still", thus describing the concept of "staying the same" (Cannon, 1939). Since its initial description, a considerable amount of additional information has broadened our basic appreciation of how living organisms function. At the basis of the homeostasis concept is the maintenance of a steady state which requires continuous work. To maintain this constant state, biochemical systems operate through the regulation of metabolic flux, gene expression, and energy transformation. All these processes rely on one common denominator: the cellular proteome. Proteins participate in almost all biological processes hence they are essential for cell function, development, and viability. In human cells, more than 10'000 different proteins are expressed (Kulak et al., 2017), most of which fold into a

well-defined three-dimensional conformation to perform their biological functions. The abundance of numerous proteins must be carefully controlled in mammalian cells. This state of balanced proteome, the so-called proteostasis, relies on a large network comprising molecular chaperones, proteolytic processes, and their regulatory proteins in which roughly 2'000 proteins are estimated to participate in (Klaips et al., 2018). The organisation and regulation of this network is of great interest in understanding the cellular adaptation response triggered upon extrinsic or intrinsic stresses, as failure in protein homeostasis is associated with aging process and associated pathologies (Cohen & Dillin, 2008; Lopez-Otin et al., 2013; Taylor & Dillin, 2011).

A.1. Protein synthesis

Proteins are produced by ribonucleoprotein structures called ribosomes. In eukaryotes, these cytosolic structures consist of two molecular subunits: small 40s and large 60s subunits. Although their function is closely connected, they have distinctive roles in the protein translation process. The small 40s subunit coordinates the interaction between an mRNA codon and the anticodon of the amino-acetylated transfer RNA (tRNA). Whereas the large 60s subunit catalyses the reaction generating the peptide bond between the nascent protein and the up-coming amino acid (Steitz, 2008). Translation starts when the ribosomal complex detects the mRNA start codon coding for methionine and terminates with an mRNA stop codon releasing factor binding and disassembly of the ribosome structure (Poole & Tate, 2000) **(Figure 1)**.

Initially, protein translation is taking place in the cytoplasm. Nevertheless, depending on the role of the newly synthetised protein, ribosomes can be localised either free in the cytosol or bound to the ER membrane. Pioneers in the protein synthesis field have established the role of cytosolic ribosomes in producing cell-retained proteins whereas ER-associated ribosomes were implicated in generating membrane-incorporated and secretory proteins (Hicks et al., 1969). Further studies have demonstrated the necessity of nascent protein to have a ~20 amino-acids N-terminal signal peptide to promote ribosome binding to the ER and facilitate their transport into the ER lumen following their synthesis (Blobel & Dobberstein, 1975).

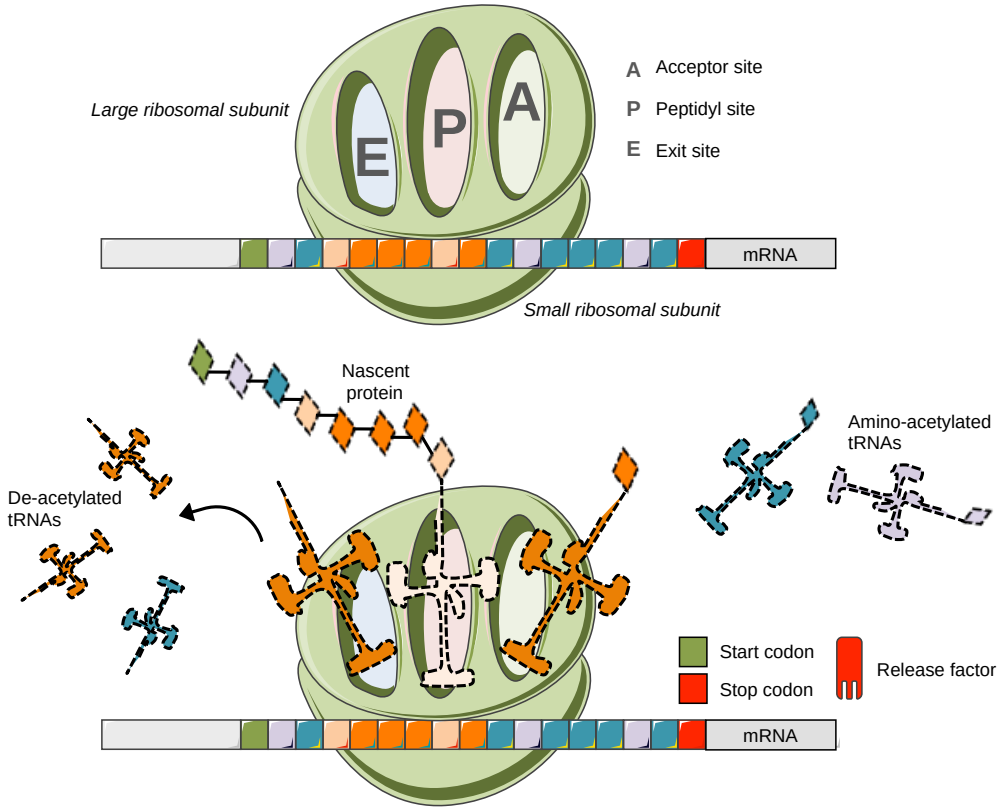

Figure 1. Protein synthesis. Proteins are newly synthetized by ribosome molecules which contain acceptor (A), peptidyl (P) and exit (E) sites. These three sites enable the interaction between the mRNA and the amino-acetylated tRNAs, to facilitate the production of the new protein. The start codon of the mRNA (shown in green) encodes a methionine as the starting amino acid of the polypeptide chain. Finally, when ribosomes detect the stop codon (shown in red), translation is terminated, and the release factor is recruited to facilitate the disassembly of the ribosome from the freshly translated mRNA. From (Bujišić & Université de Lausanne).

The protein synthesis process is tightly regulated by a set of specific factors, co-factors, and pathways. Indeed, bulk levels of newly synthetized proteins must be adjusted to the folding capacity of the cell in order to avoid accumulation of misfolded proteins. One typical example of protein synthesis regulation is translation attenuation through the inhibition of the translation initiator factor 2α (eIF2α). For instance, upon accumulation of misfolded proteins in the ER, the unfolded protein response (UPR) program is activated, which induces phosphorylation of eIF2α by the protein kinase RNA-like ER kinase (PERK), as part of the integrated stress response (ISR), thereby dampening eIF2α function in translation (Harding et al., 2001). General decrease in protein translation is critical in relieving PN overload under conformational stresses.

A.2. Protein folding and aggregation

Most of nascent proteins must fold into a three-dimensional structure to complete their function in the cell. The folding process is assisted by molecular chaperones which promote the correct protein assembly in an ATP-dependent or independent manner (Balchin et al., 2016; Kim et al., 2013; Lee et al., 2018). These chaperones are part of the small heat shock proteins family (sHSPs). In other words, chaperones participate in the folding of two-third of newly synthetised polypeptides that are destined for cytosolic function (Thul et al., 2017). For secretory proteins or proteins destined for membranes, cytosolic chaperones prevent their premature folding before the polypeptide is correctly transported into their target organelle (Balchin et al., 2016; Young et al., 2003). As for proteins whose destination is the nucleus or peroxisomes, chaperones coordinate their folding before transport. Chaperones are very abundant proteins; they represent about 2% of the total cellular protein.

One of the best-described protein folding process is the action of Calnexin-Calreticulin system which assists the folding of glycoprotein in the ER. Most proteins transported in the ER must undergo N-linked glycosylation by the enzyme Oligosaccharyl transferase (OST). This enzyme tags nascent polypeptides with a complex oligosaccharide chain on their N-terminus. Once proteins are marked by the N-linked glycan, they are prone for recognition by the Calnexin-Calreticulin complex. This complex recruits an additional protein called ERp57 that coordinates the formation of a disulfide bond and isomerization. This cascade of events leads to a slower folding of the glycoprotein, thus enhancing the folding efficiency (Ellgaard & Helenius, 2003; Hebert & Molinari, 2007) **(Figure 2)**.

Once proteins are properly folded, they exit the ER toward the Golgi apparatus where they undergo further post-translational modifications labelling them for their destined role. In most cases, the proteome is conformationally stable, but when this stability is challenged a proportion of unfolded proteins starts to accumulate in the cell, a process called protein aggregation. This phenomenon is emphasized by the presence of destabilizing factors such as mutations or environmental stresses like elevated temperature, the presence of reactive oxygen species (ROS), etc. In addition, the accumulation of aggregated proteins is cytotoxic where proteins tend to have a role unrelated to their initial biological function. To cope with protein aggregation, the PN activates the transcription of molecular chaperones involved in signalling pathway specifically leading to protein remodelling (Anckar & Sistonen, 2011; Gomez-Pastor et al., 2018). Once again, specific heat shock proteins are coordinating the re-folding of non-native proteins to achieve their structural function. Similar mechanisms are observed in the ER and in the mitochondria upon accumulation of unfolded proteins (Shpilka & Haynes, 2018; Walter & Ron, 2011).

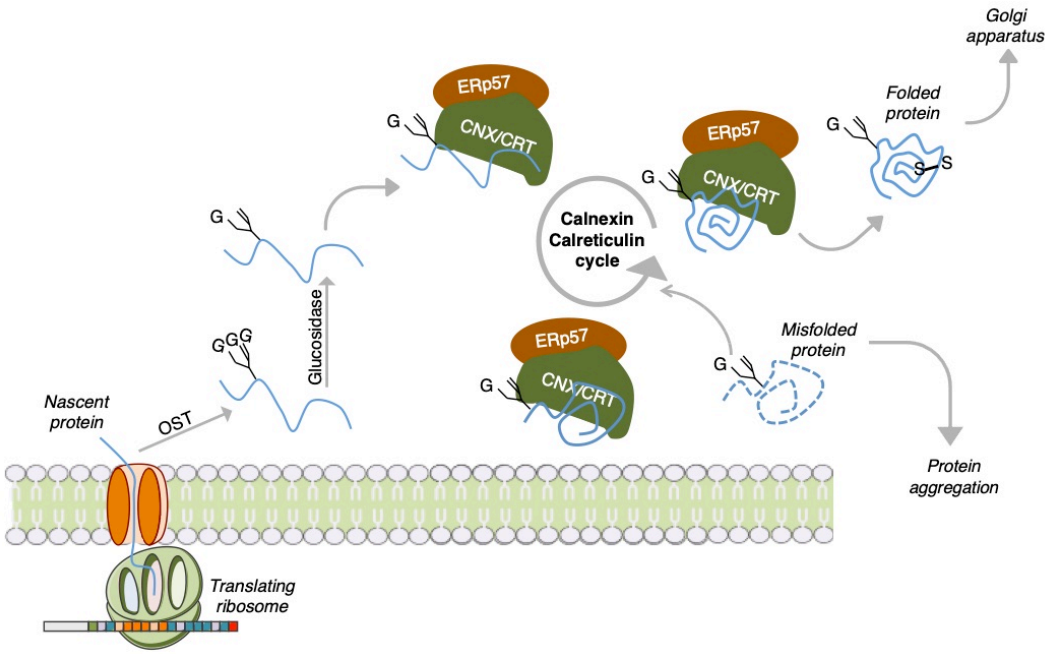

Figure 2. Protein folding. Nascent protein targeted for ER undergo N-glycosylation by OST. Subsequently, N-glycan is trimmed by a glucosidase rendering the protein suitable for folding through the Calnexin/Calreticulin (CNX/CRT) cycle. ERp57 facilitate the formation of the disulfide bond during protein folding. Properly folded proteins are then delivered to the Golgi apparatus for further maturation processes. Misfolded proteins undergo an additional Calnexin/Calreticulin cycle or start to aggregate. Adapted from (Bujišić & Université de Lausanne).

B. Cellular adaptation responses

When the cell fails to clear misfolded and aggregated proteins, chaperone-mediated pathways are activated to help redirect non-native proteins to degradation programs. These events are part of the cellular adaptation program. Cells have developed two main adaptation programs that lead to protein clearance through lysosomal-degradation pathway, also known as autophagy (Yang & Klionsky, 2010) or proteasomal-degradation pathway (Finley, 2009).

B.1. Autophagy

The autophagy concept was first introduced in 1963 by the Nobel Prize in Physiology and Medicine for lysosome discovery: Christian de Duve. In his studies, he described how cellular material is engulfed within lysosomes destined for clearance (de Duve, 1983). The etymology of autophagy derives from the combination of two Greek words: *auto,* meaning "self", and *phagein* translated as "to eat". Thus far, three mechanisms of autophagy are described in the literature: macro-autophagy, micro-autophagy, and chaperone-mediated autophagy **(Figure**

3). Among the different types of autophagy, the most described mechanism is the macro-autophagy pathway which is widely known as autophagy.

Mechanistically, autophagy is regulated by ATG proteins which sequentially form complexes orchestrating the different steps of the pathway (Klionsky et al., 2011). The different steps comprise the initiation of the phagophore formation, the phagophore elongation, the phagophore closure leading to the creation of the autophagosome structure, and the fusion of the mature autophagosome with the lysosomal compartment where the autophagosome content is degraded by lysosomal hydrolases **(Figure 3a)**.

In contrast, micro-autophagy is described as a more direct mechanism of protein clearance. Along the process, lysosomes directly engulf the cytosolic material through their own membrane invagination (Mijaljica et al., 2011) **(Figure 3c)**. As for chaperone-mediated autophagy, the pathway relies on a specific cytosolic chaperone called HSC70 which, upon recognition of misfolded proteins, translocates into the lysosome through an association with the lysosomal receptor LAMP-2A (lysosomal-associated membrane protein 2A) (Cuervo & Wong, 2014) **(Figure 3b)**.

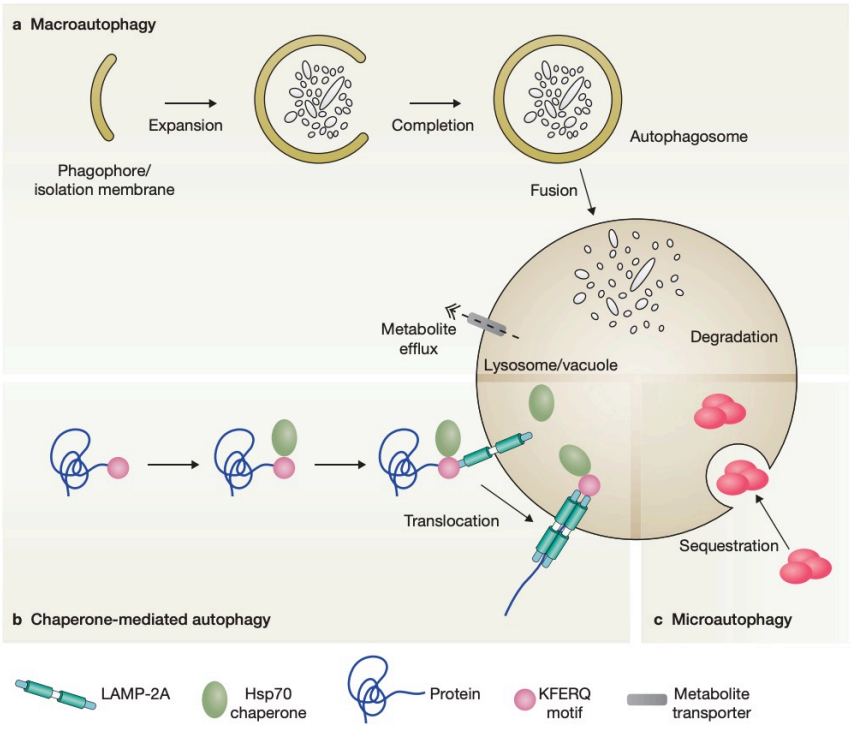

Figure 3. The different mechanisms of autophagy. (**a**) In macroautophagy, structures targeted for destruction are sequestrated in vesicles named autophagosomes. Fully mature autophagosomes fuse with endosomes first, then finally expose their content to lysosomal hydrolases. (**b**) In chaperone-mediated autophagy, the chaperone HSC70 recognizes specifically tagged misfolded proteins (KFERQ motif) and associates with LAMP-2A at the lysosomal surface. This leads to translocation of the misfolded protein into the lysosomal content. (**c**) In microautophagy, proximity targeted components are recruited to the lysosome through invagination of its membrane. From (Boya et al., 2013).

Studies on autophagy have initially presented this process as regulated by nutrient availability (Deter et al., 1967; Novikoff et al., 1964). Nutrient availability is sensed by mTORC1 (mammalian target of rapamycin C1) (Gonzalez & Hall, 2017). Bar-Peled and Sabatini have also showed how, upon fed conditions, mTORC1 keeps autophagy at basal level, and upon nutrient deprivation, mTORC1 is deactivated thus increasing autophagy (Bar-Peled & Sabatini, 2014). Later, studies have then revealed the implication of ER stress in driving autophagy activation. Indeed, all three branches of the unfolded protein response (UPR), PERK, IRE1, and ATF6, have been described as promoting autophagy through mTORC1 inhibition (Deegan et al., 2013). The stress sensor PERK is the most implicated in autophagy activation through the transcriptional upregulation of ATG5, ATG12 and LC3 genes involved in phagophore elongation via the PERK-ATF4-CHOP arm (Rashid et al., 2015; Rouschop et al., 2010).

Although the three branches of UPR are linked with upregulation of autophagy, they are also implicated in the degradation of misfolded protein through the major proteolytic system in eukaryotic cells: the ubiquitin-proteasome system, also referred as UPS.

B.2. Ubiquitin-proteasome system (UPS)

The process of protein degradation through the ubiquitination system occurs in two successive steps. Firstly, multiple ubiquitin molecules attach covalently to the protein substrate. The 26S proteasome complex then degrades the tagged protein, thus releasing reusable ubiquitin. Both ubiquitin conjugation and substrate degradation need to be tightly regulated to remove targeted proteins efficiently and specifically at the right time.

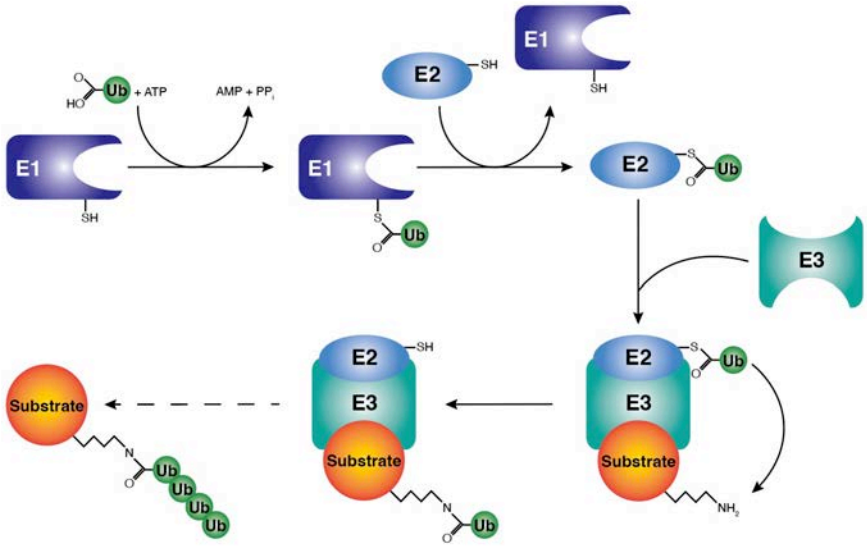

Figure 4. The protein ubiquitination pathway. The ubiquitin molecule is activated by E1 through the use of ATP, then transferred to the E2 enzyme. Following E2 activation, the ubiquitin conjugates to the substrate protein via a specific E3 ligase. Further polyubiquitination is required to target substrate proteins for degradation. Adapted from (D'Arcy et al., 2015).

The pathway consists of several components, including ubiquitin, an evolutionarily conserved protein of 76 residues that is activated by the ubiquitin-activating enzyme E1 in the presence of ATP. Subsequently to activation, an E2 enzyme transfers the activated ubiquitin to an E3 ubiquitin-protein ligase which, in return, binds to a specific substrate protein. The E3 catalyzes the covalent attachment of ubiquitin to the substrate protein generating a polyubiquitin chain that serves as a recognition marker for the proteasome **(Figure 4)**. 26S proteasomes recognize the poly-ubiquitin chain as the main tag for protein degradation, several E3 ligases can recognize substrates harboring diverse degradation signals, thus contributing to the specificity and selectivity of the UPS (Ciechanover & Iwai, 2004; Pickart, 2001; Pickart & Cohen, 2004; Voges et al., 1999; Weissman, 2001). Comparative genomic analysis has revealed that only a few genes encode for E1 ligases, about ten for E2 and a hundred for E3 ligases (Semple et al., 2003). Through E2 and E3-mediated specificity, the UPS eliminates specifically proteins while leaving other proteins untouched. In such a way, the UPS enables the cells to regulate cell fate in a dynamic fashion (Varshavsky, 2005). Where several E2 enzymes were characterized in mammalian cells and appear to act with one or more E3 ligases, E3s appear to play a crucial role in recognizing and selecting proteins for conjugation and degradation. While only a few E3 ligases have been described, it is likely that they belong to a growing family of enzymes that recognize several different cellular proteins with similar but not identical structural motifs. Some proteins are recognized through their N-terminal residues or downstream primary sequences (Varshavsky, 1992), while others are targeted through post-translational modifications, like phosphorylation, or when associated with molecular chaperones.

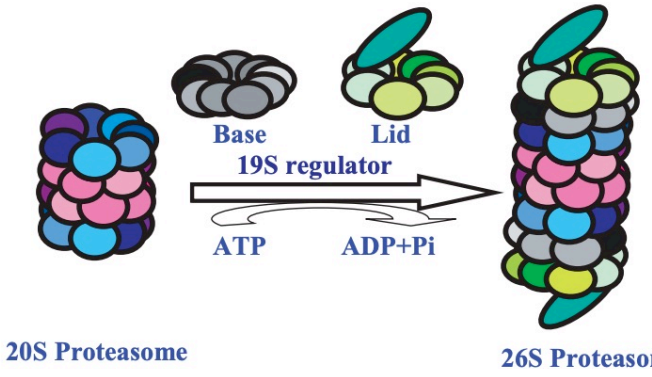

Figure 5. The 26S proteasome formation. In an ATP-dependent manner, the catalytic 20S proteasome structure assembles with the 19S regulators. Adapted from (Nandi et al., 2006).

Following conjugation, the proteasome complex degrades the protein moiety of the adduct and the resulting ubiquitin is released and can be reused (Schmidt & Kloetzel, 1997; Stock et al., 1996). The 26S proteasome complex is the most well-studied complex responsible for degrading ubiquitin-tagged proteins. Its symmetric structure is composed of a central catalytic unit called the 20S proteasome which is flanked by regulatory 19S proteasome complexes on both sides (19S-20S-19S) **(Figure 5)**. The crystal structure of the eukaryotic 20S proteasome

has been resolved at a resolution of 2.4 Å, confirming previous predictions while also revealing unexpected features (Groll et al., 1997). The yeast complex consists of four rings, each containing seven distinct subunits, with molecular masses ranging from 25–30 kDa. Topological analysis has revealed that the active sites for proteolysis reside in the three β subunits (β1 encoded by *PMSB6*, β2 by *PSMB7*, and β5 by *PSMB5*) and that the active sites for the three proteolytic activities (trypsin-like, chymotrypsin-like, and postglutamyl peptidyl hydrolytic activities) are generated by adjacently paired β-type subunits residing in different β rings. The propeptides of β subunits are essential for the biogenesis and stabilization of the proteasomal structure, and processing occurs only after assembly. The α chains, although catalytically inactive, play a crucial role in stabilizing the two-ring structure of the β chains and in binding the 19S cap complexes. The 26S proteasome is prone to structural changes in adaptive immunity upon stimuli and is named the immunoproteasome. An immunoproteasome is a proteasome-like structure expressed in immune cells and induced by interferon gamma (IFNγ) (and other proinflammatory cytokines) as well as oxidative stress. These events lead to the transcription of three catalytic subunits that are not present in the classical proteasome (Ferrington & Gregerson, 2012) **(Figure 6)**. As in the UPS, the immunoproteasome degrades ubiquitin-labeled cytosolic proteins, and its main function is to cleave specific proteins into shorter peptides to be displayed on the cell surface of immune cells to cope with infection from a pathogen.

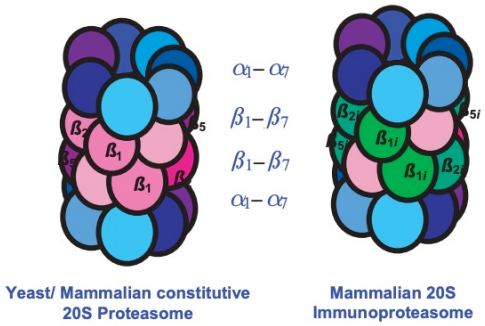

Figure 6. Schematic comparison of mammalian 20S proteasome and immunoproteasome. The mammalian 20S proteasome is composed of seven α and β subunits. The mammalian immunoproteasome is induced in response to inflammatory signals, e.g. IFNγ, where the three constitutive β subunits, β1, β2, and β5, are replaced by β1i, β2i, and β5i. Adapted from (Nandi et al., 2006).

It is now known that not all ubiquitinated proteins are targeted for proteasomal degradation, particularly mature cell surface membrane proteins (Hicke, 1997). The degradation of membrane-anchored proteins via the ubiquitin system raises unresolved mechanistic issues, particularly with regards to the combination of topologically distinct events such as misfolding in the endoplasmic reticulum and degradation in the cytosol. The role of ubiquitin modification for endocytosis of the tagged protein or its specific targeting and uptake by the lysosome remains unclear for cell surface membrane proteins. For endoplasmic reticulum proteins degraded by the cytosolic proteasome, important questions revolve around the

mechanisms underlying the retrieval of these proteins across the membrane back into the cytosol. The membrane-anchored proteins are retrotranslocated to the cytosol through the process called ER-associated degradation (ERAD) whereas for lumenal endoplasmic reticulum proteins, the remaining question centers on how they are transported back into the cytosol.

ER-associated degradation (ERAD)

The ER has developed sophisticated mechanisms to ensure that misfolded polypeptides are degraded. These misfolded proteins are labeled and extracted from the ER lumen to be degraded by cytosolic proteasomes, a process known as ER-associated degradation (ERAD) (Pisoni & Molinari, 2016).

The process starts with the progressive de-mannosylation of the N-glycan. The mannose trimming is the targeting signal for ERAD and is carried out by mannosidases such as ERmanI or EDEM proteins (Olivari et al., 2006; Olivari et al., 2005). These enzymes remove mannose sequentially in a slow process that enables the expansion of misfolded glycoproteins exposition to the action of mannosidases (Lederkremer & Glickman, 2005; Molinari, 2007). The removal of mannose is an essential step to prevent the misfolded protein to go through more Calnexin-Calreticulin cycles (mentioned earlier) (Aebi et al., 2010). Once trimmed, polypeptides are recognized by ERAD lectins known as OS-9 and XTP3-B (Bernasconi et al., 2008; Hosokawa et al., 2008).

Following recognition by ERAD lectins, labelled polypeptides must be transported from the ER to the cytosol to undergo proteasome degradation. The dislocation process of proteins from the ER lumen requires the action of large protein complexes enclosed in the ER membrane and surrounded by E3 ubiquitin ligases **(Figure 7)**.

In mammals, around twenty ER-resident E3 ubiquitin-ligases have been identified, including HRD1 (Kikkert et al., 2004), most of which play a role in ERAD **(Table 1)**. The E3 ubiquitin ligase HRD1 is the best characterized to be involved in the dislocation machinery. In yeast and mammals, analyses have revealed that the dislocation process relies on a highly elaborate protein network composed of HRD1 interactors (Carvalho et al., 2006; Christianson et al., 2011), including the scaffold protein HERP which participates in the assembly and stabilization of the machinery (Huang et al., 2014; Schulze et al., 2005), and the adaptor protein SEL1L which stabilizes HRD1 (Sun et al., 2014). Following the dislocation of misfolded proteins, polypeptides must be recognized on the cytosolic side of the dislocation machinery to be targeted for proteasomal degradation. The cytosolic ATPase VCP/p97 chaperone was characterized as part of the cytosolic HRD1 interactors (Ye et al., 2001).

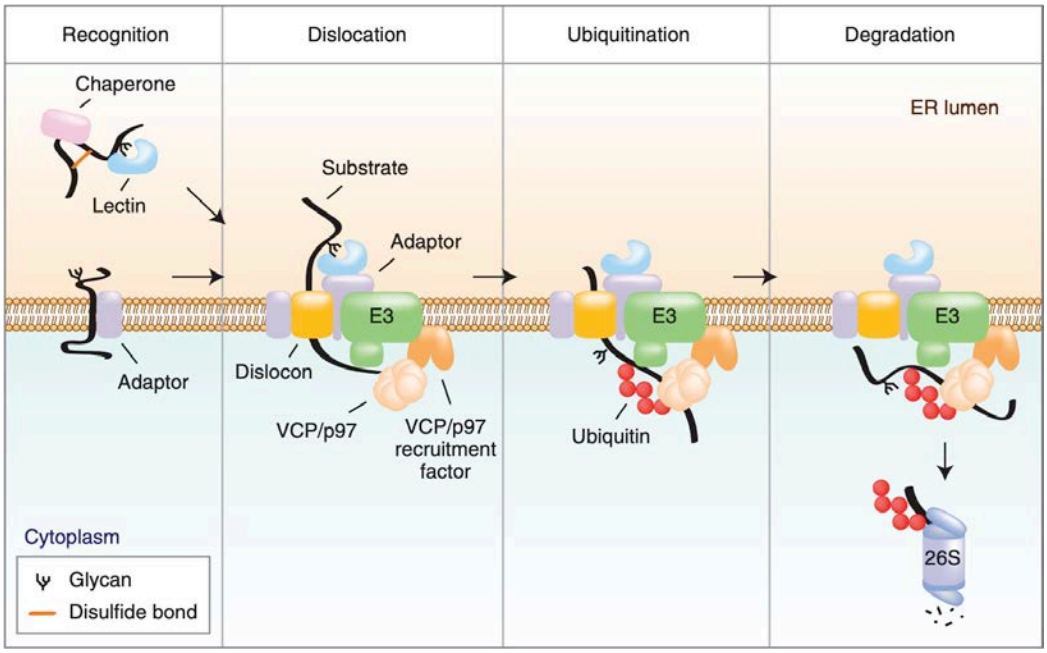

Figure 7. The key steps of ERAD. The ERAD pathway consists in the succession of temporally ordered steps, including: - Recognition: in the ER lumen, chaperones and lectins interact with misfolded substrate proteins and connect them to the dislocon through membrane-embedded adaptors. - Dislocation: Energy generated from ATP hydrolysis by VCP/p97 enables the passage of the substrates through the pores of the dislocon structure. – Ubiquitination: upon exposure to the cytosol, substrates are polyubiquitinated by E3 ligases. – Degradation: ubiquitinated substrates are transferred to the cytosolic 26S proteasome which degrades them. From (Olzmann et al., 2013).

The mechanism by which misfolded proteins are translocated from the ER lumen to the cytosol for degradation is still relatively obscure. Various proteins have been suggested to form a channel or "dislocon" through which misfolded proteins would be expelled from the ER (Lilley & Ploegh, 2004; Loureiro et al., 2006; Ye et al., 2004). According to a recently proposed model, HRD1 was suggested to form the dislocon through autoubiquitination triggering the opening of the channel (Baldridge & Rapoport, 2016; Carvalho et al., 2010; Schoebel et al., 2017). Soluble misfolded proteins may require a dislocation channel to be transported from the ER lumen to the cytosol, while other machineries will be required to extract transmembrane misfolded proteins from the ER membrane. Several proteins were suggested to be implicated in the destabilization and extraction of defective transmembrane proteins from the ER membrane (Greenblatt et al., 2011; Wunderle et al., 2016; Zettl et al., 2011).

Following dislocation, the substrate needs to be ubiquitinated, as mentioned before, to undergo proteasomal degradation. The polyubiquitination of the substrate engages the cytosolic ATPase VCP/p97 which mediates the extraction of the polypeptide from the ER lumen in concert with co-factors (Schuberth & Buchberger, 2008; Ye et al., 2001). After ATP binding, VCP/p97 enables the unfolding of the substrate by passing through its central pore (Bodnar & Rapoport, 2017).

Sometimes along the process of translocation and substrate unfolding, hydrophobic patches of the polypeptide are exposed and lead to protein aggregation. To cope with this issue, proteasomal degradation occurs simultaneously to ERAD retrotranslocation (Ikeda et al., 2009). In alternative to direct degradation, dislocated ERAD substrates are transported by cytosolic chaperones like DSK2 and RAD23 proteins (Medicherla et al., 2004).

Subsequently to ER lumen extraction, ERAD substrates are proteolytically processed and degraded through the UPS pathway, as described earlier. De-ubiquitinating enzymes (DUBs) and peptide:N-glycanase (PNGase) were described to be tightly associated with the proteasome to ensure an efficient passage through the proteasomal pore by removing ubiquitin and N-glycan (Matyskiela & Martin, 2013).

Table 1. List of some human ER-associated E3 ubiquitin protein ligases. Adapted from (Kevei et al., 2017).

E3 ligase	Target	References
STUB1/CHIP	Misfolded proteins. Hsp90 clients	(Connell et al., 2001)
UBR1	Misfolded proteins	(Eisele & Wolf, 2008; Heck et al., 2010)
UBR2	Misfolded proteins	(Nillegoda et al., 2010)
HUWE1	Unassembled proteins	(Xu et al., 2016)
SYVN1/HRD1	Misfolded proteins from the ER	(Kikkert et al., 2004)
E6AP/UBE3A	Misfolded, aggregated proteins	(Mishra et al., 2009)
RNF126	Mislocalized ER proteins	(Rodrigo-Brenni et al., 2014)
NEDD4	Heat-induced misfolded proteins. Plasma membrane proteins	(Fang et al., 2014)
RNF5/RMA1	Misfolded proteins	(Younger et al., 2006)
SKP1/CUL1/F-box	LRR domain proteins. kinetochore	(Kaplan et al., 1997)
MARCHF6/TEB4	ER and inner nuclear membrane	(Hassink et al., 2005; Schultz et al., 2018)
TRIM13/RFP2	Misfolded proteins from the ER	(Lerner et al., 2007)
RNF103	Involved in ERAD	(Maruyama et al., 2008)
RNF170	Involved in ERAD	(Lu et al., 2011)
RNF185	Misfolded proteins from the ER	(El Khouri et al., 2013)
TMEM129	Involved in ERAD	(van den Boomen et al., 2014)
RNF139/TRC8	MHC I polyubiquitination before ERAD	(Stagg et al., 2009)
ZNRF4	Misfolded proteins from the ER	(Neutzner et al., 2011)

C. UPS in health and diseases

The UPS is implicated in the degradation of a very large number of cellular proteins, thus controlling several cellular processes. As the central hub of proteostasis, it is not surprising to find it involved in the adaptive immune system as much as associated to various diseases upon dysfunction.

C.1. MHC Class I antigen processing and presentation

Antigen presentation plays a central role in the activation of adaptive immune responses. Along this process, foreign antigens are presented as short peptide fragments on cell surfaces to cytotoxic T cells (CTL), and they are presented by two main classes of major histocompatibility complexes (MHCs). MHC class II complexes are expressed only on professional antigen-presenting cells, and they present exclusively extracellular foreign antigens that have been processed in lysosomes (e.g. phagocytosis of viruses or bacteria) (Roche & Furuta, 2015; Wieczorek et al., 2017). In contrast, MHC class I complexes are expressed by all nucleated cells and present self-peptides from cellular proteins and foreign peptides that derive from intracellular pathogens like viruses. Peptides presented by MHC class I molecules are about 8-10 amino acids long and are generated through proteasome-dependent protein degradation.

Although both proteasomes and immunoproteasomes can generate peptides for MHC class I presentation, the induction of specific subunits into proteasomes have either positive or negative effects in antigen presentation. Several studies have highlighted a positive role of the immunoproteasome in initiating CTL responses against viral and bacterial antigens but it has also been described to inhibit the presentation of tumor epitopes (Chapatte et al., 2006; Chapiro et al., 2006; de Graaf et al., 2011; Guimaraes et al., 2018; Hutchinson et al., 2011; Keller et al., 2015; Kincaid et al., 2011; Morel et al., 2000; Sijts et al., 2000; Van Kaer et al., 1994). The differences in MHC class I-restricted peptide supply between the two proteasome systems can be explained by the higher cleavage rate from immunoproteasomes subunits (Mishto et al., 2014), which may result in either increased epitope generation or destruction depending on the peptide sequence.

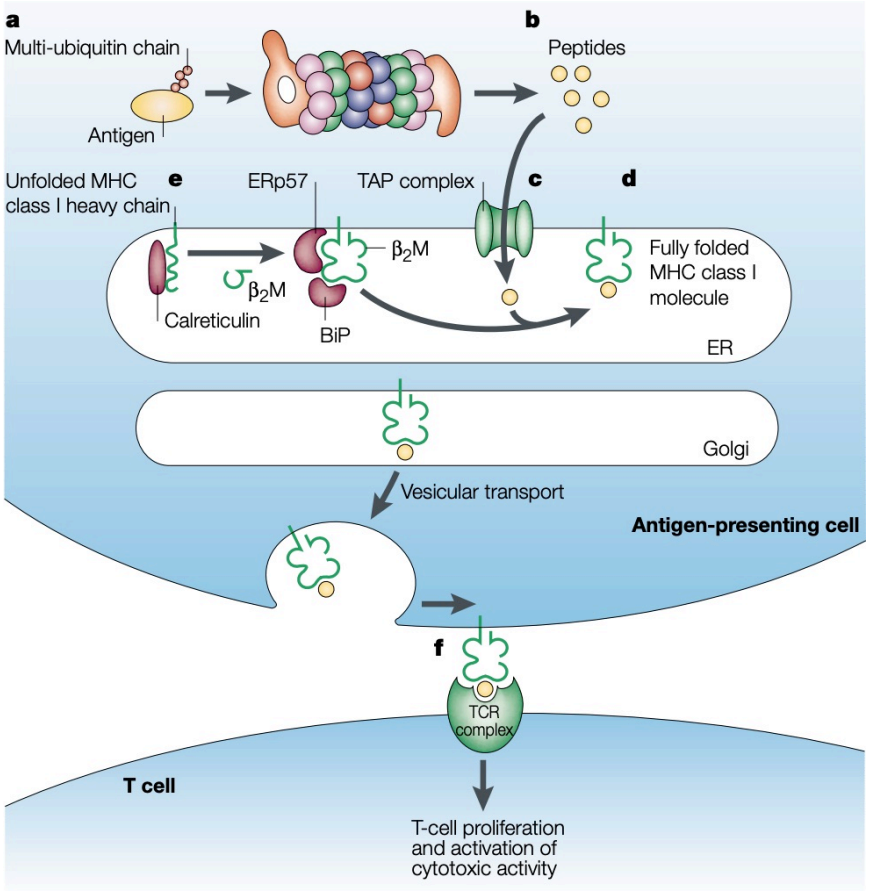

Figure 8. Proteasome catalyzed peptide splicing (PCPS) for MHC Class I antigen presentation. (**a**) Most antigenic substrates hold a polyubiquitinated chain, targeting them to the 26S complex for proteasomal degradation. (**b**) Proteasomal degradation results in the generation of peptides about 8-10 amino acid long. (**c**) These small peptides are transported to the ER via the TAP complex. (**d**) Once in the ER, peptides are loaded on the MHC Class I complex (composed of one heavy chain and a β2-microglobulin molecule). (**e**) The assembly of the MHC molecule is coordinated by ER-resident chaperones, like BiP, Calreticulin and ERp57 and only upon assembly, peptide-loaded MHC complexes can be transported to the cell surface through the Golgi apparatus. (**f**) Cytotoxic T cells (CTLs) are able to recognize the unique peptide, presented by the MHC I molecule at the cell surface, through its T-cell receptors (TCRs) to stimulate its proliferation and killing of the infected target cell. From (Kloetzel, 2001).

Both proteasomes play a vital role in generating peptides for MHC class I antigen presentation through various mechanisms, including proteasome catalyzed peptide splicing (PCPS) (Mishto & Liepe, 2017; Platteel et al., 2017) **(Figure 8)** and defective ribosomal products (DRIPs) (Reits et al., 2000; Schubert et al., 2000; Yewdell et al., 1996) **(Figure 9)**. These peptides are transported from the cytosol into the ER via the transporter associated with antigen processing (TAP) and loaded onto MHC class I molecules (Deverson et al., 1990; Monaco et al., 1990; Parham, 1990; Spies et al., 1990; Trowsdale et al., 1990) which dissociate from the ER and translocate to the cell surface for presentation to CTLs (van de Weijer et al., 2015) **(Figure 8)**. In addition to increased cleavage rate, immunoproteasomes play a crucial role in enhancing peptide supply by improving the clearance of inflammation-

induced DRIPs and inflammation-damaged proteins. This process improves the generation of peptides for MHC class I antigen presentation, thus promoting the efficient initiation of CTL responses directed against viral and bacterial antigens (Fehling et al., 1994; Kincaid et al., 2011; Seifert et al., 2010).

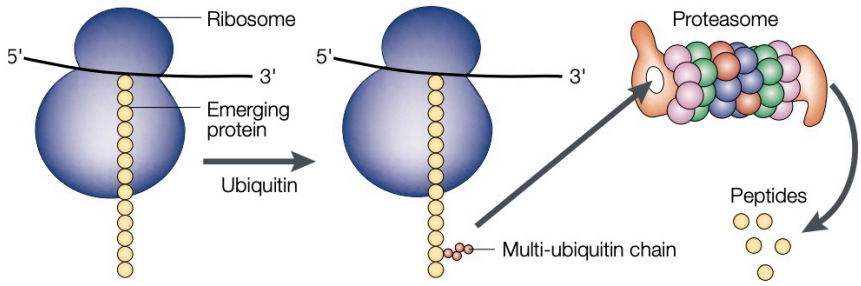

Figure 9. The DRIP model. Due to errors in translation or folding, a large number of newly synthetized proteins are never functional. These deficient proteins, named defective ribosomal products (DRIPs), are rapidly ubiquitinated and degraded by proteasomes, later loaded onto MHC I molecules as illustrated in Figure 8. From (Kloetzel, 2001).

C.2. Autoinflammatory diseases

Proteasome dysfunction has primarily been associated with proteinopathies in the central nervous system and shall be uncovered in the next chapter. It was then unexpected that patients suffering from autoinflammation were found to have genetic alterations in genes that encode proteasome components, like the loss of function mutations. Autoinflammatory disorders are characterized by early-onset fever and organ inflammation, including neuroinflammation (H. Kim et al., 2016), and are referred to as CANDLE/PRAAS (Chronic Atypical Neutrophilic Dermatosis with Lipodystrophy and Elevated temperature / Proteasome Associated Autoinflammatory Syndromes) (Torrelo, 2017; Torrelo et al., 2010). These syndromes have been identified as joint contractures, muscle atrophy, microcytic anaemia, lipodystrophy, immune dysregulation, and so on (Agarwal et al., 2010; Arima et al., 2011; Brehm et al., 2015; Kitamura et al., 2011; Liu et al., 2012). For instance, the mutations in the PSMB8 gene were the first identified in causing CANDLE/PRAAS and encode for the immunoproteasome subunit β5i/LMP7 (Agarwal et al., 2010; Kitamura et al., 2011; Liu et al., 2012). This suggests that CANDLE/PRAAS might be a disease related to immunoproteasome deficiency. Later, other mutations in proteasome and immunoproteasome genes were uncovered, thus proposing that CANDLE/PRAAS were not caused solely by immunoproteasome deficiency (Brehm et al., 2015; de Jesus et al., 2019; Poli et al., 2018; Sarrabay et al., 2020).

On top of genomic alterations, it has been noticed that one of the major consequences leading to CANDLE/PRAAS was a defect in proteasome assembly and an activity leading to the accumulation of ubiquitinated aggregates in cells (Arima et al., 2011; Brehm et al., 2015; de Jesus et al., 2019; Kitamura et al., 2011; Liu et al., 2012; Poli et al., 2018; Sarrabay et al.,

2020). It is worth noting that proteasome loss-of-function mutations do not systematically lead to systemic autoinflammation. In cases of alterations in PSMD12, PSMC3, or PSMB1, patients suffer from neurodevelopmental disorders instead of the typical CANDLE/PRAAS syndromes, and the reason behind these phenotypes require further investigation (Ansar et al., 2020; Kury et al., 2017; Liepe et al., 2018; Wahl et al., 2008).

In addition to proteasome gene alterations, other components of the UPS may also contribute to the activation of inflammatory signalling pathways such as mutations in DUBs leading to NF-κB signalling dysregulation (Beck & Aksentijevich, 2019; Kostura & Mathews, 1989; Rigante, 2020; Wertz et al., 2004) and/or, mutation of the E3 Itch leading to ITCH deficiency (Aki et al., 2018; Bachmaier et al., 2000; Lohr et al., 2010), and so on. And in the long-term, mutations compromise the breakdown of multiple targets in immune cells (Ahmed et al., 2011; Kang & Jeon, 2020; Kathania et al., 2016; Layman et al., 2017; Meuwissen et al., 2016; Theivanthiran et al., 2015; Zhang et al., 2015).

C.3. Neurodegeneration

As mentioned previously, dysregulation in the proteasome has been linked to various diseases. When it fails to destruct misfolded or damaged proteins, it leads to their accumulation which is deleterious for cells. One of the hallmarks of neurodegenerative diseases is characterized by the accumulation of proteins with abnormal shapes that form insoluble aggregates, suggesting the capacity of the cell to prevent protein aggregation declines in ageing (Chondrogianni et al., 2014). Whereas ageing is a multifactorial issue, dysregulation of proteasomal degradation has been associated to it (Chondrogianni et al., 2015; Saez & Vilchez, 2014; Vilchez et al., 2014).

Therefore, there has been a significant effort made to enhance the cellular capacity for protein degradation to slow down the progression of neurodegenerative diseases and ageing. One approach was to boost cellular autophagic capacity through mTOR1 inhibition (Dikic, 2017) since protein aggregates linked to these diseases are often too large for proteasomal destruction. Nevertheless, inhibition of TORC1 resulted in increasing both autophagy and proteasomal degradation (Rousseau & Bertolotti, 2016; Zhao & Goldberg, 2016), making it worth re-evaluating the role of proteasomal degradation in the benefits of TORC1 inhibitors. It is also worth mentioning that the precursors of protein aggregates are proteasome substrates (Bertolotti, 2011), thus providing an interesting idea to control the increase of proteasomal degradation to prevent aggregates of misfolded proteins. Unravelling new nodes of regulation of proteasomal degradation offer unique opportunities to manipulate this system for potential therapeutics, such as inhibitors of the proteasome-associated DUB USP14 (Lee et al., 2010) although their use is controversial (Marshall et al., 2013).

C.4. Cancer

Since ageing is implicated in the development of neurodegenerative diseases, it is also an important risk factor for cancer (Finkel et al., 2007; Lopez-Otin et al., 2013) due to the age-dependent enhancement of genetic mutations (Manasanch & Orlowski, 2017). Some of these mutations cause alteration of protein expression levels and/or imbalance in expression of protein complexes. These changes lead to the accumulation of misfolded or overproduced proteins, thus explaining why cancer cells often rely on high levels of proteasomes. This vulnerability was exploited through the development of proteasome inhibitors to treat some cancers (Grigoreva et al., 2015; Manasanch & Orlowski, 2017).

Bortezomib was the first proteasome inhibitor to be introduced to clinical settings in the treatment of multiple myeloma (Grigoreva et al., 2015; Manasanch & Orlowski, 2017). Whereas the use of proteasome inhibitors has been beneficial, relapses were commonly observed due to the development of resistance to the treatment. Consequently, understanding the mechanisms causing resistance to proteasome inhibitors became a significant research question to address. Interestingly, studies have shown that resistance to proteasome inhibitors increased upon the knockdown of regulatory particle subunits (Acosta-Alvear et al., 2015). As cells adjust proteasome levels to their needs, it is reasonable to assume that they adapt to the reduction of regulatory particle subunits through resistance mechanisms (Op et al., 2022) (see also chapter **VI.A. – Related articles**).

Therefore, disruption of proteasome levels holds a valuable therapeutic strategy, either alone or in conjugation with existing drugs that inhibit the catalytic activity of the proteasome, like the proteasome inhibitor Bortezomib.

D. Regulation of Proteasome levels

Because the generation of the proteasome is energy consuming for the cells, and when compromised, leads to cell death (Navon & Ciechanover, 2009), it is crucial to maintain adequate levels of proteasomes in cells.

To produce and coordinate the correct amount of proteasome subunits, yeasts use the common transcription factor Rpn4 (Mannhaupt et al., 1999; Xie & Varshavsky, 2001). Rpn4 binds the proteasome-associated control element (PACE), a nonameric box located in the promoter regions of most proteasome subunits and some other stress genes (Mannhaupt et al., 1999). Due to rapid proteasomal degradation, Rpn4 has a short half-life which results in its accumulation when proteasomal function is impaired, thus leading to upregulation of proteasome subunits (Xie & Varshavsky, 2001) **(Figure 10)**. Rpn4 expression is also regulated transcriptionally by stress-inducible transcription factors, such as Yap1 or Hsf1,

suggesting that the upregulation of proteasome genes expression may be a common mechanism for cells to adapt to environmental challenges (Ma & Liu, 2010).

In plants, two transcription factors named NAC53 and NAC78 were identified as the main regulators of genes encoding proteasome subunits in response to a proteotoxic stress (Gladman et al., 2016; Nguyen et al., 2013; Yabuta et al., 2010). They are essential for the plant survival to proteasome inhibition, and their physiological pathways may be particularly sensitive to perturbations of this proteasome stress response as they have likely evolved to ensure proteasome homeostasis is adapted to the plant's needs.

Finally, in mammals, two transcription factors were suggested to resemble the function of Rpn4 in yeast: the nuclear factor erythroid 2-related factor 1 (NRF1, also named SKN-1A in yeast) and -related factor 2 (NRF2) (Kwak et al., 2003; Radhakrishnan et al., 2010). Like Rpn4, NRF2 is an unstable protein that becomes stabilized during redox stress to boost proteasome gene expression (Kwak et al., 2003; Taguchi et al., 2011). Although NRF2 was initially thought to increase proteasome subunit expression after proteasome inhibition (Kraft et al., 2006), a later study attributed this role to NRF1 (Radhakrishnan et al., 2010). This last point will be discussed thoroughly in the following chapter along with the role of the DDI2-NRF1 pathway in proteostasis.

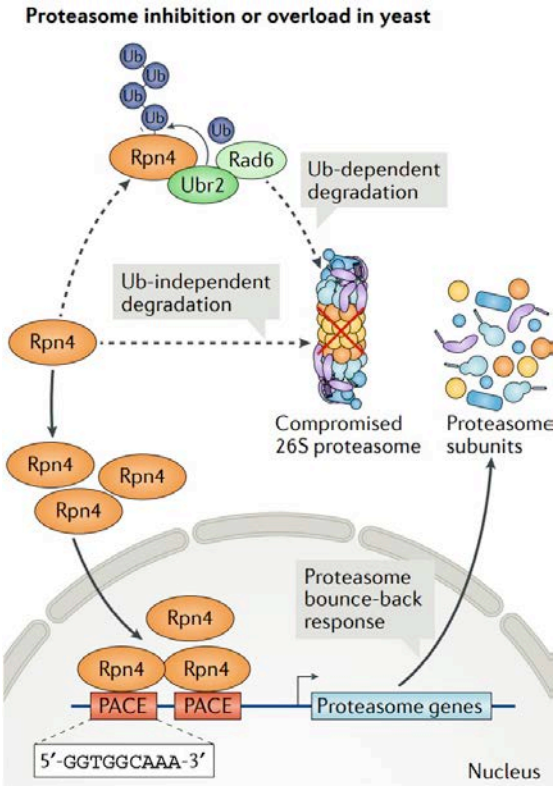

Figure 10. The regulation of proteasome subunits transcription in yeast. Upon physiological conditions, Rpn4 is constantly degraded through dependent or independent ubiquitin-degradation pathways. Upon proteasomal dysregulation, Rpn4 accumulates which permits its stabilization to translocate to the nucleus where it binds the PACE region located in the promoter region of most proteasome subunits and increase their transcription. Adapted from (Rousseau & Bertolotti, 2016).

DDI2-NRF1 pathway: a Sensor of Proteostasis Imbalance

In recent years, emerging evidence of the contribution of the DDI2-NRF1 pathway in cell-stress adaptation, for instance in response to proteasome dysfunction, was established. In mammalian cells, NRF1 is continuously degraded by the proteasome. Upon proteasome impairment, NRF1 escapes degradation and is cleaved into its active form which enables the restoration of proteasome function. Studies in the field have revealed that the aspartyl protease DDI2 is responsible for the proteolytic activation of NRF1 (Koizumi et al., 2016). However, several steps leading to DDI2-mediated NRF1 activation and how DDI2 is activated remain obscure.

In the following paragraph, we will describe thoroughly the distinct features of NRF1 and DDI2 proteins and discuss their importance in sensing proteostasis imbalance.

E. The ER membrane sensor NRF1

The vertebrate genome encodes for three different nuclear factor erythroid 2-like (NRF) transcription factors: NFE2L1/NRF1, NFE2L2/NRF2 and NFE2L3/NRF3 (Chan et al., 1993; Kobayashi et al., 1999; Moi et al., 1994). These genes are strongly conserved across species where they are control stress-responsive gene expression programs (Blackwell et al., 2015; Sykiotis & Bohmann, 2010) **(Figure 11)**. NRFs genes are part of the cap'n'collar (CnC) and basic leucine zipper (bZIP) transcription factor family where they bind to DNA by dimerization with small Maf proteins. NRF/Maf complexes recognize the antioxidant response element (ARE) within DNA sequence motif and act as transcriptional activator (Itoh et al., 1995; Johnsen et al., 1996). Whereas NRF genes resemble in structure and DNA binding mechanisms, they have distinct biological roles (Ibrahim et al., 2020; Liu et al., 2019). Upon oxidative stress, NRF2 is activated and drives antioxidant defences (Ma, 2013), while NRF3 function is not well characterised (Kobayashi, 2020) and NRF1 triggers proteasome subunits genes transcription. In *Caenorhabditis elegans* (*C. elegans*) and *Drosophila melanogaster*, NRFs genes are respectively named SKN-1 and CncC (Blackwell et al., 2015; Sykiotis & Bohmann, 2010) and their functions are similar to the different mammalian NRFs **(Figure 11)**. For instance, both SKN-1C and NRF2 are localised in the cytosol and activate antioxidant adaptation programs (Itoh et al., 1999; Xu et al., 2018). For NRF1, SKN-1A and CncC also regulate the UPS upon cytotoxic stress (Glover-Cutter et al., 2013; Grimberg et al., 2011; Lehrbach & Ruvkun, 2016; Radhakrishnan et al., 2010). Although NRF1 is widely described as a mediator of proteasome inhibitor resistance by increasing proteasome levels (Sha &

Goldberg, 2014), it also promotes protein turnover through alternative pathways such as autophagy, mitophagy, etc. (Cui et al., 2021; Yang et al., 2018). In addition, dysregulation of NRF1 is implicated in various diseases such as metabolic disorders, neurodegenerative disorders, and cancer.

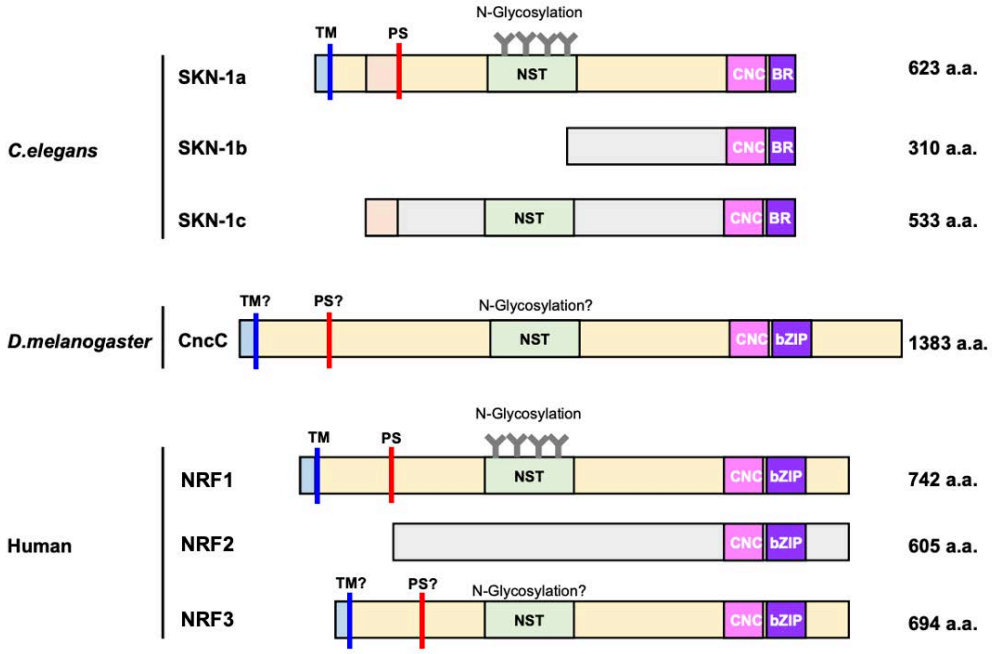

Figure 11. Domain organization of the CnC-bZIP transcription factor family across species. The illustration depicts the structural domains of seven CnC-bZIP proteins (SKN-1A, SKN-1B, SKN-1C, CncC, NRF1, NRF2, and NRF3). NRFs and CncC shares the CnC and the bZIP domain, whereas SKN1 proteins hold a basic leucine domain (BR). Only SKN-1A, CncC, NRF1 and NRF3 present a transmembrane (TM) region, located in their N-terminal domain, to tether proteins to the ER membrane. In addition, except for SKN-1B and NRF2, they all contain an Asn/Ser/Thr-rich (NST) domain targeted by N-glycosylation modification. The red bars represent the processing site (PS). Finally, regions colored in light blue are located in the cytosolic side, whereas regions colored in light yellow are located in the ER lumen. *a.a. stands for amino acids.* From (Hamazaki & Murata, 2020).

E.1. Role in health and diseases

Initially, NRF1 was identified for its role in controlling the expression of antioxidant genes driving the compensatory proteasome biogenesis to cells exposed to proteotoxic stress. More recently, a broader role for NRF1 was introduced in lipid and cholesterol homeostasis as well as an anti-cancer target and in oxidative stress responses.

E.1.1. NRF1 regulates Lipid and Cholesterol Metabolism

Cholesterol surplus in organisms causes the accumulation of glycosylated and non-glycosylated full-length NRF1 in the ER compartment. Structural studies have demonstrated that NRF1 becomes insensitive to cholesterol levels upon deletion of its CRAC (putative

cholesterol binding) domain or its N-terminus ER-targeting domain, thus suggesting that NRF1 binds to excess cholesterol in the ER, which then reduces the efficacy of ERAD retrotranslocation to the cytosol. In mice, liver-specific knockout of NRF1 triggered cholesterol-mediated hypersensitivity, emphasizing the role of NRF1 in cholesterol homeostasis in vivo (Widenmaier et al., 2017). Others have described NRF1 involvement in inflammation, liver pathology, ER stress and increased oxidative stress upon NRF1 deletion in livers (Lee et al., 2013; Xu et al., 2005). Lee and collaborators have even established the role of single NRF1 knock-out allele in mice leading to hepatic steatosis hypersensitivity upon Bortezomib. They have shown how proteasome inhibitors aggravated defects in lipid homeostasis caused by loss of NRF1 (Lee et al., 2013). In addition, deletion of NRF1 in adipocytes induced adipocyte hypertrophy further supporting the hypothesis of NRF1 implication in lipid homeostasis (Hou et al., 2018). The same observations were described in models deficient for the deglycosylating enzyme NGLY1 (Fujihira et al., 2020). Furthermore, evidence in *C. elegans* has established the conserved implication of NRF1 in lipid metabolism. Under high-carbohydrate diet, fat accumulation is prevented by gain-of-function mutations in *SKN-1* (Pang et al., 2014) and *SKN-1* enhances proteasome activity and regulation of lipid metabolism (Steinbaugh et al., 2015).

E.1.2. Physiological roles of NRF1 in Proteasome Biogenesis

NRF1 is essential for embryonic development. Indeed, homozygous deletion of NRF1 in mice is lethal (Chan et al., 1998). Studies about NRF1 disruption in specific tissues, like adipocytes, bone, brain, and liver, have caused abnormalities further cementing the essentiality of NRF1 for normal embryonic development in mammalian tissues (L. Chen et al., 2003; Kim et al., 2010; Kobayashi et al., 2011; Lee et al., 2011; Ohtsuji et al., 2008; Widenmaier et al., 2017; Xu et al., 2005). Most of these defects likely resulted from failed proteasome function. The combination of reduced basal proteasome expression and activity, with increased accumulation of ubiquitinated proteins, is observed in liver or nervous system tissues upon specific-NRF1 depletion (Kobayashi et al., 2011; Lee et al., 2013; Lee et al., 2011). Similar observations are described in *Drosophila* and *C. elegans* (Grimberg et al., 2011; Lehrbach et al., 2019; Li et al., 2011). Obviously, all evidence points towards a role for NRF1 in optimizing proteasome levels in physiological conditions and not solely in response to environmental stress. However, which endogenous signals influence NRF1 to regulate proteasome levels?

Several lines of evidence have highlighted NRF1 as a downstream target of mTORC1 which, upon activation, promotes transcription of the transcription factor (Zhang, Nicholatos, et al., 2014). Similarly, in *C. elegans* the extracellular regulated kinases, ERK1 and ERK2, were identified by genetic screening to be essential in promoting proteasome gene expression

through the action of SKN-1A (Zhang, 2021). Moreover, studies published on the role of the cytosolic O-linked N-acetylglucosamine transferase (OGT), have revealed its direct impact on proteasome regulation via modification of NRF1 (Chen et al., 2015; Han et al., 2017; Sekine et al., 2018). Overall, the regulation of SKN-1A/NRF1 through these different actors influences positively protein quality control at different states of the cell cycle.

In addition, NRF1 regulates the proteasome in response to accumulation of misfolded proteins and protein aggregates. This NRF1 function is greatly illustrated by the neurodegenerative disease, Alzheimer's disease, where the accumulation of amyloid β peptide is described as one of the main causes leading to the development the disease. In 2019, Lehrbach and Ruvkun have shown that accumulation of amyloid β in *C. elegans* led to the activation of proteasome gene subunit expression through SKN-1A (Lehrbach & Ruvkun, 2019). They further demonstrated that activation of the proteasome in this context relied on the same mechanisms as in response to proteasome inhibition. Whereas the mechanism prompting NRF1 degradation remains unclear, SKN-1A activation was directly linked to proteostasis maintenance through degradation of misfolded proteins preventing age-dependent aggregation and toxicity of amyloid β peptide. Studies in the mouse brain have further shown how NRF silencing could drive neurodegeneration and accumulation of ubiquitinated protein aggregates (Kobayashi et al., 2011; Lee et al., 2011). Again, NGLY1 deficiency in humans and rodents is also correlated with neurodegenerative symptoms and formation of protein aggregates (Asahina et al., 2020; Lam et al., 2017; Mueller et al., 2020).

E.1.3. Physiological roles of NRF1 *in vivo*

To study the significance of NRF1 *in vivo*, scientific laboratories have developed an important number of mouse models. Both genetic loss and gain-of-function mutations in mice have clearly established that the dysregulation of NRF1 led to pathological states observed in human diseases.

First, the NRF1 knock-out mouse model is embryonic lethal. This observation results from impaired foetal liver erythropoiesis (Chan et al., 1998). In consistency with this observation, Chen and others have described the essentiality of NRF1 in controlling hepatocyte homeostasis during development in mouse chimeras (L. Chen et al., 2003). Moreover, tissue-specific knock-out of NRF1 in hepatocytes have led to steatosis, inflammation, and tumorigenesis (Xu et al., 2005). Although the mechanisms driving these pathologic states remain unclear, NRF1-deficient hepatocytes display both oxidative and ER stress profiles (Lee et al., 2013; Ohtsuji et al., 2008; Xu et al., 2005). Interestingly, liver-specific NRF1 knock-out models raise its potential to study NRF1 physiological role in ER stress responses and liver diseases. Recently, studies in both human hepatocytes and mouse have established a role for NRF1 in triggering heavy metal detoxification through the restoration of proteasome

function upon Cadmium exposure (Ribeiro et al., 2022). Cadmium is an environmentally present toxic heavy metal exhibiting cytotoxic and carcinogenic effects. This study has outlined the importance of NRF1 in proteostasis maintenance to heavy metal mediated toxicity.

Moreover, NRF1 is implicated in neuronal homeostasis. Using Cam-K2 Cre transgenic mouse, researchers have developed neuron-specific conditional knock-out for NRF1. Upon NRF1-deficiency, they observed the development of age-dependent forebrain atrophy (Lee et al., 2011). Besides the neurodegenerative phenotype, the brain of these mice exhibited ubiquitinated protein accumulation and apoptosis. Another study led by Kobayashi in 2011 has revealed the role of NRF1 in neuronal and glial precursor cells. They generated NRF1-deficient neurons using Nestin-Cre system in mouse which led to motor ataxia, neurodegeneration and chromatolysis in the spinal cord (Kobayashi et al., 2011).

Additionally, gene expression studies have suggested a role for NRF1 in osteoblast homeostasis. Osteoblast-specific conditional NRF1 knock-out leads to decrease in bone size, peak bone mass, trabecular bone, and bone strength (Kim et al., 2010). NRF1 is also implicated in glucose metabolism. In a genome-wide association study (GWAS), a single nucleotide polymorphism in human NRF1 was directly associated to obesity (Speliotes et al., 2010). Paradoxically, overexpression of NRF1 in transgenic mice appears to be associated with weight loss and protection from diet-induced obesity. In addition, these transgenic mice exhibited insulin resistance profiles in liver and skeletal muscle (Hirotsu et al., 2014). Surprisingly, the NRF1 loss-of-function in pancreatic β cells is also associated with insulin resistance. Mice deficient for NRF1 in pancreatic β cells develop glucose intolerance and severe hyperinsulinemia, suggesting a role of NRF1 in the development of type-2 diabetes.

E.1.4. NRF1 in Cancer

The use of proteasome inhibitors in cancer treatment is of high relevance. Like in multiple myeloma, proteasome inhibitors challenge the proteasome capacity, but their utility is limited to cell-elicited resistance mechanisms (Wallington-Beddoe et al., 2018). The necessity to recruit NRF1 in response to proteasome dysfunction suggests it is a promising pharmacological target to enhance the drugs' efficiency. Genetic analysis in *C. elegans* has demonstrated the essential role of deglycosylation by NGLY1/PNG-1 of SKN-1A/NRF1 in response to proteasome impairment (Lehrbach et al., 2019). Additionally, recent studies in multiple myeloma models have demonstrated a role for the protease DDI2 in driving adaptation program to proteasome inhibition through the activation of NRF1 (Op et al., 2022).

E.2. Regulation and Mechanism of Activation

E.2.1. in the ER

The full-length precursor protein of NRF1 possesses an N-terminal transmembrane domain enabling its insertion in the ER via the Sec61-dependent pathway (Glover-Cutter et al., 2013; Steffen et al., 2010; Zhang et al., 2006). In the ER, the bulk of NRF1 polypeptide until the C-terminal domain resides in the ER lumen whereas a small portion of the N-terminus is protruding into the cytosol (Radhakrishnan et al., 2014; Wang & Chan, 2006; Zhang & Hayes, 2010). NRF1 then undergoes N-linked glycosylation which adds around 10 to 15 kDa to its size. At steady-state and following N-glycosylation, NRF1 is subjected to ER-associated degradation (ERAD) to return to the cytosol where it is degraded by proteasomes. ERAD is a very well described pathway specialized in ER misfolded proteins turnover (Sun & Brodsky, 2019; Wu & Rapoport, 2018). ERAD-dependent degradation of NRF1 involves the action of the ER-associated E3 ubiquitin ligase HRD1 and the extraction from the ER by p97 (also known as valosin containing protein "VCP") (Radhakrishnan et al., 2014; Steffen et al., 2010). Under proteotoxic stress or proteasome inhibition, following retrotranslocation through ERAD, NRF1 is processed in the cytosol **(Figure 12)**.

E.2.2. in the Cytosol

Proteolytic activation by DDI2

When cells are deficient for proteasome function, NRF1 is proteolytically cleaved into a different isoform. The cleavage removes around 100 amino acids from the N-terminus of the protein (Radhakrishnan et al., 2014). In *C. elegans*, SKN-1A is similarly cleaved which removes around 150 amino acids from its N-terminus (Lehrbach & Ruvkun, 2016). The truncated form of SKN-1A generated following its cleavage is capable of inducing proteasome gene expression to cope with proteasome impairment. In human and *C. elegans*, this proteolytic cleavage relies on a conserved aspartic protease named DDI2 and Ddi1 respectively (Koizumi et al., 2016; Lehrbach & Ruvkun, 2016) **(Figure 12)**. Studies have reported that when DDI2 or Ddi1 is deficient in cells, NRF1/SKN-1A remains uncleaved and fails to restore the proteasome function. However, the requirement of DDI2 in generating an active truncated NRF1 is not fully understood. Others have suggested that DDI2 is essential to release NRF1 from the ER in some cell types (Koizumi et al., 2016) but it was not conserved in *C. elegans* studies and other human cells (Lehrbach & Ruvkun, 2016; Northrop et al., 2020). NRF1 was released from the ER in its full-length form and detected in the nucleus whereas it was defective in stimulating proteasome gene expression. Moreover,

observations in *C. elegans* have suggested that Ddi1 deficiency was linked to the accumulation of NRF1 aggregates (Lehrbach & Ruvkun, 2016).

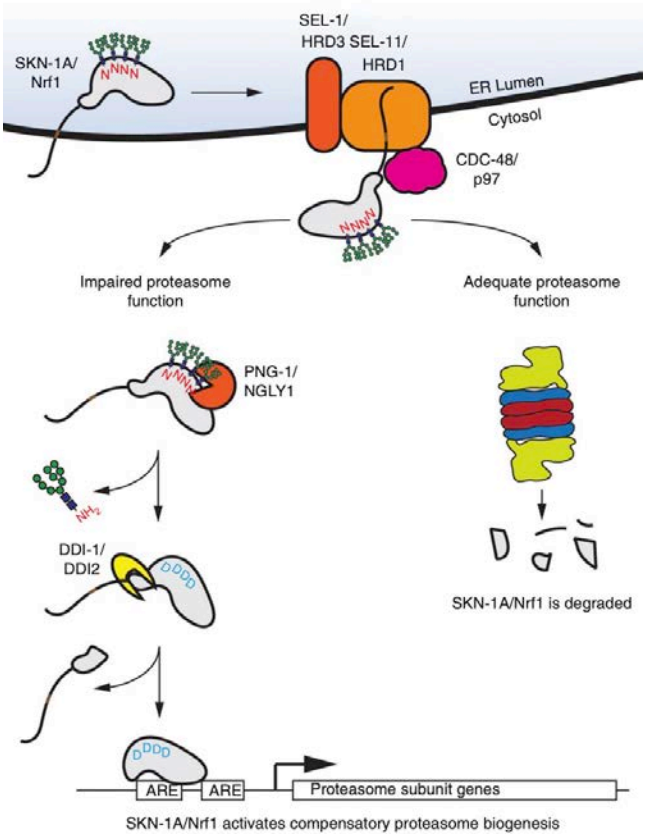

Figure 12. SKN-1A/NRF1 mechanism of activation upon proteasomal impairment. SKN-1A/NRF1 is an ER-associated protein with its N-terminal transmembrane region anchored to the ER membrane. In the ER, SKN-1A/NRF1 undergoes N-linked glycosylation. Glycosylated SKN-1a/NRF1 is then retrotranslocated from the ER via the ERAD machinery composed of SEL-1 and HRD1 factors. In addition to ERAD factors, SKN-1A/NRF1 is pulled-out from the ER via the ATPase VCP/p97 (also named CDC-48) through ATP hydrolysis. In cells with full proteasomal capacity, cytosolic SKN-1A/NRF1 is degraded by the proteasome. In cells with altered proteasome function, SKN-1A/NRF1 undergoes deglycosylation by the peptide:N-glycanase PNG-1/NGLY1 and proteolytic cleavage by Ddi1/DDI2. In this model, removal of N-glycans implies that N-glycosylated asparagines (N) are converted into aspartates (D). Proteolytically processed and edited SKN-1A/NRF1 finally enters the nucleus and binds ARE regions of proteasome subunits genes and other target genes. From (Ruvkun & Lehrbach, 2022).

Deglycosylation and Deamination by NGLY1/PNG-1

NRF1 contains seven N-glycosylation motifs (N-X-S/T) localised in its central asparagine/serine/threonine-rich domain (NST) (Zhang, Ren, et al., 2014). Since NRF1 is cotranslationally inserted into the ER, it is likely that these N-linked glycosylations occur sequentially (Yoshida et al., 2021; Zhang & Hayes, 2013; Zhang, Ren, et al., 2014). In 2019, Lehrbach and collaborators have characterized the deglycosylation-dependent mechanism of SKN-1A protein editing in *C. elegans*. In this model, SKN-1A holds a cluster of four N-linked glycosylation motifs similarly positioned as in human. The study has described the

importance of deglycosylation and deamination of the four asparagine residues into aspartic acids by the N-glycanase PNG-1 to destine SKN-1A to upregulate proteasome gene expression (Lehrbach et al., 2019; Yoshida et al., 2021; Zhang, Ren, et al., 2014). Conversely, N-glycosylation is not required to destine NRF1 for ERAD degradation, nor to accumulate into its active form in the nucleus upon proteasomal dysfunction.

The N-glycanase, termed NGLY1 in mammals and PNG-1 in *C. elegans*, is a cytosolic enzyme responsible for the deglycosylation of ERAD substrates following their retrotranslocation and prior to their degradation by the proteasome (Suzuki et al., 2016) **(Figure 12)**. In cellular model lacking the expression of this N-glycanase, both NRF1 and SKN-1A respectively fail to activate proteasome gene expression (Lehrbach & Ruvkun, 2016; Tomlin et al., 2017). The action of this enzyme consists in a coupled reaction combining the release of the N-linked glycan and the conversion of the glycosylation asparagine into an aspartic acid (Suzuki et al., 1994). NRF1/SKN-1A, engineered with the mutation of the N-linked glycosylation motifs into aspartic acids, is functionally competent and bypasses the requirement of NGLY1/PNG-1 for modulation of proteasome gene (Lehrbach et al., 2019; Yoshida et al., 2021). Interestingly, endogenous genomic mutations to bypass the requirement of NGLY1 are observed in phylogenetic comparisons of NRF1 in both human and *C. elegans* (Lehrbach et al., 2019; Ruvkun, 2021).

E.2.3. in the Nucleus

Upon entry into the nucleus in its active and processed form, NRF1 regulation is carried out by various factors. The earliest regulators implicated are small MAF (MafF, MafG and MafK) cofactors harbouring a bZIP domain, just as NRF1 (Johnsen et al., 1996; H. M. Kim et al., 2016). Through this domain, NRF1/small Maf heterodimerizes to bind the antioxidant response element (ARE) located upstream of proteasome genes or other target genes. More recently, another cofactor was identified to be implicated in NRF1 transcriptional activation upon proteasome inhibition and is named the RUVBL1-containing TIP60 chromatin regulatory complex (Vangala & Radhakrishnan, 2019). In the nucleus, NRF1 protein levels are also prone to several regulation processes. NRF1 is regulated by two Cullin-RING ubiquitin ligases (Biswas et al., 2013; Biswas et al., 2011; Tsuchiya et al., 2011b) and is also subject to regulation by phosphorylation and O-linked glycosylation (Chen et al., 2015). However, the regulatory effect of O-GlcNAcylation on NRF1 remains unclear due to discordant results in published studies (Han et al., 2017; Sekine et al., 2018). Casein kinase 2-mediated phosphorylation of NRF1 at residue Ser-497 has been shown to decrease its transcriptional activity, but the precise mechanism behind this effect is still unknown (Tsuchiya et al., 2013). The cellular location of the CK2-mediated phosphorylation event also remains elusive (Faust & Montenarh, 2000; Litchfield, 2003).

F. The aspartyl protease DDI2

The DNA-damage inducible 1 homolog 2 (DDI2) protein is an aspartic protease containing a retroviral protease-like (RVP) domain and highly conserved among eukaryotes (Perteguer et al., 2013; Siva et al., 2016a). DDI2 is ubiquitously expressed and is involved in cell stress response. However, function, regulation and molecular mechanisms driving DDI2 activity are poorly understood. Recent research conducted in *C. elegans*, yeast, and human cells have demonstrated a role for DDI2 in regulating proteasome activity to sustain protein homeostasis (Koizumi et al., 2016; Lehrbach & Ruvkun, 2016) as well as in response to cell stress during DNA replication (Kottemann et al., 2018; Serbyn et al., 2020).

F.1. Structure and Function

Aspartic proteases differ from retroviral proteases, like the HIV-1 protease (Kohl et al., 1988), in size and structure but are part of the pepsin-like family and are believed to be evolutionarily related due to homologous active site loops and the similar localisation of aspartic residues at a domain interface (Navia et al., 1989; Richter et al., 1998; Wlodawer et al., 1989). A family of eukaryotic proteins harbouring structural and sequence similarity to retroviral proteases has been characterised by the presence of a retroviral protease-like (RVP) domain with every feature of retroviral proteases conserved. (Krylov & Koonin, 2001) **(Figure 13)**.

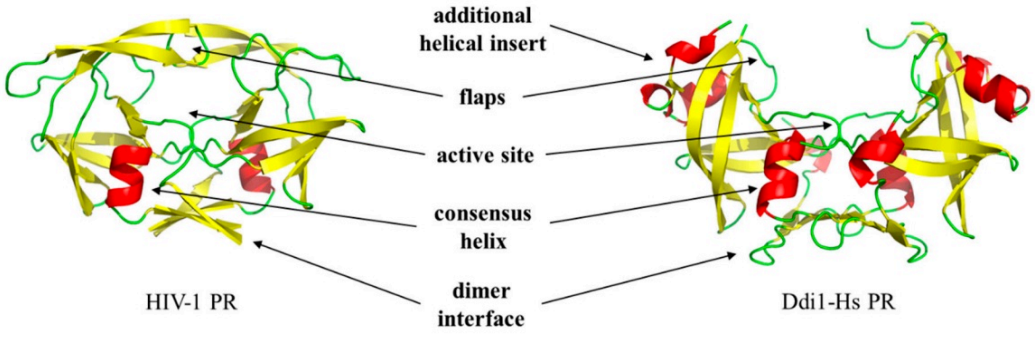

Figure 13. Structural comparison between human HIV-1 and Ddi1 proteases. Retroviral (HIV) and DNA damage inducible (Ddi) proteins shares homology structure. The arrows underline the important regions, with exception for the additional α-helical insert, which are known to contribute to dimerization. From (Motyan et al., 2020).

Several proteases have been described with an RVP domain. Among them, Ddi1 is one of the most studied and is conserved across species, from *S. pombe*, *Leishmania* species, *A. thaliana*, *S. cerevisiae*, *D. melanogaster*, up to mammals (Fatimababy et al., 2010; Liu & Xiao, 1997; Morawe et al., 2011; White et al., 2011; Wilkinson et al., 2001). More recently, by multiple sequence alignments using yeast Ddi1 as a model, we have expanded our knowledge of human RVP-like proteins. Among them are described the yeast orthologs Ddi1 and DDI2.

Evidence have shown that Ddi1 is expressed at low levels almost exclusively in testis, which suggests it to status as a pseudogene (Sirkis et al., 2006). Conversely, DDI2 appears to be expressed at higher levels than Ddi1 in human in a variety of tissues, especially in the bladder, prostate, and breast. Structurally, both Ddi1 and DDI2 hold a N-terminal ubiquitin-like (UBL) domain whereas in C-terminal, DDI2 lacks the ubiquitin-associated (UBA) domain described in its yeast ortholog. Indeed, in human C-terminal DDI2 we find a ubiquitin-interacting motif (UIM) which is described to bind weakly but specifically to mono-ubiquitinated substrates (Siva et al., 2016a) whereas the N-terminal ubiquitin fold interacts with large ubiquitylated proteins (Collins et al., 2022). Moreover, human DDI2 along with RAD23 proteins have been identified in a large-scale pull-down study of proteins interacting with proteasomes (Bousquet-Dubouch et al., 2009).

More recently and as mentioned earlier, mammalian DDI2 studies have demonstrated its role in mediating NRF1 proteolytic activation (Koizumi et al., 2016). Additionally, biochemical analysis has further suggested that purified DDI2 in presence of RAD23 co-factors promoted the cleavage of ubiquitylated substrates, including NRF1 (Dirac-Svejstrup et al., 2020b). Also, the protease was characterised to potentialize the upregulation of proteasome activity (Collins & Goldberg, 2020; Collins et al., 2022).

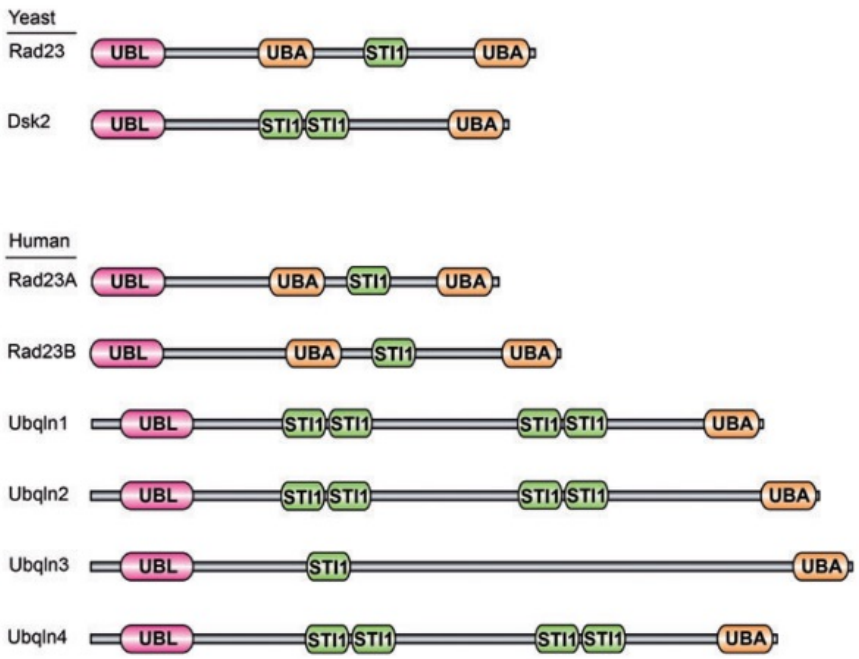

Figure 14. Schematic representations of ubiquilin proteins in yeast and mammal. Yeast Dsk2 and its mammalian orthologs Ubqln1, Ubqln2, Ubqln3, and Ubqln4, present an N-terminal UBL domain, multiple STI1 domains in their central region, and a C-terminal UBA domain. Yeast Rad23 and its mammalian orthologs Rad23A and Rad23B, have an N-terminal UBL domain, one UBA and one STI1 domain in their central region, and a C-terminal UBA domain. UBL: ubiquitin-like; UBA: ubiquitin-associated; STI1: heat shock chaperone-binding. From (Lee & Brown, 2012).

Whereas the role of DDI2 as a protease cleaving NRF1 was recently established, the involvement of RAD23 therein remained elusive. It is known that RAD23 proteins and other ubiquilins **(Figure 14)** are shuttling factors involved in protein degradation, and more recently connected to ERAD (Medicherla et al., 2004). RAD23 proteins are also able to activate proteasomes upon binding with the 26S particle (Collins & Goldberg, 2020; Kim & Goldberg, 2018). In addition, studies demonstrated that yeast Rad23 and Ddi1 can form a complex (Bertolaet et al., 2001a) furthermore supporting the hypothesis of RAD23 requirement to enable DDI2 proteolytic activity.

F.2. Physiological role in mice

Although the transcription factor NRF1 was characterized *in vivo*, as discussed earlier in the study, it remained to be investigated for its activating partner DDI2. This study was led in our laboratory (see chapter **VI.B. – Related articles**) to shed light on the DDI2-associated molecular mechanisms and physiological functions (Ribeiro et al., 2022).

To test the involvement of DDI2 in cell stress response, Cadmium (Cd) was used to trigger toxicity. Cd is a toxic heavy metal widely present in our environment and capable of triggering both cytotoxic and carcinogenic effects in mice and humans. Furthermore, studies have demonstrated that Cd can cause accumulation of ubiquitinated proteins, thus disrupting the UPS and ultimately resulting in apoptosis of both mouse and human cells (Figueiredo-Pereira et al., 1997; Yu et al., 2011). Moreover, the deletion of NRF1 gene in mouse liver was described to impair the expression of Mt1 and Mt2 genes (Ohtsuji et al., 2008) which encode for cysteine-rich and metal-binding proteins associated with metal-ions chelation and detoxification to Cadmium and Arsenic (Habeebu et al., 2000; Klaassen et al., 2009; Ohtsuji et al., 2008; Wang et al., 2020; Zhao et al., 2011). Finally, the mouse model reported in the study is using a liver specific DDI2 knockout.

The results establish that, upon Cd exposure, mice exhibited DDI2-mediated NRF1 activation and regulation of MT gene expression. In contrast, DDI2 deficiency affected the expression of proteasome subunits. However, the activation of MT genes is not exclusively controlled by DDI2 and/or NRF1 (Sabolic et al., 2010). In addition, the study uncovers the requirement of DDI2 for normal embryonic development where total DDI2 knockout mice die at mid-gestational stage, whereas lethality is not increase in liver specific DDI2 knockout upon Cd.

In conclusion, DDI2 *in vivo* is required for normal embryonic development and is involved in response to heavy metal mediated toxicity. Whereas DDI2 causing lethality at embryonic level can be compared to NRF1-deficient mice, additional investigations are essential to understand the cause(s) of death.

F.3. DDI2-NRF1, a promising anti-Cancer target

Although NRF1 was linked to different neuronal dysfunction or diabetes, the role of NRF1 when activated by the protease DDI2 remains to be characterised. In addition, among several tumorigenic cell lines, from leukaemia to skin cancer, cells are sensitive to NGLY1 deficiency as well as to NRF1 loss-of-function or to the aspartyl protease DDI2 responsible for NRF1 activation. In the Cancer Dependency Map, there are no other genes than NRF1 and/or DDI2 correlating to the necessity of NGLY1. Most of the cancer cells relying of NGLY1/NRF1/DDI2 are proliferating and present diverse oncogenic mutations. But how is proteostasis linked to the proliferation of these cancer cells? One hypothesis is that cancers elicit NRF1 constitutive activity to cope with mutations effects, thus leading to the disruption of proteostasis.

Recently, our laboratory and others, have unravelled a role for the DDI2-NRF1 pathway in mediating adaptation to proteasome inhibition in multiple myeloma (Op et al., 2022) (see chapter **VI.A. – Related articles**).

To explore the involvement of DDI2-NRF1 pathway, the proteasome inhibitor Bortezomib was used to trigger cytotoxic effect and specific resistance observed in multiple myeloma patients. The study has revealed that DDI2-deficient cells were more sensitive to Btz treatment which has underlined consistently other studies where defect in the proteasome function is observed in absence of DDI2 (Northrop et al., 2020). Furthermore, the activation of NRF1 by DDI2 contributes to the development of Btz resistance by triggering a proteasome bounce-back response which enhances proteostasis. Interestingly, Nelfinavir (NFV), a drug originally designed to target HIV protease, partially reduces DDI2 activity and improves the effectiveness of Btz in multiple myeloma. These observations were supported by promising clinical evidence showing that NFV restores sensitivity of multiple myeloma patients that are refractory to proteasome inhibition (Driessen et al., 2018; Erath et al., 2020; Hitz et al., 2019). Although, it is worth noting that NFV has additional effects on translation mechanisms that contribute to its antitumoral properties (Besse et al., 2021; De Gassart, Bujisic, et al., 2016; De Gassart, Demaria, et al., 2016). Based on this work, developing targeted DDI2 inhibitors in conjugation with proteasome inhibitors holds the potential to offer novel therapeutic approaches for multiple myeloma.

Altogether, NGLY1, NRF1 and DDI2 are represented as attractive targets for cancer therapies.

Aim of the Thesis

The focus of this thesis lies on the atypical DDI2-NRF1 signaling pathway through the characterization of the underlying mechanisms driving NRF1 activation upon proteasomal dysregulation. NRF1 transcriptional activity is preceded by ER retrotranslocation, accumulation in the cytosol, cleavage by DDI2 and entry in the nucleus to induce proteasome gene expression.

Although much progress has been made on the mechanical insight of DDI2-mediated NRF1 activation prior to and during my thesis, the regulation of NRF1 cleavage in terms of post-translational modifications and the outcome of cleaved NRF1 in other cellular programs than proteasome regulation, was unclear.

Thus, to shed light on these mechanisms, this thesis aimed at answering the following questions:

- Is ER-trafficking involved in NRF1 cleavage by DDI2?
- What NRF1 posttranslational modifications are involved in DDI2-mediated cleavage?
- How is DDI2 activated, and does it directly interact with NRF1?
- Is DDI2-mediated NRF1 cleavage required for NRF1 function?

Given that cancers like multiple myeloma and some autoinflammatory diseases are characterized by a defect in proteasome function, a detailed view of this pathway is crucial for the understanding of these pathologies and critical for future drug development.

II. RESULTS

Research Article: ER-trafficking triggers NRF1 ubiquitination to promote its proteolytic activation

Submitted manuscript

Claire Chavarria[1], Léa Zaffalon[1], Sérgio T. Ribeiro[1], Mélanie Op[1], Manfredo Quadroni[2], Maria Sofia Iatrou[1], Chloé Chapuis[1] and Fabio Martinon[1]

Affiliations:

[1]Department of Immunobiology, University of Lausanne, 155 Ch. des Boveresses, 1066, Epalinges, Switzerland

[2]Protein Analysis Facility (PAF), Center for Integrative Genomics, University of Lausanne, Lausanne 1015, Switzerland

Statement of contribution:

I designed the study together with Fabio Martinon. I conducted the experiments and downstream analysis of the study. The SDS-PAGE and mass spectrometry analysis were carried out by Manfredo Quadroni (PAF). The RNA-seq analysis was carried out by the genomic technologies facility (GTF). Léa Zaffalon performed multiple experiments related to RAD23 characterisation. Chloé Chapuis and Léa Zaffalon participated to generate plasmids. Sérgio T. Ribeiro and Mélanie Op participated in experimental design. Maria S. Iatrou generated Figure 16A. Subsequent data analysis were performed together with Fabio Martinon.

A. Summary

In this project we set out to interrogate the different biological mechanisms involved upstream of NRF1 cleavage by DDI2 and their impact on NRF1 activation.

Firstly, we aimed at investigating additional NRF1 subcellular localization and its consequence on the cleavage by DDI2. In particular, we investigated whether ER-trafficking and retrotranslocation into the cytosol were mandatory for DDI2 to execute NRF1 cleavage. Since upon ER stress, misfolded proteins are tagged to be retrotranslocated to the cytosol and degraded by the proteasome e.g. via the ERAD pathway, a mechanism proposed to lead to misfolded proteins degradation (Pisoni & Molinari, 2016), we wondered whether ERAD was implicated in the translocation of ER-associated proteins destined for transcriptional activation. To answer this question, we intended, as a first step to examine NRF1 cleavage upon ER-trafficking, or not. And, in a second step explore the extent and role of this trafficking on NRF1 transcriptional activity.

In addition, we set out to examine NRF1 post-translational modifications. Previous literature, in particular HRD1/p97-mediated ubiquitination of ERAD substrates, indicated a role for ubiquitination to target misfolded proteins for proteasomal degradation (Ye et al., 2001). While previous literature *in vitro* shows that DDI2 is a ubiquitin-directed endoprotease (Dirac-Svejstrup et al., 2020b), it is unclear whether NRF1 requires ubiquitination to be cleaved into its active form.

Moreover, while we were not able to develop an *in vitro* assay to study DDI2 activity, we focused on the nature of the relationship between NRF1 and DDI2. As previous *in vitro* studies observed, DDI2-mediated NRF1 cleavage relied on the presence of a co-factor molecule called RAD23 (Dirac-Svejstrup et al., 2020b). This part is split into characterization of the interaction of DDI2 and NRF1 and the exploration of the role of RAD23 in this process.

Finally, the last part is dedicated to NRF1 activity. Research in the last years has made pretty clear the role of NRF1 as a master regulator of proteasome gene expression. Thus, we set out to understand the potential role of DDI2 in regulating proteasomal programs through NRF1 activation and further investigate other DDI2-dependent cellular programs and their role in disease.

A.1. Abstract

The transcription factor NRF1 resides in the endoplasmic reticulum (ER) and is constantly transported to the cytosol for proteasomal degradation. However, when the proteasome is defective, NRF1 escapes degradation and undergoes proteolytic cleavage by the protease DDI2, generating a transcriptionally active form that restores proteostasis, including proteasome function. The mechanisms that regulate NRF1 proteolytic activation and transcriptional potential remain poorly understood. This study demonstrates that the ER is a crucial regulator of NRF1 function by orchestrating its ubiquitination through the E3 ubiquitin ligase HRD1. We show that HRD1-mediated NRF1 ubiquitination is necessary for DDI2-mediated processing in cells. Furthermore, we found that deficiency in both RAD23A and RAD23B impaired DDI2-mediated NRF1 processing, indicating that these genes are essential components of the DDI2 proteolytic machinery. Our findings highlight the intricate mechanism by which the ER activates NRF1 to coordinate the transcriptional activity of an adaptation response in cells and suggest potential avenues for therapeutic interventions in conditions associated with proteasome impairment.

A.2. Introduction

The endoplasmic reticulum (ER) is an organelle conserved in eukaryotes that plays a crucial role in protein synthesis, folding, and trafficking, as well as in other essential cellular functions, such as lipid synthesis, calcium storage, and carbohydrate metabolism (Lynes & Simmen, 2011; Sitia & Meldolesi, 1992). Moreover, the ER serves as a gateway to the degradation pathway by targeting misfolded proteins for degradation through the ubiquitin-proteasome system (UPS) (Christianson & Ye, 2014). This process is known as the ER-associated degradation (ERAD) pathway, whereby misfolded proteins are extracted from the ER lumen and retrotranslocated into the cytosol for degradation (Olzmann et al., 2013).

Considered a central protein folding hub, the ER governs the modifications, structural maturation, and targeted transportation of over one-third of the cellular proteome, including all proteins embedded in membranes or those retained in specific cellular compartments or released extracellularly (Stevenson et al., 2016). Furthermore, recent evidence suggests that the ER may also be involved in the posttranslational modifications of at least one cytosolic protein, the Cap'n'Collar (CnC) basic leucine zipper (bZIP) transcription factor NFE2L1, also known as NRF1 (Ruvkun & Lehrbach, 2022). In *C. elegans*, the homolog of NRF1, SKN-1A, undergoes N-glycosylation within the ER lumen. In the cytosol, the glycosylated asparagine residues are processed, and the asparagine amino acids edited into aspartic acid residues (Lehrbach et al., 2019). This amino acid change is required to unleash NRF1 transcriptional activity (Lehrbach et al., 2019).

The transcription factor NRF1 regulates genes associated with inflammation, oxidative stress response, and other cellular processes in mammals. It does so via the antioxidant response element (ARE) or the Maf recognition element (MARE) (Motohashi et al., 2002). Similar to its homolog NRF2, which initiates an appropriate adaptation response to oxidative stress (Tebay et al., 2015), NRF1 can detect various insults and trigger specific transcriptional programs. For example, NRF1 is activated as a response to proteasome impairment to restore proteasomal activity by promoting the transcription of proteasome subunit genes (Radhakrishnan et al., 2014; Radhakrishnan et al., 2010; Roeten et al., 2018). Furthermore, inhibition of NRF1 activation has been shown to increases the susceptibility of Multiple Myeloma to proteasome inhibitor-based chemotherapy (Chen et al., 2022; Collins & Goldberg, 2020; Dirac-Svejstrup et al., 2020a; Op et al., 2022). Moreover, NRF1 has been shown to be involved in the physiological response to pollutants such as cadmium (Ribeiro et al., 2022).

The stability and proteolytic maturation of the NRF1 protein are crucial steps in controlling its activation as observed upon proteasome system impairment (Steffen et al., 2010; Tsuchiya et al., 2011a). Conversely, proteasome inhibition allows NRF1 to escape degradation and orchestrate the transcriptional response that restores proteasome homeostasis (Radhakrishnan et al., 2014; Radhakrishnan et al., 2010).

Another critical step that controls NRF1 activity relies on its proteolytic maturation, which requires the protease DDI2 (Koizumi et al., 2016; Lehrbach & Ruvkun, 2016). However, the mechanisms by which DDI2 contributes to this process are poorly understood. Biochemical experiments have suggested that purified DDI2 could promote the cleavage of high molecular weight ubiquitinated substrates, including NRF1 (Dirac-Svejstrup et al., 2020a). The aspartic protease DDI2 can increase proteasome activity (Collins & Goldberg, 2020; Collins et al., 2022) and may bind substrates via ubiquitin chains through its ubiquitin-interacting motif (UIM) and ubiquitin-like domain (UBL) (Collins et al., 2022; Siva et al., 2016b).

While NRF1 cleavage has been proposed to require ubiquitination (Sha & Goldberg, 2014, 2016), cellular experiments have shown that DDI2's UBL and UIM are dispensable for NRF1 maturation (Op et al., 2022). This suggests that other domains, including the helical domain (HDD), may be involved in this process. Moreover, evidence in yeast indicates that DDI2 homologs interact with RAD23 proteins through their respective ubiquitin-associated (UBA) domains (Bertolaet et al., 2001a). In humans, DDI2 lacks the UBA domain; however, *in vitro*, RAD23 has been shown to enhance DDI2 proteolytic activity (Dirac-Svejstrup et al., 2020a), suggesting that UBL-harboring proteins may cooperate to trigger NRF1 activation in humans. NRF1 activation also requires p97/VCP, a component of the endoplasmic reticulum (ER) retrotranslocation machinery (Radhakrishnan et al., 2014; Steffen et al., 2010). This machinery is involved in the transport of misfolded proteins into the cytosol for degradation, suggesting that trafficking to the ER and subsequent retrotranslocation of NRF1 could precede maturation by cytosolic DDI2.

In this study, we show that ER trafficking function is to tag NRF1 protein for DDI2-mediated proteolytic maturation. Mechanistically, we describe that this process is independent of glycosylation and relies on NRF1 ubiquitination by the E3-ligase HRD1-mediated. The role of NRF1 ubiquitination is also supported by the observation that UBA-harboring RAD23 proteins are required for DDI2-mediated NRF1 activation. Additionally, we demonstrate that ER-dependent glycosylation in human cells plays a DDI2-independent role in promoting the transcriptional activity of NRF1. Moreover, we show that DDI2-mediated cleavage affects the transcriptional program induced by NRF1 but is not required for NRF1's ability to promote

transcription. These findings indicate that posttranslational modifications within the ER are essential and cooperate to coordinate NRF1 transcriptional responses.

A.3. Material and Methods

Plasmids and molecular biology.

Most DDI2 and NRF1 constructs (N-terminal and C-terminal deletions, C-terminal FLAG tag, N-terminal eGFP tag) were generated by PCR amplification using the Phusion High-Fidelity PCR kit and restriction enzyme cloning into a pCR3 backbone. The NRF1 30NTD (1-30 amino acids) was annealed and cloned into a pCR3-derived NRF1 construct. NRF1 and DDI2 point mutants were generated on pCR3-derived NRF1 and DDI2 expression constructs by Pfu DNA Polymerase or by standard double PCR approach. NRF1 7NA and 7ND were generated by subcloning a synthetic pre-annealed oligo, designed, and ordered at Biomatik, into a pCR3-derived NRF1 construct. Ub-NRF1 derived constructs were generated by attachment of one ubiquitin moiety (with substitution of the final C-terminal glycine of ubiquitin with a valine residue) in-frame to the N-terminus of NRF1 with pCR3-derived NRF1 constructs. Single guide RNA (sgRNA) sequences for DDI2, NRF1, Rad23A, Rad23B and HRD1 were annealed, Esp3I-digested (Biolabs), gel-purified (Cytiva kit), and ligated into pLentiCRISPRv2-Puro (Sanjana et al., 2014) and pLentiCRISPRv2-Blast for sgRad23B, using T4 DNA ligase (Thermo Scientific). All mutations were verified by sequencing.

Generation cell lines.

Gene knock-out cell lines were generated by viral transduction of pLentiCRISPRv2 (Sanjana et al., 2014) vector containing the sgRNA sequence and a puromycin selection marker. The sgRNA sequence of the Luciferase gene was used as control (sgLuci). Positive populations were selected with 2-3 μg/ml puromycin and/or blasticidin for 15 days. Clones were tested by western blot for each protein knock-out level. Gene-targeted single guide RNA sequences were designed using the CRISPRseek package of Bioconductor (version 3.6) on R. DDI2 knock-out and NRF1 knock-out ARH77 cells were infected with pINDUCER-21 lentiviruses containing the different NRF1 constructs inducible upon doxycycline treatment and a GFP selection marker. GFP-positive cells were FACS sorted 5 days following infection.

Single guide RNA design.

Gene-targeted single guide RNA sequences were designed using the CRISPRseek package of Bioconductor (version 3.6) on R.

Transient transfection.

HEK293T cells were transfected with plasmid of interest along with eGFP expression vector used as a control for transfection. After 24h, eGFP expression in HEK293T was assessed by fluorescent microscopy.

Immunoblotting.

Cell lysates were either lysed directly in Laemmli buffer 4X (10% glycerol, 2% SDS, 50mM Tris-HCl pH 6.8, 12.5mM EDTA, 0.02% Bromophenol Blue) complemented with 100 mM of dithiothreitol (DTT) or prepared with ice cold RIPA buffer (50 mM NaCl, 50 mM Tris pH 7.4, 1 mM EDTA, 0.1 % SDS, 1 % NP-40, 1 % sodium deoxycholate) supplemented with protease inhibitor cocktail (Roche, Basel, Switzerland), 10 mM Na_3VO_4, 50 mM NaF, 10 mM $Na_4P_2O_7$, and 5 μM MG132. Protein extracts were denatured, and equal amounts were separated by SDS-PAGE and transferred to nitrocellulose blotting membranes (Amersham).

Quantitative real time PCR.

Total RNA from cells was extracted with PRImeZOL (Canvax, #AN1100) and cDNA was synthetized using 2X Reverse transcription master mix (Applied Biosystems, Waltham, MA, USA) according to manufacturers' protocols. For quantitative real time PCR (RT-PCR), SYBR Green fluorescent reagent and LightCycler 480 Real-Time PCR System (Roche) were used. All RT-PCR were performed in experimental triplicate. Primer sequences are listed in Table EV1.

Immunoprecipitation assay.

HEK293T cells were lysed in lysis buffer containing 0.2% NP-40, 20 mM Tris-HCl pH 7.4, 150 mM NaCl, supplemented with protease inhibitors (cocktail from Roche) and phosphatase inhibitors (Naf, $Na_4P_2O_7$ and Na_3VO_4). Lysates were precleared for 30 minutes with Sepharose beads (6B100, Sigma-Aldrich), then anti-FLAG agarose beads (Anti-FLAG M2 A2220 Sigma-Aldrich) were added, followed by incubation for two hours at 4°C. The immunocomplexes were then washed three times with lysis buffer, resuspended in 4X Laemmli buffer and analysed by Western Blot.

Cell fractionation assay.

Confluent HEK293T or ARH77 cells grown in 10 cm^2 petri dish or T25 flask were washed once with cold PBS 1X. Cells were permeabilized in lysis buffer A (150 mM NaCl, 50 mM HEPES pH 7.4, digitonin 25 μg/ml, 1M Hexylene glycol) for 20 minutes at 4°C on a rotating wheel. Following centrifugation, supernatants corresponding to cytosolic fraction were recovered. Pellets were then washed twice and lysed in lysis buffer B (150 mM NaCl, 50 mM HEPES pH 7.4, 1% NP-40, 1M Hexylene glycol) for 30 minutes on ice. Subsequent centrifugation followed and supernatants corresponding to membrane fraction were withdrawn. Pellets corresponding to nucleic fraction were lysed in lysis buffer C (150 mM NaCl, 50 mM HEPES pH 7.4, 0.1% SDS, 0.5% sodium deoxycholate, 1M Hexylene glycol) supplemented with Benzonase. All buffers were complemented with protease inhibitors

(cocktail from Roche). The samples were mixed with 4X Laemmli buffer and analysed by Western Blot.

Microsome purification assay.

HEK293T cells, grown in 10cm^2 petri dish up to 90% confluency, were washed twice, resuspended in 10 mM HEPES-KOH pH 7.5 buffer, and incubated on ice for 10 minutes. Swollen cells were then sedimented, resuspended in homogenization buffer (10 mM HEPES-KOH pH 7.5, 10 mM KCl, 1.5 mM MgCl2, 5 mM EGTA, and 250 mM sucrose) and passed through a 27G syringe needle for five to 10 times. Homogenates were subjected to serial centrifugations at 600xg (10 min), 3000xg (10 min) and 100,000xg (60 min). Microsomes collected at the end of the ultracentrifugation step were resuspended in membrane buffer (10 mM HEPES-KOH pH 7.5, 50 mM KOAc, 2 mM $Mg(OAc)_2$, 1 mM DTT, and 250 mM sucrose). Microsomes were mock-treated or subjected to Proteinase K (0.5 µg/µl) treatment either in the absence or presence of 1% Triton X-100 for one hour on ice. Samples were then precipitated with trichloroacetic acid (TCA), resuspended in 4X Laemmli buffer and analyzed by Western blot.

High-throughput sequencing.

For RNA sequencing, RNA was extracted using RNeasy mini kit (Qiagen) from three independent wells of different ARH77 cell lines treated with 2.5 µg/ml of doxycycline and treated or not with 10 nM Btz. High-throughput sequencing was performed at the Lausanne Genomics Technologies Facility (University of Lausanne) on the Illumina HiSeq 2500 using TruSeq SBS Kit v3 reagents. For the RNA-seq analysis, we used a moderated *t*-test from the R bioconductor package "limma" (R version 3.1.1, limma version 3.20.8). The "adjusted *P*-value" corresponds to the *P*-values corrected for multiple testing using the Benjamini–Hochberg method.

Analysis of NRF1 cleavage site and post-translational modification sites by mass spectrometry.

Large-scale precipitation of proteins from control (sgLuci) and DDI2 knock-out (sgDDI2) HEK293T cell lysates transfected with FLAG-tagged NRF1 was done using anti-FLAG M2 agarose beads (see Immunoprecipitation assay section), followed by SDS-PAGE, and staining with colloidal Coomassie. Bands corresponding to NRF1 in control and DDI2 knock-out cells were excised, and after in-gel digested with trypsin and chloroacetamide as alkylating reagent. Samples were analysed by liquid chromatography – mass spectrometry (protein analysis facility at Lausanne University).

Quantification and statistical analysis.

Data from one representative independent experiment is shown. All experiments were performed two or three times, except some adaptation experiments. Statistical significances were determined using Graph Pad Prism version 9. The error bars are the standard deviation of the sample.

Table 2. List of reagents and resources.

REAGENT or RESOURCE	SOURCE	IDENTIFIER
Antibodies		
See table S1 for a list of antibodies.		
Chemicals, Peptides, and Recombinant Proteins		
Doxycycline hyclate	Sigma-Aldrich	Cat# D9891
MG-132 (Z-Leu-Leu-Leu-al)	Sigma-Aldrich	Cat# C2211
OSMI-1	Sigma-Aldrich	Cat# SML1621
NMS-873	Sigma-Aldrich	Cat# SML1128
Tunicamycin	Enzo Life Sciences	Cat# BML-CC104-0010
Puromycin	Enzo Life Sciences	Cat# BML-GR312-0250
Bortezomib	LC Laboratories	Cat# B-1408
TAK-243	Lucerna-chem	Cat# HY-100487
CP-26	Anawa	Cat# AOB13238-1
Proteinase K	Roche	Cat# 03115887001
Critical Commercial Assays		
Phusion High-Fidelity PCR kit	New England BioLabs	Cat# E0553
Pfu DNA Polymerase	Promega	Cat# M774A
2X Reverse Transcription master mix	Applied Biosystems	Cat# 4368814
Deposited Data		
Raw sequencing data RNA-seq	This paper	BioProject ID PRJNA897493
Raw mass spectrometry data	ProteomeXchange Consortium	ID PXD041331 10.6019/PXD041331
Raw data for immunoblots	Mendeley	DOI: 10.17632/dcxmrzdkvk.1
Experimental Models: Cell Lines		
HEK293T	Jürg Tschopp	N/A
ARH77	Pascal Schneider	N/A
HeLa	Pascal Schneider	N/A
See Table S2 for a list of generated cell lines used in this manuscript.		
Oligonucleotides		
See Table S3 for a list of oligonucleotides.		
Recombinant DNA		
pCR3	Pascal Schneider	N/A
pDONR-221	Thermo Fisher Scientific	Cat# 12536017
pINDUCER-21	Stephen Elledge and Thomas Westbrook	N/A
pLentiCRISPRv2-Puro	(Sanjana et al., 2014)	RRID:Addgene_52961
Software and Algorithms		
CRISPRseek Bioconductor package	(Zhu et al., 2014)	DOI: 10.18129/B9.bioc.CRISPRseek

A.4. Results

NRF1 cleavage by DDI2 requires sequences upstream and downstream of the cleavage site.

To investigate DDI2-mediated NRF1 cleavage, we generated a DDI2 knock-out population using Crispr-Cas9 technology in human embryonic kidney (HEK) 293T cells. To inhibit NRF1 constitutive degradation by the proteasome (Steffen et al., 2010), we treated the cells with Bortezomib (Btz) and monitored DDI2-mediated NRF1 cleavage by immunoblot analysis **(Figure 15A)**. DDI2-mediated processing was also observed in ARH77 (Op et al., 2022) and HeLa cells in the presence of proteasome inhibitors **(Figures 15B and S1A)**. Previous studies using Edman degradation-based N-terminal sequencing have shown that NRF1, upon overexpression, was cleaved in N-terminal at Leucine-104 (Radhakrishnan et al., 2014). To confirm that DDI2 targets this site, we mutated the putative cleavage site at residues 103 and 104 (W103A L104A). We confirmed that this mutation partially affected DDI2-dependent NRF1 processing, suggesting that DDI2 could recognize alternative sites within NRF1 **(Figure 15C)**.

To test this hypothesis, we purified FLAG-tagged NRF1 proteins expressed in cells proficient or deficient for DDI2 and investigated the cleavage site by liquid-chromatography mass-spectrometry (LC-MS) analysis. We detected only fragments with cleavage between positions 103 and 104 in DDI2-expressing cells **(Figure S1B)**. These data confirm that DDI2 cleaves NRF1 at position 103 and suggest that DDI2 may recognize structural elements in addition to particular amino acid sequences, similar to mechanisms used by the closely related protease from HIV (Pettit et al., 1991). Furthermore, phylogenetic comparisons show some conservation in the cleavage site in NRF1, indicating the region's structural preservation. NRF3, a paralog of NRF1 cleaved by similar mechanisms (Zhang et al., 2009), displays similar conservation around the cleavage site **(Figure 15D)**.

To identify the minimal regions required for DDI2-mediated processing, we generated several NRF1 deletion constructs and monitored processing in DDI2 deficient or control cells. We found that deletion within the N-terminal sequence of NRF1 completely abolished processing **(Figure 15E)**. Furthermore, adding an N-terminal FLAG tag did not impact NRF1 processing and showed comparable cleavage as NRF1 fused to a FLAG tag at the C-terminus **(Figure 15F)**. In contrast, linking a 28 kDa eGFP moiety at the N-terminus of NRF1 abrogated its processing **(Figure 15G)**.

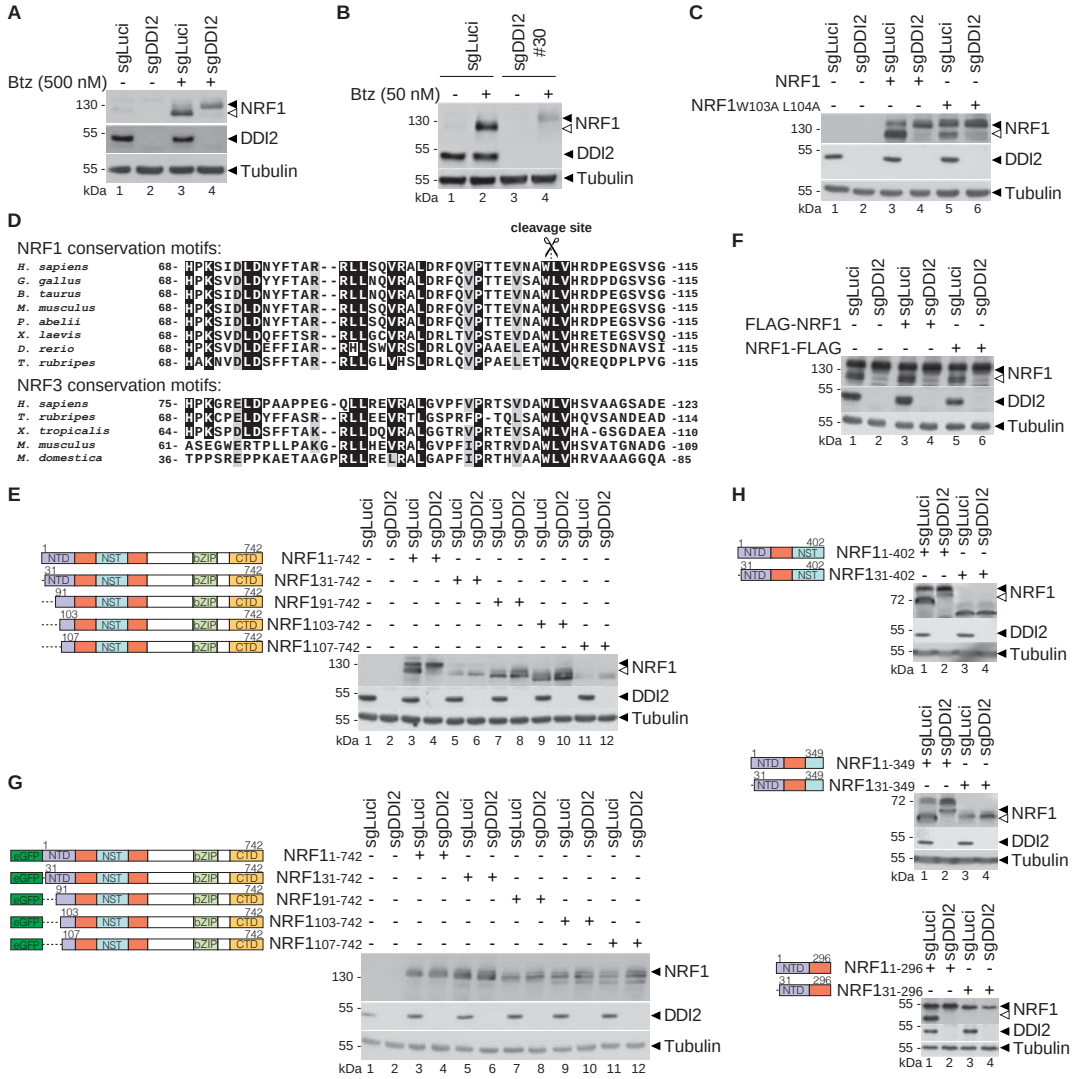

Figure 15. DDI2 mediates NRF1 cleavage at Leucin 104. (A and B) Endogenous NRF1 cleavage in control (sgLuci) and DDI2 knock-out (sgDDI2) HEK293T cells (**A**) or ARH77 cells (**B**) treated with Bortezomib (Btz) for six hours as indicated. Protein expression is measured by western blot. Tubulin is used as loading control; ◀ indicates the full-length NRF1 protein; ◁ indicates the cleaved NRF1 protein. **(C)** NRF1 cleavage in control (sgLuci) and DDI2 knock-out (sgDDI2) HEK293T transfected with NRF1 wild-type or cleavage site mutant W103A L104A. Protein expression is measured by western blot as in A. **(D)** Sequence alignment of the conserved cleavage site of NRF1 and NRF3 among representative species. **(E-H)** NRF1 cleavage in control (sgLuci) and DDI2 knock-out (sgDDI2) HEK293T transfected with NRF1 deletion constructs within the N-terminus (**E**), fused with a FLAG tag at the N-terminus or C-terminus (**F**) or fused with a eGFP tag at the N-terminus (**G**), and the C-terminus (**H**), the C-terminus (**H**), as illustrated on the left of the panels. NTD, N-terminal domain; NST, Asn/Ser/Thr-rich glycosylated domain; bZIP, Basic Leucine Zipper domain; CTD, C-terminal domain. Protein expression is measured by western blot as in A. Western blots are representative of three (A, B, E, F) or two (C, G, H) independent experiments.

To study the involvement of the C-terminal portion of NRF1, we deleted several regions in NRF1 C-terminus. We found that all constructs with sequences shorter than 1-246 could not be cleaved by DDI2 **(Figure S1C)**. Truncated NRF1 protein (amino acids 1-246) showed partial cleavage compared to full-length NRF1. In contrast, construct 1-296 corresponding to the N-Terminal region (NTD) and the intermediate domain preceding the Asn/Ser/Thr-rich

glycosylated region (NST), as well as other shorted deletions in the C-terminus showed robust DDI2-mediated cleavage **(Figure 15H)**.

Taken together, these observations indicated that NRF1 processing requires several elements upstream and downstream of its cleavage site, with the N-terminus being essential. Adding a short sequence did not affect the function of the N-terminus; however, a more prominent independent fold could impact its function.

ER localization is required for NRF1 proteolytic maturation.

Given that the N-terminal region of NRF1 was proposed to be involved in anchoring the protein within the ER (Wang & Chan, 2006; Zhang et al., 2007; Zhang, Ren, et al., 2014), we hypothesized that ER trafficking could be a prerequisite to license NRF1 for DDI2-mediated cleavage in the cytosol.

To examine the importance of NRF1 cellular localization, we tested whether the NRF1 N-terminal domain (NTD) is dispensable for DDI2-mediated activation. Structural studies suggested that the region encoding the first 30 amino acids of NRF1 (30NTD) could dictate its entry into the ER (Zhang et al., 2007). HEK293T cells expressing wild-type NRF1 (1-742) or lacking its first 30 amino acids (31-742) were fractionated, and proteins were isolated from membrane compartments of the Golgi apparatus, the mitochondria, and the ER (as indicated by the "M" fraction on the immunoblots) **(Figure 16A)**. Notably, NRF1 lacking the 30NTD was absent from the M fraction, highlighting the importance of this region in mediating NRF1 membrane localization. These findings were confirmed using the shorter version of NRF1 (1-296) and (31-296) **(Figure 16B)**.

To further examine the role of the NRF1 first 30 amino acids in facilitating ER-trafficking, microsomes were isolated from HEK293T cells expressing wild-type NRF1 (1-742) or lacking the 30NTD (31-742) **(Figure 16C)** or similar shorter constructs **(Figure 16D)**. Purified microsomes were subjected to proteinase K (PK) treatment to determine the conformation of ER-associated proteins. We monitored Calnexin, an ER-specific type I transmembrane protein as a control. The digestion of microsomes revealed a 70 kDa proteinase-resistant fragment, consistent with the fact that the majority of the Calnexin was intraluminal. Unprocessed NRF1 remained intact after PK treatment in comparison to the Calnexin control, indicating that NRF1 protein is entirely located in the ER lumen before retrotranslocation **(Figures 16C and 16D)**.

To demonstrate that ER-localization is required for proteolytic activation, the NRF1 region coding for 30NTD was fused to the N-terminus of the eGFP moiety, which abrogated NRF1

cleavage, as shown in Figure 15G. Constructs were then monitored for NRF1 processing in DDI2-deficient and control cells. Fusion of the NRF1 30NTD sequence in front of the eGFP restored DDI2-mediated NRF1 cleavage. Both the eGFP (31-742) NRF1 **(Figure 16E)** and eGFP (31-296) NRF1 **(Figure 16F)** showed DDI2-dependent cleavage, confirming that ER-localization can promote NRF1 processing.

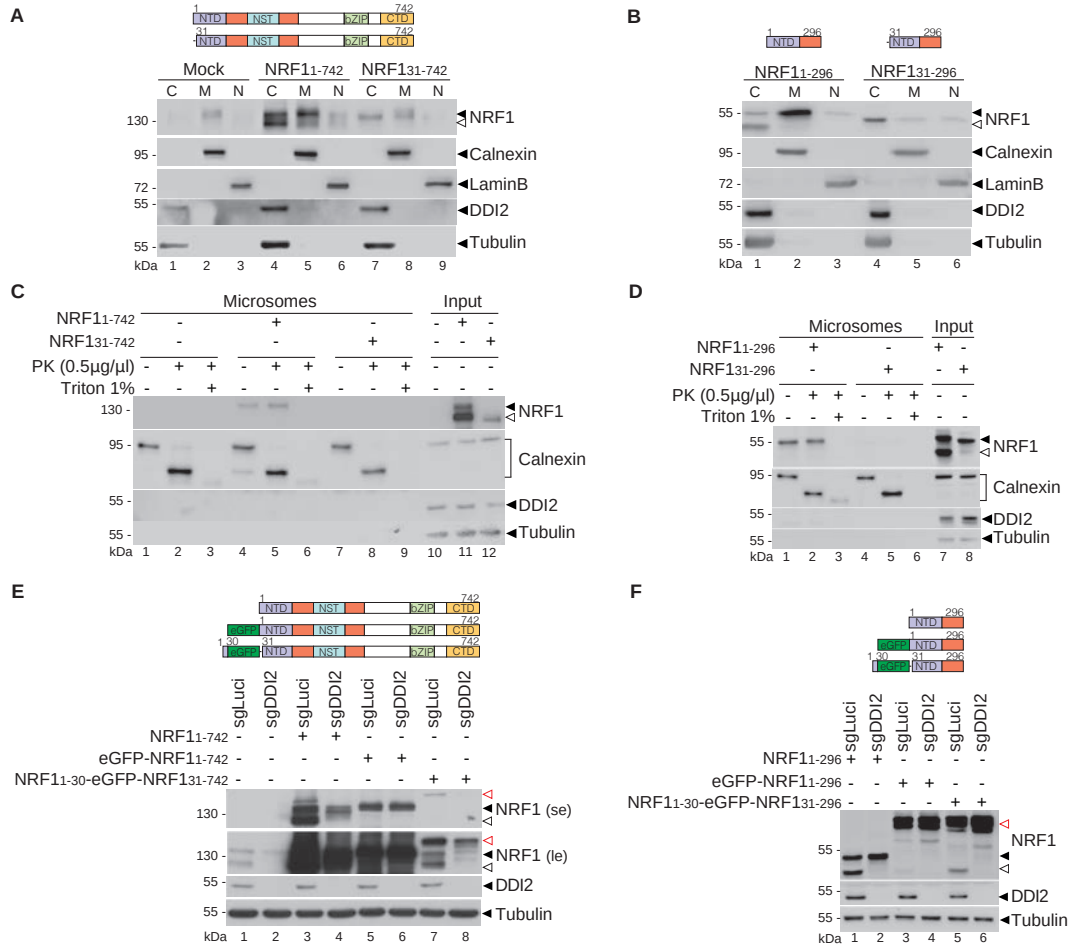

Figure 16. ER-localization of NRF1 is essential for its DDI2-mediated processing. (A and B) NRF1 full-length (1-742) or lacking a functional 30NTD (31-742) (**A**) or NRF1 (1-296) and (31-296) (**B**) were expressed in HEK293T. Lysates were fractionated by sequential centrifugation into the membrane fraction (M: ER, Golgi, mitochondria), the nucleus (N) and the cytosol (C), respectively. NRF1 was monitored by western blot. Calnexin, Lamin B and Tubulin are loading and fractionation controls. **(C and D)** NRF1 full-length (1-742) or lacking a functional 30NTD (31-742) (**C**) or NRF1 (1-296) and (31-296) (**D**) were expressed in HEK293T. Microsomes were isolated as described under "Material and Methods". Microsomes were incubated with or without Proteinase K (PK) or Triton X-100 as indicated. NRF1 was monitored by western blot. Calnexin and Tubulin are loading and microsomes controls. **(E and F)** NRF1 full-length (1-742), or fused to an N-terminal eGFP tag, or expressing the 30 first amino acids in front of the eGFP tag and lacking a functional 30NTD (**E**) or similar shorter functional constructs (**F**) were expressed in control (sgLuci) and DDI2 knock-out (sgDDI2) HEK293T. NRF1 cleavage was monitored by western blot. ◁ indicates the unprocessed NRF1 protein fused to an N-terminal eGFP tag; se: short image exposure; le: long image exposure. Tubulin is a loading control. ◀ indicates the unprocessed NRF1 protein and ◁ indicates the cleaved NRF1 protein. Western blots are representative of three (A, B, E) or two (C, D, F) independent experiments.

The fractionation assays **(Figures 16A and 16B)** are consistent with DDI2 being a cytosolic protein. Therefore, in line with previous observations (Radhakrishnan et al., 2014), we confirmed that NRF1 retrotranslocation into the cytosol is required for DDI2-mediated processing. To assess this question, we treated the cells with NMS-873, an inhibitor of p97/VCP protein. The p97/VCP protein is an essential AAA+ ATPase that contributes to the ERAD pathway (Lim et al., 2009). Upon treatment with the p97 inhibitor, NRF1 cleavage in HEK293T was partially abrogated **(Figure S2A)**. Moreover, endogenous NRF1 cleavage was blocked entirely in ARH77 cells **(Figure S2B)**. These results indicate that ER trafficking of NRF1 licenses NRF1 for cleavage by DDI2 in the cytosol. Considering the role of the ER in post-translational modification of proteins (Schwarz & Blower, 2016; Stevenson et al., 2016), we sought to interrogate NRF1 posttranslational modifications and their importance in licensing NRF1 for subsequent processing by DDI2.

DDI2-mediated NRF1 cleavage requires ubiquitination but occurs independently of its glycosylation state.

One of the most frequent ER-initiated modifications is N-glycosylation, which involves attaching a pre-existing sugar chain to an asparagine residue on a newly formed protein. In the glycodomain of NRF1 (NST), there are seven potential asparagine sites that could undergo N-glycosylation (Tomlin et al., 2017; Zhang, Ren, et al., 2014). We investigated the role of N-glycosylations by treating cells with Tunicamycin (TM), an N-glycosylation inhibitor, and monitoring DDI2-mediated NRF1 cleavage via immunoblot analysis. In the presence of TM, DDI2 retained its ability to cleave non-glycosylated NRF1 in ARH77 cells **(Figure S3A)** and full-length NRF1 protein in HEK293T cells **(Figure S3B)**.

We found that the glycodomain was not required for DDI2 mediated processing of NRF1, as NRF1 constructs with full (1-402), partially deleted (1-349), or completely deleted (1-296) glycodomain were still processed in a DDI2-dependent manner **(Figure S3C)**. Furthermore, it was shown in *C. elegans* that deglycosylation in the cytosol catalyzes a deamidation reaction that releases the glycan moiety and concomitantly converts N-glycosylated asparagine residues to aspartate (Lehrbach et al., 2019). To assess whether this mechanism in mammals contributes to DDI2-mediated NRF1 processing, we engineered NRF1 constructs where the seven glycosylated asparagines are either replaced by aspartic acids (hereafter "7ND") or alanines to mimic a deglycosylated inactive NRF1 protein (hereafter "7NA"). When expressed in HEK293T cells, both 7ND and 7NA NRF1 mutants are processed in a DDI2-dependent manner **(Figure S3D)**. Altogether these observations indicate that DDI2 mediates NRF1 cleavage independently of the status of its N-glycosylation sites.

To identify other posttranslational modifications (PTMs) of NRF1 that could regulate its processing, we purified FLAG-tagged NRF1 proteins expressed in cells proficient or deficient for DDI2 and analyzed PTMs by LC-MS (liquid chromatography-mass spectrometry) analysis **(Figure S4)**. We detected the presence of one O-glycosylated site at T98, very close to the cleavage site, and two ubiquitinated sites **(Figures S3E and S4)**. First, we investigated the involvement of the O-glycosylation at T98. To test this hypothesis, we monitored DDI2-mediated NRF1 cleavage in DDI2 deficient or control cells treated with OSMI-1, an inhibitor of O-GlcNAc transferase. In the presence of the OSMI-1 inhibitor, NRF1 cleavage was not affected **(Figure S3F)**. Mutation of the O-glycosylated site at residue 98 (T98A) did not affect DDI2-dependent NRF1 processing **(Figure S3G)**, further suggesting that NRF1 is cleaved independently of O-glycosylation.

Next, we explored the involvement of ubiquitination in NRF1 recognition by DDI2. This hypothesis is supported by previous reports indicating that an inhibitor of ubiquitination affected NRF1 activation and that DDI2 may preferentially recognize large ubiquitylated proteins for degradation by the proteasome (Collins et al., 2022; Dirac-Svejstrup et al., 2020a; Sha & Goldberg, 2014). To investigate the role of NRF1 ubiquitination in DDI2-mediated processing of NRF1, we treated HeLa cells with bortezomib and TAK-243, a UBA1 inhibitor, to block most constitutive ubiquitination. As expected, UBA1 inhibition prevented NRF1 cleavage **(Figure 17A)**. We also generated various mutations within NRF1 lysines residues identified by LC-MS **(Figure S4)** and four other lysines located within the N-terminus **(Figure 17B)**. Interestingly, when one single lysine mutation is introduced, NRF1 processing was not affected **(Figures 17C and 17D)**. Furthermore, combinations of mutations in the lysine residues also led to no change in NRF1 activation **(Figure 17E)**. In contrast, mutating all six lysine residues within NRF1 N-terminus abolished its DDI2-mediated cleavage **(Figures 17F and 17G)**. These findings suggest that DDI2-mediated NRF1 cleavage does not require a specific lysine residue, but rather any lysine residue that can be ubiquitinated. To confirm the presence of NRF1 ubiquitination, we performed immunoprecipitation of FLAG-tagged NRF1 (1-296) or a version with the six lysine residues mutated (1-296 6KA), in the presence of an HA-tagged ubiquitin moiety **(Figure 17H)**. We then monitored ubiquitin conjugation in the pull-downs. As seen in Figure 17H, NRF1 was found to be conjugated with the HA-tagged ubiquitin, whereas NRF1 lacking all six N-terminal lysine residues showed decreased ubiquitination. These results suggest that the lysines within NRF1's N-terminus play a critical role in directing its ubiquitination and subsequent cleavage by DDI2.

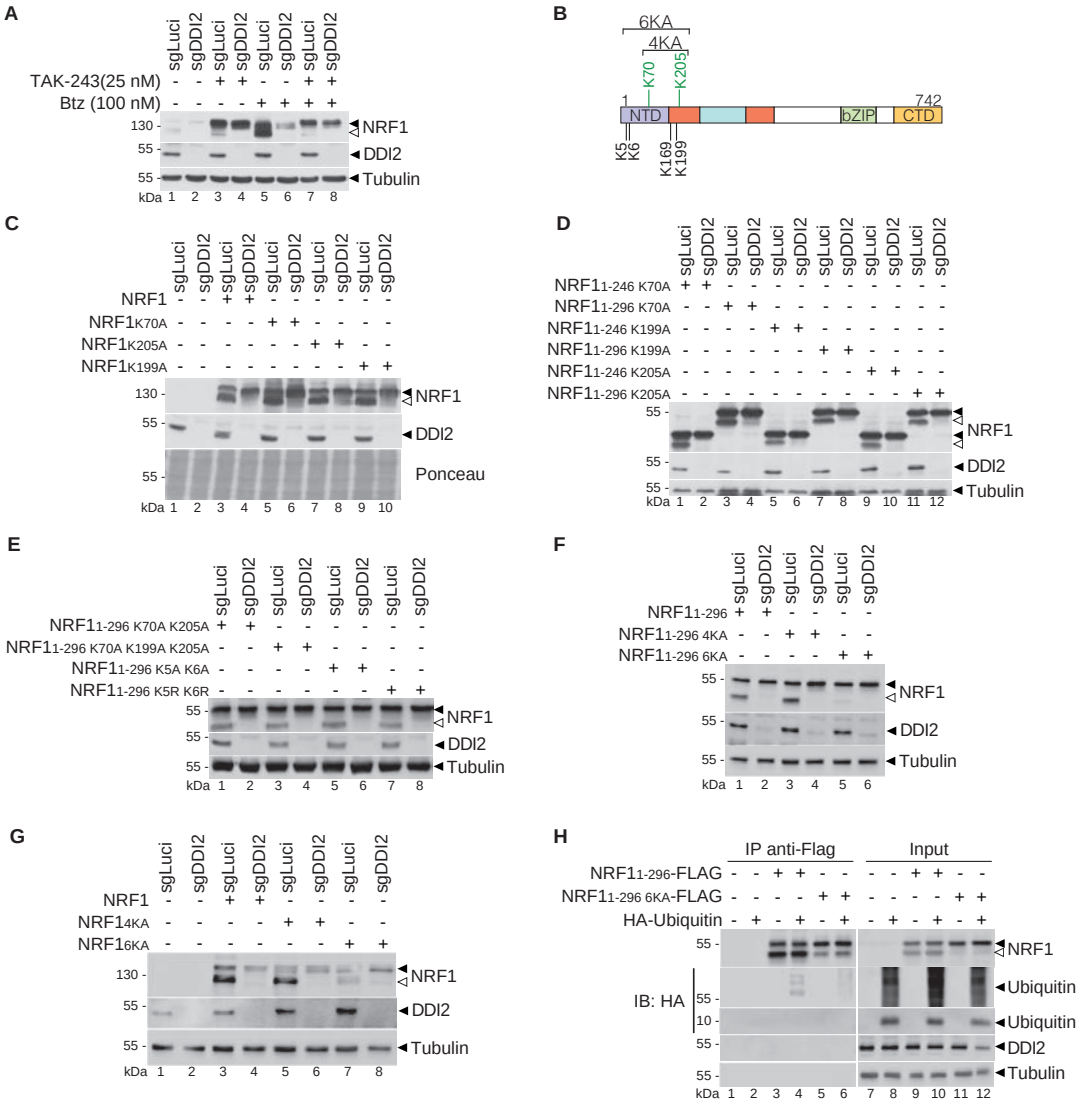

Figure 17. Ubiquitination is essential to mediate NRF1 cleavage.(A) Endogenous NRF1 cleavage in control (sgLuci) and DDI2 knock-out (sgDDI2) HeLa cells treated with TAK-243 or/and Bortezomib (Btz) for six hours as indicated. Protein expression is measured by western blot. Tubulin is used as loading control; ◀ indicates the full-length NRF1 protein; ◁ indicates the cleaved NRF1 protein. **(B)** Schematic representation of NRF1 ubiquitination sites (in green); **—** indicates four lysin residues in NTD of NRF1. **(C-G)** NRF1 cleavage in control (sgLuci) and DDI2 knock-out (sgDDI2) HEK293T transfected with full-length NRF1 with single ubiquitination site mutants (**C**), or NRF1 (1-296) or (1-246) (**D**), or with double ubiquitination site mutants (**E**), or multiple ubiquitination site mutants (**F, G**). Protein expression is measured by western blot. Ponceau or Tubulin is used as a loading control; ◀ indicates the unprocessed NRF1 protein; ◁ indicates the cleaved NRF1 protein. **(H)** NRF1 immunoprecipitation in HEK293T co-transfected with an HA tagged ubiquitin and Flag-tagged NRF1 (1-296) or (1-296 6KA). Protein expression is monitored by western blot as in A. Western blots are representative of three (C, D, E, H) or two (A, F, G) independent experiments.

ER-trafficking of NRF1 licenses its cleavage by promoting its ubiquitination.

To understand how the trafficking within the ER affects NRF1 ubiquitination, we studied NRF1 constructs that do not traffic to the ER. We previously observed that NRF1 lacking the 30NTD does not localize to the ER **(Figures 16A and 16B)**. Interestingly, NRF1 lacking the 30NTD is not ubiquitinated and therefore cannot be cleaved **(Figure 18A)**, suggesting that

ER trafficking is involved in the ubiquitination of NRF1. We used this cytosolic form of NRF1 that is not subject to ubiquitination to investigate whether we could restore the process of proteolytic maturation by fusing a ubiquitin moiety to the N-terminus of the protein.

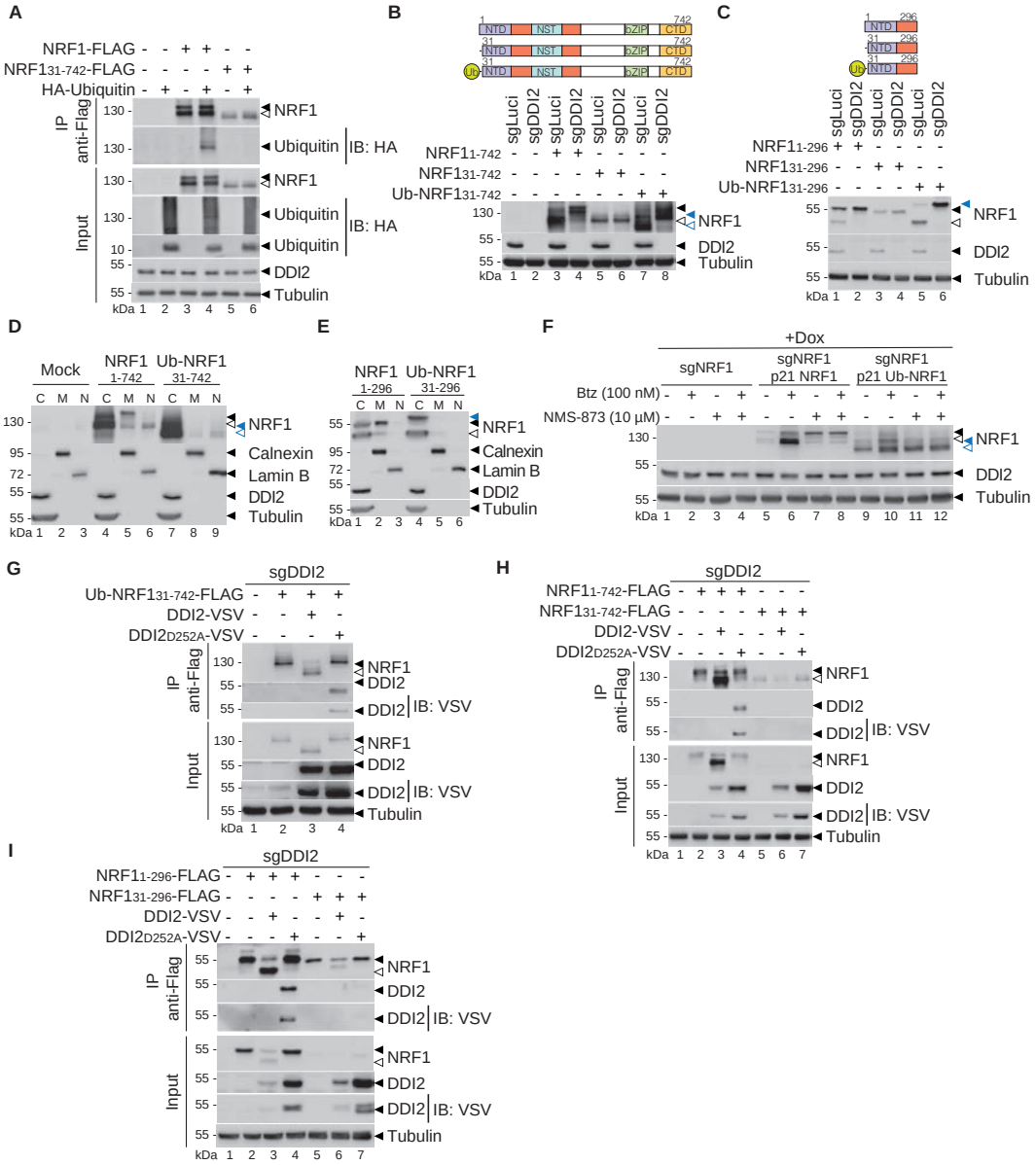

Figure 18. Without trafficking through the ER, ubiquitin-tagged NRF1 is cleaved via conjugation with DDI2. (A) Co-immunoprecipitation in HEK293T co-transfected with an HA tagged ubiquitin and Flag-tagged NRF1 or (31-742). Protein expression is monitored by western blot. Tubulin is used as a loading control; ◀ indicates the full-length NRF1 protein; ◁ indicates the cleaved NRF1 protein. **(B and C)** NRF1 cleavage in control (sgLuci) and DDI2 knock-out (sgDDI2) HEK293T transfected with NRF1 (1-742), or (31-742), or fused with a ubiquitin moiety at the N-terminus (**B**), or similar shorter functional constructs (**C**) as illustrated on the top of the panels. Protein expression is measured by western blot. Tubulin is used as a loading control; ◀ indicates the unprocessed NRF1 protein; ◁ indicates the cleaved NRF1 protein; ◀ indicates the unprocessed NRF1 protein fused to ubiquitin moiety in N-terminus; ◁ indicates the cleaved NRF1 protein fused to ubiquitin moiety in N-terminus. **(D and E)** NRF1 full-length (1-742) or (31-742) fused to ubiquitin moiety in N-terminus (**D**) or similar shorter functional constructs (**E**) were expressed in HEK293T. Lysates were fractionated by sequential centrifugation into the membrane fraction (M: ER, Golgi, mitochondria), the nucleus (N) and the cytosol (C), respectively. Calnexin, Lamin B

and Tubulin are loading and fractionation controls. NRF1 was monitored by western blot as in B. **(F)** NRF1 cleavage in NRF1 knock-out (sgNRF1) or reconstituted with full-length NRF1 (sgNRF1 p21 NRF1) or NRF1 lacking its functional 30NTD but fused to ubiquitin moiety in N-terminus (sgNRF1 p21 Ub-NRF1) upon doxycycline, in ARH77 cells treated with Btz and/or NMS-873 for six hours as indicated. Protein expression is monitored by western blot as in B. **(G)** Flag-tagged NRF1 (31-742) fused to ubiquitin moiety in N-terminus co-immunoprecipitation with DDI2 wild-type or protease domain mutant (D252A) in HEK293T cells. Protein expression is monitored by western blot as in A. **(H and I)** Flag-tagged full-length NRF1 (1-742) or lacking functional 30NTD (31-742) (**H**), or similar shorter functional constructs (**I**), co-immunoprecipitation with DDI2 wild-type or protease domain mutant (D252A) in HEK293T cells. Protein expression is monitored by western blot as in A. Western blots are representative of three (A, B, C, D, E, F) or two (G, H, I) independent experiments.

Our results revealed that adding a single ubiquitin fold to the N-terminus of NRF1 was sufficient to restore DDI2-mediated cleavage **(Figures 18B and 18C)**. Cell fractionation studies indicated that these constructs were only present in the cytosolic fraction and not in the membrane fraction **(Figures 18D and 18E)**. To confirm that the cytosolic, ubiquitinated form of NRF1 is cleaved independently of ERAD, we monitored NRF1 cleavage in ARH77 cells deficient in NRF1, reconstituted with an inducible form of full-length NRF1 or the cytosolic version (lacking the 30NTD) fused to ubiquitin at its N-terminus. We induced NRF1 expression in the presence of NMS-873. Consistently, this ERAD inhibitor blocked the proteolytic maturation of full-length NRF1 **(Figures 18F and S2A)**. However, NMS-873 did not affect the processing of the Ub-NRF1 construct at basal or upon treatment with bortezomib **(Figure 18F)**. These findings provide evidence that DDI2 is capable of processing cytosolic proteins directly and that NRF1 localization within the ER main function is to license NRF1 for cleavage by promoting its ubiquitination.

To investigate the role of NRF1 ubiquitination in its recruitment to DDI2, a protease known to interact with ubiquitinated proteins (Collins et al., 2022; Dirac-Svejstrup et al., 2020a), we expressed NRF1, lacking its functional 30NTD, and fused with a ubiquitin moiety at the N-terminus, along with either DDI2 or an enzymatic inactive form of DDI2 (D252A), in HEK293T cells deficient in DDI2. We then analyzed NRF1 pull-downs. We observed that only the enzymatically inactive DDI2 was pulled down together with NRF1 **(Figure 18G)**, suggesting that DDI2 binds to full length NRF1 and dissociates right after proteolytic processing. Additionally, we found that only NRF1 constructs that have the 30NTD and thereby can be ubiquitinated could interact with DDI2 **(Figures 18H and 18I)**. Collectively, these findings indicate that the ubiquitination at the N-terminus of NRF1 is ER-dependent and that this process is required for the recognition and the subsequent processing by DDI2.

The E3 ligase HRD1 ubiquitinates NRF1 upon retrotranslocation from the ER.

The ER plays a critical role in regulating protein quality control and ER-associated degradation (ERAD) pathways through the action of several E3 ligases. One such E3 ligase is the HMG-CoA reductase degradation 1 (HRD1), which is a transmembrane protein involved in the degradation of misfolded ER proteins via the ERAD pathway. Previous studies have suggested that HRD1 may also contribute to the degradation of NRF1 and other misfolded proteins (Dirac-Svejstrup et al., 2020a; Tsuchiya et al., 2011a; Wu et al., 2020). To investigate the potential involvement of HRD1 in NRF1 processing, we generated HRD1 knock-out cell lines and assessed the impact of HRD1 deficiency on NRF1 activation.

First, we immunoprecipitated a functional NRF1 construct co-expressed with HA-tag ubiquitin in wild-type and HRD1-deficient HEK293T cells. We observed that the ubiquitination of NRF1 was abrogated in HRD1 knock-out cells **(Figure 19A)**. Furthermore, in ARH77 cells, HRD1 deficiency led to the accumulation of NRF1 and impaired its proteolytic cleavage **(Figure 19B)**. This accumulation of NRF1 was observed in the absence of bortezomib, highlighting the dual role of HRD1 in mediating NRF1 degradation and its requirement for activation.

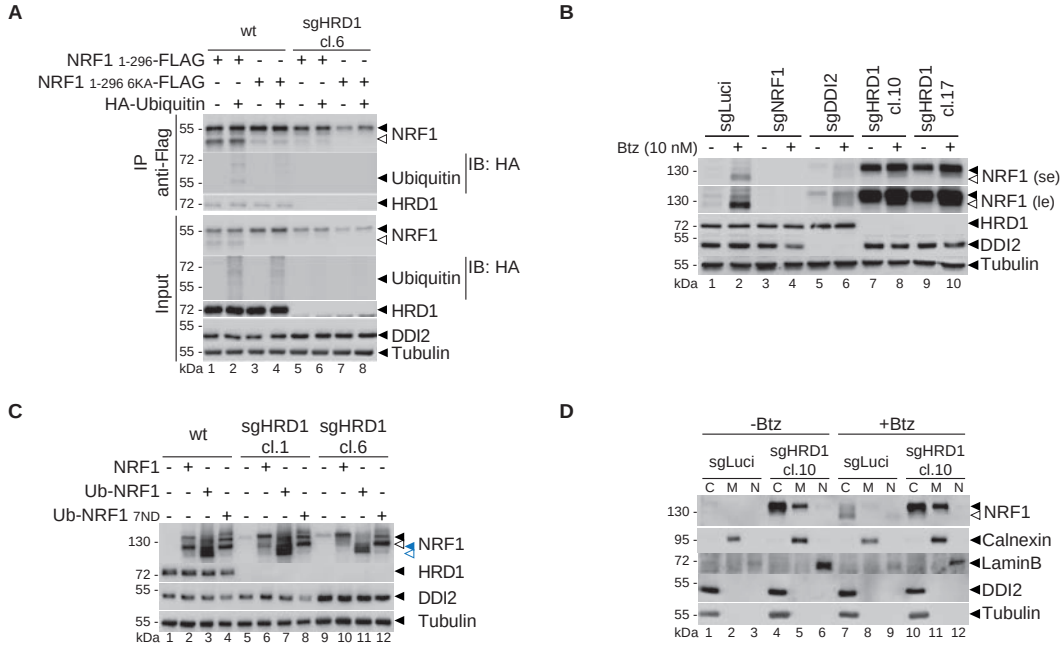

Figure 19. HRD1 mediates NRF1 ubiquitination following its retrotranslocation from the ER. (A) Flag-tagged NRF1 (1-296) or (1-296 6KA) immunoprecipitation in wild-type and HRD1 knock-out (sgHRD1 cl.6) HEK293T co-transfected with an HA tagged ubiquitin. Protein expression is monitored by western blot. Tubulin is used as a loading control; ◀ indicates the full-length NRF1 protein; ◁ indicates the cleaved NRF1 protein. **(B)** Endogenous NRF1 cleavage in control (sgLuci), NRF1 knock-out (sgNRF1), DDI2 knock-out (sgDDI2) and two clones for HRD1 knock-out (sgHRD1 cl.10 and cl.17) ARH77 cells treated with Btz for 24 hours as indicated; se: short image exposure; le: long image exposure. Protein expression is measured by western blot as in A. **(C)** NRF1 cleavage in control (sgLuci) and HRD1 knock-out (sgHRD1 cl.1 and cl.6) HEK293T transfected with NRF1 wild-type or lacking its functional 30NTD and fused to ubiquitin in N-terminus (Ub-NRF1) and with N-glycosylation sites mutations (Ub-NRF1 7ND). Protein expression is measured

by western blot as in A; ◀ indicates the unprocessed NRF1 protein fused to ubiquitin moiety in N-terminus; ◁ indicates the cleaved NRF1 protein fused to ubiquitin moiety in N-terminus. **(D)** Endogenous NRF1 localization in control (sgLuci) and HRD1 knock-out (sgHRD1 cl.10) ARH77 treated with Btz for six hours. Lysates were fractionated by sequential centrifugation into the membrane fraction (M: ER, Golgi, mitochondria), the nucleus (N) and the cytosol (C), respectively. Calnexin, Lamin B and Tubulin are loading and fractionation controls. NRF1 was monitored by western blot as in A. Western blots are representative of two (D) or one independent experiment.

To demonstrate that HRD1 did not impact DDI2 activity *per se*, we analyzed the proteolytic activation of the cytosolic versions of Ub-NRF1 and Ub-NRF1 7ND. HRD1 deficiency did not impact cytosolic Ub-NRF1 cleavage, indicating that its function is required upstream of DDI2 activation **(Figure 19C)**. Importantly, HRD1 deficiency did not affect NRF1 retrotranslocation in the cytosol, as demonstrated by fractionation studies showing that NRF1 accumulated in the cytosolic fraction of HRD1-deficient ARH77, independently of proteasome inhibition. In contrast, in HRD1-proficient cells, only the cleaved form of NRF1 was detected in the cytosol **(Figure 19D)**.

These experiments indicate that HRD1 is crucial for the ubiquitination of NRF1 at the ER, a key step that licenses NRF1 for the subsequent DDI2-mediated cleavage in the cytosol.

RAD23 is required for DDI2-mediated NRF1 cleavage.

The yeast homolog of DDI2 has a ubiquitin-associated domain (UBA), which mediates interaction with ubiquitinated proteins. However, in humans, DDI2 lacks this domain and reconstitution experiments have shown that neither the ubiquitin-like domain (UBL) nor its C-terminus are required for DDI2 activity (Op et al., 2022). Interestingly, RAD23, a UBA-containing protein, has been shown to enhance DDI2 proteolytic activity in vitro (Dirac-Svejstrup et al., 2020a). In addition, studies in yeast have shown a genetic and physical interaction between yeast Ddi1 and RAD23 (Bertolaet et al., 2001b). Therefore, we hypothesize that RAD23 may contribute to recruit ubiquitinated proteins to DDI2.

To investigate whether human RAD23 proteins are required for NRF1 maturation in cells, we generated RAD23 knock-out HEK293T by targeting the two RAD23 paralogues (Rad23a and Rad23b). We found that double deficiency of Rad23a and Rad23b, similar to DDI2 deficiency, decreased NRF1 cleavage **(Figure 20A)** whereas single deficiency of either Rad23a or Rad23b did not impaired NRF1 cleavage **(Figure S5)**. Additionally, reconstitution of Rad23a expression in the double RAD23 knock-out HEK293T cells rescued partially NRF1 cleavage upon Bortezomib **(Figure 20B)**. Moreover, RAD23 proteins were required for maximal cleavage of the cytosolic NRF1 construct lacking the 30NTD but fused to the ubiquitin fold **(Figures 20C and 20D)**. In addition, we demonstrated that RAD23 deficiency

did not impact NRF1 ubiquitination **(Figure 20E)**. These results indicate that RAD23 functions downstream of NRF1 trafficking to the ER or ubiquitination.

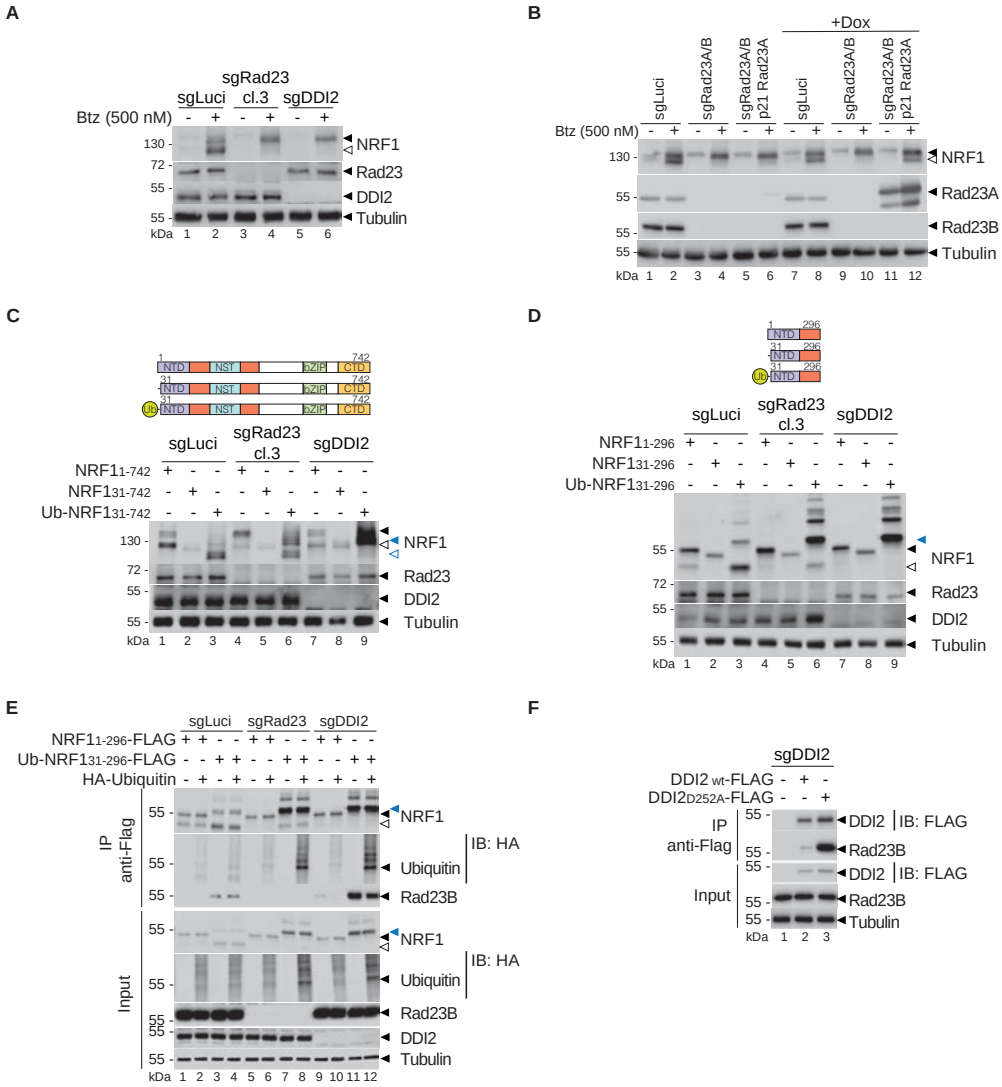

Figure 20. Rad23B conjugates to DDI2 to trigger NRF1 cleavage. (A) Endogenous NRF1 cleavage in control (sgLuci), double RAD23 knock-out (sgRad23 cl.3) and DDI2 knock-out (sgDDI2) HEK293T cells treated with Btz for six hours as indicated. Protein expression is measured by western blot. Tubulin is used as loading control; ◀ indicates the full-length NRF1 protein; ◁ indicates the cleaved NRF1 protein. **(B)** NRF1 cleavage in control (sgLuci) or double RAD23 knock-out (sgRad23A/B) reconstituted with Rad23a (p21 Rad23A), in HEK293T cells treated with Btz for six hours as indicated. Protein expression is monitored by western blot as in A. **(C and D)** NRF1 cleavage in control (sgLuci), double RAD23 knock-out (sgRad23 cl.3) and DDI2 knock-out (sgDDI2) HEK293T transfected with full-length NRF1, NRF1 lacking its functional 30NTD and with ubiquitin moiety fused in N-terminus (**C**), or with similar shorter functional constructs (**D**) as illustrated on the left of the panels. Protein expression is measured by western blot as in A. ◀ indicates the unprocessed NRF1 protein fused to ubiquitin moiety in N-terminus; ◁ indicates the cleaved NRF1 protein fused to ubiquitin moiety in N-terminus. **(E)** Flag-tagged NRF1 immunoprecipitation in wild-type (sgLuci), double RAD23 knock-out (sgRad23) and DDI2 knock-out (sgDDI2) HEK293T co-transfected with an HA tagged ubiquitin and short functional NRF1 or (31-296). Protein expression is monitored by western blot as in A. **(F)** DDI2 immunoprecipitation in DDI2-deficient HEK293T cells transfected with flag-tagged wild-type DDI2 or DDI2 proteolytically inactive (D252A). Protein expression is measured by western blot as in A. Western blots are representative of at least two independent experiments.

To investigate the possible interaction between RAD23 and DDI2, we expressed DDI2 or a catalytically inactive DDI2 construct in HEK293T cells. We found that RAD23B interacted with both active and inactive DDI2, but the interaction was more robust with inactive DDI2, suggesting that the complex is more stable when DDI2 is inactive **(Figure 20F)**. Altogether, these findings indicate that RAD23 is a co-factor protein possibly involved in shuttling ubiquitinated NRF1 to DDI2 through its interaction with DDI2.

N-D protein sequence editing and DDI2 mediated cleavage in the cytosol influence NRF1 transcriptional activity.

ER signaling contributes to NRF1 activity via two possible mechanisms. First, it promotes the glycosylation and deglycosylation of NRF1, which results in the editing of glycosylated asparagine into aspartic acids. Second, allows for ubiquitination which is essential for NRF1 activation by DDI2. To study how these events contribute to NRF1 transcriptional program, we examined gene expression in NRF1-deficient ARH77 cell line reconstituted with different NRF1 constructs. We used wild-type NRF1, NRF1 lacking its functional N-terminal domain (30NTD) fused to a ubiquitin moiety in the N-terminus (hereafter referred to as "Ub-NRF1"), NRF1 with its seven glycosylation sites replaced by alanines (hereafter referred to as "Ub-NRF1 7NA") or replaced by aspartic acids (hereafter referred to as "Ub-NRF1 7ND"). We induced the expression of the above-mentioned constructs with doxycycline and treated the cells with bortezomib to inhibit the proteasome and thereby trigger NRF1 activation. Upon doxycycline or bortezomib treatment, we confirmed that all NRF1 constructs are cleaved in ARH77 cells **(Figure 21A)** and confirmed that Ub-NRF1 constructs did not traffic to the ER **(Figure S6)**. The migration of the various products was affected by the glycosylation status and differences in charge observed with the N-D amino acid changes.

To investigate the transcriptional responses, we performed RNA-seq to compare the transcriptional profile of ARH77 control cells (sgLuci), NRF1-deficient (sgNRF1) cells, or (Ub-NRF1 7ND) cells in the presence/absence of bortezomib. Moreover, using the hierarchical clustering method, we were able to detect an overlapping set of genes triggered by bortezomib in an NRF1-dependent manner that are similarly induced in cells expressing the Ub-NRF1 7ND protein **(Figure 21B)**. These data indicate that expression of Ub-NRF1 7ND without proteasome impairment is sufficient to recapitulate the transcriptional programs triggered by NRF1 in the presence of Bortezomib.

To verify the activity of the top identified NRF1 targets, we performed real-time qPCR analysis. STYK1, and CLU gene expression were enriched upon Ub-NRF1 7ND expression, as well as wild-type NRF1 expression **(Figure 21C)**. In contrast, these genes were not induced upon expression of Ub-NRF1 and Ub-NRF1 7NA, indicating that, as previously discovered

in *C. elegans*, N-D editing of glycosylated sites is required for optimal transcriptional induction.

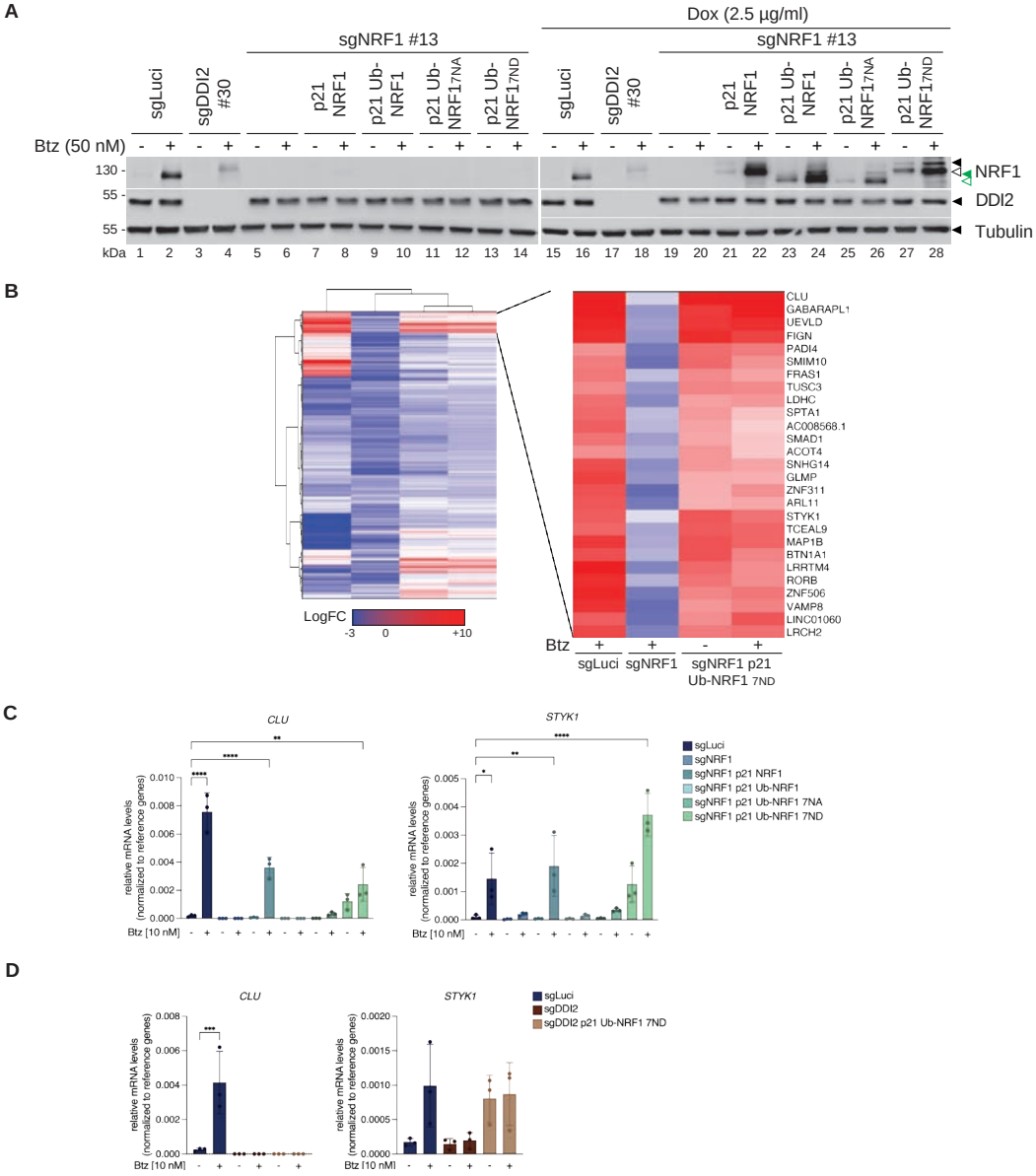

Figure 21. N-D editing and subsequent cytosolic DDI2 cleavage of NRF1 are involved controlling gene expression. (A) NRF1 cleavage in control (sgLuci), DDI2 knock-out (sgDDI2), NRF1 knock-out (sgNRF1) - or reconstituted with full-length NRF1 (p21 NRF1), or NRF1 lacking its functional 30NTD but fused to ubiquitin moiety in N-terminus (p21 Ub-NRF1), and with N-glycosylation sites mutated into alanine (p21 Ub-NRF1 7NA) or into aspartic acid (p21 Ub-NRF1 7ND) - upon doxycycline, in ARH77 cells treated with Btz for six hours as indicated. Protein expression is monitored by western blot. Tubulin is used as a loading control; ◀ indicates the unprocessed NRF1 protein; ◁ indicates the cleaved NRF1 protein; ◀ indicates the non-glycosylated unprocessed NRF1 protein; ◁ indicates the non-glycosylated cleaved NRF1 protein. **(B)** Heatmap showing the NRF1 up-regulated genes in control (sgLuci) and NRF1 knock-out (sgNRF1) reconstituted or not with Ub-NRF1 7ND, ARH77 cells treated with Btz for 24 hours. Purified RNA was analyzed for gene expression by RNA-seq. The genes are listed based on hierarchical clustering generated on NG-CHM Builder and with a P-value <0.01. The LogFC is based on the mean from the triplicates from each condition; red color indicates high expression and blue low expression. The right panel shows the more strongly 27 genes upregulated by NRF1. **(C)** As in A, but treated with Btz for 24 hours as indicated. Induction of STYK1 and CLU genes was measured by real-time

PCR relative to GAPDH and RPL19 (mean and SEM of technical triplicates of one representative experiment are shown). **(D)** NRF1 activation in control (sgLuci), DDI2 knock-out (sgDDI2 cl.30), or reconstituted with NRF1 lacking its functional 30NTD but fused to ubiquitin moiety in N-terminus and with N-glycosylation sites mutations (p21 Ub-NRF1 7ND) - upon doxycycline, in ARH77 cells treated with Btz for 24 hours as indicated. Induction of STYK1 and CLU genes was measured by real-time PCR relative to GAPDH and RPL19. Western blots and RT-PCR are representative of three (C, D) and one (A) independent experiments. RT-PCR data are represented as means ± SEM and tested for statistical significance using Sidak's multiple comparisons test (*p≤0.05, **p≤0.01, ***p≤0.001, ****p≤0.0001, are considered significant).

The fact that Ub-NRF1 7ND functions independently of treatment with bortezomib offers a unique opportunity to dissect DDI2 cleavage to its activity. To answer this question, we generated DDI2-deficient ARH77 cells expressing Ub-NRF1 7ND. We treated these cells with doxycycline to induce NRF1 expression and performed real-time qPCR analysis in these different ARH77 cell models under bortezomib treatment. We found that while some NRF1-dependent genes like CLU were induced in a DDI2-dependent manner, other genes like STYK1 could be induced in a DDI2-independent manner **(Figure 21D)**, indicating that DDI2 engagement may differentially affect NRF1's transcriptional output.

A.5. Discussion

The behavior of NRF1 is unique as it traffics to the ER before being retrotranslocated in the cytosol and eventually functions in the nucleus as a transcription factor. This process involves several layers of regulation that orchestrate NRF1 responses. Our study reveals two main regulatory functions of ER trafficking of NRF1 in mammalian cells: NRF1 ubiquitination and N-glycosylation.

Early studies have shown that NRF1 cellular localization was controlled through residues 1–30 within the N-terminus (Zhang et al., 2007). It was hypothesized that this sequence could represent an atypical signal sequence that could be regulated during stress in a fashion that ensures its incorporation into the ER at basal (Zhang et al., 2007). In line with these initial observations, our studies demonstrated that this sequence is required for NRF1 import in the ER, a process that initiates a cycle of degradation or activation of NRF1. However, the nature of the 30NTD is unclear as it does not contain a typical signal peptidase cleavage site, and the fusion of a FLAG tag at the N-terminus of NRF1 does not perturb its trafficking within the ER. In contrast, we could show that fusing this sequence in front of a cytosolic version of NRF1, harboring an eGFP at the N-terminus, restored both trafficking and DDI2-mediated cleavage. These findings suggest that this sequence alone is sufficient to direct NRF1 import into the ER. It is also possible that this sequence could contribute directly to the retrotranslocation of NRF1 via the ER-associated degradation (ERAD) pathway. However, we cannot rule out the possibility that additional motifs within the first 296 amino acids of NRF1 could also direct its trafficking to the ERAD machinery, as this portion of NRF1 is the minimal structure that traffics in and out of the ER and is required for cleavage by DDI2. The first 296 residues of NRF1 may also contain sequences required for DDI2 recognition. Several attempts at generating an uncleavable version of NRF1 by mutating the region surrounding the cleavage site failed to abolish its cleavage completely. Moreover, attempts at identifying other potential cleavage sites by mass spectrometry only identified the cleavage site between residues 103 and 104. It is, therefore, possible that DDI2 recognition may rely on additional features within the 296 first amino acids. In line with this possibility, it is worth noting that DDI2 proteolytic domain shares homology with that of HIV-1 aspartyl protease, which is known to recognize structural shapes of its substrates rather than a particular amino acid sequence (Prabu-Jeyabalan et al., 2002).

Importantly, we describe that NRF1 trafficking within the ER is a prerequisite for DDI2-mediated processing via ubiquitination by HRD1. This ERAD associated E3-ligase has been implicated in various physiological processes, including the ubiquitination of NRF1 homolog, NRF2, upon ER stress during liver cirrhosis (Wu et al., 2014). Here we found that HRD1

deficiency impaired NRF1 ubiquitination without affecting its retrotranslocation leading to its accumulation in the cytosol. In addition to its function in promoting degradation at basal levels, we show that HRD1-mediated ubiquitination is also required for NRF1 proteolytic maturation by DDI2 when proteasome is impaired. We also showed that a cytosolic version of NRF1 fused to a ubiquitin moiety can bypass this step and undergo DDI2-mediated cleavage in an HRD1-independent manner. Altogether these findings suggests that the accumulation of ubiquitylated NRF1 substrate in the cytosol is critical to elicit NRF1 responses.

Previous studies have shown that DDI2 activity on NRF1 was observed only upon the addition of recombinant RAD23 in vitro (Dirac-Svejstrup et al., 2020a). Our study using human knockout cells demonstrates that both RAD23 paralogues are necessary for both NRF1-mediated proteasome degradation and NRF1 proteolytic maturation by DDI2. RAD23 acts as a ubiquitin receptor that binds the proteasome via its N-terminal ubiquitin folds and two UBA domains that can bind ubiquitinated proteins (Collins & Goldberg, 2020; Kim & Goldberg, 2018; Wade & Auble, 2010). It functions as a shuttle or receptor to bring substrates to the proteasome and promote turnover. Interestingly, we observed that RAD23 binding to DDI2 was stabilized in the absence of DDI2 catalytic activity, suggesting that the stalling of uncleaved substrates with the complex stabilized the interaction. Overall, our findings support a model where the same mechanisms involved in NRF1 proteasomal degradation, such as HRD1-dependent ubiquitination and RAD23-mediated proteasome targeting, are also engaged, and required in promoting DDI2-mediated NRF1 cleavage.

The second step that occurs upon trafficking in the ER is glycosylation. This was described in a breakthrough study in *C. elegans* that identified the editing by the cytosolic N-glycanase PNG1 of glycosylated asparagine residues into aspartic acid (Lehrbach et al., 2019). Using several mutated constructs within the glycosylation residues, we showed that neither glycosylation nor editing of these residues impacted NRF1 processing by DDI2. In contrast, we observed that the editing of glycosylated asparagine into aspartic acid increased NRF1 transcriptional activity similar to that described in *C. elegans*. These observations suggest that this process is conserved in mammals and further defines an additional regulatory function of ER trafficking. We took advantage of this knowledge to investigate the transcriptional activity of NRF1 in cells expressing an ubiquitinated and edited NRF1 construct that does not traffic to the ER. We identified genes triggered by this cytosolic NRF1 that overlapped with the signature elicited by wild-type NRF1 in the presence of bortezomib. This finding confirmed that editing and ubiquitination were sufficient to bypass ER trafficking and restore transcriptional activity. Consistently, we observed that several of the NRF1-induced genes, including *clusterin* (*CLU*), were induced in a DDI2-dependent manner and therefore relied on

the proteolytic maturation of NRF1. *CLU* was identified as among the most NRF1-dependent genes. In contrast, we observed that some of the genes that were identified as NRF1-dependent did not rely on DDI2. For example, the kinase *STYK1* was induced by treatment with bortezomib or expression of an ubiquitinated and edited NRF1 construct in a DDI2-independent manner, suggesting that DDI2 engagement could contribute to determining NRF1 transcriptional programs. Investigation of these different programs and their physiological relevance and implication within NRF1 responses and adaption programs is an important question that remains to be addressed.

In summary, this study delineates the importance of ER trafficking for NRF1 to exert its functions. We demonstrated that editing of the N-glycosylated sites contributes to transcriptional activity and that HRD1-mediated NRF1 ubiquitination contributes to degradation as well as recognition by the RAD23-DDI2 pathway leading to the expression of distinct transcriptional program. The DDI2-dependent NRF1 pathway has been mostly proposed to contribute to susceptibility and resistance to treatments with proteasome inhibitors in multiple myeloma (Chen et al., 2022; Collins & Goldberg, 2020; Dirac-Svejstrup et al., 2020a; Op et al., 2022). The identification of these additional steps and novel proteins involved in the pathway such as HRD1 and RAD23 could shed a new light on the mechanisms of adaptation and resistance to proteasome inhibition and provide with new therapeutic targets in these diseases.

A.6. Supplementary material

Supplementary information for:

ER-trafficking triggers NRF1 ubiquitination to promote its proteolytic activation

Claire Chavarria[1], Léa Zaffalon[1], Sérgio T. Ribeiro[1], Mélanie Op[1], Manfredo Quadroni[2], Maria Sofia Iatrou[1], Chloé Chapuis[1] and Fabio Martinon[1]

[1]Department of Immunobiology, University of Lausanne, 155 Ch. des Boveresses, 1066, Epalinges, Switzerland

[2]Protein Analysis Facility (PAF), Center for Integrative Genomics, University of Lausanne, Lausanne 1015, Switzerland

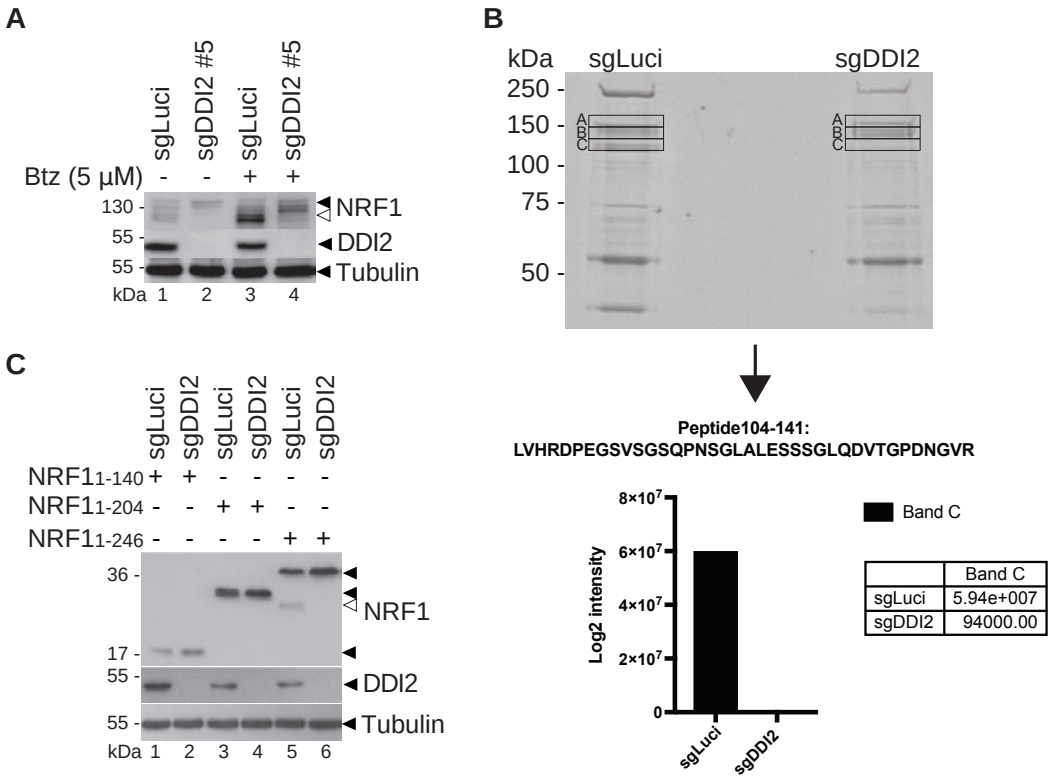

Supplementary figure 1. DDI2 mediates NRF1 cleavage at Leucine 104, related to Figure 15. (A) NRF1 cleavage in control (sgLuci) and DDI2 knock-out (sgDDI2) HeLa cells treated with Bortezomib (Btz) for six hours as indicated. Protein expression is monitored by western blot. Tubulin is used as loading control; ◀ indicates the unprocessed protein; ◁ indicates the cleaved protein. **(B)** NRF1 immunoprecipitation in control (sgLuci) and DDI2 knock-out (sgDDI2) HEK293T cells. Immunoprecipitated samples were loaded on 9% SDS-PAGE gel (top panel). Three bands per condition corresponding to full-length (A and B) and cleaved (C) NRF1 were cut off and digested with trypsin for subsequent LC-MS analysis. The increase of the characteristic peptide 104-141 (bottom panel) in fraction C of control (sgLuci) and not in DDI2 knock-out (sgDDI2) points out a cleavage site between residues 103 and 104. **(C)** NRF1 cleavage in control (sgLuci) and DDI2 knock-out (sgDDI2) HEK293T transfected with NRF1 (1-140) or (1-204) or (1-246). Protein expression is monitored as in A.

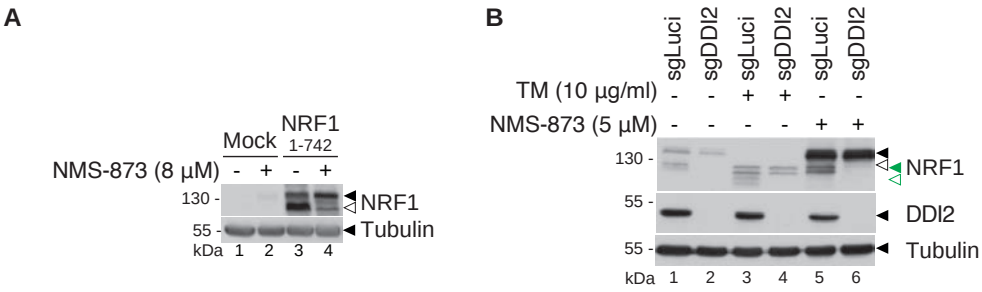

Supplementary figure 2. DDI2 mediates NRF1 cleavage upon ER-retrotranslocation blockade, related to Figure 16. (A) NRF1 cleavage in HEK293T transfected with full-length NRF1 (1-742) and treated with NMS-873 for six hours as indicated. Protein expression is measured by western blot; ◀ indicates the unprocessed protein; ◁ indicates the cleaved protein. **(B)** Endogenous NRF1 cleavage in control (sgLuci) and DDI2 knock-out (sgDDI2) ARH77 cells treated with the N-glycosylation inhibitor, Tunicamycin (TM) or NMS-873, an inhibitor of VCP/97 for six hours as indicated; ◀ indicates the deglycosylated unprocessed protein; ◁ indicates the deglycosylated cleaved protein. Protein expression is measured as in A. Western blots are representative of at least two independent experiments.

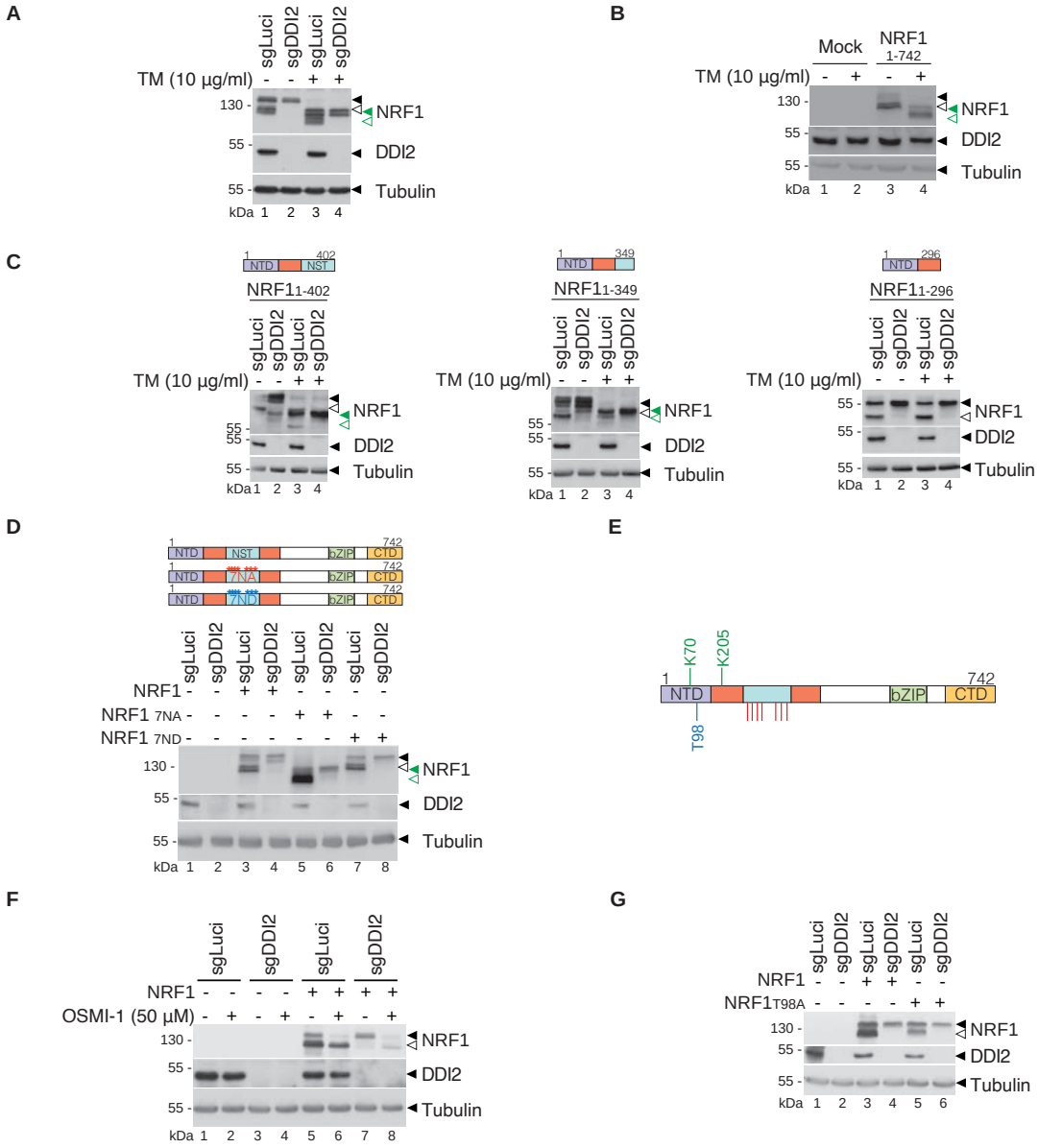

Supplementary figure 3. NRF1 is cleaved independently of its glycosylation state, related to Figure 17. (A) Endogenous NRF1 cleavage in control (sgLuci) and DDI2 knock-out (sgDDI2) ARH77 cells treated with Tunicamycin (TM) for six hours as indicated. Protein expression is measured by western blot. Tubulin is used as loading control; ◀ indicates the unprocessed NRF1 protein; ◁ indicates the cleaved NRF1 protein; ◀ indicates the deglycosylated unprocessed NRF1 protein; ◁ indicates the deglycosylated cleaved NRF1 protein. **(B)** NRF1 cleavage in HEK293T transfected with NRF1 wild-type and treated with TM for six hours. Protein expression is measured by western blot as in A. **(C)** NRF1 cleavage in control (sgLuci) and DDI2 knock-out (sgDDI2) HEK293T transfected with NRF1 deletion constructs within the C-terminus and treated with TM for six hours as illustrated on the top of the panels. Protein expression is measured by western blot as in A. **(D)** NRF1 cleavage in control (sgLuci) and DDI2 knock-out (sgDDI2) HEK293T transfected with full-length NRF1 or N-glycosylation sites mutants (7NA and 7ND) as illustrated on the top of the panel. Protein expression is measured by western blot as in A. **(E)** Schematic representation of NRF1 PTMs sites predicted by LC-MS analysis described under "Material and Methods". — indicates O-glycosylated residue; — indicate ubiquitinated residues; — indicates N-glycosylated residues. **(F)** Endogenous NRF1 cleavage in control (sgLuci) and DDI2 knock-out (sgDDI2) HEK293T cells treated with OSMI-1 for six hours as indicated. NRF1 cleavage was monitored by western blot. Tubulin is used as loading control; ◀ indicates the full-length

NRF1 protein; ◁ indicates the cleaved NRF1 protein. **(G)** NRF1 cleavage in control (sgLuci) and DDI2 knock-out (sgDDI2) HEK293T transfected with NRF1 wild-type or O-glycosylation site mutant (T98A). NRF1 cleavage was monitored by western blot as in F. Western blots are representative of three (C, F), two (B, D, E) or one (G) independent experiments.

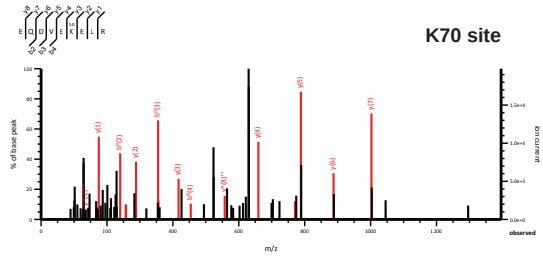

MS/MS Fragmentation of EQDVEKELR
Match to Query 2996: 1258.613728 from(630.314140,2+)
intensity(593702.7949) rtinseconds(1597.8024) index(1289)
Monoisotopic mass of neutral peptide Mr(calc): 1258.6153
Fixed modifications: Carboxymethyl (C) ;
Variable modifications: K6 : GG (K)
Ions Score: 26 Expect: 0.02

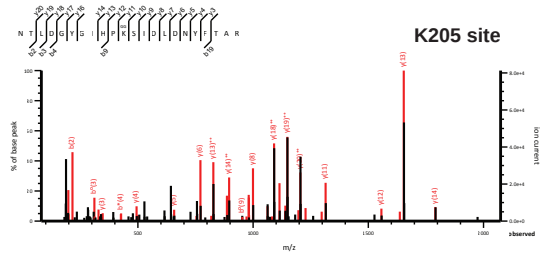

MS/MS Fragmentation of NTLDGYGIHPKSIDLDNYFTAR
Match to Query 9193: 2623.270506 from(875.430778,3+)
intensity(9249288.3594) rtinseconds(2666.79954) index(7553)
Monoisotopic mass of neutral peptide Mr(calc): 2623.2667
Fixed modifications: Carboxymethyl (C) ;
Variable modifications: K11 : GG (K)
Ions Score: 60 Expect: 2.4e-06

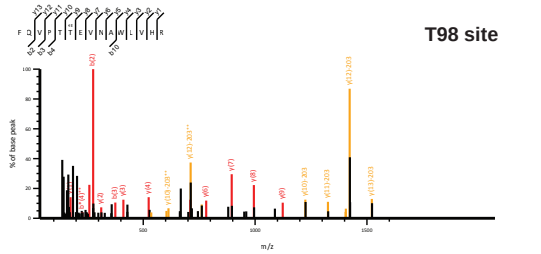

MS/MS Fragmentation of FQVPTTEVNAWLVHR
Match to Query 7603: 1999.019508 from(667.347112,3+)
intensity(7255880.2031) rtinseconds(2627.09142) index(7325)
Monoisotopic mass of neutral peptide Mr(calc): 1999.0163
Fixed modifications: Carboxymethyl (C) ;
Variable modifications: T6 : HexNAc (ST)
Ions Score: 90 Expect: 3.6e-09

Supplementary figure 4. NRF1 is ubiquitinated at lysin 70 and 205, related to Figure 17 and S3. NRF1 immunoprecipitation in control (sgLuci) and DDI2 knock-out (sgDDI2) HEK293T cells. Immunoprecipitated samples were loaded on SDS-PAGE gel. One band per condition corresponding to full-length and cleaved NRF1 respectively, were cut off and digested with trypsin for subsequent LC-MS analysis. A relevant peptide was selected for each post-translational modification and quantified based on signal intensity (precursor mass intensity). Mascot search results were imported into the MsViz software (Martin-Campos et al., 2017), which was used for validation of the PTM localization and quantitation of modified peptide intensities across samples based on extracted ion chromatograms (XIC). Peak heights in XIC traces as extracted by MSViz were used as quantitative measure.

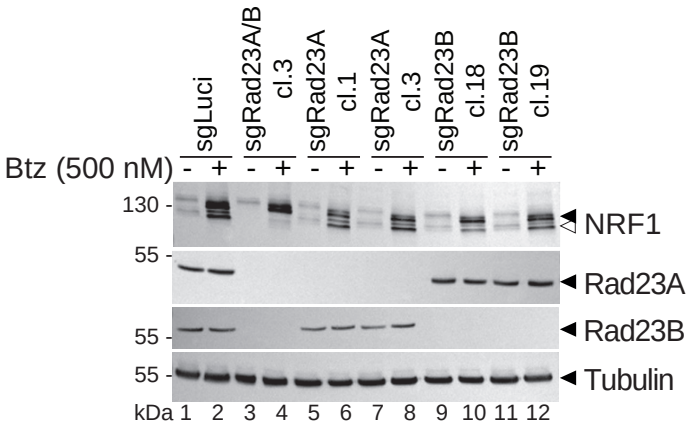

Supplementary figure 5. NRF1 cleavage requires both RAD23 paralogues, related to Figure 20. Endogenous NRF1 cleavage in control (sgLuci), double RAD23 knock-out (sgRad23A/B cl.3), RAD23A knock-out (sgRad23A cl.1 and cl.3) and RAD23B knock-out (sgRad23B cl.18 and cl.19) HEK293T cells treated with Btz for six hours as indicated. Protein expression is measured by western blot. Tubulin is used as loading control; ◀ indicates the full-length NRF1 protein; ◁ indicates the cleaved NRF1 protein.

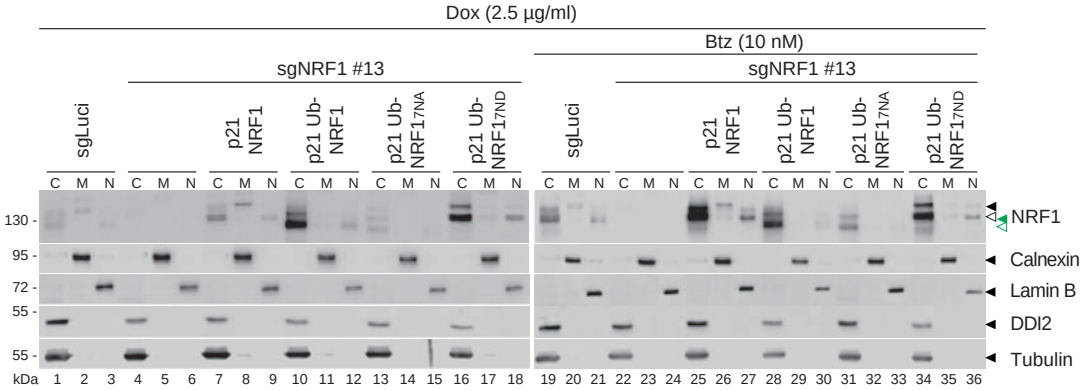

Supplementary figure 6. Ub-NRF1 constructs are cleaved in the cytosol, related to Figure 21. NRF1 cleavage in control (sgLuci), DDI2 knock-out (sgDDI2), NRF1 knock-out (sgNRF1) - or reconstituted with full-length NRF1 (p21 NRF1), or NRF1 lacking its functional NTD but fused to ubiquitin moiety in N-terminus (p21 Ub-NRF1), and with N-glycosylation sites mutated into alanine (p21 Ub-NRF1 7NA) or into aspartic acid (p21 Ub-NRF1 7ND) - upon Doxycycline, in ARH77 cells treated with Btz for six hours as indicated. Lysates were fractionated by sequential centrifugation into the membrane fraction (M: ER, Golgi, mitochondria), the nucleus (N) and the cytosol (C), respectively. Calnexin, Lamin B and Tubulin are loading and fractionation controls. Protein expression is monitored by western blot. ◀ indicates the unprocessed NRF1 protein; ◁ indicates the cleaved NRF1 protein; ◀ indicates the non-glycosylated unprocessed NRF1 protein; ◁ indicates the non-glycosylated cleaved NRF1 protein.

Supplementary table 1. List of antibodies, related to Table 2.

REAGENT or RESOURCE	SOURCE	IDENTIFIER
Antibodies		
Rabbit monoclonal anti-TCF11/NRF1	Cell Signaling Technology	Cat# 8052, RRID:AB_11178947
Rabbit monoclonal anti-SYVN1/HRD1	Cell Signaling Technology	Cat# 14773, RRID:AB_2798607
Rabbit monoclonal anti-Calnexin	Cell Signaling Technology	Cat# 2679, RRID:AB_2228381
Rabbit monoclonal anti-HA-tag	Cell Signaling Technology	Cat# 3724, RRID:AB_1549585
Human anti-alpha-Tubulin	Adipogen	Cat# AG-27B-0005, RRID:AB_2490494
Rabbit polyclonal anti-DDI2	Abcam	Cat# ab197081, RRID:AB_2928956
Rabbit monoclonal anti-Rad23A	Cell Signaling Technology	Cat# 24555, RRID:AB_2750888
Rabbit monoclonal anti-Rad23B	Cell Signaling Technology	Cat# 13525, RRID:AB_2798247
Rabbit polyclonal anti-VSV-G	Sigma-Aldrich	Cat# V4888, RRID:AB_261872
Goat polyclonal anti-Lamin B	Santa Cruz Biotechnology	Cat# sc-6217, RRID:AB_648158
Goat polyclonal anti-Mouse IgG (H+L)	Jackson ImmunoResearch Labs	Cat# 115-035-146, RRID:AB_2307392
Goat polyclonal anti-Rabbit IgG (H+L)	Jackson ImmunoResearch Labs	Cat# 111-035-144, RRID:AB_2307391
Donkey polyclonal anti-Goat IgG (H+L)	Jackson ImmunoResearch Labs	Cat# 705-035-003, RRID:AB_2340390
Donkey polyclonal anti-Human IgG (H+L)	Jackson ImmunoResearch Labs	Cat# 709-035-149, RRID:AB_2340495

Supplementary table 2. List of cell lines, related to Table 2.

REAGENT or RESOURCE	SOURCE	IDENTIFIER
Cell lines		
HEK293T sgLuci	This paper	N/A
HEK293T sgDDI2	This paper	N/A
HEK293T sgRad23A/B cl.3	This paper	N/A
HEK293T sgRad23A cl.1	L. Zaffalon	N/A
HEK293T sgRad23A cl.3	L. Zaffalon	N/A
HEK293T sgRad23B cl.18	L. Zaffalon	N/A
HEK293T sgRad23B cl.19	L. Zaffalon	N/A
HeLa sgLuci	This paper	N/A
HeLa sgDDI2 #5	This paper	N/A
ARH77 sgLuci	(Op et al., 2022)	N/A
ARH77 sgDDI2 #30	(Op et al., 2022)	N/A
ARH77 sgDDI2 #30 p21 Ub-NRF1 7ND	This paper	N/A
ARH77 sgNRF1 #13	(Op et al., 2022)	N/A
ARH77 sgNRF1 #13 p21 NRF1	(Op et al., 2022)	N/A
ARH77 sgNRF1 #13 p21 Ub-NRF1	This paper	N/A
ARH77 sgNRF1 #13 p21 Ub-NRF1 7NA	This paper	N/A
ARH77 sgNRF1 #13 p21 Ub-NRF1 7ND	This paper	N/A

Supplementary table 3. List of oligonucleotides, related to Table 2.

REAGENT or RESOURCE	SOURCE	IDENTIFIER
Oligonucleotides		
single guide RNA targeting Luciferase forward: CAC CGC TTC GAA ATG TCC GTT CGG T	(Op et al., 2022)	N/A
single guide RNA targeting Luciferase reverse: AAA CAC CGA ACG GAC ATT TCG AAG C	(Op et al., 2022)	N/A
single guide RNA targeting DDI2 forward: CAC CGG CTC GAA GTC GGC GTC GAC	(Op et al., 2022)	N/A
single guide RNA targeting DDI2 reverse: AAA CGG TCG ACG CCG ACT TCG AGC C	(Op et al., 2022)	N/A
single guide RNA targeting NRF1 forward: CAC CGC TTT CTC GCA CCC CGT TGT C	(Op et al., 2022)	N/A
single guide RNA targeting NRF1 reverse: AAA CGA CAA CGG GGT GCG AGA AAG C	(Op et al., 2022)	N/A
single guide RNA targeting Rad23A exon 2 forward: CAC CGT GAG TTT CTG TCC AGC CAC G	This paper	N/A
single guide RNA targeting Rad23A exon 2 reverse: AAA CCG TGG CTG GAC AGA AAC TCA	This paper	N/A
single guide RNA targeting Rad23B tr59139 exon 4 forward: CAC CGC TAG CCC AAC AGC AAC TGA C	This paper	N/A
single guide RNA targeting Rad23B tr59139 exon 4 reverse: AAA CGT CAG TTG CTG TTG GGC TAG	This paper	N/A
single guide RNA targeting HRD1 exon 4 #1 forward: TCC CGT GAA GAG TGC AAC AAA GCG G	This paper	N/A
single guide RNA targeting HRD1 exon 4 #1 reverse: AAA CCC GCT TTG TTG CAC TCT TCA C	This paper	N/A
single guide RNA targeting HRD1 exon 4 #2 forward: TCC CGG CTG AAG TCA TCC CGA AAA A	This paper	N/A
single guide RNA targeting HRD1 exon 4 #2 reverse: AAA CTT TTT CGG GAT GAC TTC AGC C	This paper	N/A
qPCR primer for GAPDH housekeeping gene forward: CGC TCT CTG CTC CTC CTG TT	(Op et al., 2022)	N/A
qPCR primer for GAPDH housekeeping gene reverse: CCA TGG TGT CTG AGC GAT GT	(Op et al., 2022)	N/A
qPCR primer for RPL19 housekeeping gene forward: CAA GCG GAT TCT CAT GGA ACA CAT C	This paper	N/A
qPCR primer for RPL19 housekeeping gene reverse: CTT GAT GAT CTC CTC CTT CTT GGC	This paper	N/A
qPCR primer for GABARAPL1 gene forward: CCC TCC CTT GGT TAT CAT CCA	This paper	N/A
qPCR primer for GABARAPL1 gene reverse: ACT CCC ACC CCA CAA AAT CC	This paper	N/A
qPCR primer for STYK1 gene forward: AGC GTT CTG GAC CTC AAG G	This paper	N/A
qPCR primer for STYK1 gene reverse: ATA TTG GCT CGA AAG ATG GGC	This paper	N/A
qPCR primer for CLU gene forward: CGA GAA GGC GAC GAT GAC	This paper	N/A
qPCR primer for CLU gene reverse: GGT GGA ACA GTC CAC AGA CA	This paper	N/A

B. Additional Results to Research Article

B.1. Additional Material and Methods

Metabolic labelling and *in vitro* production of radioactive-labelled NRF1 protein. The *in vitro* transcription/translation of radio-labelled NRF1 protein was performed according to the kit protocol (TnT® coupled Reticulocyte Lysate System). The translation process was performed using a pCR3 NRF1 Flag-tagged plasmid with a CMV promoter. The radioactive labelling was enabled using ^{35}S-methionine/cysteine (10 µCi/µl). The *in vitro* ^{35}S NRF1 protein was loaded on an SDS-PAGE, transferred on a PVDF membrane, and analysed by autoradiography.

Production and purification of recombinant DDI2 protein from wheat germ extract. Large-scale *in vitro* production of recombinant DDI2 was performed according to the kit protocol (ENDEXT® Technology, premium PLUS expression kit). pEU-E01 Strep-tagged DDI2 plasmid was incubated for six hours at 37°C in presence of the transcription reaction mix. The translation reaction was performed by mixing the mRNA reaction with the wheat germ extract WEPRO1240. On top of this mix, the translation buffer was layered in a 96-well and incubated o/n at RT. Then, 250 U of Pierce Nuclease was added to the mix, with 1% of n-dodecyl β-D-maltoside when required, and incubated for 30 minutes at RT on a rotating wheel, then centrifuged at max speed for 30 minutes, 4°C. The supernatant was purified using *Strep*-Tactin® Sepharose columns according to kit protocol. The elution was quantified using BCA protein kit. Purified recombinant DDI2 was monitored by Western blot.

***In vitro* protease assay using synthetic substrates.** The protease assays were performed in 50 µl of HIV buffer (0.1 M NaOAc, 1 M NaCl, 1 mM EDTA, 1 mM DTT, 10% DMSO, 1 mg/ml BSA, pH 4.7) in 200 µl PCR tubes. 20 µg or 40 µg of recombinant DDI2 protein were incubated with 1 µl of ^{35}S NRF1 substrate (50 µM) for one hour at 37°C. The resulted protease assays were loaded on SDS-PAGE for subsequent Western blot analysis.

Additional table 1. List of additional reagents and resources.

REAGENT or RESOURCE	SOURCE	IDENTIFICATION
Antibodies		
Rabbit monoclonal anti-GABARAPL1	Cell Signaling Technology	Cat# 26632
Mouse monoclonal anti-Streptavidin	IBA Lifesciences	Cat# 2-1507-001
Chemicals, Peptides, and Recombinant Proteins		
CP-26	Anawa	Cat# AOB13238-1
Pierce Nuclease	Thermo Scientific	Cat# 88700
n-dodecyl β-D-maltoside	Thermo Scientific	Cat# 89902

Critical Commercial Assays		
TnT® coupled Reticulocyte Lysate System	Promega	Cat# L4600
ENDEXT® Technology, premium PLUS expression kit	CellFree Sciences Co.	Cat# CFS-EDX-PLUS
Pierce™ BCA Protein Assay Kit	Thermo Scientific	Cat# 23225
Strep-Tactin® Sepharose columns	IBA Lifesciences	Cat# 2-1202-001
Oligonucleotides		
qPCR primer for PSMD14 gene forward: CCG TGC TGG AGT TCC AAT	(Op et al., 2022)	N/A
qPCR primer for PSMD14 gene reverse: TGC CTC CAC ACT GAC ACC	(Op et al., 2022)	N/A
qPCR primer for PSMD12 gene forward: GTG CGC GAC TGA CTA AAA CA	Ribeiro S.T.	N/A
qPCR primer for PSMD12 gene reverse: TAG GCA GAG CCT CAT TTG CT	Ribeiro S.T.	N/A
qPCR primer for PSMD11 gene forward: ATG CAG GGA GGC AGA CAG	(Op et al., 2022)	N/A
qPCR primer for PSMD11 gene reverse: GGA GCT CTG CCC GGT AAT	(Op et al., 2022)	N/A
qPCR primer for PSMB7 gene forward: TGC AAA GAG GGG ATA CAA GC	Op M.	N/A
qPCR primer for PSMB7 gene reverse: GCA ACA ACC ATC CCT TCA GT	Op M.	N/A
Recombinant DNA		
pEU-E01	Jérôme Gouttenoire	N/A

B.2. Additional results

The investigation **II.D – Research Article – Results**, showed that NRF1 cleavage required ubiquitination, following its retrotranslocation from the ER, by the ubiquitin ligase HRD1 **(Figure 19)**. To corroborate with these observations, we also intended to block HRD1 activity through pharmacological agent. We treated ARH77 cells deficient for NRF1, reconstituted with an inducible form of full-length NRF1 or the cytosolic version (lacking the N-terminal domain) fused to ubiquitin at its N-terminus, with CP-26 - a small molecule inhibitor of HRD1 (Ruan et al., 2019) – along with Btz and monitored wild-type NRF1 and ubiquitinated cytosolic NRF1 cleavage **(Additional figure 1)**. We found that NRF1 cleavage was significantly reduced and in contrast, Ub-NRF1 cleavage remained intact, furthermore confirming the role of HRD1 in mediating NRF1 ubiquitination following ER-trafficking.

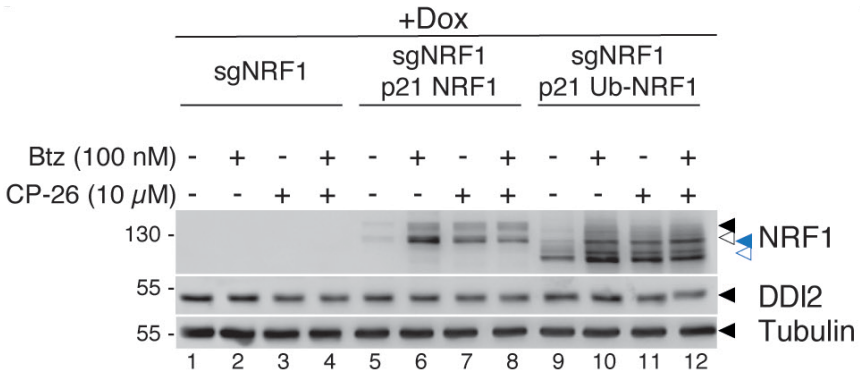

Additional figure 1. HRD1 mediates NRF1 ubiquitination following ERAD retrotranslocation. NRF1 cleavage in NRF1 knock-out (sgNRF1), or reconstituted with full-length NRF1 (sgNRF1 p21 NRF1) or NRF1 lacking its functional NTD but fused to ubiquitin moiety in N-terminus (sgNRF1 p21 Ub-NRF1) upon Doxycycline, in ARH77 cells treated with Btz and/or CP-26, an inhibitor of HRD1 for six hours as indicated. Protein expression is monitored by western blot. Tubulin is used as a loading control; ◀ indicates the unprocessed NRF1 protein; ◁ indicates the cleaved NRF1 protein; ◀ indicates the unprocessed NRF1 protein fused to ubiquitin moiety in N-terminus; ◁ indicates the cleaved NRF1 protein fused to ubiquitin moiety in N-terminus.

Moreover, while CLU gene expression profile was elicited to be DDI2 and NRF1-dependent **(Figure 21C and 21D)**, other gene expression profiles appeared to be upregulated in ARH77 cells expressing Ub-NRF1 7ND as well as upon endogenous NRF1 expression, like *STYK1* **(Figure 21C)** and *GABARAPL1* **(Additional figure 2A)**. While previous studies demonstrated the induction of *p62* and *GABARAPL1* upon proteasome inhibition (Sha et al., 2018), we were not surprised to find it following the RNA-sequencing analysis of ARH77 treated with Bortezomib. Although *Sha & collaborators* shown the induction of *GABARAPL1* upon proteasome inhibition, they did not connect it to NRF1 proteolytic activation.

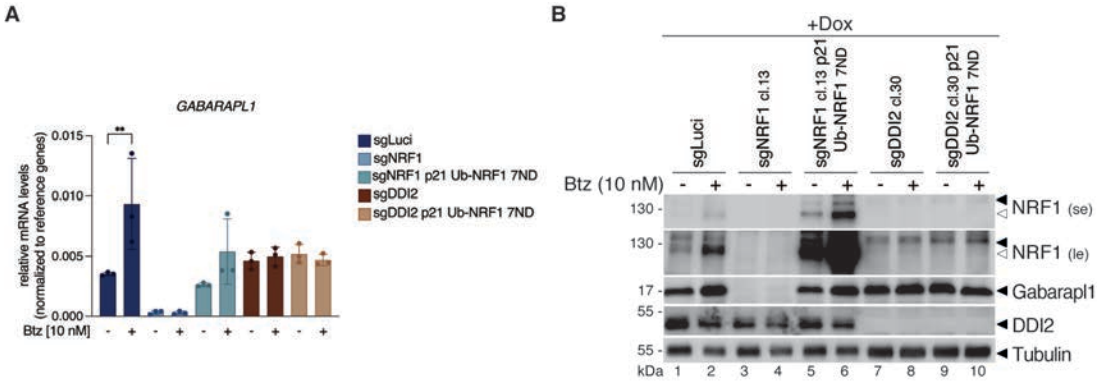

Additional figure 2. GABARAPL1 gene and protein expression profiles are NRF1-dependent. (**A**) Induction of GABARAPL1 gene measured in control (sgLuci), DDI2 knock-out (sgDDI2), NRF1 knock-out (sgNRF1) - or reconstituted with NRF1 lacking its functional NTD but fused to ubiquitin moiety in N-terminus and with N-glycosylation sites mutated into aspartic acid (p21 Ub-NRF1 7ND) - upon Doxycycline, in ARH77 cells treated with Btz for 24 hours as indicated. Gene expression profile was measured by real-time PCR relative to GAPDH and RPL19 (mean and SEM of technical triplicates of three representative experiment are shown). (**B**) As in A, but NRF1 cleavage is monitored by western blot. Tubulin is used as a loading control; ◀ indicates the unprocessed NRF1 protein; ◁ indicates the cleaved NRF1 protein; se: short image exposure; le: long image exposure.

To investigate this question, we interrogated the activity of GABARAPL1 gene upon N-D protein sequence editing of NRF1 by real-time qPCR analysis **(Additional figure 2A)** and by Western-blot **(Additional figure 2B)**. Whereas the observations by qPCR were not significantly convincing for *GABARAPL1* induction upon Ub-NRF1 7ND expression, the protein expression profile of GABARAPL1 formerly indicated that GABARAPL1 protein is dependent on NRF1 expression. Additionally, the Western-blot analysis of cells deficient for DDI2 demonstrates that GABARAPL1 expression is not dependent on NRF1 cleavage, suggesting that unprocessed NRF1 protein is able to enter the nucleus and activate downstream specific genes, such as *GABARAPL1*.

While new gene expression profiles were uncovered upon RNA-sequencing analysis, the dogma in the literature always supported the idea that the DDI2-NRF1 pathway was involved in the bounce-back response to proteasome impairment by upregulating proteasome gene expression, as mentioned earlier in the study. Although some proteasome genes were upregulated but only by 2-fold induction in the RNA-sequencing analysis, we sought to interrogate their expression by real-time qPCR.

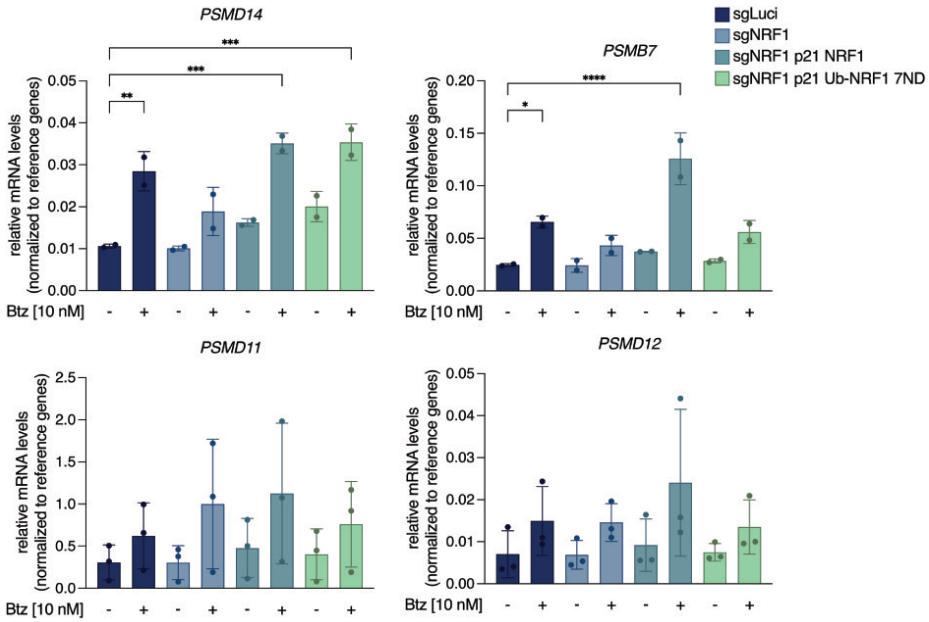

Additional figure 3. Proteasome subunits gene expression profiles upon proteasome inhibition. ARH77 control (sgLuci), NRF1 knock-out (sgNRF1) - or reconstituted with wild-type NRF1 or NRF1 lacking its functional NTD but fused to ubiquitin moiety in N-terminus and with N-glycosylation sites mutated into aspartic acid (p21 Ub-NRF1 7ND) - upon Doxycycline, cells treated with Btz for 24 hours as indicated. Proteasome subunits (PSM) mRNA expression analysis by real-time PCR relative to GAPDH and RPL19 (mean and SEM of technical triplicates of three or two representative experiments are shown).

Btz-mediated induction of proteasome subunits genes appeared irregularly regulated in the different conditions **(Additional figure 3)**. Whereas *PSMD14* and *PSMB7* were significantly upregulated upon NRF1 expression, and also upon Ub-NRF1 7ND for *PSMD14*, *PSMD11* and *PSMD12* profiles were inconsistent. To corroborate studies performed in our laboratory (Op et al., 2022) and the results of the RNA-sequencing analysis, these observations indicated that the DDI2-NRF1 pathway contributes, at least in part, to the proteasome feedback-loop in ARH77 cells.

Finally, in chapter **I – Aim of the Thesis**, we sought to answer the following question: How is DDI2 activated? Although we described in detail the different steps leading to DDI2-mediated NRF1 cleavage and activation, the question about DDI2 activity remained to be answered.

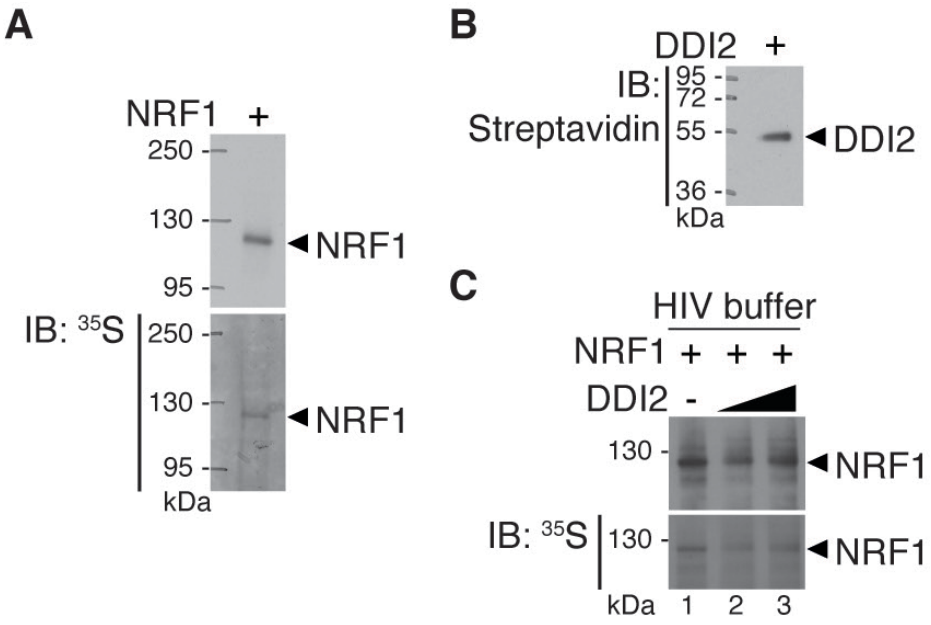

Additional figure 4. Cell-free based protein synthesis and assay. (**A-B**) Western-blot analysis of radio-labelled ^{35}S NRF1 *in vitro* translated protein (**A**) and recombinant Streptavidin-tagged DDI2 protein (**B**). (**C**) *In vitro* cleavage assay of ^{35}S NRF1 in presence of increasing concentration of recombinant DDI2 (20 µg and 40 µg), in HIV buffer for one hour at 37°C. Protein expression is assessed by Western-blot analysis.

As explained in chapter **I.F.1. – Introduction**, the HIV-1 protease and DDI2 shares strong homology structure. It is naturally that our investigations towards DDI2 activity turned to the studies investigating the activation of the HIV-1 protease.

Beforehand, we first successfully generated soluble *in vitro* protein for NRF1 and DDI2 **(Additional figures 4A and 4B)**. To avoid non-specific interaction due to inherent proximity-induced in a cell-free based assay, both proteins were synthetized through two different approaches (see **II.G.1. – Results**). Since we demonstrated that DDI2 was interacting with NRF1 **(Figures 18G, 18H and 18I)**, we simplified our study model by using in vitro translated NRF1 as a read-out of DDI2 activity following incubation in a buffer at acidic pH (hereafter "HIV buffer") since it is an essential parameter enabling the correct protonation of the aspartic acids localized in the active site of aspartyl proteases (Xie et al., 1997). Results demonstrated that radio-labelled NRF1 protein remained uncleaved following incubation in HIV buffer in presence of recombinant DDI2 **(Additional figure 4C)**. In conclusion, these conditions did not enable the activation of DDI2 *in vitro*. Further studies on the biochemical characteristics of this protease are required to gain a better understanding of its mechanism of activation.

In the literature, HIV-PIs were demonstrated to target the RVP domain of the HIV protease and, *de facto*, several indications reported that the RVP domain of DDI2 is responsible for its proteolytic activity. In addition, on top of being extensively conserved through evolution in eukaryotes, the DDI2 RVP domain is present in bacteria and lower organisms (Krylov & Koonin, 2001; Morawe et al., 2011; Sato et al., 2000; Sirkis et al., 2006). This highly sequence conservation indicates that the RVP domain is responsible for essential functions in these organisms, like the proteolytic cleavage of substrates. To reinforce the proteolytic activity hypothesis of DDI2, its ortholog in *Leishmania* and its homolog in human, the SASPase protein, were identified as active proteases (Matsui et al., 2011; Perteguer et al., 2013). Moreover, HIV-PIs have demonstrated their inhibitory capacity by blocking the substrate cleavage of these proteins (Bernard et al., 2005; White et al., 2011). Recent studies suggested that the HIV-PIs, Nelfinavir (NFV), inhibits DDI2 (Gu et al., 2020). NFV was initially developed to target the RVP domain of HIV protease and was reported with off-target effects in human presenting anti-cancer properties (Kawabata et al., 2012; Kraus et al., 2013). Because of the shared homology structure of HIV and DDI2 RVP domains, NFV was the first candidate inhibitor to study DDI2 activity.

To investigate DDI2 activity, our approach aimed at producing a recombinant protein for DDI2 and analyze its activity against a synthetic substrate. To overcome the inconveniences of synthetically producing conformationally active protein, we took advantage of the intensive thesis work of a former colleague, Gianluca Frera, where he uncovered different techniques to produce soluble synthetic substrates (Frera, 2015). Particularly, he showed that he could produce high levels of recombinant proteins using wheat germ extract, which were formerly successfully used for the generation of an active HCV protease (Pieroni et al., 1997). In addition, at this time in the laboratory, the current literature just reported NRF1 as a substrate of DDI2 (Koizumi et al., 2016).

Nevertheless, synthetic NRF1 cleavage failed, following incubation at acidic pH, in presence of purified recombinant DDI2. Although, one example of *in vitro* protease assay was described in this study **(Additional figure 4C)**, we have tested several conditions in an attempt to trigger DDI2 activity *in vitro*. It seems that other factors are required to convey *in vitro* reconstitution of NRF1 cleavage by DDI2, such as a set of specific experimental set-up, co-activators of DDI2, and substrate unfolding.

As of experimental conditions, the reaction buffer composition is of primary importance when designing an *in vitro* protease assay. To boost synthetic DDI2 activity, we thought an acidic pH would be adapted as it enables the correct protonation required for the proteolytic activity of aspartic proteases (Suguna et al., 1987). In addition, where these enzymes usually reside in

acidic compartments, such as lysosomes (Conner, 1992; Kinoshita et al., 2003; Matsui et al., 2011; Richter et al., 1998), DDI2 appeared to be localized in the cytosol **(Figures 16A and 16B)**. A few biochemical techniques are established to investigate the optimal buffer required for a specific proteolytic activity, but their success rely on the substrate cleavage efficiency. Therefore, it is of high importance to gain more insights on DDI2 cellular function, – which could uncover the presence of specific co-activators essential to mediate its activity *in vitro* – and on the mechanisms of activation of DDI2 substrate, NRF1.

IV. DISCUSSION

At the beginning of my PhD, DDI2 was discovered as the executor protease of NRF1 cleavage. Early papers showed that DDI2 was cleaving NRF1 at the N-terminus (at Tryptophan 103) to enforce proteasome subunit synthesis in response to proteasomal impairment (Koizumi et al., 2016; Radhakrishnan et al., 2014). Subsequently, we and others found that NRF1 N-terminus triggers ER-trafficking where it is N-glycosylated before being retrotranslocated through the ERAD pathway for subsequent proteasomal degradation. The discovery of DDI2 proteolytic cleavage ensued many questions surrounding the mechanism of activation of its substrate NRF1 and its role in re-establishing proteasomal integrity in response to proteasome dysfunction.

During my PhD work I focused on the different mechanistic steps involved upstream of NRF1 cleavage in presence or absence of DDI2. In all, I was able to contribute to the deeper characterization and understanding of these mechanisms e.g. demonstrating the essentiality of ER-trafficking and ubiquitination in allowing DDI2-mediated NRF1 cleavage and also provided new evidence that proteolytically active NRF1 triggers different transcriptional programs than the proteasome bounce-back response.

Here I will integrate our findings with present literature, critically interrogate our data and pin-point shortcomings and future perspectives of this project.

The ER is widely known for its role in targeted transportation of proteins that are embedded in membranes, retained in specific cellular compartments, or released extracellularly (Stevenson et al., 2016). Therefore, today we conveyed a new role for the ER in orchestrating the transportation of a protein destined for proteolytic activation in the cytosol: the transcription factor NRF1. We shed light on the two main regulatory functions of the ER in enabling NRF1 processing which are its ubiquitination and N-glycosylation.

Our work shows that a 30-amino acid sequence within the N-terminus of NRF1 is required for its import into the ER and subsequent processing by DDI2. The study also highlights the role of HRD1 in directing NRF1 to proteolytic maturation by DDI2 when proteasome-mediated degradation is impaired. Additionally, we describe the involvement of RAD23 in both NRF1-mediated proteasome degradation and NRF1 proteolytic maturation by DDI2. Finally, the study shows that glycosylation and editing of glycosylated asparagine residues into aspartic acid do not impact NRF1 processing by DDI2. Altogether, these data convey a rather complicated but unique signal transduction of NRF1 upstream of its cleavage by DDI2 **(Figure 22)**.

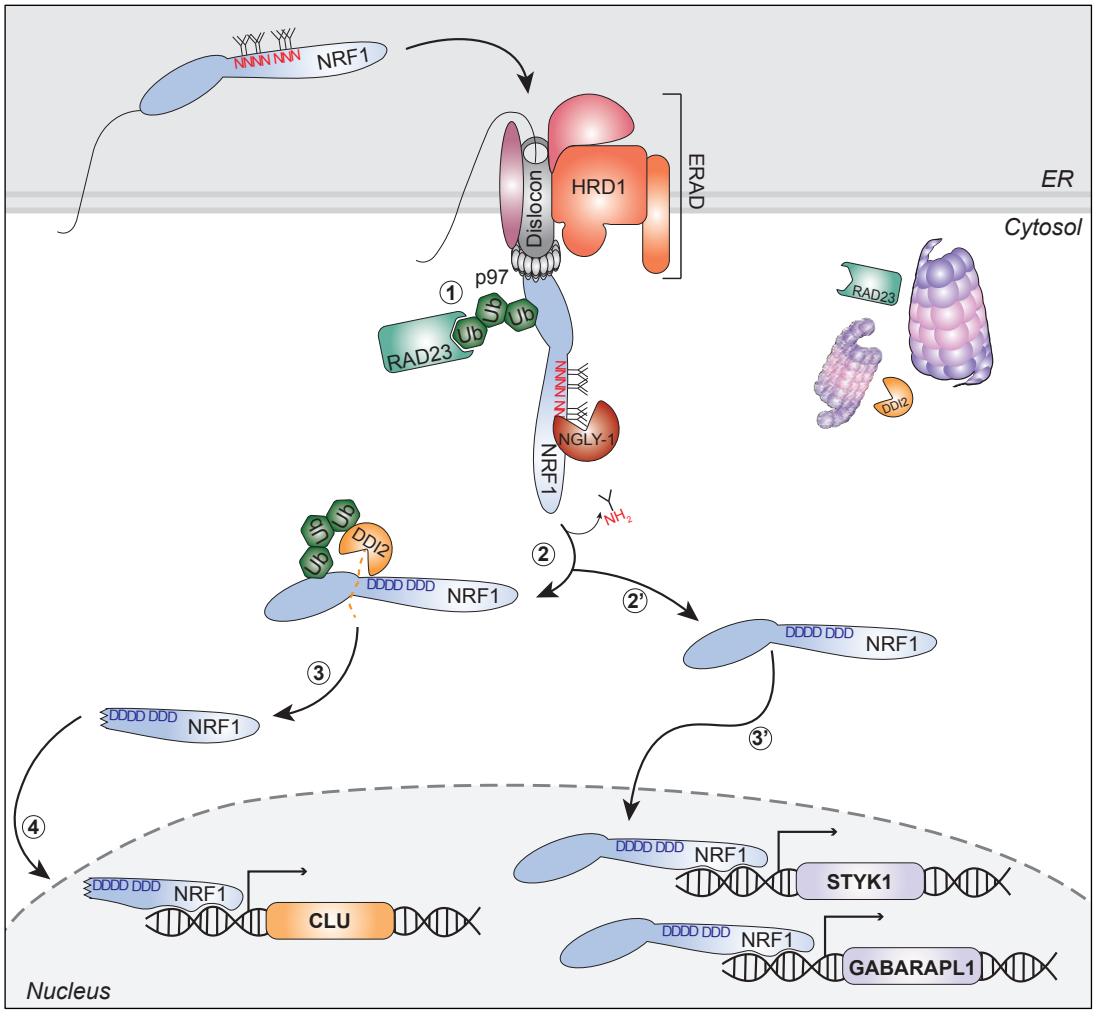

Figure 22. The signal transduction of NRF1 upon proteasome inhibition or overload. NRF1 is an ER-associated protein with its N-terminal transmembrane region anchored to the ER membrane. In the ER, NRF1 undergoes N-glycosylation. Upon proteasomal dysfunction, glycosylated NRF1 is retrotranslocated through ERAD. Following retrotranslocation, glycosylated and ubiquitinated NRF1 is (**1**) recognized by RAD23 and (**2**) concomitantly deglycosylated by the peptide:N-glycanase NGLY-1. (**3**) The shuttle protein RAD23 then transmit deglycosylated NRF1 to DDI2 for subsequent proteolytic cleavage. (**4**) Deglycosylated and cleaved NRF1 enters the nucleus to activate DDI2-dependent genes, like *CLU*. Alternatively, we may have uncovered that (**2'**) subsequently to deglycosylation by NGLY-1, (**3'**) deglycosylated and uncleaved NRF1 can enter the nucleus to induce the activation of NRF1-dependent and DDI2-independent genes, like *STYK1* or *GABARAPL1*.

Why is NRF1 mechanism of activation so complicated?

In line with the discovery on the role of NRF1 in sensing cholesterol excess in the ER (Widenmaier et al., 2017), we cannot rule out the possibility that NRF1 may have additional functions within the ER. It may function as a sensor of ER homeostasis. Indeed, it was suggested that cholesterol regulates NRF1 localization, processing, turnover and transcriptional activity (Widenmaier et al., 2017). In our study, we underlined how NRF1 localization, modification, processing, and transcriptional activity are influenced by proteasomal dysfunction. Overall, we can hypothesize that NRF1, upon entry in the ER, senses environmental stimuli that will influence its fate in the cell. How this sensing is done, or which triggers are involved, have yet to be investigated.

Another important observation we made is the fact that the biological mechanisms involved in NRF1 stabilization also control the susceptibility to DDI2 cleavage. We showed that RAD23 binding to DDI2 is stabilized in presence of proteolytically inactive DDI2. RAD23 is described as a ubiquitin receptor, able to bind the proteasome through its N-terminus ubiquitin fold and holds two UBA domains which bind ubiquitinated substrates upon ERAD-retrotranslocation (Collins & Goldberg, 2020; Kim & Goldberg, 2018; Wade & Auble, 2010). This observation is consistent with the fact that RAD23 may function as a proteasome receptor that targets NRF1 to the proteasome while functioning also as a DDI2 receptor required for NRF1 targeting by DDI2. As for how RAD23 decides to act as a proteasome shuttle or a receptor for DDI2 remain to be elucidated. Here, the factor that will influence this decision is the proteasome function. Indeed, DDI2 is engaged only when the proteasome is non-functional. Whether DDI2 function within the proteasome complex or within a separate complex, with RAD23 possibly, is a question that remains to be addressed.

Importantly, our observations highlighted the conservation of NRF1 deamidation by the N-glycanase PNG-1/NGLY-1 in mammals. Similarly, to ER-trafficking and ubiquitination, NRF1 deamidation is a key step in determining the activation of different transcriptional program. The conservation of such a phenomenon across species is reflective of an important functional role in maintaining NRF1 activity. This process underlines the immense diversity of the proteome where the final amino acid sequence of a protein is not directly encoded in the DNA but reassembled enzymatically in an ER-dependent process.

It is also worth noting that whereas it was suggested that uncleaved NRF1 was inactive in the nucleus (Northrop et al., 2020), our real-time PCR data demonstrated that unprocessed NRF1 was able to activate different transcriptional program that are DDI2-independent. These observations suggested that uncleaved and deaminated NRF1 is transcriptionally active in the nucleus. Altogether, these findings propose a leading role for NGLY-1 in determining cell fate through NRF1 deamination. It is unlikely that NRF1 is the only substrate subject to

NGLY-1 deglycosylation and therefore, it would be interesting to investigate additional substrates, their function, and their conservation among species.

Although we strengthened our knowledge on the underlying biological regulation of DDI2-mediated NRF1 cleavage, the biological characterization of DDI2 remains to be evaluated in detail to convey its function. As a result, we also worked on the molecular characterization of DDI2 activity *in vitro*.

How is the protease DDI2 activated?

For the treatment of HIV positive patients, HIV protease inhibitors (HIV-PIs) are widely used in the clinic. Nevertheless, the presence of undesired side effects remains and results as an off-target effect blocking cellular pathways. Our working hypothesis suggests that HIV-PIs are able to target and block cellular proteins while interfering with cellular processes, thus generating the secondary effects observed. To interrogate this question, we studied the aspartyl protease DDI2, which shares structural homology with the HIV protease, to provide a functional rationale of the side effects pathophysiology of HIV-PIs. In human, no evidence pointed out this protease as a target of HIV-PIs. Additionally, no functional studies ever reported proof of DDI2 cellular function to our knowledge.

To investigate DDI2 activity, our approach aimed at using a recombinant DDI2 protein and analyze its activity against an NRF1 synthetic substrate. We were not able to convey synthetic NRF1 cleavage *in vitro* **(Additional figure 4C)** at acidic pH, we have tested several conditions in an attempt to trigger DDI2 activity *in vitro*. We concluded that other factors are required to convey *in vitro* reconstitution of NRF1 cleavage by DDI2, such as a set of specific experimental set-up, co-activators of DDI2, and substrate unfolding.

As a result of unsuccessful *in vitro* characterization of DDI2 activity, the quest of finding DDI2 inhibitors became challenging. Whereas, as mentioned earlier, NFV was presented as an excellent candidate for DDI2 inhibition, it became challenging to test its inhibitory properties. Therefore, our laboratory started to interrogate DDI2 function in a different system. This study was led by a former colleague, Mélanie Op, and we demonstrated that NFV was able to disrupt NRF1 cleavage at basal conditions **(VI.A. – Figure 5a)**, suggesting a likely NFV-mediated DDI2 inhibition (Op et al., 2022). Although NRF1 cleavage was disrupted, NFV only partially inhibited DDI2 in this set-up in comparison to its effect on HIV-1 protease. We also tested several analogs to NFV, and none conveyed an impact on NRF1 cleavage (Op et al., 2022). Whereas NFV was designed to inhibit HIV-1, we suspect that the affinity of NFV for DDI2 is not sufficient to elicit a strong inhibition.

Additionally, in this study we gained insights on potential DDI2 co-factors involved in its proteolytic activity. We uncovered the conjugation of Rad23B with DDI2 **(Figure 20F)**, thereby promoting NRF1 cleavage and may explain our failures at engineering a working *in*

vitro assay for DDI2 activity. This discovery corroborated the initial findings of Dirac-Svejstrup *& al.* where they showed that DDI2 cleaves NRF1 *in vitro* uniquely in presence of Rad23 (Dirac-Svejstrup et al., 2020b), as well as the findings on yeast Ddi1 and Rad23 being able to form a complex (Bertolaet et al., 2001a). If Rad23B and other ubiquilins (UBQLNs; the mammalian Dsk2 homologs) **(Figure 14)** are established as shuttling factors involved in ERAD (Medicherla et al., 2004), DDI2 was recently suggested to serve as a shuttling factor, despite the absence of the typical Ub-binding domain (UBA domain) (Collins et al., 2022). The term "shuttling factor" implies a delivery process from one site to proteasomes (Medicherla et al., 2004; Richly et al., 2005). Literature have shown that Rad23B can activate proteasomes when it binds the 26S particle (Collins & Goldberg, 2020; Kim & Goldberg, 2018) and dissociate once the proteasome begins to process the ubiquitylated substrate (Kuo & Goldberg, 2017). And DDI2 has been similarly described to activate proteasomes (Kim & Goldberg, 2018). Paradoxically, our findings suggest that DDI2 requires Rad23B *in vivo* rather than working as a shuttling factor of NRF1 following its retrotranslocation from the ER. Hence, to explain Rad23B conjugation with DDI2, it is possible that Rad23 is functioning as a shuttling factor while DDI2 acquired different function such as its proteolytic activity towards NRF1.

Finally, as mentioned, when designing an *in vitro* assay, the folding of the substrate is always of great challenge. In the case of NRF1, we demonstrated the multiple steps NRF1 has to go through to be cleaved by DDI2 *in vivo*. Remarkably, we generated a cytosolic version of NRF1 fused to a ubiquitin moiety that is able to bypass the requirement of ER-trafficking and retrotranslocation but can undergo DDI2 cleavage in an HRD1-independent manner. The development of this tool holds the potential to be a game-changer when establishing an *in vitro* system to test for DDI2 activity.

Altogether, these studies offer a promising hope in producing a synthetically active recombinant Rad23 to test *in vitro* along with recombinant DDI2, towards a Ub-NRF1 synthetic substrate, in adequate conditions. Such an approach will allow not only to screen for multiple chemical compounds, like commercial libraries of HIV inhibitors, but also to generate other analogs of NFV through bioinformatic approaches to find the best match for DDI2 (Guan et al., 2015).

The extensive interest to target DDI2 in cancer therapy is no more to be presented. Following our findings on the role of DDI2 in multiple myeloma (Op et al., 2022) and in response to heavy metal mediated toxicity (Ribeiro et al., 2022), DDI2 is at the center of stress related-pathways where the necessity to understand its function(s) would be game-changing in the clinic.

But what is the function of DDI2?

Physiological investigations of the role of DDI2 *in vivo* allowed us to uncover that DDI2 knock-out in mice is embryonic lethal (Ribeiro et al., 2022), indicating a role for the protease during development. This observation corroborated with the essential role of NRF1 during embryonic development. Indeed, studies in the field revealed the essentiality of NRF1 to sustain normal embryonic development in mammals and established that defect in NRF1 most likely resulted in failed proteasomal function (L. Chen et al., 2003; Kim et al., 2010; Kobayashi et al., 2011; Lee et al., 2011; Ohtsuji et al., 2008; Widenmaier et al., 2017; Xu et al., 2005). From our observations from DDI2 knock-out mice, we can speculate that the disruption of the DDI2-NRF1 pathway is the leading cause of proteasome dysfunction, triggering embryonic lethality in mammals.

Interestingly, while the implication of the UPS in the development of neurodegenerative diseases and NRF1 in neuronal homeostasis are widely established, this work enabled to uncover a potential role for DDI2 in driving this phenotype. Earlier, we discussed on the function of CLU gene which mRNA levels appeared to be enriched in a DDI2-dependent manner **(Figure 21D)**. Gene ontology revealed its involvement in the regulation of neuronal signal transduction and in positive regulation of neuronal proteins assembly. Moreover, GWAS studies depicted that single nucleotide polymorphisms (SNPs) within *CLU* are representative risk factors of Alzheimer's diseases (AD) (Bertram et al., 2007; Harold et al., 2009) and CLU proteins levels are correlated to the severity of cerebral amyloid angiopathy (Miners et al., 2017). In fact, the role of the CLU gene in AD is widely studied and depicted at the current moment (Wilson & Zoubeidi, 2017). Together our data encourage the hypothesis that the DDI2-NRF1 pathway is involved in neurodegeneration phenotypes. We can propose a role for DDI2 which, upon proteasomal dysregulation, leads to the transcription of CLU proteins which accumulates, thus driving the development of neurodegenerative diseases.

In comparison to *CLU*, STYK1 mRNA levels were not enriched in a DDI2-dependent manner **(Figure 21D)**. Although, both genes are widely described in the literature as involved in many human cancers (X. Chen et al., 2003; Fang et al., 2018; Girard et al., 2010; July et al., 2002; Lai et al., 2021; Lai et al., 2019; Li et al., 2020; Miyake, Gleave, et al., 2002; Miyake, Hara, et al., 2002; Miyake et al., 2005; Redondo et al., 2000; Steinberg et al., 1997). CLU and STYK1 are depicted as essential proteins of protein homeostasis and, whereas there are not classified as oncogenes, their high expression is correlated with higher grade tumors and poor prognosis. In combination with our knowledge on the key role of the UPS in the maintenance of proteostasis, we suspect that overexpression of *CLU* and *STYK1* upon DDI2-mediated NRF1 cleavage is one of the leading causes of the development of these cancers.

While inhibition over-time of the proteasome irretrievably induces the accumulation of ubiquitinated proteins in the cytosol, the cellular adaptation programs activate autophagy pathway, and these proteins are degraded through lysosomal degradation (Korolchuk et al., 2010; Pankiv et al., 2007). Interestingly, STYK1 was recently described as a new upstream regulator of autophagy (Zhou et al., 2020). Whereas GABARAPL1 gene turned-out enriched in the RNA-sequencing analysis **(Figure 21B)** and by real-time PCR for NRF1 wild-type **(Additional figure 2A)**, as well as by Western-blot analysis **(Additional figure 2B)**, the gene did not seem to be dependent of DDI2-mediated cleavage. Nevertheless, the GABARAPL1 gene was established as involved in the phagophore maturation during autophagy (An et al., 2019; Chakrama et al., 2010; Chen et al., 2006; Chino et al., 2019). Together with STYK1, these observations allow us to extrapolate on a potential role for NRF1 – along with DDI2 or not – in enhancing autophagy-related pathway in response to proteasome inhibition. Particularly, autophagy is described to reduce cellular stress induced by proteasome inhibitors and would probably impact the efficiency of proteasome inhibitors on multiple myeloma therapies. In this situation, targeting DDI2 in multiple myeloma phenotypes holds the potential to decrease both proteasomal and lysosomal degradation of misfolded proteins, and would drastically enhance the sensitivity of multiple myeloma cancer cells to proteasome inhibition.

Collectively, the current knowledge on DDI2 function is wide and still remain to be characterized in more detail. These discoveries enabled to shed light on new physiological roles of the DDI2-NRF1 pathway and emphasized the essentiality to study DDI2 activity more than ever as a key protease of protein homeostasis.

In conclusion, this study reported new discoveries essential to understand better the role of the DDI2-NRF1 pathway. We showed that not only ER-trafficking and subsequent ubiquitination were implicated in targeting proteins for proteasomal degradation but were essential in enabling DDI2-mediated NRF1 cleavage. Interestingly, we uncovered a potential new role for the shuttling factor Rad23B in triggering DDI2 activity. Finally, we conveyed that N-D sequence editing of NRF1 following its retrotranslocation from the ER was a pre-requisite for its transcriptional activation in mammals. Altogether, these data brought new insights on the mechanisms of activation of NRF1 which are essential to deepen our study of DDI2 activity. A better understanding of DDI2 would allow to screen for pharmacological inhibitors which holds the potential to improve targeted cancer therapies, and eventually other diseases.

Overall, since the beginning of my PhD, great advances have been made in uncovering new mechanistical details of DDI2-mediated NRF1 activation. These studies open the way for important questions that remain to be answered and will need to be interrogated in the future.

V. REFERENCES

Acosta-Alvear, D., Cho, M. Y., Wild, T., Buchholz, T. J., Lerner, A. G., Simakova, O., Hahn, J., Korde, N., Landgren, O., Maric, I., Choudhary, C., Walter, P., Weissman, J. S., & Kampmann, M. (2015). Paradoxical resistance of multiple myeloma to proteasome inhibitors by decreased levels of 19S proteasomal subunits. *Elife*, *4*, e08153. https://doi.org/10.7554/eLife.08153

Aebi, M., Bernasconi, R., Clerc, S., & Molinari, M. (2010). N-glycan structures: recognition and processing in the ER. *Trends Biochem Sci*, *35*(2), 74-82. https://doi.org/10.1016/j.tibs.2009.10.001

Agarwal, A. K., Xing, C., DeMartino, G. N., Mizrachi, D., Hernandez, M. D., Sousa, A. B., Martinez de Villarreal, L., dos Santos, H. G., & Garg, A. (2010). PSMB8 encoding the beta5i proteasome subunit is mutated in joint contractures, muscle atrophy, microcytic anemia, and panniculitis-induced lipodystrophy syndrome. *Am J Hum Genet*, *87*(6), 866-872. https://doi.org/10.1016/j.ajhg.2010.10.031

Ahmed, N., Zeng, M., Sinha, I., Polin, L., Wei, W. Z., Rathinam, C., Flavell, R., Massoumi, R., & Venuprasad, K. (2011). The E3 ligase Itch and deubiquitinase Cyld act together to regulate Tak1 and inflammation. *Nat Immunol*, *12*(12), 1176-1183. https://doi.org/10.1038/ni.2157

Aki, D., Li, H., Zhang, W., Zheng, M., Elly, C., Lee, J. H., Zou, W., & Liu, Y. C. (2018). The E3 ligases Itch and WWP2 cooperate to limit T(H)2 differentiation by enhancing signaling through the TCR. *Nat Immunol*, *19*(7), 766-775. https://doi.org/10.1038/s41590-018-0137-8

An, H., Ordureau, A., Paulo, J. A., Shoemaker, C. J., Denic, V., & Harper, J. W. (2019). TEX264 Is an Endoplasmic Reticulum-Resident ATG8-Interacting Protein Critical for ER Remodeling during Nutrient Stress. *Mol Cell*, *74*(5), 891-908 e810. https://doi.org/10.1016/j.molcel.2019.03.034

Anckar, J., & Sistonen, L. (2011). Regulation of HSF1 function in the heat stress response: implications in aging and disease. *Annu Rev Biochem*, *80*, 1089-1115. https://doi.org/10.1146/annurev-biochem-060809-095203

Ansar, M., Ebstein, F., Ozkoc, H., Paracha, S. A., Iwaszkiewicz, J., Gesemann, M., Zoete, V., Ranza, E., Santoni, F. A., Sarwar, M. T., Ahmed, J., Kruger, E., Bachmann-Gagescu, R., & Antonarakis, S. E. (2020). Biallelic variants in PSMB1 encoding the proteasome subunit beta6 cause impairment of proteasome function, microcephaly, intellectual disability, developmental delay and short stature. *Hum Mol Genet*, *29*(7), 1132-1143. https://doi.org/10.1093/hmg/ddaa032

Arima, K., Kinoshita, A., Mishima, H., Kanazawa, N., Kaneko, T., Mizushima, T., Ichinose, K., Nakamura, H., Tsujino, A., Kawakami, A., Matsunaka, M., Kasagi, S., Kawano, S., Kumagai, S., Ohmura, K., Mimori, T., Hirano, M., Ueno, S., Tanaka, K., . . . Yoshiura, K. (2011). Proteasome assembly defect due to a proteasome subunit beta type 8 (PSMB8) mutation causes the autoinflammatory disorder, Nakajo-Nishimura syndrome. *Proc Natl Acad Sci U S A*, *108*(36), 14914-14919. https://doi.org/10.1073/pnas.1106015108

Asahina, M., Fujinawa, R., Nakamura, S., Yokoyama, K., Tozawa, R., & Suzuki, T. (2020). Ngly1 -/- rats develop neurodegenerative phenotypes and pathological abnormalities in their peripheral and central nervous systems. *Hum Mol Genet*, *29*(10), 1635-1647. https://doi.org/10.1093/hmg/ddaa059

Bachmaier, K., Krawczyk, C., Kozieradzki, I., Kong, Y. Y., Sasaki, T., Oliveira-dos-Santos, A., Mariathasan, S., Bouchard, D., Wakeham, A., Itie, A., Le, J., Ohashi, P. S., Sarosi, I., Nishina, H., Lipkowitz, S., & Penninger, J. M. (2000). Negative regulation of lymphocyte activation and autoimmunity by the molecular adaptor Cbl-b. *Nature*, *403*(6766), 211-216. https://doi.org/10.1038/35003228

Balch, W. E., Morimoto, R. I., Dillin, A., & Kelly, J. W. (2008). Adapting proteostasis for disease intervention. *Science*, *319*(5865), 916-919. https://doi.org/10.1126/science.1141448

Balchin, D., Hayer-Hartl, M., & Hartl, F. U. (2016). In vivo aspects of protein folding and quality control. *Science*, *353*(6294), aac4354. https://doi.org/10.1126/science.aac4354

Baldridge, R. D., & Rapoport, T. A. (2016). Autoubiquitination of the Hrd1 Ligase Triggers Protein Retrotranslocation in ERAD. *Cell*, *166*(2), 394-407. https://doi.org/10.1016/j.cell.2016.05.048

Bar-Peled, L., & Sabatini, D. M. (2014). Regulation of mTORC1 by amino acids. *Trends Cell Biol*, *24*(7), 400-406. https://doi.org/10.1016/j.tcb.2014.03.003

Beck, D. B., & Aksentijevich, I. (2019). Biochemistry of Autoinflammatory Diseases: Catalyzing Monogenic Disease. *Front Immunol*, *10*, 101. https://doi.org/10.3389/fimmu.2019.00101

Bernard, C., Greene, H. C., & Henderson, L. J. (1927). *An Introduction to the Study of Experimental Medicine ... Translated by Henry Copley Creene ... With an introduction by Lawrence J. Henderson*. Macmillan Co.

Bernard, D., Mehul, B., Thomas-Collignon, A., Delattre, C., Donovan, M., & Schmidt, R. (2005). Identification and characterization of a novel retroviral-like aspartic protease specifically expressed in human epidermis. *J Invest Dermatol*, *125*(2), 278-287. https://doi.org/10.1111/j.0022-202X.2005.23816.x

Bernasconi, R., Pertel, T., Luban, J., & Molinari, M. (2008). A dual task for the Xbp1-responsive OS-9 variants in the mammalian endoplasmic reticulum: inhibiting secretion of misfolded protein conformers and enhancing their disposal. *J Biol Chem*, *283*(24), 16446-16454. https://doi.org/10.1074/jbc.M802272200

Bertolaet, B. L., Clarke, D. J., Wolff, M., Watson, M. H., Henze, M., Divita, G., & Reed, S. I. (2001a). UBA domains mediate protein-protein interactions between two DNA damage-inducible proteins. *Journal of Molecular Biology*, *313*(5), 955-963. https://doi.org/10.1006/jmbi.2001.5105

Bertolaet, B. L., Clarke, D. J., Wolff, M., Watson, M. H., Henze, M., Divita, G., & Reed, S. I. (2001b). UBA domains of DNA damage-inducible proteins interact with ubiquitin. *Nat Struct Biol*, *8*(5), 417-422. https://doi.org/10.1038/87575

Bertolotti, A. (2011). *Protein Chaperones and Protection from Neurodegenerative diseases* (S. N. Witt, Ed.). Wiley-Blackwell.

Bertram, L., McQueen, M. B., Mullin, K., Blacker, D., & Tanzi, R. E. (2007). Systematic meta-analyses of Alzheimer disease genetic association studies: the AlzGene database. *Nat Genet*, *39*(1), 17-23. https://doi.org/10.1038/ng1934

Besse, L., Besse, A., Stolze, S. C., Sobh, A., Zaal, E. A., van der Ham, A. J., Ruiz, M., Phuyal, S., Buchler, L., Sathianathan, M., Florea, B. I., Boren, J., Stahlman, M., Huber, J., Bolomsky, A., Ludwig, H., Hannich, J. T., Loguinov, A., Everts, B., . . . Driessen, C. (2021). Treatment with HIV-Protease Inhibitor Nelfinavir Identifies Membrane Lipid Composition and Fluidity as a Therapeutic Target in Advanced Multiple Myeloma. *Cancer Res*, *81*(17), 4581-4593. https://doi.org/10.1158/0008-5472.CAN-20-3323

Biswas, M., Kwong, E. K., Park, E., Nagra, P., & Chan, J. Y. (2013). Glycogen synthase kinase 3 regulates expression of nuclear factor-erythroid-2 related transcription factor-1 (Nrf1) and inhibits pro-survival function of Nrf1. *Experimental Cell Research*, *319*(13), 1922-1931. https://doi.org/10.1016/j.yexcr.2013.04.013

Biswas, M., Phan, D., Watanabe, M., & Chan, J. Y. (2011). The Fbw7 Tumor Suppressor Regulates Nuclear Factor E2-related Factor 1 Transcription Factor Turnover through Proteasome-mediated Proteolysis. *Journal of Biological Chemistry*, *286*(45), 39282-39289. https://doi.org/10.1074/jbc.M111.253807

Blackwell, T. K., Steinbaugh, M. J., Hourihan, J. M., Ewald, C. Y., & Isik, M. (2015). SKN-1/Nrf, stress responses, and aging in Caenorhabditis elegans. *Free Radic Biol Med*, *88*(Pt B), 290-301. https://doi.org/10.1016/j.freeradbiomed.2015.06.008

Blobel, G., & Dobberstein, B. (1975). Transfer of proteins across membranes. I. Presence of proteolytically processed and unprocessed nascent immunoglobulin light chains on membrane-bound ribosomes of murine myeloma. *J Cell Biol*, *67*(3), 835-851. https://doi.org/10.1083/jcb.67.3.835

Bodnar, N. O., & Rapoport, T. A. (2017). Molecular Mechanism of Substrate Processing by the Cdc48 ATPase Complex. *Cell*, *169*(4), 722-735 e729. https://doi.org/10.1016/j.cell.2017.04.020

Bousquet-Dubouch, M. P., Baudelet, E., Guerin, F., Matondo, M., Uttenweiler-Joseph, S., Burlet-Schiltz, O., & Monsarrat, B. (2009). Affinity Purification Strategy to Capture Human Endogenous Proteasome Complexes Diversity and to Identify Proteasome-interacting Proteins. *Molecular & Cellular Proteomics*, *8*(5), 1150-1164. https://doi.org/10.1074/mcp.M800193-MCP200

Boya, P., Reggiori, F., & Codogno, P. (2013). Emerging regulation and functions of autophagy. *Nature Cell Biology*, *15*(7), 713-720. https://doi.org/10.1038/ncb2788

Brehm, A., Liu, Y., Sheikh, A., Marrero, B., Omoyinmi, E., Zhou, Q., Montealegre, G., Biancotto, A., Reinhardt, A., Almeida de Jesus, A., Pelletier, M., Tsai, W. L., Remmers, E. F., Kardava, L., Hill, S., Kim, H., Lachmann, H. J., Megarbane, A., Chae, J. J., . . . Goldbach-Mansky, R. (2015). Additive loss-of-function proteasome subunit mutations in CANDLE/PRAAS patients promote type I IFN production. *J Clin Invest*, *125*(11), 4196-4211. https://doi.org/10.1172/JCI81260

Bujisic, B., De Gassart, A., Tallant, R., Demaria, O., Zaffalon, L., Chelbi, S., Gilliet, M., Bertoni, F., & Martinon, F. (2017). Impairment of both IRE1 expression and XBP1 activation is a hallmark of GCB DLBCL and contributes to tumor growth. *Blood*, *129*(17), 2420-2428. https://doi.org/10.1182/blood-2016-09-741348

Bujišić, B., & Université de Lausanne. *Regulation of IRE1 expression modulates the nature of ER stress response and contributes to tumor growth in DLBCL*.

Cannon, W. B. (1939). *The Wisdom of the body* (Rev ed.). W.W. Norton & Company Inc.

Carvalho, P., Goder, V., & Rapoport, T. A. (2006). Distinct ubiquitin-ligase complexes define convergent pathways for the degradation of ER proteins. *Cell*, *126*(2), 361-373. https://doi.org/10.1016/j.cell.2006.05.043

Carvalho, P., Stanley, A. M., & Rapoport, T. A. (2010). Retrotranslocation of a misfolded luminal ER protein by the ubiquitin-ligase Hrd1p. *Cell*, *143*(4), 579-591. https://doi.org/10.1016/j.cell.2010.10.028

Chakrama, F. Z., Seguin-Py, S., Le Grand, J. N., Fraichard, A., Delage-Mourroux, R., Despouy, G., Perez, V., Jouvenot, M., & Boyer-Guittaut, M. (2010). GABARAPL1 (GEC1) associates with autophagic vesicles. *Autophagy*, *6*(4), 495-505. https://doi.org/10.4161/auto.6.4.11819

Chan, J. Y., Han, X. L., & Kan, Y. W. (1993). Cloning of Nrf1, an NF-E2-related transcription factor, by genetic selection in yeast. *Proc Natl Acad Sci U S A*, *90*(23), 11371-11375. https://doi.org/10.1073/pnas.90.23.11371

Chan, J. Y., Kwong, M., Lu, R., Chang, J., Wang, B., Yen, T. S., & Kan, Y. W. (1998). Targeted disruption of the ubiquitous CNC-bZIP transcription factor, Nrf-1, results in anemia and embryonic lethality in mice. *EMBO J*, *17*(6), 1779-1787. https://doi.org/10.1093/emboj/17.6.1779

Chapatte, L., Ayyoub, M., Morel, S., Peitrequin, A. L., Levy, N., Servis, C., Van den Eynde, B. J., Valmori, D., & Levy, F. (2006). Processing of tumor-associated antigen by the proteasomes of dendritic cells controls in vivo T-cell responses. *Cancer Res*, *66*(10), 5461-5468. https://doi.org/10.1158/0008-5472.CAN-05-4310

Chapiro, J., Claverol, S., Piette, F., Ma, W., Stroobant, V., Guillaume, B., Gairin, J. E., Morel, S., Burlet-Schiltz, O., Monsarrat, B., Boon, T., & Van den Eynde, B. J. (2006). Destructive cleavage of antigenic peptides either by the immunoproteasome or by the standard proteasome results in differential antigen presentation. *J Immunol*, *176*(2), 1053-1061. https://doi.org/10.4049/jimmunol.176.2.1053

Chen, C., Li, J. G., Chen, Y., Huang, P., Wang, Y., & Liu-Chen, L. Y. (2006). GEC1 interacts with the kappa opioid receptor and enhances expression of the receptor. *J Biol Chem*, *281*(12), 7983-7993. https://doi.org/10.1074/jbc.M509805200

Chen, J., Liu, X., Lu, F., Liu, X., Ru, Y., Ren, Y., Yao, L., & Zhang, Y. (2015). Transcription factor Nrf1 is negatively regulated by its O-GlcNAcylation status. *FEBS Lett*, *589*(18), 2347-2358. https://doi.org/10.1016/j.febslet.2015.07.030

Chen, L., Kwong, M., Lu, R., Ginzinger, D., Lee, C., Leung, L., & Chan, J. Y. (2003). Nrf1 is critical for redox balance and survival of liver cells during development. *Mol Cell Biol*, *23*(13), 4673-4686. https://doi.org/10.1128/MCB.23.13.4673-4686.2003

Chen, T., Ho, M., Briere, J., Moscvin, M., Czarnecki, P. G., Anderson, K. C., Blackwell, T. K., & Bianchi, G. (2022). Multiple myeloma cells depend on the DDI2/NRF1-mediated proteasome stress response for survival. *Blood Adv*, *6*(2), 429-440. https://doi.org/10.1182/bloodadvances.2020003820

Chen, X., Halberg, R. B., Ehrhardt, W. M., Torrealba, J., & Dove, W. F. (2003). Clusterin as a biomarker in murine and human intestinal neoplasia. *Proc Natl Acad Sci U S A*, *100*(16), 9530-9535. https://doi.org/10.1073/pnas.1233633100

Chino, H., Hatta, T., Natsume, T., & Mizushima, N. (2019). Intrinsically Disordered Protein TEX264 Mediates ER-phagy. *Mol Cell*, *74*(5), 909-921 e906. https://doi.org/10.1016/j.molcel.2019.03.033

Chondrogianni, N., Sakellari, M., Lefaki, M., Papaevgeniou, N., & Gonos, E. S. (2014). Proteasome activation delays aging in vitro and in vivo. *Free Radic Biol Med*, *71*, 303-320. https://doi.org/10.1016/j.freeradbiomed.2014.03.031

Chondrogianni, N., Voutetakis, K., Kapetanou, M., Delitsikou, V., Papaevgeniou, N., Sakellari, M., Lefaki, M., Filippopoulou, K., & Gonos, E. S. (2015). Proteasome activation: An innovative promising approach for delaying aging and retarding age-related diseases. *Ageing Res Rev*, *23*(Pt A), 37-55. https://doi.org/10.1016/j.arr.2014.12.003

Christianson, J. C., Olzmann, J. A., Shaler, T. A., Sowa, M. E., Bennett, E. J., Richter, C. M., Tyler, R. E., Greenblatt, E. J., Harper, J. W., & Kopito, R. R. (2011). Defining human ERAD networks through an integrative mapping strategy. *Nature Cell Biology*, *14*(1), 93-105. https://doi.org/10.1038/ncb2383

Christianson, J. C., & Ye, Y. (2014). Cleaning up in the endoplasmic reticulum: ubiquitin in charge. *Nat Struct Mol Biol*, *21*(4), 325-335. https://doi.org/10.1038/nsmb.2793

Ciechanover, A., & Iwai, K. (2004). The ubiquitin system: from basic mechanisms to the patient bed. *IUBMB Life*, *56*(4), 193-201. https://doi.org/10.1080/15216540420002236l6

Cohen, E., & Dillin, A. (2008). The insulin paradox: aging, proteotoxicity and neurodegeneration. *Nat Rev Neurosci*, *9*(10), 759-767. https://doi.org/10.1038/nrn2474

Collins, G. A., & Goldberg, A. L. (2020). Proteins containing ubiquitin-like (Ubl) domains not only bind to 26S proteasomes but also induce their activation. *Proc Natl Acad Sci U S A*, *117*(9), 4664-4674. https://doi.org/10.1073/pnas.1915534117

Collins, G. A., Sha, Z., Kuo, C. L., Erbil, B., & Goldberg, A. L. (2022). Mammalian Ddi2 is a shuttling factor containing a retroviral protease domain that influences binding of ubiquitylated proteins and proteasomal degradation. *J Biol Chem*, *298*(5), 101875. https://doi.org/10.1016/j.jbc.2022.101875

Connell, P., Ballinger, C. A., Jiang, J., Wu, Y., Thompson, L. J., Hohfeld, J., & Patterson, C. (2001). The co-chaperone CHIP regulates protein triage decisions mediated by heat-shock proteins. *Nature Cell Biology*, *3*(1), 93-96. https://doi.org/10.1038/35050618

Conner, G. E. (1992). The role of the cathepsin D propeptide in sorting to the lysosome. *J Biol Chem*, *267*(30), 21738-21745. https://www.ncbi.nlm.nih.gov/pubmed/1400484

Cuervo, A. M., & Wong, E. (2014). Chaperone-mediated autophagy: roles in disease and aging. *Cell Res*, *24*(1), 92-104. https://doi.org/10.1038/cr.2013.153

Cui, M., Atmanli, A., Morales, M. G., Tan, W., Chen, K., Xiao, X., Xu, L., Liu, N., Bassel-Duby, R., & Olson, E. N. (2021). Nrf1 promotes heart regeneration and repair by regulating proteostasis and redox balance. *Nat Commun*, *12*(1), 5270. https://doi.org/10.1038/s41467-021-25653-w

D'Arcy, P., Wang, X., & Linder, S. (2015). Deubiquitinase inhibition as a cancer therapeutic strategy. *Pharmacol Ther*, *147*, 32-54. https://doi.org/10.1016/j.pharmthera.2014.11.002

de Duve, C. (1983). Lysosomes revisited. *Eur J Biochem*, *137*(3), 391-397. https://doi.org/10.1111/j.1432-1033.1983.tb07841.x

De Gassart, A., Bujisic, B., Zaffalon, L., Decosterd, L. A., Di Micco, A., Frera, G., Tallant, R., & Martinon, F. (2016). An inhibitor of HIV-1 protease modulates constitutive eIF2alpha dephosphorylation to trigger a specific integrated stress response. *Proc Natl Acad Sci U S A*, *113*(2), E117-126. https://doi.org/10.1073/pnas.1514076113

De Gassart, A., Demaria, O., Panes, R., Zaffalon, L., Ryazanov, A. G., Gilliet, M., & Martinon, F. (2016). Pharmacological eEF2K activation promotes cell death and inhibits cancer progression. *EMBO Rep*, *17*(10), 1471-1484. https://doi.org/10.15252/embr.201642194

de Graaf, N., van Helden, M. J., Textoris-Taube, K., Chiba, T., Topham, D. J., Kloetzel, P. M., Zaiss, D. M., & Sijts, A. J. (2011). PA28 and the proteasome immunosubunits play a central and independent role in the production of MHC class I-binding peptides in vivo. *Eur J Immunol*, *41*(4), 926-935. https://doi.org/10.1002/eji.201041040

de Jesus, A. A., Brehm, A., VanTries, R., Pillet, P., Parentelli, A. S., Montealegre Sanchez, G. A., Deng, Z., Paut, I. K., Goldbach-Mansky, R., & Kruger, E. (2019). Novel proteasome assembly chaperone mutations in PSMG2/PAC2 cause the autoinflammatory interferonopathy CANDLE/PRAAS4. *J Allergy Clin Immunol*, *143*(5), 1939-1943 e1938. https://doi.org/10.1016/j.jaci.2018.12.1012

Deegan, S., Saveljeva, S., Gorman, A. M., & Samali, A. (2013). Stress-induced self-cannibalism: on the regulation of autophagy by endoplasmic reticulum stress. *Cell Mol Life Sci*, *70*(14), 2425-2441. https://doi.org/10.1007/s00018-012-1173-4

Deter, R. L., Baudhuin, P., & De Duve, C. (1967). Participation of lysosomes in cellular autophagy induced in rat liver by glucagon. *J Cell Biol*, *35*(2), C11-16. https://doi.org/10.1083/jcb.35.2.c11

Deverson, E. V., Gow, I. R., Coadwell, W. J., Monaco, J. J., Butcher, G. W., & Howard, J. C. (1990). MHC class II region encoding proteins related to the multidrug resistance family of transmembrane transporters. *Nature*, *348*(6303), 738-741. https://doi.org/10.1038/348738a0

Dikic, I. (2017). Proteasomal and Autophagic Degradation Systems. *Annu Rev Biochem*, *86*, 193-224. https://doi.org/10.1146/annurev-biochem-061516-044908

Dirac-Svejstrup, A. B., Walker, J., Faull, P., Encheva, V., Akimov, V., Puglia, M., Perkins, D., Kumper, S., Hunjan, S. S., Blagoev, B., Snijders, A. P., Powell, D. J., & Svejstrup, J. Q. (2020a). DDI2 Is a Ubiquitin-Directed Endoprotease Responsible for Cleavage of Transcription Factor NRF1. *Mol Cell*, *79*(2), 332-341 e337. https://doi.org/10.1016/j.molcel.2020.05.035

Dirac-Svejstrup, A. B., Walker, J., Faull, P., Encheva, V., Akimov, V., Puglia, M., Perkins, D., Kumper, S., Hunjan, S. S., Blagoev, B., Snijders, A. P., Powell, D. J., & Svejstrup, J. Q. (2020b). DDI2 Is a Ubiquitin-Directed Endoprotease Responsible for Cleavage of Transcription Factor NRF1. *Molecular Cell*, *79*(2), 332-+. https://doi.org/10.1016/j.molcel.2020.05.035

Driessen, C., Muller, R., Novak, U., Cantoni, N., Betticher, D., Mach, N., Rufer, A., Mey, U., Samaras, P., Ribi, K., Besse, L., Besse, A., Berset, C., Rondeau, S., Hawle, H., Hitz, F., Pabst, T., & Zander, T. (2018). Promising activity of nelfinavir-bortezomib-dexamethasone in proteasome inhibitor-refractory multiple myeloma. *Blood*, *132*(19), 2097-2100. https://doi.org/10.1182/blood-2018-05-851170

Eisele, F., & Wolf, D. H. (2008). Degradation of misfolded protein in the cytoplasm is mediated by the ubiquitin ligase Ubr1. *FEBS Lett*, *582*(30), 4143-4146. https://doi.org/10.1016/j.febslet.2008.11.015

El Khouri, E., Le Pavec, G., Toledano, M. B., & Delaunay-Moisan, A. (2013). RNF185 is a novel E3 ligase of endoplasmic reticulum-associated degradation (ERAD) that targets cystic fibrosis transmembrane conductance regulator (CFTR). *J Biol Chem*, *288*(43), 31177-31191. https://doi.org/10.1074/jbc.M113.470500

Ellgaard, L., & Helenius, A. (2003). Quality control in the endoplasmic reticulum. *Nat Rev Mol Cell Biol*, *4*(3), 181-191. https://doi.org/10.1038/nrm1052

Erath, A., Patel, D. A., Hosack, E. A., Patanella, J. E., Ibach, D. M., & Kassim, A. A. (2020). Overcoming Proteasome Inhibitor-Refractory Multiple Myeloma With Elotuzumab, Bortezomib, Nelfinavir, and Dexamethasone. *World J Oncol*, *11*(1), 33-36. https://doi.org/10.14740/wjon1241

Fang, J., Wang, H., Fang, X., Li, N., Hu, H., Bian, M., & Yang, P. (2018). Low STYK1 expression indicates poor prognosis in gastric cancer. *Cancer Manag Res*, *10*, 6669-6676. https://doi.org/10.2147/CMAR.S181910

Fang, N. N., Chan, G. T., Zhu, M., Comyn, S. A., Persaud, A., Deshaies, R. J., Rotin, D., Gsponer, J., & Mayor, T. (2014). Rsp5/Nedd4 is the main ubiquitin ligase that targets cytosolic misfolded proteins following heat stress. *Nature Cell Biology*, *16*(12), 1227-1237. https://doi.org/10.1038/ncb3054

Fatimababy, A. S., Lin, Y. L., Usharani, R., Radjacommare, R., Wang, H. T., Tsai, H. L., Lee, Y. F., & Fu, H. Y. (2010). Cross-species divergence of the major recognition pathways of ubiquitylated substrates for ubiquitin/26S proteasome-mediated proteolysis. *Febs Journal*, *277*(3), 796-816. https://doi.org/10.1111/j.1742-4658.2009.07531.x

Faust, M., & Montenarh, M. (2000). Subcellular localization of protein kinase CK2 - A key to its function? *Cell and Tissue Research*, *301*(3), 329-340. https://doi.org/DOI 10.1007/s004410000256

Fehling, H. J., Swat, W., Laplace, C., Kuhn, R., Rajewsky, K., Muller, U., & von Boehmer, H. (1994). MHC class I expression in mice lacking the proteasome subunit LMP-7. *Science*, *265*(5176), 1234-1237. https://doi.org/10.1126/science.8066463

Ferrington, D. A., & Gregerson, D. S. (2012). Immunoproteasomes: structure, function, and antigen presentation. *Prog Mol Biol Transl Sci*, *109*, 75-112. https://doi.org/10.1016/B978-0-12-397863-9.00003-1

Figueiredo-Pereira, M. E., Yakushin, S., & Cohen, G. (1997). Accumulation of ubiquitinated proteins in mouse neuronal cells induced by oxidative stress. *Mol Biol Rep*, *24*(1-2), 35-38. https://doi.org/10.1023/a:1006848405975

Finkel, T., Serrano, M., & Blasco, M. A. (2007). The common biology of cancer and ageing. *Nature*, *448*(7155), 767-774. https://doi.org/10.1038/nature05985

Finley, D. (2009). Recognition and processing of ubiquitin-protein conjugates by the proteasome. *Annu Rev Biochem*, *78*, 477-513. https://doi.org/10.1146/annurev.biochem.78.081507.101607

Frera, G. (2015). *Characterization of the HIV protease inhibitor Nelfinavir cellular targets* [Thèse Univ Lausanne, s.n. ,]. S.l.

Fujihira, H., Masahara-Negishi, Y., Akimoto, Y., Hirayama, H., Lee, H. C., Story, B. A., Mueller, W. F., Jakob, P., Clauder-Munster, S., Steinmetz, L. M., Radhakrishnan, S. K., Kawakami, H., Kamada, Y., Miyoshi, E., Yokomizo, T., & Suzuki, T. (2020). Liver-specific deletion of Ngly1 causes abnormal nuclear morphology and lipid metabolism under food stress. *Biochim Biophys Acta Mol Basis Dis*, *1866*(3), 165588. https://doi.org/10.1016/j.bbadis.2019.165588

Girard, F. P., Byrne, J., Downes, M., Fanning, D., Desgrandchamps, F., Fitzpatrick, J. M., & Watson, R. W. (2010). Detecting soluble clusterin in in-vitro and in-vivo models of prostate cancer. *Neoplasma*, *57*(5), 488-493. https://doi.org/10.4149/neo_2010_05_488

Gladman, N. P., Marshall, R. S., Lee, K. H., & Vierstra, R. D. (2016). The Proteasome Stress Regulon Is Controlled by a Pair of NAC Transcription Factors in Arabidopsis. *Plant Cell*, *28*(6), 1279-1296. https://doi.org/10.1105/tpc.15.01022

Glover-Cutter, K. M., Lin, S., & Blackwell, T. K. (2013). Integration of the unfolded protein and oxidative stress responses through SKN-1/Nrf. *PLoS Genet*, *9*(9), e1003701. https://doi.org/10.1371/journal.pgen.1003701

Gomez-Pastor, R., Burchfiel, E. T., & Thiele, D. J. (2018). Regulation of heat shock transcription factors and their roles in physiology and disease. *Nat Rev Mol Cell Biol*, *19*(1), 4-19. https://doi.org/10.1038/nrm.2017.73

Gonzalez, A., & Hall, M. N. (2017). Nutrient sensing and TOR signaling in yeast and mammals. *EMBO J*, *36*(4), 397-408. https://doi.org/10.15252/embj.201696010

Greenblatt, E. J., Olzmann, J. A., & Kopito, R. R. (2011). Derlin-1 is a rhomboid pseudoprotease required for the dislocation of mutant alpha-1 antitrypsin from the endoplasmic reticulum. *Nat Struct Mol Biol*, *18*(10), 1147-1152. https://doi.org/10.1038/nsmb.2111

Grigoreva, T. A., Tribulovich, V. G., Garabadzhiu, A. V., Melino, G., & Barlev, N. A. (2015). The 26S proteasome is a multifaceted target for anti-cancer therapies. *Oncotarget*, *6*(28), 24733-24749. https://doi.org/10.18632/oncotarget.4619

Grimberg, K. B., Beskow, A., Lundin, D., Davis, M. M., & Young, P. (2011). Basic leucine zipper protein Cnc-C is a substrate and transcriptional regulator of the Drosophila 26S proteasome. *Mol Cell Biol*, *31*(4), 897-909. https://doi.org/10.1128/MCB.00799-10

Groll, M., Ditzel, L., Lowe, J., Stock, D., Bochtler, M., Bartunik, H. D., & Huber, R. (1997). Structure of 20S proteasome from yeast at 2.4 A resolution. *Nature*, *386*(6624), 463-471. https://doi.org/10.1038/386463a0

Gu, Y., Wang, X., Wang, Y., Wang, Y., Li, J., & Yu, F. X. (2020). Nelfinavir inhibits human DDI2 and potentiates cytotoxicity of proteasome inhibitors. *Cell Signal*, *75*, 109775. https://doi.org/10.1016/j.cellsig.2020.109775

Guan, M., Su, L., Yuan, Y. C., Li, H., & Chow, W. A. (2015). Nelfinavir and nelfinavir analogs block site-2 protease cleavage to inhibit castration-resistant prostate cancer. *Sci Rep*, *5*, 9698. https://doi.org/10.1038/srep09698

Guimaraes, G., Gomes, M. T. R., Campos, P. C., Marinho, F. V., de Assis, N. R. G., Silveira, T. N., & Oliveira, S. C. (2018). Immunoproteasome Subunits Are Required for CD8(+) T Cell Function and Host Resistance to Brucella abortus Infection in Mice. *Infect Immun*, *86*(3). https://doi.org/10.1128/IAI.00615-17

Habeebu, S. S., Liu, J., Liu, Y., & Klaassen, C. D. (2000). Metallothionein-null mice are more sensitive than wild-type mice to liver injury induced by repeated exposure to cadmium. *Toxicol Sci*, *55*(1), 223-232. https://doi.org/10.1093/toxsci/55.1.223

Hamazaki, J., & Murata, S. (2020). ER-Resident Transcription Factor Nrf1 Regulates Proteasome Expression and Beyond. *Int J Mol Sci*, *21*(10). https://doi.org/10.3390/ijms21103683

Han, J. W., Valdez, J. L., Ho, D. V., Lee, C. S., Kim, H. M., Wang, X., Huang, L., & Chan, J. Y. (2017). Nuclear factor-erythroid-2 related transcription factor-1 (Nrf1) is regulated by O-GlcNAc transferase. *Free Radic Biol Med*, *110*, 196-205. https://doi.org/10.1016/j.freeradbiomed.2017.06.008

Harding, H. P., Novoa, I., Bertolotti, A., Zeng, H., Zhang, Y., Urano, F., Jousse, C., & Ron, D. (2001). Translational regulation in the cellular response to biosynthetic load on the endoplasmic reticulum. *Cold Spring Harb Symp Quant Biol*, *66*, 499-508. https://doi.org/10.1101/sqb.2001.66.499

Harold, D., Abraham, R., Hollingworth, P., Sims, R., Gerrish, A., Hamshere, M. L., Pahwa, J. S., Moskvina, V., Dowzell, K., Williams, A., Jones, N., Thomas, C., Stretton, A., Morgan, A. R., Lovestone, S., Powell, J., Proitsi, P., Lupton, M. K., Brayne, C., . . . Williams, J. (2009). Genome-wide association study identifies variants at CLU and PICALM associated with Alzheimer's disease. *Nat Genet*, *41*(10), 1088-1093. https://doi.org/10.1038/ng.440

Hassink, G., Kikkert, M., van Voorden, S., Lee, S. J., Spaapen, R., van Laar, T., Coleman, C. S., Bartee, E., Fruh, K., Chau, V., & Wiertz, E. (2005). TEB4 is a C4HC3 RING finger-containing ubiquitin ligase of the endoplasmic reticulum. *Biochem J*, *388*(Pt 2), 647-655. https://doi.org/10.1042/BJ20041241

Hebert, D. N., & Molinari, M. (2007). In and out of the ER: protein folding, quality control, degradation, and related human diseases. *Physiol Rev*, *87*(4), 1377-1408. https://doi.org/10.1152/physrev.00050.2006

Heck, J. W., Cheung, S. K., & Hampton, R. Y. (2010). Cytoplasmic protein quality control degradation mediated by parallel actions of the E3 ubiquitin ligases Ubr1 and San1. *Proc Natl Acad Sci U S A*, *107*(3), 1106-1111. https://doi.org/10.1073/pnas.0910591107

Hicke, L. (1997). Ubiquitin-dependent internalization and down-regulation of plasma membrane proteins. *Faseb Journal*, *11*(14), 1215-1226. https://doi.org/10.1096/fasebj.11.14.9409540

Hicks, S. J., Drysdale, J. W., & Munro, H. N. (1969). Preferential synthesis of ferritin and albumin by different populations of liver polysomes. *Science*, *164*(3879), 584-585. https://doi.org/10.1126/science.164.3879.584

Hirotsu, Y., Higashi, C., Fukutomi, T., Katsuoka, F., Tsujita, T., Yagishita, Y., Matsuyama, Y., Motohashi, H., Uruno, A., & Yamamoto, M. (2014). Transcription factor NF-E2-related factor 1 impairs glucose metabolism in mice. *Genes Cells*, *19*(8), 650-665. https://doi.org/10.1111/gtc.12165

Hitz, F., Kraus, M., Pabst, T., Hess, D., Besse, L., Silzle, T., Novak, U., Seipel, K., Rondeau, S., Studeli, S., Vilei, S. B., Samaras, P., Mey, U., Driessen, C., & Swiss Group for Clinical Cancer Research, S. (2019). Nelfinavir and lenalidomide/dexamethasone in patients with lenalidomide-refractory multiple myeloma. A phase I/II Trial (SAKK 39/10). *Blood Cancer J*, *9*(9), 70. https://doi.org/10.1038/s41408-019-0228-2

Hosokawa, N., Wada, I., Nagasawa, K., Moriyama, T., Okawa, K., & Nagata, K. (2008). Human XTP3-B forms an endoplasmic reticulum quality control scaffold with the HRD1-SEL1L ubiquitin ligase complex and BiP. *J Biol Chem*, *283*(30), 20914-20924. https://doi.org/10.1074/jbc.M709336200

Hou, Y., Liu, Z., Zuo, Z., Gao, T., Fu, J., Wang, H., Xu, Y., Liu, D., Yamamoto, M., Zhu, B., Zhang, Y., Andersen, M. E., Zhang, Q., & Pi, J. (2018). Adipocyte-specific deficiency of Nfe2l1 disrupts plasticity of white adipose tissues and metabolic homeostasis in mice. *Biochem Biophys Res Commun*, *503*(1), 264-270. https://doi.org/10.1016/j.bbrc.2018.06.013

Huang, C. H., Chu, Y. R., Ye, Y., & Chen, X. (2014). Role of HERP and a HERP-related protein in HRD1-dependent protein degradation at the endoplasmic reticulum. *J Biol Chem*, *289*(7), 4444-4454. https://doi.org/10.1074/jbc.M113.519561

Hutchinson, S., Sims, S., O'Hara, G., Silk, J., Gileadi, U., Cerundolo, V., & Klenerman, P. (2011). A dominant role for the immunoproteasome in CD8+ T cell responses to murine cytomegalovirus. *PLoS One*, *6*(2), e14646. https://doi.org/10.1371/journal.pone.0014646

Ibrahim, L., Mesgarzadeh, J., Xu, I., Powers, E. T., Wiseman, R. L., & Bollong, M. J. (2020). Defining the Functional Targets of Cap'n'collar Transcription Factors NRF1, NRF2, and NRF3. *Antioxidants (Basel)*, *9*(10). https://doi.org/10.3390/antiox9101025

Ikeda, Y., Demartino, G. N., Brown, M. S., Lee, J. N., Goldstein, J. L., & Ye, J. (2009). Regulated endoplasmic reticulum-associated degradation of a polytopic protein: p97 recruits proteasomes to Insig-1 before extraction from membranes. *J Biol Chem*, *284*(50), 34889-34900. https://doi.org/10.1074/jbc.M109.044875

Itoh, K., Igarashi, K., Hayashi, N., Nishizawa, M., & Yamamoto, M. (1995). Cloning and characterization of a novel erythroid cell-derived CNC family transcription factor heterodimerizing with the small Maf family proteins. *Mol Cell Biol*, *15*(8), 4184-4193. https://doi.org/10.1128/MCB.15.8.4184

Itoh, K., Wakabayashi, N., Katoh, Y., Ishii, T., Igarashi, K., Engel, J. D., & Yamamoto, M. (1999). Keap1 represses nuclear activation of antioxidant responsive elements by Nrf2 through binding to the amino-terminal Neh2 domain. *Genes Dev*, *13*(1), 76-86. https://doi.org/10.1101/gad.13.1.76

Johnsen, O., Skammelsrud, N., Luna, L., Nishizawa, M., Prydz, H., & Kolsto, A. B. (1996). Small Maf proteins interact with the human transcription factor TCF11/Nrf1/LCR-F1. *Nucleic Acids Res*, *24*(21), 4289-4297. https://doi.org/10.1093/nar/24.21.4289

July, L. V., Akbari, M., Zellweger, T., Jones, E. C., Goldenberg, S. L., & Gleave, M. E. (2002). Clusterin expression is significantly enhanced in prostate cancer cells following androgen withdrawal therapy. *Prostate*, *50*(3), 179-188. https://doi.org/10.1002/pros.10047

Kang, J. A., & Jeon, Y. J. (2020). Emerging Roles of USP18: From Biology to Pathophysiology. *Int J Mol Sci*, *21*(18). https://doi.org/10.3390/ijms21186825

Kaplan, K. B., Hyman, A. A., & Sorger, P. K. (1997). Regulating the yeast kinetochore by ubiquitin-dependent degradation and Skp1p-mediated phosphorylation. *Cell*, *91*(4), 491-500. https://doi.org/10.1016/s0092-8674(00)80435-3

Kathania, M., Khare, P., Zeng, M., Cantarel, B., Zhang, H., Ueno, H., & Venuprasad, K. (2016). Itch inhibits IL-17-mediated colon inflammation and tumorigenesis by ROR-

gammat ubiquitination. *Nat Immunol*, *17*(8), 997-1004. https://doi.org/10.1038/ni.3488

Kawabata, S., Gills, J. J., Mercado-Matos, J. R., Lopiccolo, J., Wilson, W., 3rd, Hollander, M. C., & Dennis, P. A. (2012). Synergistic effects of nelfinavir and bortezomib on proteotoxic death of NSCLC and multiple myeloma cells. *Cell Death Dis*, *3*(7), e353. https://doi.org/10.1038/cddis.2012.87

Keller, M., Ebstein, F., Burger, E., Textoris-Taube, K., Gorny, X., Urban, S., Zhao, F., Dannenberg, T., Sucker, A., Keller, C., Saveanu, L., Kruger, E., Rothkotter, H. J., Dahlmann, B., Henklein, P., Voigt, A., Kuckelkorn, U., Paschen, A., Kloetzel, P. M., & Seifert, U. (2015). The proteasome immunosubunits, PA28 and ER-aminopeptidase 1 protect melanoma cells from efficient MART-126-35 -specific T-cell recognition. *Eur J Immunol*, *45*(12), 3257-3268. https://doi.org/10.1002/eji.201445243

Kevei, E., Pokrzywa, W., & Hoppe, T. (2017). Repair or destruction-an intimate liaison between ubiquitin ligases and molecular chaperones in proteostasis. *FEBS Lett*, *591*(17), 2616-2635. https://doi.org/10.1002/1873-3468.12750

Kikkert, M., Doolman, R., Dai, M., Avner, R., Hassink, G., van Voorden, S., Thanedar, S., Roitelman, J., Chau, V., & Wiertz, E. (2004). Human HRD1 is an E3 ubiquitin ligase involved in degradation of proteins from the endoplasmic reticulum. *J Biol Chem*, *279*(5), 3525-3534. https://doi.org/10.1074/jbc.M307453200

Kim, H., Sanchez, G. A., & Goldbach-Mansky, R. (2016). Insights from Mendelian Interferonopathies: Comparison of CANDLE, SAVI with AGS, Monogenic Lupus. *J Mol Med (Berl)*, *94*(10), 1111-1127. https://doi.org/10.1007/s00109-016-1465-5

Kim, H. M., Han, J. W., & Chan, J. Y. (2016). Nuclear Factor Erythroid-2 Like 1 (NFE2L1): Structure, function and regulation. *Gene*, *584*(1), 17-25. https://doi.org/10.1016/j.gene.2016.03.002

Kim, H. T., & Goldberg, A. L. (2018). UBL domain of Usp14 and other proteins stimulates proteasome activities and protein degradation in cells. *Proc Natl Acad Sci U S A*, *115*(50), E11642-E11650. https://doi.org/10.1073/pnas.1808731115

Kim, J., Xing, W., Wergedal, J., Chan, J. Y., & Mohan, S. (2010). Targeted disruption of nuclear factor erythroid-derived 2-like 1 in osteoblasts reduces bone size and bone formation in mice. *Physiol Genomics*, *40*(2), 100-110. https://doi.org/10.1152/physiolgenomics.00105.2009

Kim, Y. E., Hipp, M. S., Bracher, A., Hayer-Hartl, M., & Hartl, F. U. (2013). Molecular chaperone functions in protein folding and proteostasis. *Annu Rev Biochem*, *82*, 323-355. https://doi.org/10.1146/annurev-biochem-060208-092442

Kincaid, E. Z., Che, J. W., York, I., Escobar, H., Reyes-Vargas, E., Delgado, J. C., Welsh, R. M., Karow, M. L., Murphy, A. J., Valenzuela, D. M., Yancopoulos, G. D., & Rock, K. L. (2011). Mice completely lacking immunoproteasomes show major changes in antigen presentation. *Nat Immunol*, *13*(2), 129-135. https://doi.org/10.1038/ni.2203

Kinoshita, A., Fukumoto, H., Shah, T., Whelan, C. M., Irizarry, M. C., & Hyman, B. T. (2003). Demonstration by FRET of BACE interaction with the amyloid precursor protein at the cell surface and in early endosomes. *J Cell Sci*, *116*(Pt 16), 3339-3346. https://doi.org/10.1242/jcs.00643

Kitamura, A., Maekawa, Y., Uehara, H., Izumi, K., Kawachi, I., Nishizawa, M., Toyoshima, Y., Takahashi, H., Standley, D. M., Tanaka, K., Hamazaki, J., Murata, S., Obara, K., Toyoshima, I., & Yasutomo, K. (2011). A mutation in the immunoproteasome subunit PSMB8 causes autoinflammation and lipodystrophy in humans. *J Clin Invest*, *121*(10), 4150-4160. https://doi.org/10.1172/JCI58414

Klaassen, C. D., Liu, J., & Diwan, B. A. (2009). Metallothionein protection of cadmium toxicity. *Toxicol Appl Pharmacol*, *238*(3), 215-220. https://doi.org/10.1016/j.taap.2009.03.026

Klaips, C. L., Jayaraj, G. G., & Hartl, F. U. (2018). Pathways of cellular proteostasis in aging and disease. *J Cell Biol*, *217*(1), 51-63. https://doi.org/10.1083/jcb.201709072

Klionsky, D. J., Baehrecke, E. H., Brumell, J. H., Chu, C. T., Codogno, P., Cuervo, A. M., Debnath, J., Deretic, V., Elazar, Z., Eskelinen, E. L., Finkbeiner, S., Fueyo-Margareto, J., Gewirtz, D., Jaattela, M., Kroemer, G., Levine, B., Melia, T. J., Mizushima, N., Rubinsztein, D. C., . . . Tooze, S. A. (2011). A comprehensive glossary of autophagy-related molecules and processes (2nd edition). *Autophagy*, *7*(11), 1273-1294. https://doi.org/10.4161/auto.7.11.17661

Kloetzel, P. M. (2001). Antigen processing by the proteasome. *Nat Rev Mol Cell Biol*, *2*(3), 179-187. https://doi.org/10.1038/35056572

Kobayashi, A. (2020). Roles of NRF3 in the Hallmarks of Cancer: Proteasomal Inactivation of Tumor Suppressors. *Cancers (Basel)*, *12*(9). https://doi.org/10.3390/cancers12092681

Kobayashi, A., Ito, E., Toki, T., Kogame, K., Takahashi, S., Igarashi, K., Hayashi, N., & Yamamoto, M. (1999). Molecular cloning and functional characterization of a new Cap'n' collar family transcription factor Nrf3. *J Biol Chem*, *274*(10), 6443-6452. https://doi.org/10.1074/jbc.274.10.6443

Kobayashi, A., Tsukide, T., Miyasaka, T., Morita, T., Mizoroki, T., Saito, Y., Ihara, Y., Takashima, A., Noguchi, N., Fukamizu, A., Hirotsu, Y., Ohtsuji, M., Katsuoka, F., & Yamamoto, M. (2011). Central nervous system-specific deletion of transcription factor Nrf1 causes progressive motor neuronal dysfunction. *Genes Cells*, *16*(6), 692-703. https://doi.org/10.1111/j.1365-2443.2011.01522.x

Kohl, N. E., Emini, E. A., Schleif, W. A., Davis, L. J., Heimbach, J. C., Dixon, R. A. F., Scolnick, E. M., & Sigal, I. S. (1988). Active Human Immunodeficiency Virus Protease Is Required for Viral Infectivity. *Proceedings of the National Academy of Sciences of the United States of America*, *85*(13), 4686-4690. https://doi.org/DOI 10.1073/pnas.85.13.4686

Koizumi, S., Irie, T., Hirayama, S., Sakurai, Y., Yashiroda, H., Naguro, I., Ichijo, H., Hamazaki, J., & Murata, S. (2016). The aspartyl protease DDI2 activates Nrf1 to compensate for proteasome dysfunction. *Elife*, *5*. https://doi.org/10.7554/eLife.18357

Korolchuk, V. I., Menzies, F. M., & Rubinsztein, D. C. (2010). Mechanisms of cross-talk between the ubiquitin-proteasome and autophagy-lysosome systems. *FEBS Lett*, *584*(7), 1393-1398. https://doi.org/10.1016/j.febslet.2009.12.047

Kostura, M., & Mathews, M. B. (1989). Purification and activation of the double-stranded RNA-dependent eIF-2 kinase DAI. *Mol Cell Biol*, *9*(4), 1576-1586. https://doi.org/10.1128/mcb.9.4.1576-1586.1989

Kottemann, M. C., Conti, B. A., Lach, F. P., & Smogorzewska, A. (2018). Removal of RTF2 from Stalled Replisomes Promotes Maintenance of Genome Integrity. *Molecular Cell*, *69*(1), 24-+. https://doi.org/10.1016/j.molcel.2017.11.035

Kraft, D. C., Deocaris, C. C., Wadhwa, R., & Rattan, S. I. (2006). Preincubation with the proteasome inhibitor MG-132 enhances proteasome activity via the Nrf2 transcription factor in aging human skin fibroblasts. *Ann N Y Acad Sci*, *1067*, 420-424. https://doi.org/10.1196/annals.1354.060

Kraus, M., Bader, J., Overkleeft, H., & Driessen, C. (2013). Nelfinavir augments proteasome inhibition by bortezomib in myeloma cells and overcomes bortezomib and carfilzomib resistance. *Blood Cancer J*, *3*(3), e103. https://doi.org/10.1038/bcj.2013.2

Krylov, D. M., & Koonin, E. V. (2001). A novel family of predicted retroviral-like aspartyl proteases with a possible key role in eukaryotic cell cycle control. *Current Biology*, *11*(15), R584-R587. https://doi.org/Doi 10.1016/S0960-9822(01)00357-8

Kulak, N. A., Geyer, P. E., & Mann, M. (2017). Loss-less Nano-fractionator for High Sensitivity, High Coverage Proteomics. *Mol Cell Proteomics*, *16*(4), 694-705. https://doi.org/10.1074/mcp.O116.065136

Kuo, C. L., & Goldberg, A. L. (2017). Ubiquitinated proteins promote the association of proteasomes with the deubiquitinating enzyme Usp14 and the ubiquitin ligase Ube3c. *Proc Natl Acad Sci U S A*, *114*(17), E3404-E3413. https://doi.org/10.1073/pnas.1701734114

Kury, S., Besnard, T., Ebstein, F., Khan, T. N., Gambin, T., Douglas, J., Bacino, C. A., Craigen, W. J., Sanders, S. J., Lehmann, A., Latypova, X., Khan, K., Pacault, M., Sacharow, S., Glaser, K., Bieth, E., Perrin-Sabourin, L., Jacquemont, M. L., Cho, M. T., . . . Isidor, B. (2017). De Novo Disruption of the Proteasome Regulatory Subunit PSMD12 Causes a Syndromic Neurodevelopmental Disorder. *Am J Hum Genet*, *100*(4), 689. https://doi.org/10.1016/j.ajhg.2017.03.003

Kwak, M. K., Wakabayashi, N., Greenlaw, J. L., Yamamoto, M., & Kensler, T. W. (2003). Antioxidants enhance mammalian proteasome expression through the Keap1-Nrf2 signaling pathway. *Mol Cell Biol*, *23*(23), 8786-8794. https://doi.org/10.1128/MCB.23.23.8786-8794.2003

Labbadia, J., & Morimoto, R. I. (2015). The biology of proteostasis in aging and disease. *Annu Rev Biochem*, *84*, 435-464. https://doi.org/10.1146/annurev-biochem-060614-033955

Lai, Y., Lin, F., Wang, X., Zhang, J., Xia, J., Sun, Y., Wen, M., Li, X., Zhang, Z., & Zhao, J. (2021). STYK1/NOK Promotes Metastasis and Epithelial-Mesenchymal Transition in Non-small Cell Lung Cancer by Suppressing FoxO1 Signaling. *Front Cell Dev Biol*, *9*, 621147. https://doi.org/10.3389/fcell.2021.621147

Lai, Y., Zhang, Z., Li, J., Li, W., Huang, Z., Zhang, C., Li, X., & Zhao, J. (2019). STYK1/NOK correlates with ferroptosis in non-small cell lung carcinoma. *Biochem Biophys Res Commun*, *519*(4), 659-666. https://doi.org/10.1016/j.bbrc.2019.09.032

Lam, C., Ferreira, C., Krasnewich, D., Toro, C., Latham, L., Zein, W. M., Lehky, T., Brewer, C., Baker, E. H., Thurm, A., Farmer, C. A., Rosenzweig, S. D., Lyons, J. J., Schreiber, J. M., Gropman, A., Lingala, S., Ghany, M. G., Solomon, B., Macnamara, E., . . . Wolfe, L. (2017). Prospective phenotyping of NGLY1-CDDG, the first congenital

disorder of deglycosylation. *Genet Med*, *19*(2), 160-168. https://doi.org/10.1038/gim.2016.75

Layman, A. A. K., Sprout, S. L., Phillips, D., & Oliver, P. M. (2017). Ndfip1 restricts Th17 cell potency by limiting lineage stability and proinflammatory cytokine production. *Sci Rep*, *7*, 39649. https://doi.org/10.1038/srep39649

Lederkremer, G. Z., & Glickman, M. H. (2005). A window of opportunity: timing protein degradation by trimming of sugars and ubiquitins. *Trends Biochem Sci*, *30*(6), 297-303. https://doi.org/10.1016/j.tibs.2005.04.010

Lee, B. H., Lee, M. J., Park, S., Oh, D. C., Elsasser, S., Chen, P. C., Gartner, C., Dimova, N., Hanna, J., Gygi, S. P., Wilson, S. M., King, R. W., & Finley, D. (2010). Enhancement of proteasome activity by a small-molecule inhibitor of USP14. *Nature*, *467*(7312), 179-184. https://doi.org/10.1038/nature09299

Lee, C., Kim, H., & Bardwell, J. C. A. (2018). Electrostatic interactions are important for chaperone-client interaction in vivo. *Microbiology (Reading)*, *164*(7), 992-997. https://doi.org/10.1099/mic.0.000676

Lee, C. S., Ho, D. V., & Chan, J. Y. (2013). Nuclear factor-erythroid 2-related factor 1 regulates expression of proteasome genes in hepatocytes and protects against endoplasmic reticulum stress and steatosis in mice. *FEBS J*, *280*(15), 3609-3620. https://doi.org/10.1111/febs.12350

Lee, C. S., Lee, C., Hu, T., Nguyen, J. M., Zhang, J., Martin, M. V., Vawter, M. P., Huang, E. J., & Chan, J. Y. (2011). Loss of nuclear factor E2-related factor 1 in the brain leads to dysregulation of proteasome gene expression and neurodegeneration. *Proc Natl Acad Sci U S A*, *108*(20), 8408-8413. https://doi.org/10.1073/pnas.1019209108

Lee, D. Y., & Brown, E. J. (2012). Ubiquilins in the crosstalk among proteolytic pathways. *Biol Chem*, *393*(6), 441-447. https://doi.org/10.1515/hsz-2012-0120

Lehrbach, N. J., Breen, P. C., & Ruvkun, G. (2019). Protein Sequence Editing of SKN-1A/Nrf1 by Peptide:N-Glycanase Controls Proteasome Gene Expression. *Cell*, *177*(3), 737-750 e715. https://doi.org/10.1016/j.cell.2019.03.035

Lehrbach, N. J., & Ruvkun, G. (2016). Proteasome dysfunction triggers activation of SKN-1A/Nrf1 by the aspartic protease DDI-1. *Elife*, *5*. https://doi.org/10.7554/eLife.17721

Lehrbach, N. J., & Ruvkun, G. (2019). Endoplasmic reticulum-associated SKN-1A/Nrf1 mediates a cytoplasmic unfolded protein response and promotes longevity. *Elife*, *8*. https://doi.org/10.7554/eLife.44425

Lerner, M., Corcoran, M., Cepeda, D., Nielsen, M. L., Zubarev, R., Ponten, F., Uhlen, M., Hober, S., Grander, D., & Sangfelt, O. (2007). The RBCC gene RFP2 (Leu5) encodes a novel transmembrane E3 ubiquitin ligase involved in ERAD. *Mol Biol Cell*, *18*(5), 1670-1682. https://doi.org/10.1091/mbc.e06-03-0248

Li, X., Matilainen, O., Jin, C., Glover-Cutter, K. M., Holmberg, C. I., & Blackwell, T. K. (2011). Specific SKN-1/Nrf stress responses to perturbations in translation elongation and proteasome activity. *PLoS Genet*, *7*(6), e1002119. https://doi.org/10.1371/journal.pgen.1002119

Li, X. L., Huang, Y. Y., Yuan, T. J., Lian, X. P., & Bi, H. L. (2020). STYK1 promotes the malignant progression of laryngeal squamous cell carcinoma through targeting TGF-

beta1. *Eur Rev Med Pharmacol Sci*, *24*(11), 6166-6174. https://doi.org/10.26355/eurrev_202006_21512

Liepe, J., Ovaa, H., & Mishto, M. (2018). Why do proteases mess up with antigen presentation by re-shuffling antigen sequences? *Curr Opin Immunol*, *52*, 81-86. https://doi.org/10.1016/j.coi.2018.04.016

Lilley, B. N., & Ploegh, H. L. (2004). A membrane protein required for dislocation of misfolded proteins from the ER. *Nature*, *429*(6994), 834-840. https://doi.org/10.1038/nature02592

Lim, P. J., Danner, R., Liang, J., Doong, H., Harman, C., Srinivasan, D., Rothenberg, C., Wang, H., Ye, Y., Fang, S., & Monteiro, M. J. (2009). Ubiquilin and p97/VCP bind erasin, forming a complex involved in ERAD. *J Cell Biol*, *187*(2), 201-217. https://doi.org/10.1083/jcb.200903024

Litchfield, D. W. (2003). Protein kinase CK2: structure, regulation and role in cellular decisions of life and death. *Biochemical Journal*, *369*, 1-15. https://doi.org/10.1042/Bj20021469

Liu, P., Kerins, M. J., Tian, W., Neupane, D., Zhang, D. D., & Ooi, A. (2019). Differential and overlapping targets of the transcriptional regulators NRF1, NRF2, and NRF3 in human cells. *J Biol Chem*, *294*(48), 18131-18149. https://doi.org/10.1074/jbc.RA119.009591

Liu, Y., Ramot, Y., Torrelo, A., Paller, A. S., Si, N., Babay, S., Kim, P. W., Sheikh, A., Lee, C. C., Chen, Y., Vera, A., Zhang, X., Goldbach-Mansky, R., & Zlotogorski, A. (2012). Mutations in proteasome subunit beta type 8 cause chronic atypical neutrophilic dermatosis with lipodystrophy and elevated temperature with evidence of genetic and phenotypic heterogeneity. *Arthritis Rheum*, *64*(3), 895-907. https://doi.org/10.1002/art.33368

Liu, Y. L., & Xiao, W. (1997). Bidirectional regulation of two DNA-damage-inducible genes, MAG1 and DDI1, from Saccharomyces cerevisiae. *Molecular Microbiology*, *23*(4), 777-789. https://doi.org/DOI 10.1046/j.1365-2958.1997.2701631.x

Lohr, N. J., Molleston, J. P., Strauss, K. A., Torres-Martinez, W., Sherman, E. A., Squires, R. H., Rider, N. L., Chikwava, K. R., Cummings, O. W., Morton, D. H., & Puffenberger, E. G. (2010). Human ITCH E3 ubiquitin ligase deficiency causes syndromic multisystem autoimmune disease. *Am J Hum Genet*, *86*(3), 447-453. https://doi.org/10.1016/j.ajhg.2010.01.028

Lopez-Otin, C., Blasco, M. A., Partridge, L., Serrano, M., & Kroemer, G. (2013). The hallmarks of aging. *Cell*, *153*(6), 1194-1217. https://doi.org/10.1016/j.cell.2013.05.039

Loureiro, J., Lilley, B. N., Spooner, E., Noriega, V., Tortorella, D., & Ploegh, H. L. (2006). Signal peptide peptidase is required for dislocation from the endoplasmic reticulum. *Nature*, *441*(7095), 894-897. https://doi.org/10.1038/nature04830

Lu, J. P., Wang, Y., Sliter, D. A., Pearce, M. M., & Wojcikiewicz, R. J. (2011). RNF170 protein, an endoplasmic reticulum membrane ubiquitin ligase, mediates inositol 1,4,5-trisphosphate receptor ubiquitination and degradation. *J Biol Chem*, *286*(27), 24426-24433. https://doi.org/10.1074/jbc.M111.251983

Lynes, E. M., & Simmen, T. (2011). Urban planning of the endoplasmic reticulum (ER): how diverse mechanisms segregate the many functions of the ER. *Biochim Biophys Acta*, *1813*(10), 1893-1905. https://doi.org/10.1016/j.bbamcr.2011.06.011

Ma, M., & Liu, Z. L. (2010). Comparative transcriptome profiling analyses during the lag phase uncover YAP1, PDR1, PDR3, RPN4, and HSF1 as key regulatory genes in genomic adaptation to the lignocellulose derived inhibitor HMF for Saccharomyces cerevisiae. *BMC Genomics*, *11*, 660. https://doi.org/10.1186/1471-2164-11-660

Ma, Q. (2013). Role of nrf2 in oxidative stress and toxicity. *Annu Rev Pharmacol Toxicol*, *53*, 401-426. https://doi.org/10.1146/annurev-pharmtox-011112-140320

Manasanch, E. E., & Orlowski, R. Z. (2017). Proteasome inhibitors in cancer therapy. *Nat Rev Clin Oncol*, *14*(7), 417-433. https://doi.org/10.1038/nrclinonc.2016.206

Mannhaupt, G., Schnall, R., Karpov, V., Vetter, I., & Feldmann, H. (1999). Rpn4p acts as a transcription factor by binding to PACE, a nonamer box found upstream of 26S proteasomal and other genes in yeast. *FEBS Lett*, *450*(1-2), 27-34. https://doi.org/10.1016/s0014-5793(99)00467-6

Marshall, A. G., Watson, J. A., Hallengren, J. J., Walters, B. J., Dobrunz, L. E., Francillon, L., Wilson, J. A., Phillips, S. E., & Wilson, S. M. (2013). Genetic background alters the severity and onset of neuromuscular disease caused by the loss of ubiquitin-specific protease 14 (usp14). *PLoS One*, *8*(12), e84042. https://doi.org/10.1371/journal.pone.0084042

Martin-Campos, T., Mylonas, R., Masselot, A., Waridel, P., Petricevic, T., Xenarios, I., & Quadroni, M. (2017). MsViz: A Graphical Software Tool for In-Depth Manual Validation and Quantitation of Post-translational Modifications. *J Proteome Res*, *16*(8), 3092-3101. https://doi.org/10.1021/acs.jproteome.7b00194

Maruyama, Y., Yamada, M., Takahashi, K., & Yamada, M. (2008). Ubiquitin ligase Kf-1 is involved in the endoplasmic reticulum-associated degradation pathway. *Biochem Biophys Res Commun*, *374*(4), 737-741. https://doi.org/10.1016/j.bbrc.2008.07.126

Matsui, T., Miyamoto, K., Kubo, A., Kawasaki, H., Ebihara, T., Hata, K., Tanahashi, S., Ichinose, S., Imoto, I., Inazawa, J., Kudoh, J., & Amagai, M. (2011). SASPase regulates stratum corneum hydration through profilaggrin-to-filaggrin processing. *EMBO Mol Med*, *3*(6), 320-333. https://doi.org/10.1002/emmm.201100140

Matyskiela, M. E., & Martin, A. (2013). Design principles of a universal protein degradation machine. *Journal of Molecular Biology*, *425*(2), 199-213. https://doi.org/10.1016/j.jmb.2012.11.001

Medicherla, B., Kostova, Z., Schaefer, A., & Wolf, D. H. (2004). A genomic screen identifies Dsk2p and Rad23p as essential components of ER-associated degradation. *EMBO Rep*, *5*(7), 692-697. https://doi.org/10.1038/sj.embor.7400164

Meuwissen, M. E., Schot, R., Buta, S., Oudesluijs, G., Tinschert, S., Speer, S. D., Li, Z., van Unen, L., Heijsman, D., Goldmann, T., Lequin, M. H., Kros, J. M., Stam, W., Hermann, M., Willemsen, R., Brouwer, R. W., Van, I. W. F., Martin-Fernandez, M., de Coo, I., . . . Mancini, G. M. (2016). Human USP18 deficiency underlies type 1 interferonopathy leading to severe pseudo-TORCH syndrome. *J Exp Med*, *213*(7), 1163-1174. https://doi.org/10.1084/jem.20151529

Mijaljica, D., Prescott, M., & Devenish, R. J. (2011). Microautophagy in mammalian cells: revisiting a 40-year-old conundrum. *Autophagy*, *7*(7), 673-682. https://doi.org/10.4161/auto.7.7.14733

Miners, J. S., Clarke, P., & Love, S. (2017). Clusterin levels are increased in Alzheimer's disease and influence the regional distribution of Abeta. *Brain Pathol*, *27*(3), 305-313. https://doi.org/10.1111/bpa.12392

Mishra, A., Godavarthi, S. K., Maheshwari, M., Goswami, A., & Jana, N. R. (2009). The ubiquitin ligase E6-AP is induced and recruited to aggresomes in response to proteasome inhibition and may be involved in the ubiquitination of Hsp70-bound misfolded proteins. *J Biol Chem*, *284*(16), 10537-10545. https://doi.org/10.1074/jbc.M806804200

Mishto, M., & Liepe, J. (2017). Post-Translational Peptide Splicing and T Cell Responses. *Trends Immunol*, *38*(12), 904-915. https://doi.org/10.1016/j.it.2017.07.011

Mishto, M., Liepe, J., Textoris-Taube, K., Keller, C., Henklein, P., Weberruss, M., Dahlmann, B., Enenkel, C., Voigt, A., Kuckelkorn, U., Stumpf, M. P., & Kloetzel, P. M. (2014). Proteasome isoforms exhibit only quantitative differences in cleavage and epitope generation. *Eur J Immunol*, *44*(12), 3508-3521. https://doi.org/10.1002/eji.201444902

Miyake, H., Gleave, M., Kamidono, S., & Hara, I. (2002). Overexpression of clusterin in transitional cell carcinoma of the bladder is related to disease progression and recurrence. *Urology*, *59*(1), 150-154. https://doi.org/10.1016/s0090-4295(01)01484-4

Miyake, H., Hara, S., Arakawa, S., Kamidono, S., & Hara, I. (2002). Over expression of clusterin is an independent prognostic factor for nonpapillary renal cell carcinoma. *J Urol*, *167*(2 Pt 1), 703-706. https://doi.org/10.1016/S0022-5347(01)69130-4

Miyake, H., Yamanaka, K., Muramaki, M., Kurahashi, T., Gleave, M., & Hara, I. (2005). Enhanced expression of the secreted form of clusterin following neoadjuvant hormonal therapy as a prognostic predictor in patients undergoing radical prostatectomy for prostate cancer. *Oncol Rep*, *14*(5), 1371-1375. https://www.ncbi.nlm.nih.gov/pubmed/16211311

Moi, P., Chan, K., Asunis, I., Cao, A., & Kan, Y. W. (1994). Isolation of NF-E2-related factor 2 (Nrf2), a NF-E2-like basic leucine zipper transcriptional activator that binds to the tandem NF-E2/AP1 repeat of the beta-globin locus control region. *Proc Natl Acad Sci U S A*, *91*(21), 9926-9930. https://doi.org/10.1073/pnas.91.21.9926

Molinari, M. (2007). N-glycan structure dictates extension of protein folding or onset of disposal. *Nat Chem Biol*, *3*(6), 313-320. https://doi.org/10.1038/nchembio880

Monaco, J. J., Cho, S., & Attaya, M. (1990). Transport protein genes in the murine MHC: possible implications for antigen processing. *Science*, *250*(4988), 1723-1726. https://doi.org/10.1126/science.2270487

Morawe, T., Honemann-Capito, M., von Stein, W., & Wodarz, A. (2011). Loss of the extraproteasomal ubiquitin receptor Rings lost impairs ring canal growth in Drosophila oogenesis. *Journal of Cell Biology*, *193*(1), 71-80. https://doi.org/10.1083/jcb.201009142

Morel, S., Levy, F., Burlet-Schiltz, O., Brasseur, F., Probst-Kepper, M., Peitrequin, A. L., Monsarrat, B., Van Velthoven, R., Cerottini, J. C., Boon, T., Gairin, J. E., & Van den

Eynde, B. J. (2000). Processing of some antigens by the standard proteasome but not by the immunoproteasome results in poor presentation by dendritic cells. *Immunity*, *12*(1), 107-117. https://doi.org/10.1016/s1074-7613(00)80163-6

Motohashi, H., O'Connor, T., Katsuoka, F., Engel, J. D., & Yamamoto, M. (2002). Integration and diversity of the regulatory network composed of Maf and CNC families of transcription factors. *Gene*, *294*(1-2), 1-12. https://doi.org/10.1016/s0378-1119(02)00788-6

Motyan, J. A., Miczi, M., & Tozser, J. (2020). Dimer Interface Organization is a Main Determinant of Intermonomeric Interactions and Correlates with Evolutionary Relationships of Retroviral and Retroviral-Like Ddi1 and Ddi2 Proteases. *Int J Mol Sci*, *21*(4). https://doi.org/10.3390/ijms21041352

Mueller, W. F., Jakob, P., Sun, H., Clauder-Munster, S., Ghidelli-Disse, S., Ordonez, D., Boesche, M., Bantscheff, M., Collier, P., Haase, B., Benes, V., Paulsen, M., Sehr, P., Lewis, J., Drewes, G., & Steinmetz, L. M. (2020). Loss of N-Glycanase 1 Alters Transcriptional and Translational Regulation in K562 Cell Lines. *G3 (Bethesda)*, *10*(5), 1585-1597. https://doi.org/10.1534/g3.119.401031

Nandi, D., Tahiliani, P., Kumar, A., & Chandu, D. (2006). The ubiquitin-proteasome system. *J Biosci*, *31*(1), 137-155. https://doi.org/10.1007/BF02705243

Navia, M. A., Fitzgerald, P. M. D., Mckeever, B. M., Leu, C. T., Heimbach, J. C., Herber, W. K., Sigal, I. S., Darke, P. L., & Springer, J. P. (1989). 3-Dimensional Structure of Aspartyl Protease from Human Immunodeficiency Virus Hiv-1. *Nature*, *337*(6208), 615-620. https://doi.org/DOI 10.1038/337615a0

Navon, A., & Ciechanover, A. (2009). The 26 S proteasome: from basic mechanisms to drug targeting. *J Biol Chem*, *284*(49), 33713-33718. https://doi.org/10.1074/jbc.R109.018481

Neutzner, A., Neutzner, M., Benischke, A. S., Ryu, S. W., Frank, S., Youle, R. J., & Karbowski, M. (2011). A systematic search for endoplasmic reticulum (ER) membrane-associated RING finger proteins identifies Nixin/ZNRF4 as a regulator of calnexin stability and ER homeostasis. *J Biol Chem*, *286*(10), 8633-8643. https://doi.org/10.1074/jbc.M110.197459

Nguyen, H. M., Schippers, J. H., Goni-Ramos, O., Christoph, M. P., Dortay, H., van der Hoorn, R. A., & Mueller-Roeber, B. (2013). An upstream regulator of the 26S proteasome modulates organ size in Arabidopsis thaliana. *Plant J*, *74*(1), 25-36. https://doi.org/10.1111/tpj.12097

Nillegoda, N. B., Theodoraki, M. A., Mandal, A. K., Mayo, K. J., Ren, H. Y., Sultana, R., Wu, K., Johnson, J., Cyr, D. M., & Caplan, A. J. (2010). Ubr1 and Ubr2 function in a quality control pathway for degradation of unfolded cytosolic proteins. *Mol Biol Cell*, *21*(13), 2102-2116. https://doi.org/10.1091/mbc.e10-02-0098

Northrop, A., Vangala, J. R., Feygin, A., & Radhakrishnan, S. K. (2020). Disabling the Protease DDI2 Attenuates the Transcriptional Activity of NRF1 and Potentiates Proteasome Inhibitor Cytotoxicity. *Int J Mol Sci*, *21*(1). https://doi.org/10.3390/ijms21010327

Novikoff, A. B., Essner, E., & Quintana, N. (1964). Golgi Apparatus and Lysosomes. *Fed Proc*, *23*, 1010-1022. https://www.ncbi.nlm.nih.gov/pubmed/14209792

Ohtsuji, M., Katsuoka, F., Kobayashi, A., Aburatani, H., Hayes, J. D., & Yamamoto, M. (2008). Nrf1 and Nrf2 play distinct roles in activation of antioxidant response element-dependent genes. *J Biol Chem*, *283*(48), 33554-33562. https://doi.org/10.1074/jbc.M804597200

Olivari, S., Cali, T., Salo, K. E., Paganetti, P., Ruddock, L. W., & Molinari, M. (2006). EDEM1 regulates ER-associated degradation by accelerating de-mannosylation of folding-defective polypeptides and by inhibiting their covalent aggregation. *Biochem Biophys Res Commun*, *349*(4), 1278-1284. https://doi.org/10.1016/j.bbrc.2006.08.186

Olivari, S., Galli, C., Alanen, H., Ruddock, L., & Molinari, M. (2005). A novel stress-induced EDEM variant regulating endoplasmic reticulum-associated glycoprotein degradation. *J Biol Chem*, *280*(4), 2424-2428. https://doi.org/10.1074/jbc.C400534200

Olzmann, J. A., Kopito, R. R., & Christianson, J. C. (2013). The mammalian endoplasmic reticulum-associated degradation system. *Cold Spring Harb Perspect Biol*, *5*(9). https://doi.org/10.1101/cshperspect.a013185

Op, M., Ribeiro, S. T., Chavarria, C., De Gassart, A., Zaffalon, L., & Martinon, F. (2022). The aspartyl protease DDI2 drives adaptation to proteasome inhibition in multiple myeloma. *Cell Death Dis*, *13*(5), 475. https://doi.org/10.1038/s41419-022-04925-3

Pang, S., Lynn, D. A., Lo, J. Y., Paek, J., & Curran, S. P. (2014). SKN-1 and Nrf2 couples proline catabolism with lipid metabolism during nutrient deprivation. *Nat Commun*, *5*, 5048. https://doi.org/10.1038/ncomms6048

Pankiv, S., Clausen, T. H., Lamark, T., Brech, A., Bruun, J. A., Outzen, H., Overvatn, A., Bjorkoy, G., & Johansen, T. (2007). p62/SQSTM1 binds directly to Atg8/LC3 to facilitate degradation of ubiquitinated protein aggregates by autophagy. *J Biol Chem*, *282*(33), 24131-24145. https://doi.org/10.1074/jbc.M702824200

Parham, P. (1990). Antigen processing. Transporters of delight. *Nature*, *348*(6303), 674-675. https://doi.org/10.1038/348674a0

Perteguer, M. J., Gomez-Puertas, P., Canavate, C., Dagger, F., Garate, T., & Valdivieso, E. (2013). Ddi1-like protein from Leishmania major is an active aspartyl proteinase. *Cell Stress & Chaperones*, *18*(2), 171-181. https://doi.org/10.1007/s12192-012-0368-9

Pettit, S. C., Simsic, J., Loeb, D. D., Everitt, L., Hutchison, C. A., 3rd, & Swanstrom, R. (1991). Analysis of retroviral protease cleavage sites reveals two types of cleavage sites and the structural requirements of the P1 amino acid. *J Biol Chem*, *266*(22), 14539-14547. https://www.ncbi.nlm.nih.gov/pubmed/1860860

Pickart, C. M. (2001). Mechanisms underlying ubiquitination. *Annu Rev Biochem*, *70*, 503-533. https://doi.org/10.1146/annurev.biochem.70.1.503

Pickart, C. M., & Cohen, R. E. (2004). Proteasomes and their kin: proteases in the machine age. *Nat Rev Mol Cell Biol*, *5*(3), 177-187. https://doi.org/10.1038/nrm1336

Pieroni, L., Santolini, E., Fipaldini, C., Pacini, L., Migliaccio, G., & La Monica, N. (1997). In vitro study of the NS2-3 protease of hepatitis C virus. *J Virol*, *71*(9), 6373-6380. https://doi.org/10.1128/JVI.71.9.6373-6380.1997

Pisoni, G. B., & Molinari, M. (2016). Five Questions (with their Answers) on ER-Associated Degradation. *Traffic*, *17*(4), 341-350. https://doi.org/10.1111/tra.12373

Platteel, A. C. M., Liepe, J., van Eden, W., Mishto, M., & Sijts, A. (2017). An Unexpected Major Role for Proteasome-Catalyzed Peptide Splicing in Generation of T Cell Epitopes: Is There Relevance for Vaccine Development? *Front Immunol*, *8*, 1441. https://doi.org/10.3389/fimmu.2017.01441

Poli, M. C., Ebstein, F., Nicholas, S. K., de Guzman, M. M., Forbes, L. R., Chinn, I. K., Mace, E. M., Vogel, T. P., Carisey, A. F., Benavides, F., Coban-Akdemir, Z. H., Gibbs, R. A., Jhangiani, S. N., Muzny, D. M., Carvalho, C. M. B., Schady, D. A., Jain, M., Rosenfeld, J. A., Emrick, L., . . . Orange, J. S. (2018). Heterozygous Truncating Variants in POMP Escape Nonsense-Mediated Decay and Cause a Unique Immune Dysregulatory Syndrome. *Am J Hum Genet*, *102*(6), 1126-1142. https://doi.org/10.1016/j.ajhg.2018.04.010

Poole, E., & Tate, W. (2000). Release factors and their role as decoding proteins: specificity and fidelity for termination of protein synthesis. *Biochim Biophys Acta*, *1493*(1-2), 1-11. https://doi.org/10.1016/s0167-4781(00)00162-7

Powers, E. T., Morimoto, R. I., Dillin, A., Kelly, J. W., & Balch, W. E. (2009). Biological and chemical approaches to diseases of proteostasis deficiency. *Annu Rev Biochem*, *78*, 959-991. https://doi.org/10.1146/annurev.biochem.052308.114844

Prabu-Jeyabalan, M., Nalivaika, E., & Schiffer, C. A. (2002). Substrate shape determines specificity of recognition for HIV-1 protease: analysis of crystal structures of six substrate complexes. *Structure*, *10*(3), 369-381. https://doi.org/10.1016/s0969-2126(02)00720-7

Radhakrishnan, S. K., den Besten, W., & Deshaies, R. J. (2014). p97-dependent retrotranslocation and proteolytic processing govern formation of active Nrf1 upon proteasome inhibition. *Elife*, *3*, e01856. https://doi.org/10.7554/eLife.01856

Radhakrishnan, S. K., Lee, C. S., Young, P., Beskow, A., Chan, J. Y., & Deshaies, R. J. (2010). Transcription factor Nrf1 mediates the proteasome recovery pathway after proteasome inhibition in mammalian cells. *Mol Cell*, *38*(1), 17-28. https://doi.org/10.1016/j.molcel.2010.02.029

Rashid, H. O., Yadav, R. K., Kim, H. R., & Chae, H. J. (2015). ER stress: Autophagy induction, inhibition and selection. *Autophagy*, *11*(11), 1956-1977. https://doi.org/10.1080/15548627.2015.1091141

Redondo, M., Villar, E., Torres-Munoz, J., Tellez, T., Morell, M., & Petito, C. K. (2000). Overexpression of clusterin in human breast carcinoma. *Am J Pathol*, *157*(2), 393-399. https://doi.org/10.1016/S0002-9440(10)64552-X

Reits, E. A., Vos, J. C., Gromme, M., & Neefjes, J. (2000). The major substrates for TAP in vivo are derived from newly synthesized proteins. *Nature*, *404*(6779), 774-778. https://doi.org/10.1038/35008103

Ribeiro, S. T., de Gassart, A., Bettigole, S., Zaffalon, L., Chavarria, C., Op, M., Nugraha, K., & Martinon, F. (2022). The protease DDI2 regulates NRF1 activation in response to cadmium toxicity. *iScience*, *25*(10), 105227. https://doi.org/10.1016/j.isci.2022.105227

Richly, H., Rape, M., Braun, S., Rumpf, S., Hoege, C., & Jentsch, S. (2005). A series of ubiquitin binding factors connects CDC48/p97 to substrate multiubiquitylation and proteasomal targeting. *Cell*, *120*(1), 73-84. https://doi.org/10.1016/j.cell.2004.11.013

Richter, C., Tanaka, T., & Yada, R. Y. (1998). Mechanism of activation of the gastric aspartic proteinases: pepsinogen, progastricsin and prochymosin. *Biochemical Journal*, *335*, 481-490. https://doi.org/DOI 10.1042/bj3350481

Rigante, D. (2020). Phenotype variability of autoinflammatory disorders in the pediatric patient: A pictorial overview. *J Evid Based Med*, *13*(3), 227-245. https://doi.org/10.1111/jebm.12406

Roche, P. A., & Furuta, K. (2015). The ins and outs of MHC class II-mediated antigen processing and presentation. *Nat Rev Immunol*, *15*(4), 203-216. https://doi.org/10.1038/nri3818

Rodrigo-Brenni, M. C., Gutierrez, E., & Hegde, R. S. (2014). Cytosolic quality control of mislocalized proteins requires RNF126 recruitment to Bag6. *Mol Cell*, *55*(2), 227-237. https://doi.org/10.1016/j.molcel.2014.05.025

Roeten, M. S. F., Cloos, J., & Jansen, G. (2018). Positioning of proteasome inhibitors in therapy of solid malignancies. *Cancer Chemother Pharmacol*, *81*(2), 227-243. https://doi.org/10.1007/s00280-017-3489-0

Rouschop, K. M., van den Beucken, T., Dubois, L., Niessen, H., Bussink, J., Savelkouls, K., Keulers, T., Mujcic, H., Landuyt, W., Voncken, J. W., Lambin, P., van der Kogel, A. J., Koritzinsky, M., & Wouters, B. G. (2010). The unfolded protein response protects human tumor cells during hypoxia through regulation of the autophagy genes MAP1LC3B and ATG5. *J Clin Invest*, *120*(1), 127-141. https://doi.org/10.1172/JCI40027

Rousseau, A., & Bertolotti, A. (2016). An evolutionarily conserved pathway controls proteasome homeostasis. *Nature*, *536*(7615), 184-189. https://doi.org/10.1038/nature18943

Ruan, J., Rothan, H. A., Zhong, Y., Yan, W., Henderson, M. J., Chen, F., & Fang, S. (2019). A small molecule inhibitor of ER-to-cytosol protein dislocation exhibits anti-dengue and anti-Zika virus activity. *Sci Rep*, *9*(1), 10901. https://doi.org/10.1038/s41598-019-47532-7

Ruvkun, G., & Lehrbach, N. (2022). Regulation and Functions of the ER-Associated Nrf1 Transcription Factor. *Cold Spring Harb Perspect Biol*. https://doi.org/10.1101/cshperspect.a041266

Ruvkun, G. J., F.; Sadreyev, R. I. (2021). Phylogenetic evidence for asparagine to aspartic acid protein editing of N-glycosylated SARS-CoV-2 viral proteins by NGLY1 deglycosylation/deamidation suggests an unusual vaccination strategy. *bioRxiv*. https://doi.org/10.1101/2021.09.11.459891

Sabolic, I., Breljak, D., Skarica, M., & Herak-Kramberger, C. M. (2010). Role of metallothionein in cadmium traffic and toxicity in kidneys and other mammalian organs. *Biometals*, *23*(5), 897-926. https://doi.org/10.1007/s10534-010-9351-z

Saez, I., & Vilchez, D. (2014). The Mechanistic Links Between Proteasome Activity, Aging and Age-related Diseases. *Curr Genomics*, *15*(1), 38-51. https://doi.org/10.2174/1389202915011403061133344

Sanjana, N. E., Shalem, O., & Zhang, F. (2014). Improved vectors and genome-wide libraries for CRISPR screening. *Nat Methods*, *11*(8), 783-784. https://doi.org/10.1038/nmeth.3047

Sarrabay, G., Mechin, D., Salhi, A., Boursier, G., Rittore, C., Crow, Y., Rice, G., Tran, T. A., Cezar, R., Duffy, D., Bondet, V., Boudhane, L., Broca, C., Kant, B. P., VanGijn, M., Grandemange, S., Richard, E., Apparailly, F., & Touitou, I. (2020). PSMB10, the last immunoproteasome gene missing for PRAAS. *J Allergy Clin Immunol*, *145*(3), 1015-1017 e1016. https://doi.org/10.1016/j.jaci.2019.11.024

Sato, S., Nakamura, Y., Kaneko, T., Katoh, T., Asamizu, E., & Tabata, S. (2000). Structural analysis of Arabidopsis thaliana chromosome 3. I. Sequence features of the regions of 4,504,864 bp covered by sixty P1 and TAC clones. *DNA Res*, *7*(2), 131-135. https://doi.org/10.1093/dnares/7.2.131

Schmidt, M., & Kloetzel, P. M. (1997). Biogenesis of eukaryotic 20S proteasomes: the complex maturation pathway of a complex enzyme. *Faseb Journal*, *11*(14), 1235-1243. https://doi.org/10.1096/fasebj.11.14.9409542

Schoebel, S., Mi, W., Stein, A., Ovchinnikov, S., Pavlovicz, R., DiMaio, F., Baker, D., Chambers, M. G., Su, H., Li, D., Rapoport, T. A., & Liao, M. (2017). Cryo-EM structure of the protein-conducting ERAD channel Hrd1 in complex with Hrd3. *Nature*, *548*(7667), 352-355. https://doi.org/10.1038/nature23314

Schubert, U., Anton, L. C., Gibbs, J., Norbury, C. C., Yewdell, J. W., & Bennink, J. R. (2000). Rapid degradation of a large fraction of newly synthesized proteins by proteasomes. *Nature*, *404*(6779), 770-774. https://doi.org/10.1038/35008096

Schuberth, C., & Buchberger, A. (2008). UBX domain proteins: major regulators of the AAA ATPase Cdc48/p97. *Cell Mol Life Sci*, *65*(15), 2360-2371. https://doi.org/10.1007/s00018-008-8072-8

Schultz, M. L., Krus, K. L., Kaushik, S., Dang, D., Chopra, R., Qi, L., Shakkottai, V. G., Cuervo, A. M., & Lieberman, A. P. (2018). Coordinate regulation of mutant NPC1 degradation by selective ER autophagy and MARCH6-dependent ERAD. *Nat Commun*, *9*(1), 3671. https://doi.org/10.1038/s41467-018-06115-2

Schulze, A., Standera, S., Buerger, E., Kikkert, M., van Voorden, S., Wiertz, E., Koning, F., Kloetzel, P. M., & Seeger, M. (2005). The ubiquitin-domain protein HERP forms a complex with components of the endoplasmic reticulum associated degradation pathway. *Journal of Molecular Biology*, *354*(5), 1021-1027. https://doi.org/10.1016/j.jmb.2005.10.020

Schwarz, D. S., & Blower, M. D. (2016). The endoplasmic reticulum: structure, function and response to cellular signaling. *Cell Mol Life Sci*, *73*(1), 79-94. https://doi.org/10.1007/s00018-015-2052-6

Seifert, U., Bialy, L. P., Ebstein, F., Bech-Otschir, D., Voigt, A., Schroter, F., Prozorovski, T., Lange, N., Steffen, J., Rieger, M., Kuckelkorn, U., Aktas, O., Kloetzel, P. M., & Kruger, E. (2010). Immunoproteasomes preserve protein homeostasis upon interferon-induced oxidative stress. *Cell*, *142*(4), 613-624. https://doi.org/10.1016/j.cell.2010.07.036

Sekine, H., Okazaki, K., Kato, K., Alam, M. M., Shima, H., Katsuoka, F., Tsujita, T., Suzuki, N., Kobayashi, A., Igarashi, K., Yamamoto, M., & Motohashi, H. (2018). O-GlcNAcylation Signal Mediates Proteasome Inhibitor Resistance in Cancer Cells by Stabilizing NRF1. *Mol Cell Biol*, *38*(17). https://doi.org/10.1128/MCB.00252-18

Semple, C. A., Group, R. G., & Members, G. S. L. (2003). The comparative proteomics of ubiquitination in mouse. *Genome Res*, *13*(6B), 1389-1394. https://doi.org/10.1101/gr.980303

Serbyn, N., Noireterre, A., Bagdiul, I., Plank, M., Michel, A. H., Loewith, R., Kornmann, B., & Stutz, F. (2020). The Aspartic Protease Ddi1 Contributes to DNA-Protein Crosslink Repair in Yeast. *Molecular Cell*, *77*(5), 1066-+. https://doi.org/10.1016/j.molcel.2019.12.007

Sha, Z., & Goldberg, A. L. (2014). Proteasome-mediated processing of Nrf1 is essential for coordinate induction of all proteasome subunits and p97. *Curr Biol*, *24*(14), 1573-1583. https://doi.org/10.1016/j.cub.2014.06.004

Sha, Z., & Goldberg, A. L. (2016). Reply to Vangala et al.: Complete inhibition of the proteasome reduces new proteasome production by causing Nrf1 aggregation. *Curr Biol*, *26*(18), R836-R837. https://doi.org/10.1016/j.cub.2016.08.030

Sha, Z., Schnell, H. M., Ruoff, K., & Goldberg, A. (2018). Rapid induction of p62 and GABARAPL1 upon proteasome inhibition promotes survival before autophagy activation. *J Cell Biol*, *217*(5), 1757-1776. https://doi.org/10.1083/jcb.201708168

Shpilka, T., & Haynes, C. M. (2018). The mitochondrial UPR: mechanisms, physiological functions and implications in ageing. *Nat Rev Mol Cell Biol*, *19*(2), 109-120. https://doi.org/10.1038/nrm.2017.110

Sijts, A. J., Standera, S., Toes, R. E., Ruppert, T., Beekman, N. J., van Veelen, P. A., Ossendorp, F. A., Melief, C. J., & Kloetzel, P. M. (2000). MHC class I antigen processing of an adenovirus CTL epitope is linked to the levels of immunoproteasomes in infected cells. *J Immunol*, *164*(9), 4500-4506. https://doi.org/10.4049/jimmunol.164.9.4500

Sirkis, R., Gerst, J. E., & Fass, D. (2006). Ddi1, a eukaryotic protein with the retroviral protease fold. *Journal of Molecular Biology*, *364*(3), 376-387. https://doi.org/10.1016/j.jmb.2006.08.086

Sitia, R., & Meldolesi, J. (1992). Endoplasmic reticulum: a dynamic patchwork of specialized subregions. *Mol Biol Cell*, *3*(10), 1067-1072. https://doi.org/10.1091/mbc.3.10.1067

Siva, M., Svoboda, M., Veverka, V., Trempe, J. F., Hofmann, K., Kozisek, M., Hexnerova, R., Sedlak, F., Belza, J., Brynda, J., Sacha, P., Hubalek, M., Starkova, J., Flaisigova, I., Konvalinka, J., & Saskova, K. G. (2016a). Human DNA-Damage-Inducible 2 Protein Is Structurally and Functionally Distinct from Its Yeast Ortholog. *Scientific Reports*, *6*. https://doi.org/ARTN 30443
10.1038/srep30443

Siva, M., Svoboda, M., Veverka, V., Trempe, J. F., Hofmann, K., Kozisek, M., Hexnerova, R., Sedlak, F., Belza, J., Brynda, J., Sacha, P., Hubalek, M., Starkova, J., Flaisigova, I., Konvalinka, J., & Saskova, K. G. (2016b). Human DNA-Damage-Inducible 2 Protein Is Structurally and Functionally Distinct from Its Yeast Ortholog. *Sci Rep*, *6*, 30443. https://doi.org/10.1038/srep30443

Speliotes, E. K., Willer, C. J., Berndt, S. I., Monda, K. L., Thorleifsson, G., Jackson, A. U., Lango Allen, H., Lindgren, C. M., Luan, J., Magi, R., Randall, J. C., Vedantam, S., Winkler, T. W., Qi, L., Workalemahu, T., Heid, I. M., Steinthorsdottir, V., Stringham, H. M., Weedon, M. N., . . . Loos, R. J. (2010). Association analyses of 249,796 individuals reveal 18 new loci associated with body mass index. *Nat Genet*, *42*(11), 937-948. https://doi.org/10.1038/ng.686

Spies, T., Bresnahan, M., Bahram, S., Arnold, D., Blanck, G., Mellins, E., Pious, D., & DeMars, R. (1990). A gene in the human major histocompatibility complex class II

region controlling the class I antigen presentation pathway. *Nature*, *348*(6303), 744-747. https://doi.org/10.1038/348744a0

Stagg, H. R., Thomas, M., van den Boomen, D., Wiertz, E. J., Drabkin, H. A., Gemmill, R. M., & Lehner, P. J. (2009). The TRC8 E3 ligase ubiquitinates MHC class I molecules before dislocation from the ER. *J Cell Biol*, *186*(5), 685-692. https://doi.org/10.1083/jcb.200906110

Steffen, J., Seeger, M., Koch, A., & Kruger, E. (2010). Proteasomal degradation is transcriptionally controlled by TCF11 via an ERAD-dependent feedback loop. *Mol Cell*, *40*(1), 147-158. https://doi.org/10.1016/j.molcel.2010.09.012

Steinbaugh, M. J., Narasimhan, S. D., Robida-Stubbs, S., Moronetti Mazzeo, L. E., Dreyfuss, J. M., Hourihan, J. M., Raghavan, P., Operana, T. N., Esmaillie, R., & Blackwell, T. K. (2015). Lipid-mediated regulation of SKN-1/Nrf in response to germ cell absence. *Elife*, *4*. https://doi.org/10.7554/eLife.07836

Steinberg, J., Oyasu, R., Lang, S., Sintich, S., Rademaker, A., Lee, C., Kozlowski, J. M., & Sensibar, J. A. (1997). Intracellular levels of SGP-2 (Clusterin) correlate with tumor grade in prostate cancer. *Clin Cancer Res*, *3*(10), 1707-1711. https://www.ncbi.nlm.nih.gov/pubmed/9815554

Steitz, T. A. (2008). A structural understanding of the dynamic ribosome machine. *Nat Rev Mol Cell Biol*, *9*(3), 242-253. https://doi.org/10.1038/nrm2352

Stevenson, J., Huang, E. Y., & Olzmann, J. A. (2016). Endoplasmic Reticulum-Associated Degradation and Lipid Homeostasis. *Annu Rev Nutr*, *36*, 511-542. https://doi.org/10.1146/annurev-nutr-071715-051030

Stock, D., Nederlof, P. M., Seemuller, E., Baumeister, W., Huber, R., & Lowe, J. (1996). Proteasome: from structure to function. *Curr Opin Biotechnol*, *7*(4), 376-385. https://doi.org/10.1016/s0958-1669(96)80111-x

Suguna, K., Padlan, E. A., Smith, C. W., Carlson, W. D., & Davies, D. R. (1987). Binding of a reduced peptide inhibitor to the aspartic proteinase from Rhizopus chinensis: implications for a mechanism of action. *Proc Natl Acad Sci U S A*, *84*(20), 7009-7013. https://doi.org/10.1073/pnas.84.20.7009

Sun, S., Shi, G., Han, X., Francisco, A. B., Ji, Y., Mendonca, N., Liu, X., Locasale, J. W., Simpson, K. W., Duhamel, G. E., Kersten, S., Yates, J. R., 3rd, Long, Q., & Qi, L. (2014). Sel1L is indispensable for mammalian endoplasmic reticulum-associated degradation, endoplasmic reticulum homeostasis, and survival. *Proc Natl Acad Sci U S A*, *111*(5), E582-591. https://doi.org/10.1073/pnas.1318114111

Sun, Z., & Brodsky, J. L. (2019). Protein quality control in the secretory pathway. *J Cell Biol*, *218*(10), 3171-3187. https://doi.org/10.1083/jcb.201906047

Suzuki, T., Huang, C., & Fujihira, H. (2016). The cytoplasmic peptide:N-glycanase (NGLY1) - Structure, expression and cellular functions. *Gene*, *577*(1), 1-7. https://doi.org/10.1016/j.gene.2015.11.021

Suzuki, T., Seko, A., Kitajima, K., Inoue, Y., & Inoue, S. (1994). Purification and enzymatic properties of peptide:N-glycanase from C3H mouse-derived L-929 fibroblast cells. Possible widespread occurrence of post-translational remodification of proteins by N-deglycosylation. *J Biol Chem*, *269*(26), 17611-17618. https://www.ncbi.nlm.nih.gov/pubmed/8021270

Sykiotis, G. P., & Bohmann, D. (2010). Stress-activated cap'n'collar transcription factors in aging and human disease. *Sci Signal*, *3*(112), re3. https://doi.org/10.1126/scisignal.3112re3

Taguchi, K., Motohashi, H., & Yamamoto, M. (2011). Molecular mechanisms of the Keap1-Nrf2 pathway in stress response and cancer evolution. *Genes Cells*, *16*(2), 123-140. https://doi.org/10.1111/j.1365-2443.2010.01473.x

Taylor, R. C., & Dillin, A. (2011). Aging as an event of proteostasis collapse. *Cold Spring Harb Perspect Biol*, *3*(5). https://doi.org/10.1101/cshperspect.a004440

Tebay, L. E., Robertson, H., Durant, S. T., Vitale, S. R., Penning, T. M., Dinkova-Kostova, A. T., & Hayes, J. D. (2015). Mechanisms of activation of the transcription factor Nrf2 by redox stressors, nutrient cues, and energy status and the pathways through which it attenuates degenerative disease. *Free Radic Biol Med*, *88*(Pt B), 108-146. https://doi.org/10.1016/j.freeradbiomed.2015.06.021

Theivanthiran, B., Kathania, M., Zeng, M., Anguiano, E., Basrur, V., Vandergriff, T., Pascual, V., Wei, W. Z., Massoumi, R., & Venuprasad, K. (2015). The E3 ubiquitin ligase Itch inhibits p38alpha signaling and skin inflammation through the ubiquitylation of Tab1. *Sci Signal*, *8*(365), ra22. https://doi.org/10.1126/scisignal.2005903

Thul, P. J., Akesson, L., Wiking, M., Mahdessian, D., Geladaki, A., Ait Blal, H., Alm, T., Asplund, A., Bjork, L., Breckels, L. M., Backstrom, A., Danielsson, F., Fagerberg, L., Fall, J., Gatto, L., Gnann, C., Hober, S., Hjelmare, M., Johansson, F., . . . Lundberg, E. (2017). A subcellular map of the human proteome. *Science*, *356*(6340). https://doi.org/10.1126/science.aal3321

Tomlin, F. M., Gerling-Driessen, U. I. M., Liu, Y. C., Flynn, R. A., Vangala, J. R., Lentz, C. S., Clauder-Muenster, S., Jakob, P., Mueller, W. F., Ordonez-Rueda, D., Paulsen, M., Matsui, N., Foley, D., Rafalko, A., Suzuki, T., Bogyo, M., Steinmetz, L. M., Radhakrishnan, S. K., & Bertozzi, C. R. (2017). Inhibition of NGLY1 Inactivates the Transcription Factor Nrf1 and Potentiates Proteasome Inhibitor Cytotoxicity. *ACS Cent Sci*, *3*(11), 1143-1155. https://doi.org/10.1021/acscentsci.7b00224

Torrelo, A. (2017). CANDLE Syndrome As a Paradigm of Proteasome-Related Autoinflammation. *Front Immunol*, *8*, 927. https://doi.org/10.3389/fimmu.2017.00927

Torrelo, A., Patel, S., Colmenero, I., Gurbindo, D., Lendinez, F., Hernandez, A., Lopez-Robledillo, J. C., Dadban, A., Requena, L., & Paller, A. S. (2010). Chronic atypical neutrophilic dermatosis with lipodystrophy and elevated temperature (CANDLE) syndrome. *J Am Acad Dermatol*, *62*(3), 489-495. https://doi.org/10.1016/j.jaad.2009.04.046

Trowsdale, J., Hanson, I., Mockridge, I., Beck, S., Townsend, A., & Kelly, A. (1990). Sequences encoded in the class II region of the MHC related to the 'ABC' superfamily of transporters. *Nature*, *348*(6303), 741-744. https://doi.org/10.1038/348741a0

Tsuchiya, Y., Morita, T., Kim, M., Iemura, S., Natsume, T., Yamamoto, M., & Kobayashi, A. (2011a). Dual regulation of the transcriptional activity of Nrf1 by beta-TrCP- and Hrd1-dependent degradation mechanisms. *Mol Cell Biol*, *31*(22), 4500-4512. https://doi.org/10.1128/MCB.05663-11

Tsuchiya, Y., Morita, T., Kim, M., Iemura, S. I., Natsume, T., Yamamoto, M., & Kobayashi, A. (2011b). Dual Regulation of the Transcriptional Activity of Nrf1 by beta-TrCP-

and Hrd1-Dependent Degradation Mechanisms. *Molecular and Cellular Biology*, *31*(22), 4500-4512. https://doi.org/10.1128/Mcb.05663-11

Tsuchiya, Y., Taniguchi, H., Ito, Y., Morita, T., Karim, M. R., Ohtake, N., Fukagai, K., Ito, T., Okamuro, S., Iemura, S., Natsume, T., Nishida, E., & Kobayashi, A. (2013). The Casein Kinase 2-Nrf1 Axis Controls the Clearance of Ubiquitinated Proteins by Regulating Proteasome Gene Expression. *Molecular and Cellular Biology*, *33*(17), 3461-3472. https://doi.org/10.1128/Mcb.01271-12

van de Weijer, M. L., Luteijn, R. D., & Wiertz, E. J. (2015). Viral immune evasion: Lessons in MHC class I antigen presentation. *Semin Immunol*, *27*(2), 125-137. https://doi.org/10.1016/j.smim.2015.03.010

van den Boomen, D. J., Timms, R. T., Grice, G. L., Stagg, H. R., Skodt, K., Dougan, G., Nathan, J. A., & Lehner, P. J. (2014). TMEM129 is a Derlin-1 associated ERAD E3 ligase essential for virus-induced degradation of MHC-I. *Proc Natl Acad Sci U S A*, *111*(31), 11425-11430. https://doi.org/10.1073/pnas.1409099111

Van Kaer, L., Ashton-Rickardt, P. G., Eichelberger, M., Gaczynska, M., Nagashima, K., Rock, K. L., Goldberg, A. L., Doherty, P. C., & Tonegawa, S. (1994). Altered peptidase and viral-specific T cell response in LMP2 mutant mice. *Immunity*, *1*(7), 533-541. https://doi.org/10.1016/1074-7613(94)90043-4

Vangala, J. R., & Radhakrishnan, S. K. (2019). Nrf1-mediated transcriptional regulation of the proteasome requires a functional TIP60 complex. *Journal of Biological Chemistry*, *294*(6), 2036-2045. https://doi.org/10.1074/jbc.RA118.006290

Varshavsky, A. (1992). The N-end rule. *Cell*, *69*(5), 725-735. https://doi.org/10.1016/0092-8674(92)90285-k

Varshavsky, A. (2005). Regulated protein degradation. *Trends Biochem Sci*, *30*(6), 283-286. https://doi.org/10.1016/j.tibs.2005.04.005

Vilchez, D., Saez, I., & Dillin, A. (2014). The role of protein clearance mechanisms in organismal ageing and age-related diseases. *Nat Commun*, *5*, 5659. https://doi.org/10.1038/ncomms6659

Voges, D., Zwickl, P., & Baumeister, W. (1999). The 26S proteasome: a molecular machine designed for controlled proteolysis. *Annu Rev Biochem*, *68*, 1015-1068. https://doi.org/10.1146/annurev.biochem.68.1.1015

Wade, S. L., & Auble, D. T. (2010). The Rad23 ubiquitin receptor, the proteasome and functional specificity in transcriptional control. *Transcription*, *1*(1), 22-26. https://doi.org/10.4161/trns.1.1.12201

Wahl, C., Kautzmann, S., Krebiehl, G., Strauss, K., Woitalla, D., Muller, T., Bauer, P., Riess, O., & Kruger, R. (2008). A comprehensive genetic study of the proteasomal subunit S6 ATPase in German Parkinson's disease patients. *J Neural Transm (Vienna)*, *115*(8), 1141-1148. https://doi.org/10.1007/s00702-008-0054-3

Wallington-Beddoe, C. T., Sobieraj-Teague, M., Kuss, B. J., & Pitson, S. M. (2018). Resistance to proteasome inhibitors and other targeted therapies in myeloma. *Br J Haematol*, *182*(1), 11-28. https://doi.org/10.1111/bjh.15210

Walter, P., & Ron, D. (2011). The unfolded protein response: from stress pathway to homeostatic regulation. *Science*, *334*(6059), 1081-1086. https://doi.org/10.1126/science.1209038

Wang, S., Cheng, H., Wang, L., Zhao, R., & Guan, D. (2020). Overexpression of NRF1-742 or NRF1-772 Reduces Arsenic-Induced Cytotoxicity and Apoptosis in Human HaCaT Keratinocytes. *Int J Mol Sci*, *21*(6). https://doi.org/10.3390/ijms21062014

Wang, W., & Chan, J. Y. (2006). Nrf1 is targeted to the endoplasmic reticulum membrane by an N-terminal transmembrane domain. Inhibition of nuclear translocation and transacting function. *J Biol Chem*, *281*(28), 19676-19687. https://doi.org/10.1074/jbc.M602802200

Weissman, A. M. (2001). Themes and variations on ubiquitylation. *Nat Rev Mol Cell Biol*, *2*(3), 169-178. https://doi.org/10.1038/35056563

Wertz, I. E., O'Rourke, K. M., Zhou, H., Eby, M., Aravind, L., Seshagiri, S., Wu, P., Wiesmann, C., Baker, R., Boone, D. L., Ma, A., Koonin, E. V., & Dixit, V. M. (2004). De-ubiquitination and ubiquitin ligase domains of A20 downregulate NF-kappaB signalling. *Nature*, *430*(7000), 694-699. https://doi.org/10.1038/nature02794

White, R. E., Powell, D. J., & Berry, C. (2011). HIV proteinase inhibitors target the Ddi1-like protein of Leishmania parasites. *Faseb Journal*, *25*(5), 1729-1736. https://doi.org/10.1096/fj.10-178947

Widenmaier, S. B., Snyder, N. A., Nguyen, T. B., Arduini, A., Lee, G. Y., Arruda, A. P., Saksi, J., Bartelt, A., & Hotamisligil, G. S. (2017). NRF1 Is an ER Membrane Sensor that Is Central to Cholesterol Homeostasis. *Cell*, *171*(5), 1094-1109 e1015. https://doi.org/10.1016/j.cell.2017.10.003

Wieczorek, M., Abualrous, E. T., Sticht, J., Alvaro-Benito, M., Stolzenberg, S., Noe, F., & Freund, C. (2017). Major Histocompatibility Complex (MHC) Class I and MHC Class II Proteins: Conformational Plasticity in Antigen Presentation. *Front Immunol*, *8*, 292. https://doi.org/10.3389/fimmu.2017.00292

Wilkinson, C. R. M., Seeger, M., Hartmann-Petersen, R., Stone, M., Wallace, M., Semple, C., & Gordon, C. (2001). Proteins containing the UBA domain are able to bind to multi-ubiquitin chains. *Nature Cell Biology*, *3*(10), 939-943. https://doi.org/DOI 10.1038/ncb1001-939

Wilson, M. R., & Zoubeidi, A. (2017). Clusterin as a therapeutic target. *Expert Opin Ther Targets*, *21*(2), 201-213. https://doi.org/10.1080/14728222.2017.1267142

Wlodawer, A., Miller, M., Jaskolski, M., Sathyanarayana, B. K., Baldwin, E., Weber, I. T., Selk, L. M., Clawson, L., Schneider, J., & Kent, S. B. H. (1989). Conserved Folding in Retroviral Proteases - Crystal-Structure of a Synthetic Hiv-1 Protease. *Science*, *245*(4918), 616-621. https://doi.org/DOI 10.1126/science.2548279

Wu, T., Zhao, F., Gao, B., Tan, C., Yagishita, N., Nakajima, T., Wong, P. K., Chapman, E., Fang, D., & Zhang, D. D. (2014). Hrd1 suppresses Nrf2-mediated cellular protection during liver cirrhosis. *Genes Dev*, *28*(7), 708-722. https://doi.org/10.1101/gad.238246.114

Wu, X., & Rapoport, T. A. (2018). Mechanistic insights into ER-associated protein degradation. *Curr Opin Cell Biol*, *53*, 22-28. https://doi.org/10.1016/j.ceb.2018.04.004

Wu, X., Siggel, M., Ovchinnikov, S., Mi, W., Svetlov, V., Nudler, E., Liao, M., Hummer, G., & Rapoport, T. A. (2020). Structural basis of ER-associated protein degradation mediated by the Hrd1 ubiquitin ligase complex. *Science*, *368*(6489). https://doi.org/10.1126/science.aaz2449

Wunderle, L., Knopf, J. D., Kuhnle, N., Morle, A., Hehn, B., Adrain, C., Strisovsky, K., Freeman, M., & Lemberg, M. K. (2016). Rhomboid intramembrane protease RHBDL4 triggers ER-export and non-canonical secretion of membrane-anchored TGFalpha. *Sci Rep*, *6*, 27342. https://doi.org/10.1038/srep27342

Xie, D., Gulnik, S., Collins, L., Gustchina, E., Suvorov, L., & Erickson, J. W. (1997). Dissection of the pH dependence of inhibitor binding energetics for an aspartic protease: direct measurement of the protonation states of the catalytic aspartic acid residues. *Biochemistry*, *36*(51), 16166-16172. https://doi.org/10.1021/bi971550l

Xie, Y., & Varshavsky, A. (2001). RPN4 is a ligand, substrate, and transcriptional regulator of the 26S proteasome: a negative feedback circuit. *Proc Natl Acad Sci U S A*, *98*(6), 3056-3061. https://doi.org/10.1073/pnas.071022298

Xu, Y., Anderson, D. E., & Ye, Y. (2016). The HECT domain ubiquitin ligase HUWE1 targets unassembled soluble proteins for degradation. *Cell Discov*, *2*, 16040. https://doi.org/10.1038/celldisc.2016.40

Xu, Z., Chen, L., Leung, L., Yen, T. S., Lee, C., & Chan, J. Y. (2005). Liver-specific inactivation of the Nrf1 gene in adult mouse leads to nonalcoholic steatohepatitis and hepatic neoplasia. *Proc Natl Acad Sci U S A*, *102*(11), 4120-4125. https://doi.org/10.1073/pnas.0500660102

Xu, Z., Hu, Y., Deng, Y., Chen, Y., Hua, H., Huang, S., Nie, Q., Pan, Q., Ma, D. K., & Ma, L. (2018). WDR-23 and SKN-1/Nrf2 Coordinate with the BLI-3 Dual Oxidase in Response to Iodide-Triggered Oxidative Stress. *G3 (Bethesda)*, *8*(11), 3515-3527. https://doi.org/10.1534/g3.118.200586

Yabuta, Y., Morishita, T., Kojima, Y., Maruta, T., Nishizawa-Yokoi, A., & Shigeoka, S. (2010). Identification of recognition sequence of ANAC078 protein by the cyclic amplification and selection of targets technique. *Plant Signal Behav*, *5*(6), 695-697. https://doi.org/10.4161/psb.5.6.11577

Yang, K., Huang, R., Fujihira, H., Suzuki, T., & Yan, N. (2018). N-glycanase NGLY1 regulates mitochondrial homeostasis and inflammation through NRF1. *J Exp Med*, *215*(10), 2600-2616. https://doi.org/10.1084/jem.20180783

Yang, Z., & Klionsky, D. J. (2010). Mammalian autophagy: core molecular machinery and signaling regulation. *Curr Opin Cell Biol*, *22*(2), 124-131. https://doi.org/10.1016/j.ceb.2009.11.014

Ye, Y., Meyer, H. H., & Rapoport, T. A. (2001). The AAA ATPase Cdc48/p97 and its partners transport proteins from the ER into the cytosol. *Nature*, *414*(6864), 652-656. https://doi.org/10.1038/414652a

Ye, Y., Shibata, Y., Yun, C., Ron, D., & Rapoport, T. A. (2004). A membrane protein complex mediates retro-translocation from the ER lumen into the cytosol. *Nature*, *429*(6994), 841-847. https://doi.org/10.1038/nature02656

Yewdell, J. W., Anton, L. C., & Bennink, J. R. (1996). Defective ribosomal products (DRiPs): a major source of antigenic peptides for MHC class I molecules? *J Immunol*, *157*(5), 1823-1826. https://www.ncbi.nlm.nih.gov/pubmed/8757297

Yoshida, Y., Asahina, M., Murakami, A., Kawawaki, J., Yoshida, M., Fujinawa, R., Iwai, K., Tozawa, R., Matsuda, N., Tanaka, K., & Suzuki, T. (2021). Loss of peptide:N-glycanase causes proteasome dysfunction mediated by a sugar-recognizing ubiquitin ligase. *Proc Natl Acad Sci U S A*, *118*(27). https://doi.org/10.1073/pnas.2102902118

Young, J. C., Hoogenraad, N. J., & Hartl, F. U. (2003). Molecular chaperones Hsp90 and Hsp70 deliver preproteins to the mitochondrial import receptor Tom70. *Cell*, *112*(1), 41-50. https://doi.org/10.1016/s0092-8674(02)01250-3

Younger, J. M., Chen, L., Ren, H. Y., Rosser, M. F., Turnbull, E. L., Fan, C. Y., Patterson, C., & Cyr, D. M. (2006). Sequential quality-control checkpoints triage misfolded cystic fibrosis transmembrane conductance regulator. *Cell*, *126*(3), 571-582. https://doi.org/10.1016/j.cell.2006.06.041

Yu, X., Sidhu, J. S., Hong, S., Robinson, J. F., Ponce, R. A., & Faustman, E. M. (2011). Cadmium induced p53-dependent activation of stress signaling, accumulation of ubiquitinated proteins, and apoptosis in mouse embryonic fibroblast cells. *Toxicol Sci*, *120*(2), 403-412. https://doi.org/10.1093/toxsci/kfr010

Zettl, M., Adrain, C., Strisovsky, K., Lastun, V., & Freeman, M. (2011). Rhomboid family pseudoproteases use the ER quality control machinery to regulate intercellular signaling. *Cell*, *145*(1), 79-91. https://doi.org/10.1016/j.cell.2011.02.047

Zhang, P. Q. H. W. Z. N. H. H. J. Z. F. Z. F. I. M. W. A. J. M. F. (2021). ERK signaling licenses SKN-1A/NRF1 for proteasome production
and proteasomal stress resistance *bioRxiv*. https://doi.org/10.1101/2021.01.04.425272

Zhang, X., Bogunovic, D., Payelle-Brogard, B., Francois-Newton, V., Speer, S. D., Yuan, C., Volpi, S., Li, Z., Sanal, O., Mansouri, D., Tezcan, I., Rice, G. I., Chen, C., Mansouri, N., Mahdaviani, S. A., Itan, Y., Boisson, B., Okada, S., Zeng, L., . . . Pellegrini, S. (2015). Human intracellular ISG15 prevents interferon-alpha/beta over-amplification and auto-inflammation. *Nature*, *517*(7532), 89-93. https://doi.org/10.1038/nature13801

Zhang, Y., Crouch, D. H., Yamamoto, M., & Hayes, J. D. (2006). Negative regulation of the Nrf1 transcription factor by its N-terminal domain is independent of Keap1: Nrf1, but not Nrf2, is targeted to the endoplasmic reticulum. *Biochem J*, *399*(3), 373-385. https://doi.org/10.1042/BJ20060725

Zhang, Y., & Hayes, J. D. (2010). Identification of topological determinants in the N-terminal domain of transcription factor Nrf1 that control its orientation in the endoplasmic reticulum membrane. *Biochem J*, *430*(3), 497-510. https://doi.org/10.1042/BJ20100471

Zhang, Y., & Hayes, J. D. (2013). The membrane-topogenic vectorial behaviour of Nrf1 controls its post-translational modification and transactivation activity. *Sci Rep*, *3*, 2006. https://doi.org/10.1038/srep02006

Zhang, Y., Kobayashi, A., Yamamoto, M., & Hayes, J. D. (2009). The Nrf3 transcription factor is a membrane-bound glycoprotein targeted to the endoplasmic reticulum through its N-terminal homology box 1 sequence. *J Biol Chem*, *284*(5), 3195-3210. https://doi.org/10.1074/jbc.M805337200

Zhang, Y., Lucocq, J. M., Yamamoto, M., & Hayes, J. D. (2007). The NHB1 (N-terminal homology box 1) sequence in transcription factor Nrf1 is required to anchor it to the endoplasmic reticulum and also to enable its asparagine-glycosylation. *Biochem J*, *408*(2), 161-172. https://doi.org/10.1042/BJ20070761

Zhang, Y., Nicholatos, J., Dreier, J. R., Ricoult, S. J., Widenmaier, S. B., Hotamisligil, G. S., Kwiatkowski, D. J., & Manning, B. D. (2014). Coordinated regulation of protein synthesis and degradation by mTORC1. *Nature*, *513*(7518), 440-443. https://doi.org/10.1038/nature13492

Zhang, Y., Ren, Y., Li, S., & Hayes, J. D. (2014). Transcription factor Nrf1 is topologically repartitioned across membranes to enable target gene transactivation through its acidic glucose-responsive domains. *PLoS One*, *9*(4), e93458. https://doi.org/10.1371/journal.pone.0093458

Zhao, J., & Goldberg, A. L. (2016). Coordinate regulation of autophagy and the ubiquitin proteasome system by MTOR. *Autophagy*, *12*(10), 1967-1970. https://doi.org/10.1080/15548627.2016.1205770

Zhao, R., Hou, Y., Xue, P., Woods, C. G., Fu, J., Feng, B., Guan, D., Sun, G., Chan, J. Y., Waalkes, M. P., Andersen, M. E., & Pi, J. (2011). Long isoforms of NRF1 contribute to arsenic-induced antioxidant response in human keratinocytes. *Environ Health Perspect*, *119*(1), 56-62. https://doi.org/10.1289/ehp.1002304

Zhou, C., Qian, X., Hu, M., Zhang, R., Liu, N., Huang, Y., Yang, J., Zhang, J., Bai, H., Yang, Y., Wang, Y., Ali, D., Michalak, M., Chen, X. Z., & Tang, J. (2020). STYK1 promotes autophagy through enhancing the assembly of autophagy-specific class III phosphatidylinositol 3-kinase complex I. *Autophagy*, *16*(10), 1786-1806. https://doi.org/10.1080/15548627.2019.1687212

Zhu, L. J., Holmes, B. R., Aronin, N., & Brodsky, M. H. (2014). CRISPRseek: a bioconductor package to identify target-specific guide RNAs for CRISPR-Cas9 genome-editing systems. *PLoS One*, *9*(9), e108424. https://doi.org/10.1371/journal.pone.0108424

VI. RELATED ARTICLES

A. The aspartyl protease DDI2 drives adaptation to proteasome inhibition in multiple myeloma

Cell Death and Disease. 2022 May 13:475

Op M[1], Ribeiro ST[1], Chavarria C[1], De Gassart A[1,2], Zaffalon L[1], Martinon F[1]

Affiliations:

[1]Department of Immunobiology, University of Lausanne, 155 Ch. des Boveresses, 1066, Epalinges, Switzerland

[2]ImCheck Therapeutics, 13009, Marseille, France

Statement of contribution:

I optimized the protocol for chromatin immunoprecipitation (ChIP) in ARH77 cells and validated the primers for PSMD11, PSMD14, PSMB6 and PSMB5 used for ChIP.

CDDpress

www.nature.com/cddis

ARTICLE OPEN

Check for updates

The aspartyl protease DDI2 drives adaptation to proteasome inhibition in multiple myeloma

Mélanie Op[1], Sérgio T. Ribeiro[1], Claire Chavarria[1], Aude De Gassart[1,2], Léa Zaffalon[1] and Fabio Martinon[1]✉

Proteasome inhibitors, such as bortezomib, are first-line therapy against multiple myeloma (MM). Unfortunately, patients frequently become refractory to this treatment. The transcription factor NRF1 has been proposed to initiate an adaptation program that regulates proteasome levels. In the context of proteasome inhibition, the cytosolic protease DDI2 cleaves NRF1 to release an active fragment that translocates to the nucleus to promote the transcription of new proteasome subunits. However, the contribution of the DDI2-NRF1 pathway to bortezomib resistance is poorly understood. Here we show that upon prolonged bortezomib treatment, MM cells become resistant to proteasome inhibition by increasing the expression of DDI2 and consequently activation of NRF1. Furthermore, we found that many MM cells became more sensitive to proteasome impairment in the context of DDI2 deficiency. Mechanistically, we demonstrate that both the protease and the HDD domains of DDI2 are required to activate NRF1. Finally, we show that partial inhibition of the DDI2-protease domain with the antiviral drug nelfinavir increased bortezomib susceptibility in treated MM cells. Altogether, these findings define the DDI2-NRF1 pathway as an essential program contributing to proteasome inhibition responses and identifying DDI2 domains that could be targets of interest in bortezomib-treated MM patients.

Cell Death and Disease (2022)13:475 ; https://doi.org/10.1038/s41419-022-04925-3

INTRODUCTION

Multiple myeloma (MM) is a plasma cell cancer representing the second most common hematologic malignancy in Western countries [1, 2]. Plasma cells are terminally differentiated B-lineage lymphocytes that secrete large amounts of immunoglobulins. Previous studies suggested that each plasma cell can secrete the equivalent of its mass in immunoglobulins, overloading the translation, folding, and secretory capacity of the cell [3]. Consequently, to maintain cellular proteostasis and survival, secretory plasma cell malignancies rely on adaptation programs and stress response pathways [4]. The Ubiquitin-Proteasome System plays a crucial role in proteostasis by degrading misfolded proteins [5]. Alteration of the proteostasis network may explain why proteasome inhibitors (PI) decrease the viability of MM cells and significantly improve the prognosis of MM patients [6, 7].

Since the FDA approved the PI bortezomib (BTZ) for the treatment of MM and mantle cell lymphoma (MCL) in 2003, clinical evidence showed that targeting the catalytic activity of the proteasome was a breakthrough in the treatment of these cancers [8, 9]. Unfortunately, drug resistance is a significant drawback in PI therapy, leading to relapses in MM patients [10]. Acquired resistance to BTZ is complex, multifactorial, and poorly understood. It includes overexpression of efflux pumps, mutations within BTZ's target PSMB5, and the induction of compensatory proteolytic pathways [11].

Recently the Nuclear Factor, Erythroid 2 Like 1 (NFE2L1) transcription factor, commonly known as NRF1, has been shown to contribute to the maintenance of proteasome function [12–14]. The mechanisms of activation of NRF1 are atypical. Under basal conditions, NRF1 is localized in the endoplasmic reticulum (ER) and undergoes translocation and degradation in the cytosol. In the context of impaired proteasome activity, NRF1 degradation is decreased. As a result, part of the NRF1 pool that reaches the cytosol undergoes post-translational modifications that promote its nuclear translocation and transcriptional activity leading to the expression of proteasome subunits [12, 15, 16]. These findings support a model in which the amount of proteasome activity is regulated by an adaptation program induced by transcriptionally active NRF1.

The mechanisms controlling the activation of NRF1 are still poorly understood. Within the ER, NRF1 undergoes N-glycosylation. Then, NRF1 is targeted to the ERAD machinery for retrotranslocation in the cytosol where it undergoes a series of modifications that contributes to its activation. Deglycosylation by NGLY1 was shown to be required for NRF1 activity [17]. In C. elegans, deglycosylation of NRF1 homolog (SKN-1) by PNG-1 is coupled with the editing of N-glycosylated asparagine residues to aspartic acid. This post-translational change of the amino acid sequence is required for maximal transcriptional activity [18].

Proteolytic processing of NRF1 in the cytosol by the aspartyl protease DDI2 is another crucial mechanism that regulates NRF1 activity [19]. Alterations of DDI2 functions were found to potentiate the cytotoxicity of PI in a triple-negative breast cancer model, indicating that this protease could interfere with clinical responses to proteasome inhibition [20]. However, DDI2 is still a poorly understood cytosolic protease, whose only substrate identified to date is NRF1.

[1]Department of Immunobiology, University of Lausanne, 155 Ch. des Boveresses, 1066 Epalinges, Switzerland. [2]Present address: ImCheck Therapeutics, 13009 Marseille, France. ✉email: Fabio.Martinon@unil.ch

Received: 14 December 2021 Revised: 2 May 2022 Accepted: 6 May 2022
Published online: 19 May 2022

Official journal of CDDpress

SPRINGER NATURE
CDDpress

In this study, we investigated the contribution of the DDI2-NRF1 pathway to BTZ-mediated toxicity and in the course of drug resistance acquisition in MM. We demonstrated that DDI2 plays an essential role in response to treatment with BTZ in MM cells. Activation of NRF1 by DDI2 contributes to the mechanisms driving BTZ resistance by initiating a proteasome bounce-back response that confers cell proteostasis. Interestingly, we found that nelfinavir, a drug designed to target the HIV protease, partially decreased the activity of DDI2 and potentiated BTZ efficacy in MM. Our study indicates that the development of specific DDI2 inhibitors, in combination with PI, may present new therapeutic opportunities in MM.

MATERIALS AND METHODS

Cell culture

ARH77, U266, and L363 cell lines were provided by Prof. Pascal Schneider, University of Lausanne, Switzerland. AMO-1, and RPMI8226 cell lines were provided by Dr. Lenka Besse, Kantonsspital St. Gallen, Switzerland. MM.1 S cells were purchased from ATCC (CRL-2974™). All those cell lines were cultured in RPMI 1640 supplemented with 10% fetal bovine serum (FBS). Cells were tested regularly for mycoplasma contamination. Cell Line Authentication was performed for the cells used in the study using highly-polymorphic short tandem repeat loci (STRs) (Microsynth).

Generation of stable cell lines

LentiCRISPR-v2 for DDI2 and NRF1 targeting: Optimized CRISPR target sequences were cloned into the lentiCRISPR-v2 vector (Addgene#52961). A sequence targeting luciferase was used as a control single guide RNA (sgRNA). The primers are listed in supplementary table 1.

Crispr/Cas9 lentiviruses were produced as previously describe [21]. Briefly, 40 µl of viral preparation was used to infect the cells. Positive populations were selected with 2–3 µg/ml puromycin for 15 days. To obtain full KO cell lines, populations were cloned by limit dilution. The selected clones are referred to as clX in the figure legends.

The different constructs and RVP-contained proteins were subcloned into the pENTR-1A dual selection vector (Invitrogen) and then insert by LR reaction in a pINDUCER21, a doxycycline-inducible lentiviral vector plasmid. Lentiviruses were produced as previously described [22]. All the constructs have an N-terminal FLAG-tag.

RNA isolation, reverse transcription, and RT-PCR

Total RNA from cells and tissues was extracted with Trizol (Invitrogen) according to the manufacturer's protocol. For the reverse transcription, 10 µl of RNA sample diluted in DEPC treated water (0.4–2 µg of RNA) was mixed with 10 µl of 2× Reverse Transcription master mix (Applied Biosystems).

For the quantitative real-time PCR, the SYBR Green fluorescent reagent was used, and the PCR was run on a LightCycler480 Real-Time PCR System from Roche.

Cytotoxic assay

Multiple myeloma and EBV-positive B cells were plated in 96-well plates at a final concentration of $0.4–0.6 \times 10^6$ cells/ml in 80 µl RPMI medium per well. Then 5× concentrated proteasome inhibitor treatments were added in 20 µl of medium making 1× final concentration in the total volume of 100 µl per well. After defined incubation time cell viability was assessed using a 3 - (4,5-dimethylthiazol-2-yl) - 5 - (3-carboxymethoxyphenyl) - 2 - (4-sulfonphenyl) - 2H tetrazolium (MTS) assay (Promega, Madison, WI). Twenty microliters of the MTS reagent was added to each well and the plates were incubated for 2 h at 37 °C. The viability of the samples was estimated by measuring sample absorbance at 492 nm using a spectrophotometric microplate reader. The inhibition of cell proliferation was expressed as the percentage of vehicle control-treated cells.

RESULTS

DDI2 contributes to adaptation to Bortezomib treatment in multiple myeloma cells

To study the resistance mechanisms of multiple myeloma (MM) to PI treatments, we generated a resistant cell line model based on MM.1 S cells [23]. These cells have a high proteasomal workload compared to other MM, making them particularly sensitive to BTZ treatments [24, 25]. To generate a PI-resistant cell population, we cultured MM.1 S cells with a sub-lethal concentration of BTZ (Fig. 1a). After 4 weeks of BTZ treatment, adapted cells were characterized 48 h after treatment withdrawal.

When we analyzed the NRF1-DDI2 pathways, we found that compared to parental cells, adapted MM.1 S.5B cells showed increased expression of DDI2 and increased cleavage of NRF1 upon treatment with the PIs BTZ or Carfilzomib (CFZ) (Fig. 1b). Moreover, adapted cells were less sensitive to proteasome inhibition compared to parental cells (Fig. 1c). Importantly BTZ resistance was conserved even after 3 months of culture in the absence of BTZ, suggesting the engagement of a stable adaptation response (Fig. 1c, right panel). To interrogate DDI2 contribution to this adaptation response, we used the CRISPR-Cas9 technology to delete DDI2 in adapted MM.1 S.5B cells. In unstressed cells, including MM.1 S.5B cells, we could generate DDI2-deficient populations with similar efficacy as control cells expressing a sgRNA targeting luciferase, suggesting that DDI2 is not an essential protease in multiple myeloma. In contrast, we found that in stressed cells treated with BTZ, DDI2 deletion decreased NRF1 proteolytic maturation (Fig. 1d) and restored complete sensitization to BTZ treatment (Fig. 1e). These findings suggest that DDI2 may contribute to BTZ adaptation in MM cells.

DDI2 deficiency increases bortezomib sensitivity of several myeloma cell lines

We analyzed several MM cell lines for NRF1 maturation (Fig. 2a). The ARH77 line was established from a patient diagnosed with an IgG Plasma Cell Leukemia (PCL), an advanced stage of MM [26, 27]. We observed that ARH77 were among the less BTZ sensitive cell lines of our panel similar to the L-363, also described as originating from a PCL (Fig. 2b) [28]. Furthermore, we found that in response to BTZ, the myeloma cells tested showed variability of sensitivity and diverse patterns of NRF1 maturation. For example, compared to L-363, ARH77 showed a more robust maturation of NRF1 after proteasome inhibition (Fig. 2a). Altogether, these findings are consistent with the fact that different mechanisms of BTZ resistance can arise in MM and indicate that increased NRF1 activation could be one such mechanism.

Because ARH77 appeared as a model of resistant cell lines with robust NRF1 maturation, we selected this model to investigate DDI2 and NRF1 contribution to BTZ treatment. We used the CRISPR-Cas9 technology to delete DDI2 and NRF1 in these cells (Fig. 2c, Fig. s1a). We observed that DDI2 deficiency increased BTZ sensitivity (Fig. 2d, Fig. s1a), similar to the response seen in NRF1-deficient cells (Fig. s1a). To confirm that the observed phenotype is caused by DDI2 deletion, we reconstituted a representative DDI2-deficient population with a construct expressing a CRISPR-resistant DDI2. Consistently, we found that DDI2 reconstitution restored BTZ resistance in ARH77 (Fig. 2c, d).

To further validate these observations, we next investigated DDI2 involvement in additional cell lines. In line with a recent report [29], several MM lines showed increased sensitivity to BTZ treatment upon DDI2 depletion. We found that AMO-1, an established MM cell line [30], showed increased sensitivity to BTZ treatment upon DDI2 deficiency (Fig. 2e, f). Similarly, we observed that in RPMI8226 cells, which have a solid overall proteasomal activity [24], DDI2 deletion increased BTZ sensitivity (Fig. 2g, h). Moreover, we found that DDI2 deficiency affected BTZ susceptibility in other cell types, including 293T HAP-1 and HeLa cells (Fig. S1b-d). These observations are consistent with observations showing increased susceptibility to proteasome inhibition upon expression of a defective DDI2 protein in the colorectal carcinoma cell line, HCT116 [31], or upon DDI2 deficiency in the triple-negative breast cancer cell line, MDA-MB-231 [20].

In contrast, we found that the viability of L-363 cells, which showed weak NRF1 maturation, was not affected upon BTZ

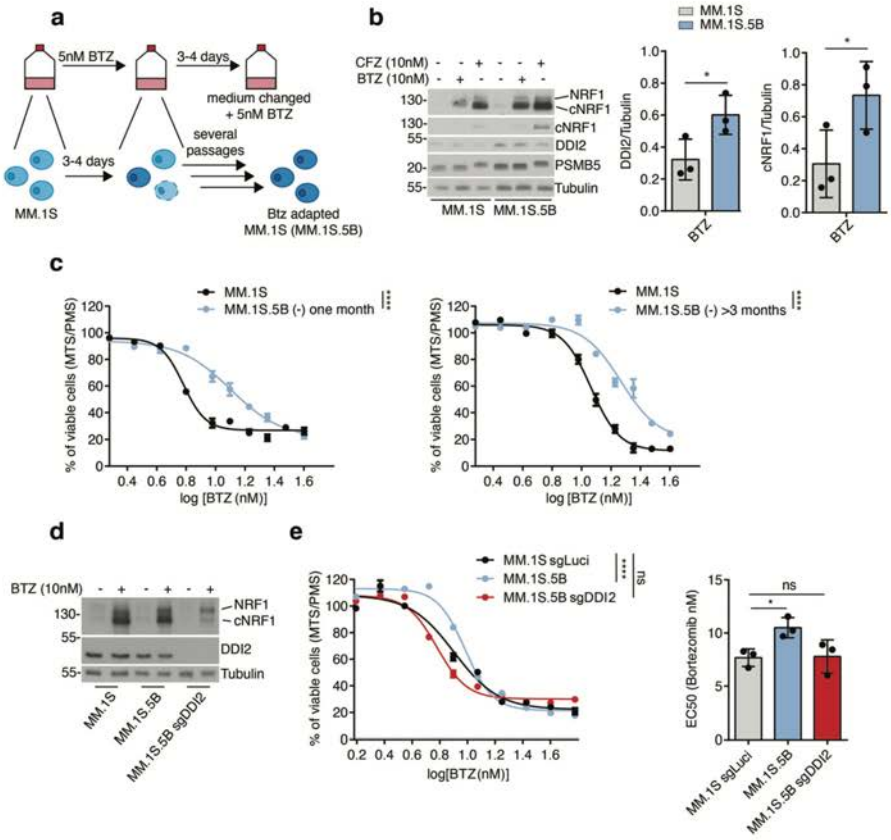

Fig. 1 DDI2 deletion restores bortezomib sensitivity in adapted multiple myeloma cells. a MM.1 S were cultured for more than three weeks in presence of a 5 nM bortezomib (BTZ). Culture medium is replaced every 3–4 days. For further analysis adapted MM.1 S.5B cells were cultured in absence of bortezomib for more than 48 h, before analysis. **b** Adapted MM.1 S.5B cells and parental cells were treated with vehicle or 10 nM of proteasome inhibitors BTZ or carfilzomib (CFZ) as indicated. Protein levels of NRF1, DDI2, and PSMB5 were analyzed by immunoblotting, tubulin is used as a loading control, cNRF1, indicates cleaved NRF1. DDI2 and cNRF1 were quantified using Image J (right panel), *P*-values were calculated using two-tailed unpaired Student's *t*-tests (left panel). **c** Viability assay of parental cells and MM.1 S.5B cultured 3 weeks or 3 months without BTZ treatment. *P*-values were calculated using two-way ANOVA. **d**, **e** Adapted MM.1 S.5B expressing a DDI2 sgRNA (MM.1 S.5B sgDDI2) were generated. Expression of DDI2 and NRF1 cleavage upon treatment with BTZ was analyzed by immunoblotting (**d**). Bortezomib sensitivity of the luciferase control and DDI2-deficient population was assessed by viability assay (**e**, left panel), Dots (bar) graph represents the EC50 (half-maximal effective concentration) of the dose responses, data are from three independent experiments performed in triplicate (**e**, right panel). *P*-values were calculated using one-way ANOVA followed by Dunnett's multiple comparison tests.

treatment after DDI2 depletion (Fig. 2i, j). These observations suggest that impairing DDI2 activity could decrease BTZ resistance in most but not all MM cells.

DDI2 contributes to proteasome adaptation by increasing proteasome activity

Because MM cells with high proteasomal activity relied on DDI2 for survival upon treatment with BTZ, we investigated the contribution of the DDI2-NRF1 pathway to proteasome activity at basal and upon treatment with BTZ. We used a Suc-LLVY-AMC fluorogenic peptide substrate that produced fluorescence after degradation to measure the chymotrypsin-like activity of the proteasome. As expected, BTZ treatment decreased the proteasome activity of the control ARH77 population expressing sgLuci (Fig. 3a). Interestingly we found that in clones with DDI2 or NRF1 deficiency, basal proteasome activity was reduced to the same level observed upon BTZ treatment (Fig. 3a). These data indicated that in these cells, DDI2 and NRF1 are required to maintain optimal DDI2-NRF1 pathway, independently of proteasome inhibition.

Then, because BTZ treatment increases proteasome expression, and NRF1 is a regulator of proteasome subunit gene expression, we investigated the contribution of NRF1 and DDI2 to this proteasome bounce-back response in MM. Using chromatin immunoprecipitation, we tested several PSM subunits and found that upon BTZ treatment, NRF1 was recruited to PSMD11, PSMD14, PSMB6, and PSMB5 promoters in a DDI2 dependent manner (Fig. 3b). In addition, BTZ-mediated increase of these proteasome subunits mRNA was reduced in DDI2 and NRF1-deficient clones compared to control populations (Fig. 3c). These

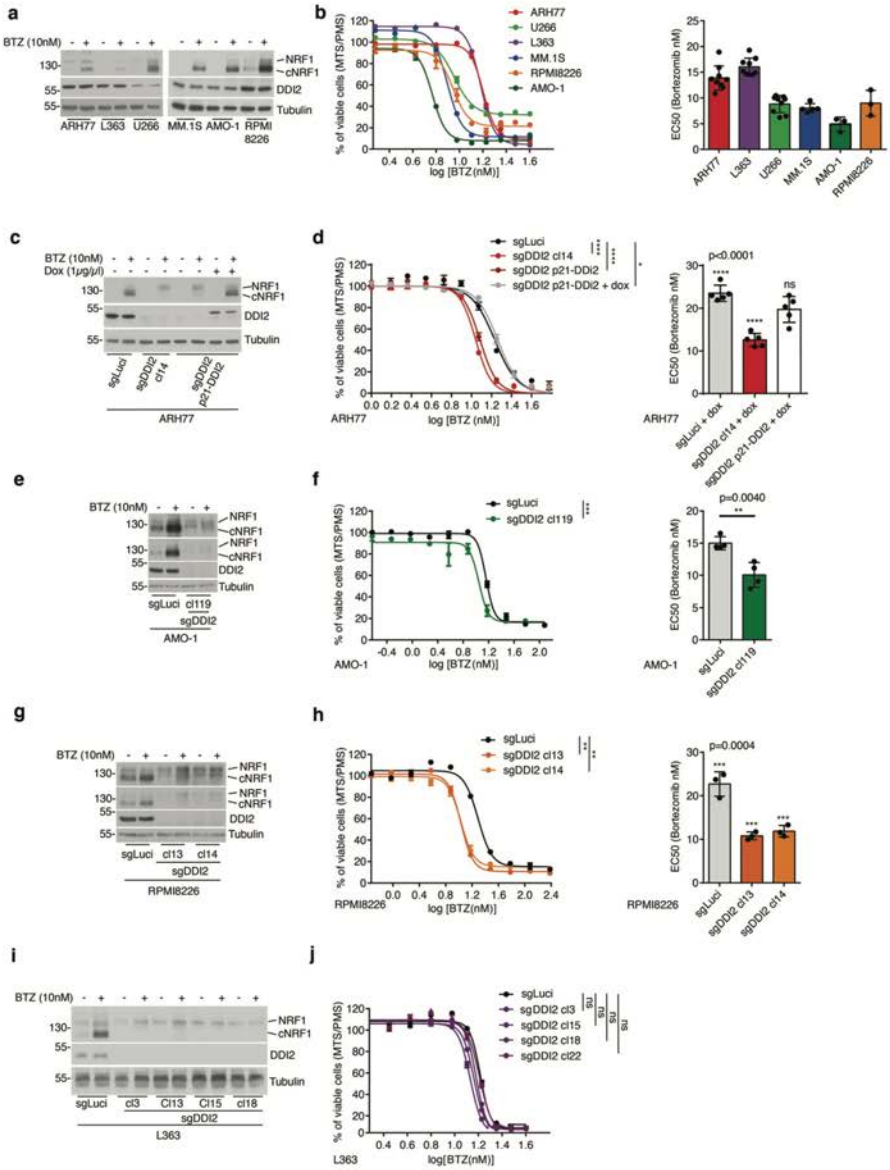

Fig. 2 DDI2 deficiency affects Bortezomib sensitivity of sensitive and resistant Myeloma cells. a, **b** Indicated multiple myeloma cell lines were treated with BTZ or vehicle and analyzed by immunoblot for protein expression of DDI2 and NRF1, cNRF1, indicates cleaved NRF1. Tubulin is used as a loading control (**a**). Viability assay was assessed by MTS/PMS assay. Dots graph represents the EC50 (half-maximal effective concentration) of the dose responses (**b**). **c**, **d** A representative ARH77 clone expressing DDI2 sgRNA and deficient for DDI2 expression was reconstituted with an inducible N-ter FLAG-DDI2 construct (backbone PINDUCER21) and treated with BTZ and doxycycline (Dox) as indicated. The expression of DDI2, NRF1, and cNRF1 was monitored by immunoblotting (**c**). Viability assay of control cells and reconstituted cells treated with BTZ or Dox was performed as indicated (**d**). **e**–**j** AMO-1, RPMI8226, and L363 populations expressing control luciferase (Luci) sgRNA or representative clonal DDI2-deficient populations were treated with BTZ or vehicle as indicated and analyzed by immunoblotting for expression of DDI2, NRF1, and cNRF1 (**e**, **g**, **i**). Sensitivity to BTZ of control cells and representative DDI2-deficient clones were analyzed by viability assay (**f**, **h**, **j**). Curve graphs are from one representative experiment of two or three replicates. *P*-values were calculated using two-way ANOVA between control cells and KO cells. Dots graph represents the EC50 (half-maximal effective concentration) of the dose responses; data are from at least three independent experiments performed in triplicate. *P*-values were calculated using one-way ANOVA followed by Dunnett's multiple comparison tests (**d**, **h**) or using two-tailed unpaired Student's *t*-tests (**f**).

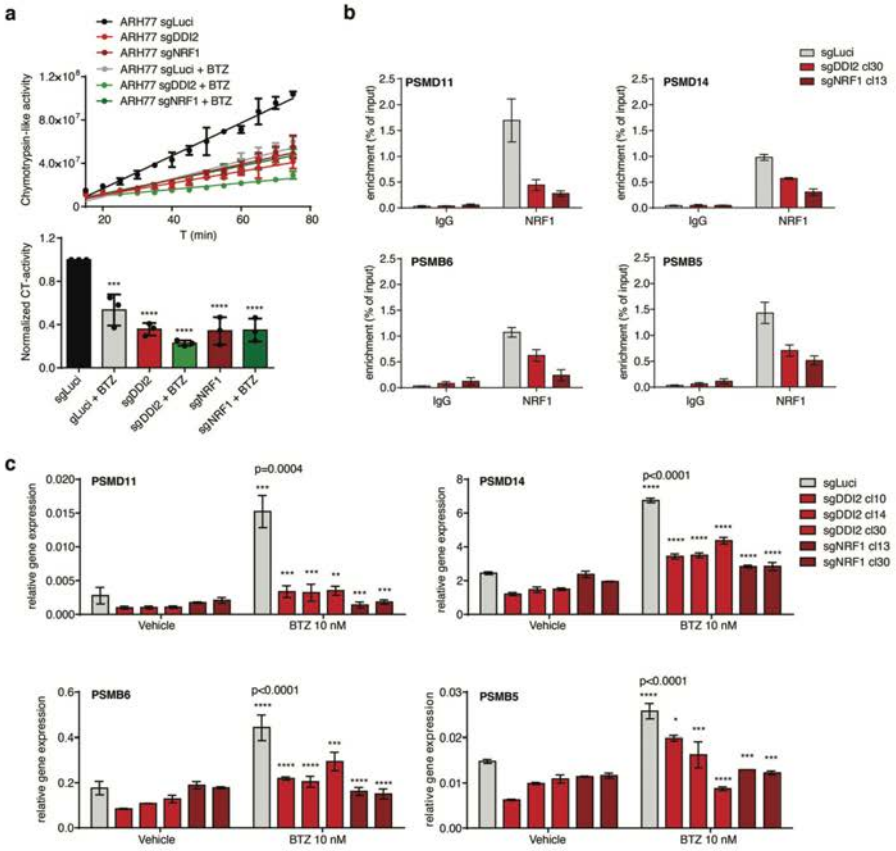

Fig. 3 DDI2 deficiency impairs the chymotrypsin-like activity of the proteasome. a ARH77 populations expressing sgLuci (control), sgDDI2 (DDI2 deficient), or sgNRF1 (NRF1 deficient) were treated with 100 nM BTZ for 6 h. Chymotrypsin-like activity of the proteasome was measured using fluorescent substrates. Dots (bar) graph represents the chymotrypsin-like (CT) activity of the different groups normalized with the untreated ARH77 expressing sgLuci. Data are from three independent experiments performed in duplicate. Significance was calculated using one-way ANOVA followed by Dunnett's multiple comparison tests. **b** ChIP was performed on ARH77 sgLuci populations or representative DDI2 and NRF1-deficient clones treated for 24 h with 10 nM BTZ using NRF1-specific antibody or IgG control. Enrichments of indicated proteasome subunit promoters were probed by real-time PCR (mean and SD of technical triplicates of one representative experiment of three). **c** Indicated cells were treated 12 h with 10 nM BTZ and analyzed for proteasome subunits (PSM) mRNA expression by real-time PCR. Normalization was done relative to SRPR levels. *P*-values were calculated using one-way ANOVA followed by Dunnett's multiple comparison tests.

observations suggest that the transcriptional activity of the DDI2-NRF1 pathway contributes, at least in part, to the proteasome bounce-back response in ARH77 cells.

The HDD and RVP domains of DDI2 are required for NRF1 activation

While the structure of human DDI2 has been partly described the function of its different domains is still not fully understood [32]. DDI2 harbors a ubiquitin-like (UBL) domain at the N-terminus and a putative ubiquitin interacting motif (UIM) at the C-terminus. The UBL is followed by the helical domain of Ddi1 (HDD), an ~100 amino acid-long region that is conserved among the different Ddi1 orthologs [32]. The retroviral protease-like domain (RVP) harbors the catalytic domain of DDI2 that was proposed to cleave the target proteins [19]. To determine the different DDI2 domains required for NRF1 maturation, we reconstituted the DDI2-deficient ARH77 cells with different versions of DDI2. We used doxycycline-inducible vectors coding for DDI2, a version of DDI2 with a mutation in the active site of the RVP, and a series of truncated DDI2 constructs (Fig. 4a). We analyzed NRF1 maturation following DDI2 expression in the context of BTZ treatment. As expected, we observed that the protease-deficient DDI2 construct could not promote the proteolytic maturation of NRF1. However, the RVP domain coupled with the UIM motif was not sufficient to cleave NRF1 (Fig. 4b). In contrast, the combination of the HDD and the RVP domains of DDI2 fully restored NRF1 maturation and increased PSMB5 expression (Fig. 4b, Fig. s2a). This observation was confirmed in DDI2-deficient HeLa cells transiently reconstituted with DDI2 constructs (Fig. s2b). These findings identify the RVP and the HDD regions as crucial mediators of DDI2 proteolytic function and suggest that the UIM and UBL domains are dispensable for NRF1 activation.

To study DDI2 specificity in recognizing and cleaving NRF1, we interrogated whether other known proteins harboring the RVP fold could compensate for DDI2 deficiency (Fig. 4c). We reconstituted DDI2-deficient ARH77 cells with DDI1, a paralogue

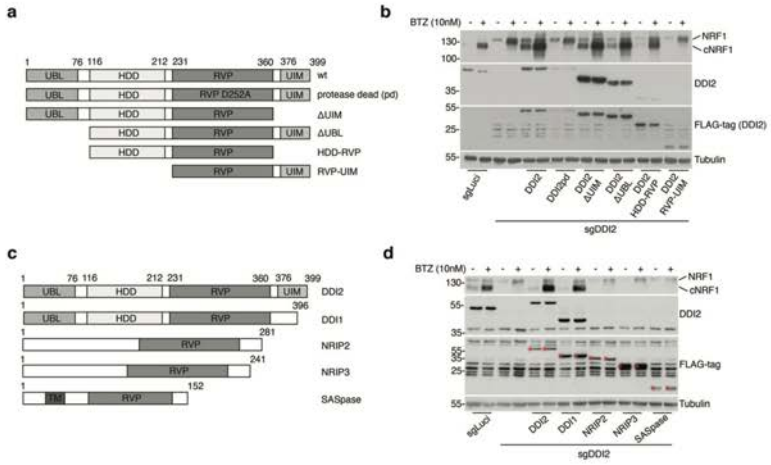

Fig. 4 The RVP and HDD domains of DDI2 are essential and sufficient for NRF1 maturation. a Schematic diagram of the different doxycycline-inducible and N-ter FLAG-tagged DDI2 constructs used in this study. These constructs were engineered with a silent mutation impairing Crispr/Cas9 cleavage and stably introduced in ARH77 cells deficient for DDI2. **b** Protein expression of NRF1, DDI2, and FLAG was analyzed by immunoblot blot upon treatment with doxycycline, in the presence or absence of BTZ. **c** Schematic diagram of the different doxycycline-inducible and FLAG-tagged constructs expressing known RVP-containing proteases. **d** DDI2-deficient ARH77 cells were stably reconstituted with the constructs depicted in **c**. Cells were treated with doxycycline and BTZ as indicated, and protein expression for NRF1, DDI2, and FLAG-tagged proteins was analyzed by immunoblotting. Tubulin is used as a loading control. The white stars are there to differentiate the FLAG-tagged proteins from the background noise.

of DDI2, NRIP2, and NRIP3, two members of the nuclear receptor-interacting protein group, and SASpase, an RVP-containing protein primarily expressed in the epidermis [33, 34]. We found that the expression of DDI1 could compensate for DDI2 deficiency and mediated NRF1 maturation in the presence of BTZ (Fig. 4d, Fig. s2a). In contrast, RVP-containing proteins that lack the HDD region, including the SASpase and NRIP proteins, could not compensate for DDI2 absence (Fig. 4d).

The protease inhibitor nelfinavir partially inhibits DDI2 and potentiates BTZ toxicity in MM cells

Nelfinavir (NFV) is a clinical available antiviral drug initially developed to target the RVP domain of the HIV protease. It has been reported that treatment with nelfinavir has off-target effects in humans that show anti-cancer properties [35, 36]. Several pathways have been proposed to contribute to NFV antitumoral properties, including the induction of ER-stress and the regulation of translation elongation [37, 38]. However, the direct target of NFV in humans has not been identified yet. Recent studies suggested that NFV inhibits DDI2, and may therefore affect MM growth [31, 39]. Because the HIV and DDI2 RVP domains share structural similarities, it has been proposed that NFV may target DDI2 [31]. To test this hypothesis in our model, we challenged the ARH77 cells expressing sgLuci or sgDDI2 with BTZ in the presence or absence of NFV. Consistent with our previous findings, we observed that treatment with NFV activates the Integrated Stress Response (ISR) as measured by ATF4 protein production [21]. Engagement of the ISR is observed in both DDI2 proficient and deficient cells, indicating that DDI2 is not involved in NFV regulation of translation initiation (Fig. 5a). In addition, we observed that in the presence of NFV, basal activation of NRF1 was consistently reduced compared to untreated cells (Fig. 5a). However, in the presence of BTZ, while we observed increased accumulation of uncleaved NRF1 precursor, DDI2-mediated NRF1 maturation was still detected (Fig. 5a). These findings indicate that in the context of robust activation of NRF1, NFV-mediated inhibition of DDI2 cannot abolish its enzymatic activity. To identify better DDI2 inhibitors, we tested several analogs of NFV identified in the NCI Open Chemical Repository Collection [40]. Still, none of these molecules showed a robust impact on the maturation of NRF1 (Fig. s3a). NFR-mediated inhibition of NRF1 was also observed in HeLa, HAP-1, and AMO-1 cells (Fig. s3b–d). NFV was particularly effective in HeLa cells as measured by decreased BTZ-mediated NRF1 cleavage. While expression of DDI2 was required HeLa cells, reconstitution with increasing amounts of DDI2 did not restore NRF1 cleavage in the presence of NFV, further indicating that NFV is particularly effective in this model (Fig. s3e).

To determine if NFV-mediated cytotoxicity potentiates BTZ treatments in MM, we treated ARH77 cells with BTZ in the combination with NFV. We observed that NFV significantly improved the efficacy of BTZ treatment (Fig. 5b). To determine if NFV sensitization relied on DDI2, we treated DDI2-deficient cells with NFV combined with BTZ. In this context, NFV could still increase the sensitivity of DDI2-deficient cells. The statistical significance was decreased compared to the same experiment in DDI2 proficient cells (Fig. 5b). However, the trend was consistent and suggested that while NFV function by decreasing DDI2 proteolytic activity, additional targets contribute to NFV-mediated toxicity in cancer [38].

DISCUSSION

In this study, we propose that adaptation to treatment with BTZ in MM can rely on a stable increase in the DDI2-NRF1 pathway. The mechanisms involved are still unclear. A possible mechanism may involve epigenetic changes [41]. Like the mechanisms observed in the context of trained immunity [42], proteasome stress may activate long-term functional reprogramming of cells, to maintain proteostasis. Evidence that mechanisms are controlling the amount of the DDI2-NRF1 pathway is also supported by the observation that different MM cell lines have variable protein amounts of the pathway. Some cell lines analyzed in this study, such as the L363, display a relatively weak NRF1 activation. In contrast, other cells have robust NRF1 maturation that is detected

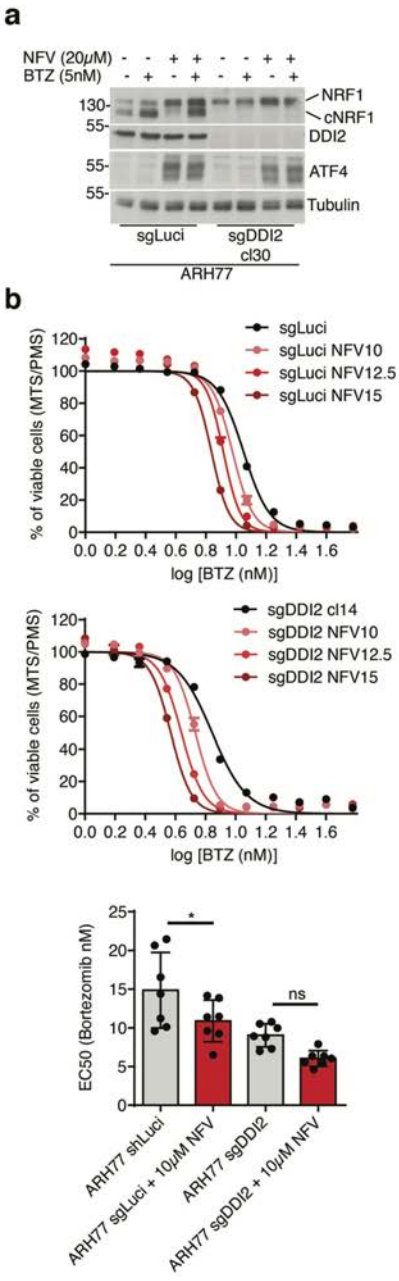

Fig. 5 Nelfinavir increased Bortezomib sensitivity. a, b ARH77 cells control population, or deficient for DDI2 were treated with BTZ in the presence or absence of Nelfinavir (NFV) as indicated. Protein expression of DDI2, NRF1, and ATF4 was assessed by immunoblot Blot. Tubulin is used as a loading control (**a**). BTZ sensitivity was analyzed by viability assay; curves are from one representative experiment performed in triplicate. Dots graph represents the EC50 (half-maximal effective concentration) of the dose responses; data are from independent experiments performed in triplicate. *P*-values were calculated using one-way ANOVA with Bonferroni multiple comparison post-tests.

in the absence of BTZ treatment, suggesting that some MM may engage the DDI2-NRF1 pathways constitutively, either to respond to a very high demand in proteasome activity or as part of developed mechanisms of resistance. In line with the observed constitutive activation of NRF1, we found that DDI2 deficiency impacted basal proteasomal activity in MM. These cells may, therefore, constitutively engage the DDI2-NRF1 pathway to maintain full proteasome activity. However, despite constitutive engagement of the DDI2-NRF1 pathway, we were able to select and expand DDI2 or NRF1-deficient MM monoclones to the same efficacy as with control populations, suggesting that neither DDI2 nor NRF1 are essential for MM survival in unstressed conditions.

How the DDI2-NRF1 pathway contributes to the maintenance of proteostasis is still unclear. Consistently with other studies [20], we observed a defect in proteasome function in the absence of DDI2. However, decreased expression of proteasome subunits was significant but relatively modest in MM. DDI2 deficiency resulted in less than a two-fold decrease in the transcriptional induction of proteasome subunits. Thus, while these defects may account for the increased BTZ susceptibility, additional pathways engaged by DDI2 may also contribute. DDI2 may directly regulate proteasome function as suggested by a recent study showing that the UBL domain of DDI2 promotes the ATPase activity of the proteasome [43]. In contrast, our reconstitution experiments showed that the lack of the UBL domain did not impair DDI2 ability to function as an NRF1 activating factor. These observations indicate that aspects of DDI2-mediated proteasome regulatory functions could be separated from its contribution to NRF1 maturation.

We demonstrated that both the RVP protease and HDD domains are essential for DDI2 proteolytic activation of NRF1. This HDD fold may contribute to substrate recruitment. In yeast, the homolog of DDI2, Ddi1, was described to recognize long ubiquitin chains. This process was shown to rely in part on a functional HDD region [44]. The HDD may also be involved in DDI2 activation, the α-helical domain of the HDD region is present in Rad23 and Dsk2, two proteasome shuttle proteins that interact with the proteasome [32]. This region may therefore interact with the proteasome, possibly sensing its overall fitness to regulate effector mechanisms. The crucial role of the HDD in mediating NRF1 maturation is also supported by the fact that, among RVP-containing proteins, DDI1, the only one harboring an HDD, was found to restore NRF1 activation. DDI1 is a paralogue of DDI2; however, while this protein retains function, its expression is undetectable in human tissues. By immunoblotting, we could not detect the presence of this protein in MM, including in cells with DDI2 deficiency. However, we cannot exclude that in specific contexts, DDI1 may compensate for the lack of DDI2.

A functional RVP domain is required for DDI2 proteolytic activity. In this study, we found that in MM, targeting the RVP domain with the anti-HIV drug NFV, blocked basal maturation of NRF1 and partially decreased DDI2 activity upon treatment with BTZ. These observations suggest that NFV could be repositioned in MM to restore sensitivity to BTZ. In support of this hypothesis, phase II clinical trials have provided promising clinical evidence that NFV may resensitize proteasome inhibitor-refractory MM to proteasome inhibition [45–47]. Our data demonstrating that DDI2 can contribute to proteasome inhibition adaptation may explain this response. NFV-mediated DDI2 inhibition likely disrupts a mechanism of resistance in MM. In addition, NFV could exacerbate

BTZ effects by blocking the NRF1-dependent proteasome bounce-back response. However, this interpretation should be cautioned by the fact that NFV has additional effects, including modulation of translation mechanisms that also contribute to its antitumoral properties [21, 38, 48].

To clarify this issue, the development of specific DDI2 inhibitors will help determine the beneficial effects of impairing DDI2 in MM. Based on the genetic studies presented in this study, we can speculate that DDI2-specific drugs could restore responses to BTZ in resistant tumors. In addition, as part of the first line of treatment, this strategy could also synergize with BTZ therapies, possibly increasing its activity and thereby decreasing the rates of MM resistance and relapse.

DATA AVAILABILITY

All data supporting the findings of this study are available from the corresponding author on reasonable request.

REFERENCES

1. Palumbo A, Anderson K. Multiple myeloma. N Engl J Med. 2011;364:1046–60.
2. Kazandjian D. Multiple myeloma epidemiology and survival: a unique malignancy. Semin Oncol. 2016;43:676–81.
3. Honjo T, Alt FW, Neuberger MS. Molecular biology of B cells. Amsterdam: Elsevier; 2004. xiv, pp. 589.
4. Hipp MS, Kasturi P, Hartl FU. The proteostasis network and its decline in ageing. Nat Rev Mol Cell Biol. 2019;20:421–35.
5. Collins GA, Goldberg AL. The logic of the 26S proteasome. Cell. 2017;169:792–806.
6. Adams J. The development of proteasome inhibitors as anticancer drugs. Cancer Cell. 2004;5:417–21.
7. Hideshima T, Richardson P, Chauhan D, Palombella VJ, Elliott PJ, Adams J, et al. The proteasome inhibitor PS-341 inhibits growth, induces apoptosis, and overcomes drug resistance in human multiple myeloma cells. Cancer Res. 2001;61:3071–6.
8. Okazuka K, Ishida T. Proteasome inhibitors for multiple myeloma. Jpn J Clin Oncol. 2018;48:785–93.
9. Besse A, Besse L, Kraus M, Mendez-Lopez M, Bader J, Xin BT, et al. Proteasome inhibition in multiple myeloma: head-to-head comparison of currently available proteasome inhibitors. Cell Chem Biol. 2019;26:340–51. e3
10. Niewerth D, Jansen G, Assaraf YG, Zweegman S, Kaspers GJ, Cloos J. Molecular basis of resistance to proteasome inhibitors in hematological malignancies. Drug Resist Updat. 2015;18:18–35.
11. Gonzalez-Santamarta M, Quinet G, Reyes-Garau D, Sola B, Roue G, Rodriguez MS. Resistance to the proteasome inhibitors: lessons from multiple myeloma and mantle cell lymphoma. Adv Exp Med Biol. 2020;1233:153–74.
12. Radhakrishnan SK, Lee CS, Young P, Beskow A, Chan JY, Deshaies RJ. Transcription factor Nrf1 mediates the proteasome recovery pathway after proteasome inhibition in mammalian cells. Mol Cell. 2010;38:17–28.
13. Li X, Matilainen O, Jin C, Glover-Cutter KM, Holmberg CI, Blackwell TK. Specific SKN-1/Nrf stress responses to perturbations in translation elongation and proteasome activity. PLoS Genet. 2011;7:e1002119.
14. Steffen J, Seeger M, Koch A, Kruger E. Proteasomal degradation is transcriptionally controlled by TCF11 via an ERAD-dependent feedback loop. Mol Cell. 2010;40:147–58.
15. Sha Z, Goldberg AL. Proteasome-mediated processing of Nrf1 is essential for coordinate induction of all proteasome subunits and p97. Curr Biol. 2014;24:1573–83.
16. Hagenbuchner J, Ausserlechner MJ. Targeting transcription factors by small compounds—current strategies and future implications. Biochem Pharmacol. 2016;107:1–13.
17. Tomlin FM, Gerling-Driessen UIM, Liu YC, Flynn RA, Vangala JR, Lentz CS, et al. Inhibition of NGLY1 inactivates the transcription factor Nrf1 and potentiates proteasome inhibitor cytotoxicity. ACS Cent Sci. 2017;3:1143–55.
18. Lehrbach NJ, Breen PC, Ruvkun G. Protein sequence editing of SKN-1A/Nrf1 by peptide:N-glycanase controls proteasome gene expression. Cell. 2019;177:737–50.
19. Koizumi S, Irie T, Hirayama S, Sakurai Y, Yashiroda H, Naguro I, et al. The aspartyl protease DDI2 activates Nrf1 to compensate for proteasome dysfunction. elife. 2016;5:e18357.
20. Northrop A, Vangala JR, Feygin A, Radhakrishnan SK. Disabling the protease DDI2 attenuates the transcriptional activity of NRF1 and potentiates proteasome inhibitor cytotoxicity. Int J Mol Sci. 2020;21:327.
21. De Gassart A, Bujisic B, Zaffalon L, Decosterd LA, Di Micco A, Frera G, et al. An inhibitor of HIV-1 protease modulates constitutive eIF2alpha dephosphorylation to trigger a specific integrated stress response. Proc Natl Acad Sci USA. 2016;113:E117–26.
22. Meerbrey KL, Hu G, Kessler JD, Roarty K, Li MZ, Fang JE, et al. The pINDUCER lentiviral toolkit for inducible RNA interference in vitro and in vivo. Proc Natl Acad Sci USA. 2011;108:3665–70.
23. Greenstein S, Krett NL, Kurosawa Y, Ma C, Chauhan D, Hideshima T, et al. Characterization of the MM.1 human multiple myeloma (MM) cell lines: a model system to elucidate the characteristics, behavior, and signaling of steroid-sensitive and -resistant MM cells. Exp Hematol. 2003;31:271–82.
24. Bianchi G, Oliva L, Cascio P, Pengo N, Fontana F, Cerruti F, et al. The proteasome load versus capacity balance determines apoptotic sensitivity of multiple myeloma cells to proteasome inhibition. Blood. 2009;113:3040–9.
25. Shabaneh TB, Downey SL, Goddard AL, Screen M, Lucas MM, Eastman A, et al. Molecular basis of differential sensitivity of myeloma cells to clinically relevant bolus treatment with bortezomib. PLoS ONE. 2013;8:e56132.
26. Canturk Z, Dikmen M, Artagan O, Ozarda MG, Ozturk N. Cytotoxic effects of resveratrol, rutin and rosmarinic acid on ARH-77 human (multiple myeloma) cell line. Nat Prod Commun. 2016;11:1441–4.
27. Drewinko B, Mars W, Minowada J, Burk KH, Trujillo JM. ARH-77, an established human IgG-producing myeloma cell line. I. Morphology, B-cell phenotypic marker profile, and expression of Epstein-Barr virus. Cancer. 1984;54:1883–92.
28. Drexler HG, Matsuo Y. Malignant hematopoietic cell lines: in vitro models for the study of multiple myeloma and plasma cell leukemia. Leuk Res. 2000;24:681–703.
29. Chen T, Ho M, Briere J, Moscvin M, Czarnecki PG, Anderson KC, et al. Multiple myeloma cells depend on the DDI2/NRF1-mediated proteasome stress response for survival. Blood Adv. 2022;6:429–40.
30. Shimizu S, Takiguchi T, Fukutoku M, Yoshioka R, Hirose Y, Fukuhara S, et al. Establishment of a CD4-positive plasmacytoma cell line (AMO1). Leukemia. 1993;7:274–80.
31. Gu Y, Wang X, Wang Y, Wang Y, Li J, Yu FX. Nelfinavir inhibits human DDI2 and potentiates cytotoxicity of proteasome inhibitors. Cell Signal. 2020;75:109775.
32. Siva M, Svoboda M, Veverka V, Trempe JF, Hofmann K, Kozisek M, et al. Human DNA-damage-inducible 2 protein is structurally and functionally distinct from its yeast ortholog. Sci Rep. 2016;6:30443.
33. Bernard D, Mehul B, Thomas-Collignon A, Delattre C, Donovan M, Schmidt R. Identification and characterization of a novel retroviral-like aspartic protease specifically expressed in human epidermis. J Invest Dermatol. 2005;125:278–87.
34. Matsui T, Kinoshita-Ida Y, Hayashi-Kisumi F, Hata M, Matsubara K, Chiba M, et al. Mouse homologue of skin-specific retroviral-like aspartic protease involved in wrinkle formation. J Biol Chem. 2006;281:27512–25.
35. Kawabata S, Gills JJ, Mercado-Matos JR, Lopiccolo J, Wilson W 3rd, Hollander MC, et al. Synergistic effects of nelfinavir and bortezomib on proteotoxic death of NSCLC and multiple myeloma cells. Cell Death Dis. 2012;3:e353.
36. Kraus M, Bader J, Overkleeft H, Driessen C. Nelfinavir augments proteasome inhibition by bortezomib in myeloma cells and overcomes bortezomib and carfilzomib resistance. Blood Cancer J. 2013;3:e103.
37. Gills JJ, Lopiccolo J, Tsurutani J, Shoemaker RH, Best CJ, Abu-Asab MS, et al. Nelfinavir, A lead HIV protease inhibitor, is a broad-spectrum, anticancer agent that induces endoplasmic reticulum stress, autophagy, and apoptosis in vitro and in vivo. Clin Cancer Res. 2007;13:5183–94.
38. De Gassart A, Demaria O, Panes R, Zaffalon L, Ryazanov AG, Gilliet M, et al. Pharmacological eEF2K activation promotes cell death and inhibits cancer progression. EMBO Rep. 2016;17:1471–84.
39. Fassmannova D, Sedlak F, Sedlacek J, Spicka I, Grantz Saskova K. Nelfinavir inhibits the TCF11/Nrf1-mediated proteasome recovery pathway in multiple myeloma. Cancers (Basel). 2020;12:1065.
40. Guan M, Su L, Yuan YC, Li H, Chow WA. Nelfinavir and nelfinavir analogs block site-2 protease cleavage to inhibit castration-resistant prostate cancer. Sci Rep. 2015;5:9698.
41. Ge M, Qiao Z, Kong Y, Liang H, Sun Y, Lu H, et al. Modulating proteasome inhibitor tolerance in multiple myeloma: an alternative strategy to reverse inevitable resistance. Br J Cancer. 2021;124:770–6.
42. Netea MG, Dominguez-Andres J, Barreiro LB, Chavakis T, Divangahi M, Fuchs E, et al. Defining trained immunity and its role in health and disease. Nat Rev Immunol. 2020;20:375–88.
43. Collins GA, Goldberg AL. Proteins containing ubiquitin-like (Ubl) domains not only bind to 26S proteasomes but also induce their activation. Proc Natl Acad Sci USA. 2020;117:4664–74.
44. Yip MCJ, Bodnar NO, Rapoport TA. Ddi1 is a ubiquitin-dependent protease. Proc Natl Acad Sci USA. 2020;117:7776–81.
45. Driessen C, Muller R, Novak U, Cantoni N, Betticher D, Mach N, et al. Promising activity of nelfinavir-bortezomib-dexamethasone in proteasome inhibitor-refractory multiple myeloma. Blood. 2018;132:2097–100.
46. Erath A, Patel DA, Hosack EA, Patanella JE, Ibach DM, Kassim AA. Overcoming proteasome inhibitor-refractory multiple myeloma with elotuzumab, bortezomib, nelfinavir, and dexamethasone. World J Oncol. 2020;11:33–6.

47. Hitz F, Kraus M, Pabst T, Hess D, Besse L, Silzle T, et al. Nelfinavir and lenalidomide/dexamethasone in patients with lenalidomide-refractory multiple myeloma. A phase I/II Trial (SAKK 39/10). Blood Cancer J. 2019;9:70.
48. Besse L, Besse A, Stolze SC, Sobh A, Zaal EA, van der Ham AJ, et al. Treatment with HIV-protease inhibitor nelfinavir identifies membrane lipid composition and fluidity as a therapeutic target in advanced multiple myeloma. Cancer Res. 2021;81:4581–93.

ACKNOWLEDGEMENTS

We thank Christoph Driessen and Lenka Besse (Kantonsspital, St. Gallen, Switzerland), as well as Pascal Schneider (Biochemistry department, Epalinges, Switzerland) for discussions and sharing reagents and cell lines. We thank the labs of Margot Thome Miazza, Pascal Schneider, Petr Broz, Manuele Rebsamen, and Alexis Jourdain (Biochemistry department, Epalinges, Switzerland) for their feedback.

AUTHOR CONTRIBUTIONS

FM and MO conceptualized and developed the study methodology and wrote the manuscript. MO, STR, CC, LZ, and ADG performed the experiments and analyzed the data.

FUNDING

This project is supported by a Swiss Cancer league grant KFS-4230-08-2017.

COMPETING INTERESTS

The authors declare no competing interests.

ADDITIONAL INFORMATION

Supplementary information The online version contains supplementary material available at https://doi.org/10.1038/s41419-022-04925-3.

Correspondence and requests for materials should be addressed to Fabio Martinon.

Reprints and permission information is available at http://www.nature.com/reprints

Publisher's note Springer Nature remains neutral with regard to jurisdictional claims in published maps and institutional affiliations.

Supplementary information for:

The aspartyl protease DDI2 drives adaptation to proteasome inhibition in multiple myeloma

Mélanie Op[1], Sérgio T. Ribeiro[1], Claire Chavaria[1], Aude de Gassart[1,2], Léa Zaffalon[1], and Fabio Martinon[1*]

[1] Dept. of Biochemistry, University of Lausanne, 155 Ch. des Boveresses, Epalinges 1066, Switzerland

[2] present address: ImCheck Therapeutics, Marseille, 13009, France

Supplementary figures S1; S2; S3

Supplementary Methods

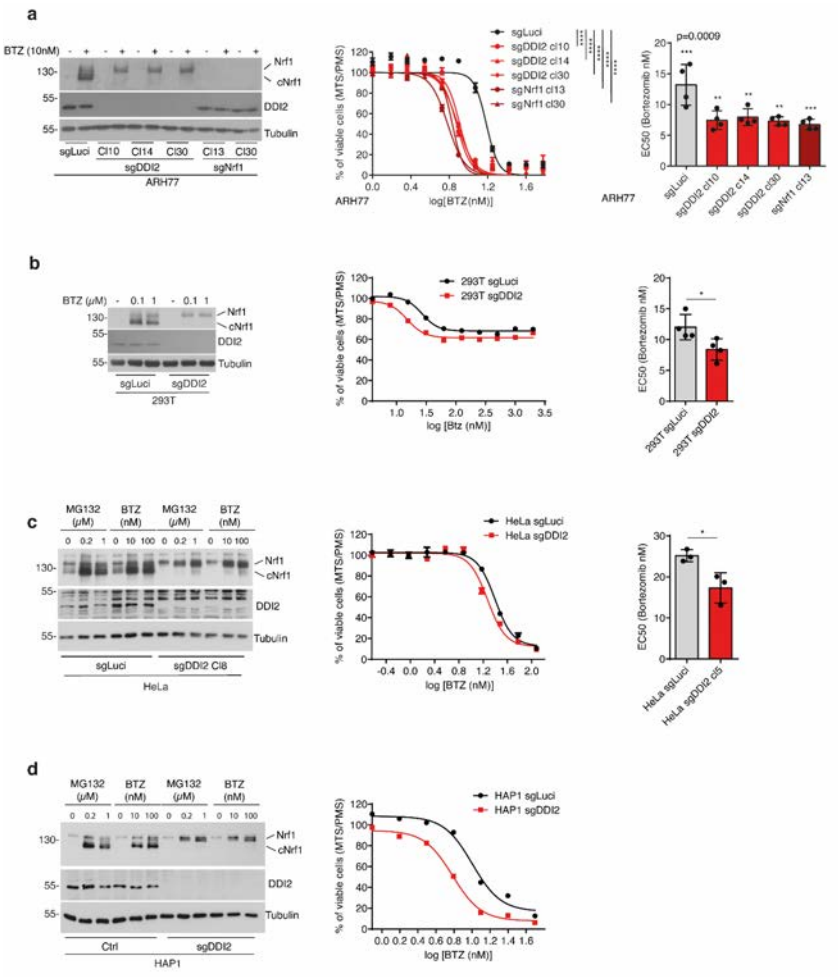

Figure S1: DDI2 deficiency affects Bortezomib sensitivity of common cell lines

a ARH77 population expressing control luciferase (Luci) sgRNA or representative clonal DDI2 deficient populations and representative clonal NRF1 deficient populations were treated with BTZ or vehicle as indicated and analyzed by immunoblotting for expression of DDI2 and NRF1, cNRF1, indicates cleaved NRF1. Sensitivity to BTZ of control cells and representative DDI2 or NRF1 deficient clones was analyzed by viability assay. **b-d** 293T, HeLa, and HAP1 populations expressing control luciferase (Luci) sgRNA or representative DDI2 deficient populations were treated with BTZ or vehicle as indicated and analyzed by immunoblotting for expression of DDI2 and NRF1. Sensitivity to BTZ was analyzed by viability assay. Curve graphs are from one representative experiment of three performed in triplicate. P-values were calculated using two-way ANOVA between control cells and KO cells. Dots graph represents the EC50 (half-maximal effective concentration) of the dose responses; data are from at least three independent experiments performed in triplicate. P-values were calculated using one-way ANOVA followed by Dunnett's multiple comparison tests.

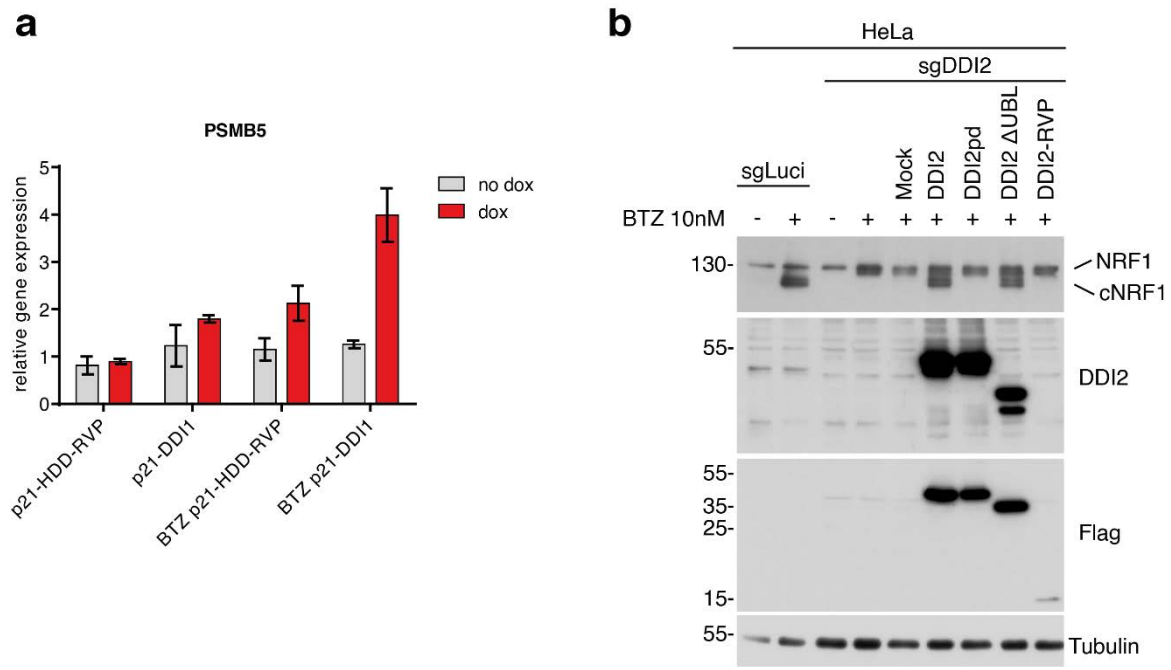

Figure S2: DDI2 reconstitution in DDI2-deficient HeLa cells

a Indicated ARH77 cells were primed or not with doxycycline and treated 24 h with 10 nM BTZ and analyzed for PSMB5 mRNA expression by real-time PCR. Normalization was done relative to HPRT levels (representative of 2). **b** The protein expression of NRF1, DDI2, and FLAG was analyzed by Western Blot in HeLa cells transfected with some of the FLAG-DDI2 constructs. Doxycycline is used to induce their expressions. Tubulin is used as a loading control.

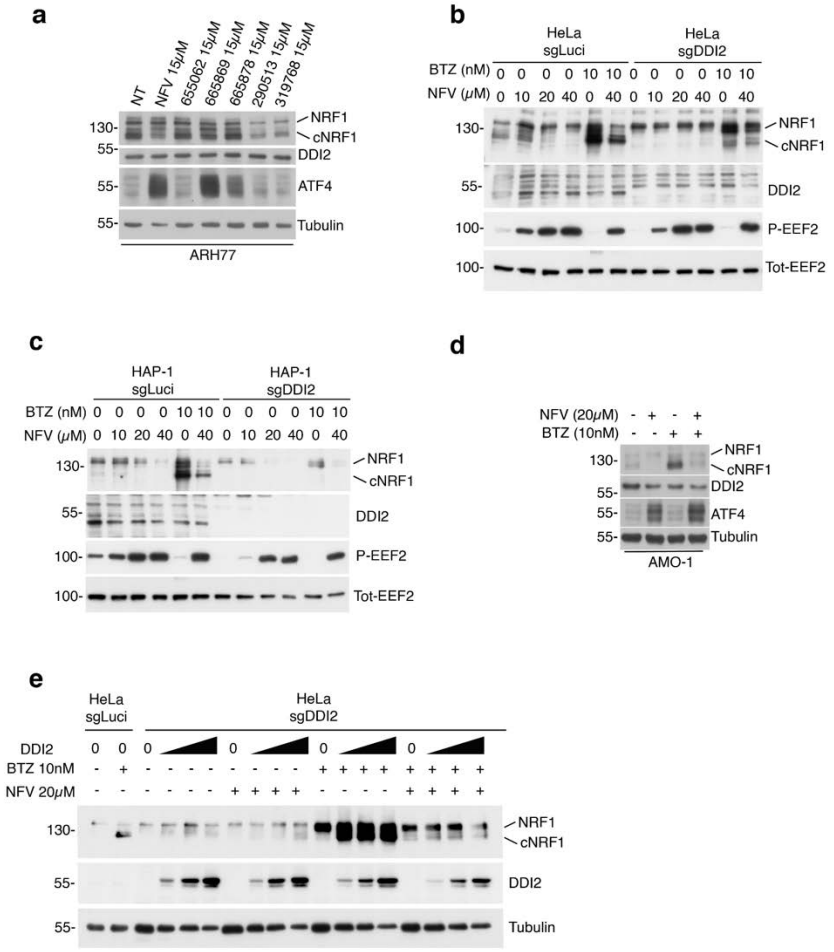

Figure S3: Effects of nelfinavir analogues effects on NRF1 maturation

a ARH77 were treated with different analogues of nelfinavir (NFV) identified in the NCI Open Chemical Repository Collection. The protein expression of DDI2, NRF1, and ATF4 after treatment was assessed by Immunoblotting. cNRF1 indicates cleaved NRF1. Tubulin is used as a loading control. **b-c** Indicated cells were treated with increased doses of NFV, in combination with BTZ. The protein expression of DDI2, NRF1, P-EEF2 after treatment was assessed by Immunoblotting. cNRF1 indicates cleaved NRF1. Tot-EEF2 was used as a loading control. **d** Parental AMO-1 cells were treated with BTZ and NFV. The protein expression of DDI2, NRF1, and ATF4 after treatment was assessed by Immunoblotting. cNRF1 indicates cleaved NRF1. Tubulin is used as a loading control. **c** A representative HeLa clone expressing DDI2 sgRNA and deficient for DDI2 expression was reconstituted with an inducible FLAG-DDI2 construct (backbone PINDUCER21) and treated with BTZ and increased doses of doxycycline (Dox) as indicated. The expression of DDI2 and NRF1 was monitored by immunoblotting.

Materials and methods

Antibodies and materials

Bortezomib and Carfilzomib were from LC-Laboratories. Nelfinavir Mesylate (CAS 159989-65-8) was from Axon Medchem. 1,4-Dithiothreitol (DTT) and Doxycycline were from AppliChem. The anti-NRF1 (8052), anti-PSMB5 (12919) were purchased from Cell Signalling. The anti-FLAG (F425) was purchased from Sigma. The anti-ATF4 (sc-200) was purchased from Santa Cruz. The anti-Tubulin (AG-27B-0005-C100) was purchased from Adipogen. The anti-DDI2 antibody was purified in our lab from human DDI2 immunized-rabbit serum using HiTrap NHS activated HP columns (GE Healthcare).

Western blotting

Cells were directly lysed in sodium dodecyl sulfate (SDS) loading buffer (10% glycerol, 2% SDS, 50 mM Tris-HCl pH 6.8, 12.5 mM EDTA, 0.02% Bromophenol Blue) containing 80-120 mM of dithiothreitol (DTT). Extracts were separated by SDS-PAGE and transferred to nitrocellulose blotting membranes (Amersham).

Proteasome activity assay

Between 3 and 5.10^6 cells were lysed in 120µl of Proteasome lysis Buffer (50 mM HEPES pH 7.8, 10mM NaCl, 1.5mM $MgCl_2$, 1mM EDTA, 1mM EGTA, 250mM sucrose and 5mM DTT in PBS without Ca^{2+} or Mg^{2+}). The cell lysates were sonicated 3 sec using microtip output set on ~3, then they were centrifuged at 16000 RCF for 10min at 4°C. The supernatants were transferred in new tubes.

For the assay, the Proteasome lysis Buffer is complemented with ATP 2 mM. The proteasome substrates used for the assay are Suc-LLVY-AMC chymotrypsin-like activity substrate from Enzo (BML-P802-0005), Z-ARR-AMC trypsin-like activity substrate from Calbiochem (CAS 90468-18-1), and Z-LLE-AMC caspase-like activity substrate from Adipogen (CAS 348086-66-8). The AMC positive control comes from Biovision (#K245-100-4). Each well is filled with 30-50µg of total proteins and one of the proteasome substrates concentrated at 100 µM. During 60 min, the $A_{360}ex/A_{360}em$ is measured on a fluorescent plate reader at 37°C.

Chromatin immunoprecipitation

This experiment was performed as previously described. (Bujisic et al., 2017). Briefly, for each ChIP reaction cells were harvested and fixed in 1% formaldehyde. Reactions were stopped in 0.18 M glycine. The cells were lysed in 0.5% NP-40 buffer (10 mM Tris pH 8, 1 mM EDTA, 0.5% NP-40) which was followed by the second round of lysis in 1% Triton X-100 (10 mM Tris pH 8, 1 mM EDTA, 1% Triton X-100, 0.5% Na-DOC, 0.5% Sarcosyl, 0.5M NaCl). Lysis buffers were supplemented with Protease's inhibitors cocktail (Roche). Lysates were sonicated using Diagenode's Bioruptor® Sonicator. For each ChIP reaction, 30 µg of chromatin was pre-cleared by co-incubation with Protein G sepharose beads (4 Fast Flow; GE Health Care Life Sciences), BSA, and Salmon Sperm DNA (UltraPureTM Salmon Sperm DNA Solution; ThermoFisher). Next, a fraction (10%) of pre-cleared chromatin was kept as input and the remaining part of the chromatin was incubated overnight with antibodies. The next day, immunoprecipitation was done using Protein G Sepharose beads. After washes beads were resuspended in elution buffer (111mM Tris pH 8, 1.11% SDS), heated, and treated overnight with Proteinase K. Following day DNA was extracted by phenol-chloroform-isoamyl alcohol (25:24:1). Real-time PCR was performed using Kapa SYBR Fast qPCR kit. Primer sequences used in ChIP experiments are shown in Table 1.

Statistical analysis

Data from one representative independent experiment is shown. All experiments were performed two or three times, except some adaptation experiments of the MM.1S. Statistical significances were determined using Graph Pad Prism version 6 as described in the figure legends. The error bars are the standard deviation of the sample. Significant differences were considered as follow *P ≤ .05, **P ≤ .01, ***P ≤ .001, or **** P ≤ .0001.

Table 1: List of primers used in this study:

Purpose	Genes	Forward primer (5'-3')	Reverse (5'-3)
CRISPR	***hDDI2***	CACCGGCTCGAAGTCGGCGTCGAC	AAACGGTCGACGCCGACTTCGAGCC
CRISPR	***hNRF1***	CACCGCTTTCTCGCACCCCGTTGTC	AAACGACAACGGGGTGCGAGAAAGC
CRISPR	**luciferase**	CACCGCTTCGAAATGTCCGTTCGGT	AAACACCGAACGGACATTTCGAAGC
RT-PCR	***hGAPDH***	CGCTCTCTGCTCCTCCTGTT	CCATGGTGTCTGAGCGATGT
RT-PCR	***hSRPR***	GTCCTGAGAACGGAGTAGAACT	ACCCCTCCCATGCTTCTGAAT
RT-PCR	***hPSMB5***	AGGAACGCATCTCTGTAGCAG	AGGGCCTCTCTTATCCCAGC
RT-PCR	***hPSMB6***	CTGATGGCGGGAATCATC	CCAATGGCAAAGGACTGC
RT-PCR	***hPSMD11***	ATGCAGGGAGGCAGACAG	GGAGCTCTGCCCGGTAAT
RT-PCR	***hPSMD14***	CCGTGCTGGAGTTCCAAT	TGCCTCCACACTGACACC
CHIP	***hGAPDH***	TACTAGCGGTTTTACGGGCG	TCGAACAGGAGGAGCAGAGAGCGA
CHIP	***hGata1***	GCCTCAACTGTGTGTCCCAC	GAAGGTACTGGAAAAGTCAG
CHIP	***PSMB5***	GGACTCACCGCTAAGGGTTC	CGTCCATGTTGCGTAAGGGA
CHIP	***PSMB6***	TTCTTTTCCCTTCTGCCGTC	ACTGTCGTAAAGCGCTCTGTC
CHIP	***PSMD11***	CGGTGTGAGAGCGGTAAGAT	CCGATGGAGTGGAGGATGTC
CHIP	***PSMD14***	GCTGCTGTTGCCTCTGTCTT	GCCTGCCTTCTGGGTCTTAC

B. The protease DDI2 regulates NRF1 activation in response to Cadmium toxicity

iScience. 2022 September 25:105227

Ribeiro ST[1], De Gassart A[1,3], Bettigole S[2], Zaffalon L[1], Chavarria C[1], Op M[1], Nugraha K[1], Martinon F[1]

Affiliations:

[1]Department of Immunobiology, University of Lausanne, 155 Ch. des Boveresses, 1066, Epalinges, Switzerland

[2]Volastra Therapeutics, 10027, New-York, USA

[3]ImCheck Therapeutics, 13009, Marseille, France

Statement of contribution:

Together with Sérgio T. Ribeiro we sacrificed mice and harvested organs for the study.

iScience

CellPress
OPEN ACCESS

Article

The protease DDI2 regulates NRF1 activation in response to cadmium toxicity

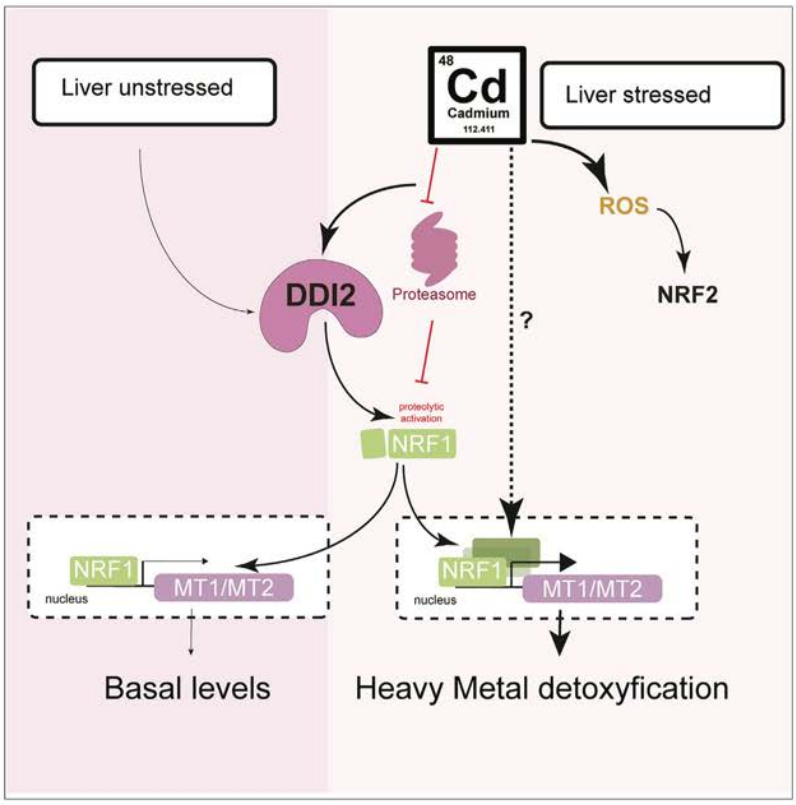

Sérgio T. Ribeiro, Aude de Gassart, Sarah Bettigole, ..., Melanie Op, Kalvin Nugraha, Fabio Martinon

Fabio.Martinon@unil.ch

Highlights

DDI2 is required for embryonic development

DDI2 contributes to MT1 and MT2 expression

Cadmium mediated proteasome inhibition activates DDI2 mediated NRF1 activity

DDI2 contributes to cell survival on Cadmium-induced toxicity

Ribeiro et al., iScience 25, 105227
October 21, 2022
https://doi.org/10.1016/j.isci.2022.105227

iScience

CellPress
OPEN ACCESS

Article

The protease DDI2 regulates NRF1 activation in response to cadmium toxicity

Sérgio T. Ribeiro,[1] Aude de Gassart,[1,3] Sarah Bettigole,[2] Lea Zaffalon,[1] Claire Chavarria,[1] Melanie Op,[1] Kalvin Nugraha,[1] and Fabio Martinon[1,4,*]

SUMMARY

DNA-damage inducible 1 homolog 2 (DDI2) is a protease that activates the transcription factor NRF1. Cellular models have shown that this pathway contributes to cell-stress adaptation, for example, on proteasome inhibition. However, DDI2 physiological function is unknown. Ddi2 Knock-out (KO) mice were embryonic lethal. Therefore, we generated liver-specific Ddi2-KO animals and used comprehensive genetic analysis to identify the molecular pathways regulated by DDI2. Here, we demonstrate that DDI2 contributes to metallothionein (MT) expression in mouse and human hepatocytes at basal and upon cadmium (Cd) exposure. This transcriptional program is dependent on DDI2-mediated NRF1 proteolytic maturation. In contrast, NRF1 homolog NRF2 does not contribute to MT production. Mechanistically, we observed that Cd exposure inhibits proteasome activity, resulting in DDI2-mediated NRF1 proteolytic maturation. In line with these findings, DDI2 deficiency sensitizes cells to Cd toxicity. This study identifies a function for DDI2 that links proteasome homeostasis to heavy metal mediated toxicity.

INTRODUCTION

The molecular mechanisms of cell stress response play a central role in cell homeostasis as well as in pathogenesis in different diseases such as cancer and neurodegeneration (Cubillos-Ruiz et al., 2017). The DNA Damage Inducible 1 Homolog 2 (DDI2) is an aspartic protease containing a retroviral protease-like (RVP) domain, highly conserved in eukaryotes (Perteguer et al., 2013; Siva et al., 2016). DDI2 is ubiquitously expressed and implicated in cell stress response. However, DDI2 function, regulation, and downstream molecular mechanisms are largely unknown. Recent data from *Caenorhabditis elegans*, yeast, and human cells demonstrate the involvement of DDI2 in protein homeostasis by regulating proteasome activity (Koizumi et al., 2016; Lehrbach and Ruvkun, 2016), as well as in cell stress response during DNA replication (Kottemann et al., 2018; Serbyn et al., 2020). Koizumi and collaborators reported that DDI2 modulates proteasome subunits through activation of the transcription factor Nuclear factor erythroid-2–related factor 1 (NRF1, encoded by the *NFE2L1* gene) (Koizumi et al., 2016; Rousseau and Bertolotti, 2018). At basal, NRF1 is glycosylated in the ER and translocated to the cytoplasm, where the proteasome continuously degrades it. However, NRF1 accumulates in the cytoplasm on proteasome inhibition and is proteolytically cleaved by DDI2. This process releases an active form of NRF1 that translocates to the nucleus and induces a transcriptional program including the expression of proteasomal (PSM) genes. This adaptation mechanism is known as the proteasome bounce-back response (Koizumi et al., 2016; Radhakrishnan et al., 2010, 2014; Zhang et al., 2007). Consistent with NRF1 contribution to proteasome homeostasis, homozygous deletion of *Nfe2l1* is lethal in mice (Chan et al., 1998) and late-stage deletion of *Nfe2l1* in neuronal cells leads to neurodegeneration (Lee et al., 2011). Although NRF1 target genes are poorly understood, it is described that NRF1 binds the antioxidant response elements (ARE), found in the promoter region of *PSM* and metallothionein (*Mt*) genes. In addition, the depletion of *Nfe2l1* in the mouse liver impairs the expression of *Mt1* and *Mt2* genes (Ohtsuji et al., 2008). MT1/2 are small cysteine-rich and metal-binding proteins, involved in metal-ions chelation and detoxification of Cadmium and Arsenic. (Habeebu et al., 2000; Klaassen et al., 2009; Ohtsuji et al., 2008; Wang et al., 2020; Zhao et al., 2011). Cd is a toxic heavy metal widely present in the environment and exhibits cytotoxic and carcinogenic effects in both mice and humans. It is known that Cd induces the accumulation of ubiquitinated proteins, affects the Ubiquitin Proteasome System (UPS), and causes cytotoxicity and apoptosis in both mouse and human cells (Figueiredo-Pereira et al., 1997; Yu et al., 2011). Moreover, the UPS has been shown to mediate the degradation of abnormal proteins and cell resistance to Cd exposure (Jungmann et al., 1993). Previous studies suggested

[1]Department of Immunobiology, University of Lausanne, 155 Ch. des Boveresses, Epalinges 1066, Switzerland

[2]Volastra Therapeutics, 1361 Amsterdam Avenue, Suite 520, New York, NY 10027, USA

[3]Present address: ImCheck Therapeutics, Marseille, 13009, France

[4]Lead contact

*Correspondence: Fabio.Martinon@unil.ch

https://doi.org/10.1016/j.isci.2022.105227

CellPress
OPEN ACCESS

iScience
Article

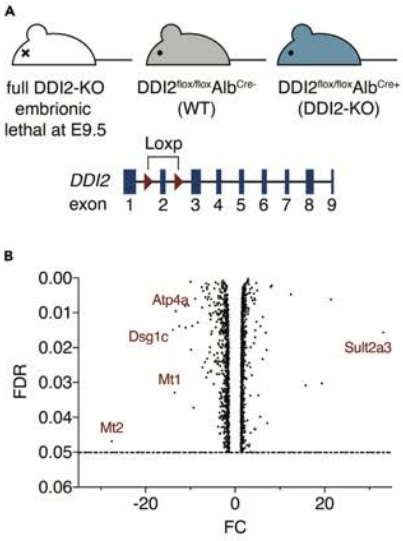

Figure 1. DDI2 modulates metallothionein gene expression *in vivo*

(A) Schematic of mouse models: Full DDI2-knockout (KO); wild-type (WT) and liver specific DDI2-KO (up) and representation of *DDI2* locus highlighting the *LoxP* sites used to generate the $DDI2^{flox/flox}$ mice (down).

(B) Volcano plot from RNA-sequencing data from liver samples of DDI2-KO compared to WT littermate control mice. The fold change (FC) is plotted on the xaxis, and the false discovery rate (FDR) (adjusted pvalue) is plotted on the yaxis. The represented genes have an FDR lower than 0.05 (horizontal dash line). Some genes are highlighted. The full raw data can be found on the supplementary material. Data points generated from two biological replicates.

the use of Cd complexes as proteasome inhibitors that activate cell stress and induce apoptosis in human cancer cells (Yeh et al., 2022; Zhang et al., 2015).

Similar to NRF1, NRF2 is able to bind to ARE regions and mount a cell stress response to promote cell survival. However, the regulatory mechanisms for NRF2 activation, target genes, and its requirement for normal mouse development seem to be distinct from NRF1 (Chan et al., 1996; Ohtsuji et al., 2008).

Here, we found that DDI2 is required for normal embryonic development in mice. The depletion of *Ddi2* in the mouse liver resulted in an impaired NRF1 activation and reduced downstream *MT* gene expression, independently of NRF2. Furthermore, DDI2 appeared to play a central role during metal-based treatments with Cadmium because DDI2-KO cells are more sensitive to cell death compared to WT DDI2 sufficient cells. Overall, we present further understandings into the molecular mechanisms of the DDI2-NRF1-MT pathway during cell stress response in both human cells and mice.

RESULTS

DDI2 modulates steady-state metallothionein expression *in vivo*

The aspartic protease DDI2 is highly conserved between species and ubiquitously expressed; however, its function is poorly understood. DDI2 was recently described to mediate the activation of NRF1 during proteasome inhibition (Koizumi et al., 2016). To further elucidate DDI2 function, we generated DDI2 deficient mice. Full body depletion of DDI2, using gene-trap technology, was embryonic lethal at middle gestational stage with decreased viability observed at E9.5 (Figures 1A and S1), confirming previous observations (Siva et al., 2020). However, a DDI2 liver-specific depletion, using conditional deletion of DDI2-floxed under albumin control was viable and the toxicology results were similar to WT animals at steady state, except for catalase activity, that was reduced (Figure S2A). At non-stressed conditions, DDI2-KO mice presented similar liver tissue structure and morphology compared to the WT animals. To identify DDI2 downstream target genes, we performed mRNA sequencing using liver samples from DDI2-KO mice and littermate controls (Figure 1B). Gene ontology (GO) analysis of molecular function showed that many genes affected by DDI2 deficiency belong to the category of DNA binding and transcriptional regulators (Figure S2B). Several genes involved in the metabolic process (Atp4a, Slc25), cellular response to ions and transcription regulation (Mt1, Mt2) are disturbed in DDI2-deficient livers (Figure 1B and S2B). The top downregulated hits identified in the genetic screening were the metallothionein genes, *Mt1* and *Mt2* (Figure 1B). *MT* genes were previously described to be under the control of the transcription factor NRF1 (Ohtsuji et al., 2008),

iScience
Article

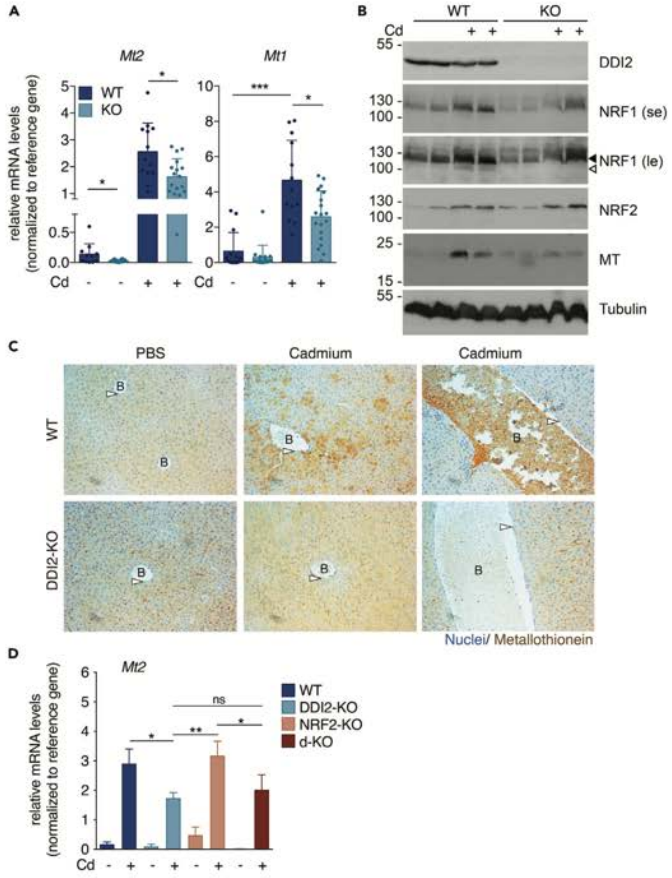

Figure 2. DDI2 activates metallothionein in response to cadmium exposure

(A and B) Relative mRNA levels (A) and protein levels (B) from liver samples of DDI2-KO (KO) and wild-type (WT) mice after 16 h of intraperitoneal injection of PBS or 8 mg/kg of $CdCl_2$ (Cd). (A) mRNA levels of metallothioneins, *Mt1* and *Mt2*, normalized with *Actin* mRNA levels, each dot represents a single animal. n = 11, 14 for WT and n = 13, 17 for DDI2-KO, treated with PBS or Cd, respectively. (B) Representative immunoblotting (n = 3) showing the relative protein levels of DDI2, NRF1, NRF2, MT and tubulin as loading control, of liver samples as in (A). Each line represents one animal and the protein molecular weights in KDa are indicated. ◄ indicates the full-length protein, ◅ indicates the cleaved protein, se: short image exposure, le: long image exposure.

(C) Representative micrographs (n = 3) of immunohistochemistry staining of MT proteins from liver tissues as in (A).

(D) mRNA levels of *Mt2*, normalized with *Actin*, from liver samples from WT, DDI2-KO, NRF2-KO, and DDI2- and NRF2-double-KO (d-KO) from animals treated as in (A) (n = 5). p values were calculated using two-tailed unpaired Mann-Whitney t-tests and error bars denote SD. *p<0.05; **p<0.01; ***p<0.001; B, blood vessel; arrow, epithelial cells.

suggesting that DDI2 may contribute to NRF1 activation at basal in the mouse liver. These findings were confirmed by real-time PCR mRNA expression analysis in the liver of deficient animals (Figure 2A). To analyze stress-induced *Mt* genes expression, we challenged mice with heavy metals. Intraperitoneal injection of acute doses of cadmium (Cd) induced a robust *Mt* gene expression in the liver of WT animals. In contrast, DDI2-KO mice presented a reduced *Mt1* and *Mt2* genes induction after 16 h of Cd treatment (Figure 2A). Importantly, we found that Cd exposure triggered proteolytic activation of NRF1 in the mouse liver

(Figure 2B) as well as in human HepG2 cell line (Figure S3A). We observed that NRF1 protein levels increase following Cd treatment because of an impairment in NRF1 protein degradation whereas NRF1 mRNA levels remained unchanged (Figure S3B). Moreover, similar to previous studies in human cell lines treated with proteasome inhibitors (Koizumi et al., 2016), we found that DDI2 depletion in mouse hepatocytes prevented Cd-mediated NRF1 cleavage and activation in the liver (Figure 2B). In addition, we confirmed that, similarly to proteasome inhibitors, treatment with Cd can promote NRF1 cleavage in human HepG2 cells (Figure S3C).

To further analyze the contribution of DDI2 to Cd exposure, we immunohistochemically stained MT proteins in liver tissue sections. We confirmed that MT is increased following 16 h of Cd injection (Figures 2B and2C). The WT mouse showed a high MT protein expression with a heterogeneous pattern throughout the liver (Figure 2C, mid-panel). When we stained a transversal cut of the blood vessel, it was possible to identify the high levels of secreted MT protein (Figure 2C, top right panel). These results confirmed the previous reports suggesting that MT proteins chelate Cd molecules in the liver, the MT-Cd complexes are transported to the bloodstream to be later filtered in the kidneys and eliminated from the body through urine (Sabolic et al., 2010). In contrast, after Cd exposure, DDI2-KO animals expressed a diffused pattern of MT in the liver, and showed less secreted MT into the blood vessels than WT animals (Figure 2C, bottom panel).

In addition to NRF1 activation, we also observed an accumulation of NRF2 protein following Cd treatment, independent of DDI2 (Figure 2B). Our results align with previous reports where NRF2 was described to mediate an adaptive cellular response to Cd-induced oxidative stress (Chen et al., 2021; Chen and Shaikh, 2009). To determine if NRF2 could be involved in MT induction in the absence of DDI2, we generated a double KO mouse (d-KO) with complete deficiency of functional NRF2 and liver-specific DDI2 deletion. Our results indicated that NRF2 is not involved in MT induction following Cd treatment. In the NRF2-KO mouse, we observed MT genes induction following Cd treatment, similar to the WT mouse. In contrast, the double DDI2 and NRF2-KO mice presented a reduced MT response following Cd treatment, identical to that observed in the DDI2-KO mice (Figure 2D). These findings demonstrate the partial but specific contribution of the DDI2-NRF1 pathway to the Cd-mediated MT-gene expression.

Cadmium induces DDI2-mediated cleavage and nuclear translocation of NRF1 in human HepG2 cells

To further confirm the *MT* gene induction following Cd treatment, we used an NRF1-responsive luciferase reporter assay (8xARE-Luc construct characterized in (Ohtsuji et al., 2008)). We transfected the reporter in the human hepatocyte cell line (HepG2). Consistently with MT expression observed in the mouse model, the MT-promoter was activated following Cd treatment (Figure 3A). In addition, in line with previous reports (Chen et al., 2014), Arsenic or Zinc treatments could also increase the MT-promoter activity. In contrast, Bortezomib (BTZ) or Carfilzomib (CFZ), two proteasome inhibitors that promote DDI2-mediated NRF1 activation, could not induce MT-promoter activation *per se*, indicating that Cd, in addition to NRF1, relies on additional factors to trigger MT gene expression. In agreement with our *in-vivo* data where we demonstrate that MT activation is independent of NRF2 activity, the chemical activation of NRF2 with tert-butylhydroquinone (tBHQ) treatment did not induce the MT-promoter activation in HepG2 cells (Figure 3A).

Cd-induced NRF1 accumulation and cleavage is rapid and occurs within hours in a DDI2-dependent manner (Figure 3B). In addition, cell fractionation studies confirmed that proteolytically cleaved NRF1 localized in the nucleus upon Cd treatment whereas uncleaved NRF1 accumulated in the cytoplasm (Figure 3C).

To further confirm the contribution of DDI2 and NRF1 to Cd-mediated *MT* gene expression, we engineered HepG2 with DDI2 and NRF1 deficiency. In agreement with the observations made in DDI2-KO mice, we found that DDI2 or NRF1 deficiency comparably affected Cd-induced MT-promoter activity (Figure 3D). Moreover, NRF1-deficient cells presented undetected levels of MT protein at both basal and Cd-treated conditions (Figure S3A).

Cadmium inhibits proteasome activity

Although we analyzed NRF1 activation, we observed increased detection of ubiquitinated proteins following Cd treatment (Figure 3C), suggesting that Cd may affect proteasome activity. Because

iScience
Article

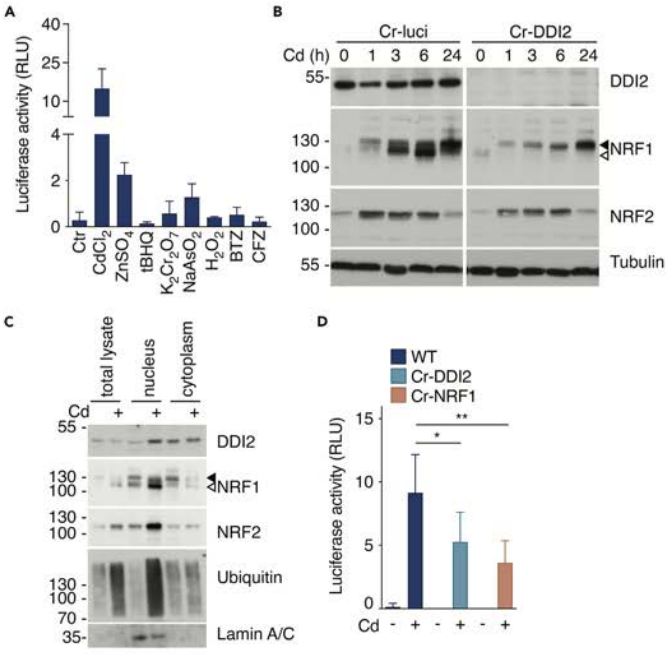

Figure 3. Cadmium induces DDI2-mediated cleavage and nucleus translocation of NRF1

(A) Activation of MT1 promoter-driven luciferase activity in HepG2 cells after 6 h exposure to $CdCl_2$ (5 μM), $ZnSO_4$ (100 μM), tBHQ (50 μM), $K_2Cr_2O_7$ (50 μM), $NaAsO_2$ (12.5 μM), H_2O_2 (1 mM), bortezomib (BTZ, 10 nM), carfilzomib (CFZ, 10 nM) or DMSO as a control (Ctr).

(B) Representative immunoblotting (n = 3) showing the relative protein levels of DDI2, NRF1, NRF2 and tubulin as loading control, of CRISPR KO (Cr)-DDI2 or Cr-luciferase (luci) HepG2 cells treated with Cd (5 μM) during the indicated time in hours (h).

(C) Representative immunoblotting (n = 3) showing subcellular fractionation of endogenous DDI2, NRF1, NRF2, Ubiquitin and Lamin A/C in total cell lysates, nucleus and cytoplasm from HepG2 cells treated with or without Cd (5 μM) during 6 h.

(D) Activation of MT1 promoter-driven luciferase activity in Cr-DDI2, Cr-NRF1 or HepG2 parental cells (WT) after 6 h exposure to Cd (5 μM). Each bar represents the mean, and error bars denote SD of at least three independent experiments. p values were calculated using one-way ANOVA followed by Bonferroni's multiple comparison test. *p<0.05; **p<0.01. ◄ indicates the full-length protein, ◅ indicates the cleaved protein.

proteasome inhibition can trigger the proteolytic activation of NRF1 (Koizumi et al., 2016; Radhakrishnan et al., 2014), we hypothesized that proteasome impairment could be the upstream mechanism of NRF1 activation following Cd exposure. Surprisingly, we found that Cd treatment in HepG2 cells impaired the proteasome activity, similarly to the proteasome inhibitor, CFZ. The treatment with Cd decreased most proteolytic activities of the proteasome including, chymotrypsin, trypsin, and caspase-like activities (Figure 4A). To determine if Cd directly binds and impairs the proteasome function, we evaluated the proteasome activity using cell-free purified proteasome complexes in the presence of Cd molecules. As expected, CFZ directly interacted with the purified proteasome and blocked the substrate degradation. In contrast, Cd did not inhibit the proteasome in the cell-free assay (Figure 4B), indicating that its mechanism of action is indirect and may affect upstream events required for proteasome function.

Consistent with proteasome inhibition, we observed in mice, that DDI2 deficiency in livers increased K48-linked ubiquitinated proteins (Figure S3D). However, in these conditions we could not observe a robust induction of proteasome genes (Figure S4A). In contrast, treatment with cadmium decreased *PSMA4* mRNA levels in wildtype and NRF2 deficient animals. Because DDI2 deficiency impaired expression of this gene at

CellPress
OPEN ACCESS

iScience
Article

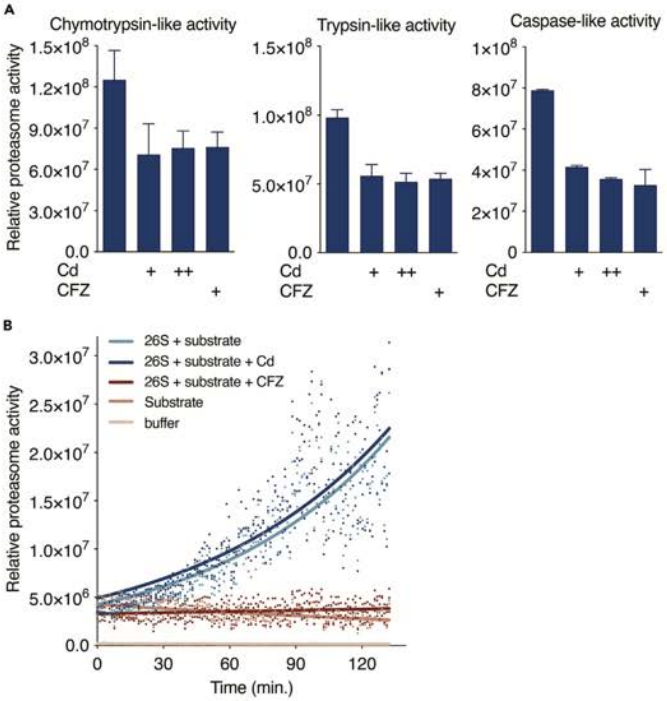

Figure 4. Cadmium indirectly inhibits the proteasome

(A) Relative proteasome activity of HepG2 cells treated with $CdCl_2$ (Cd; + 1 μM or ++ 5 μM) or carfilzomib (CFZ, 10 nM) during 6 h. Each bar represents the mean, and error bars denote SD of at least three independent experiments.

(B) Relative proteasome activity of purified 26S proteasome complexes incubated with the substrate Suc-LLVY-AMC and treated with or without Cd (1 μM) or CFZ (10 nM) during the indicated time in minutes (n = 3).

basal no additional defect was observed on treatment with Cd (Figure S4A). In contrast, in HepG2 cells, cadmium increased PSMA4 gene expression following Cd treatment. As expected, both DDI2- or NRF1-KO cells failed to modulate PSMA4 induction (Figure S4B). These observations indicate that the proteasome bounce back response can be activated but is not always engaged as observed in mice.

DDI2 contributes to increased cell survival on cadmium-induced toxicity

Metallothioneins contribute to the detoxification of heavy metals. We, therefore, tested whether DDI2-mediated *MT* expression could decrease Cd-mediated toxicity. We analyzed *MT* genes expressions in HepG2 cells harboring DDI2 deficiency. In line with the promoter-reporter assays, we observed decreased induction of the human homologs of *MT* genes on treatment with Cd compared with the control population (Figure 5A). We also found that the expression of previously described NRF1 target genes, like *NQO1*, were slightly reduced in Cd-treated HepG2 cells deficient for DDI2, compared to the WT cells (Figure 5A). Moreover, we showed that cellular survival is decreased in DDI2- or NRF1 deficient cells exposed to Cd (Figure 5B), further suggesting that depleting DDI2, consequently preventing NRF1 activation, sensitizes cells to Cd toxicity. Then, we tested if mouse lacking DDI2 in the liver are more sensitive to Cd toxicity. Surprisingly, we did not verify differences in mouse survival, when comparing WT and DDI2-KO, following Cd exposure (Figure S5). However, this observation may be due to the fact that other organs, compensate for MT proteins expression as reported previously (Sabolic et al., 2010), accounting for Cd detoxification and mouse survival.

iScience
Article

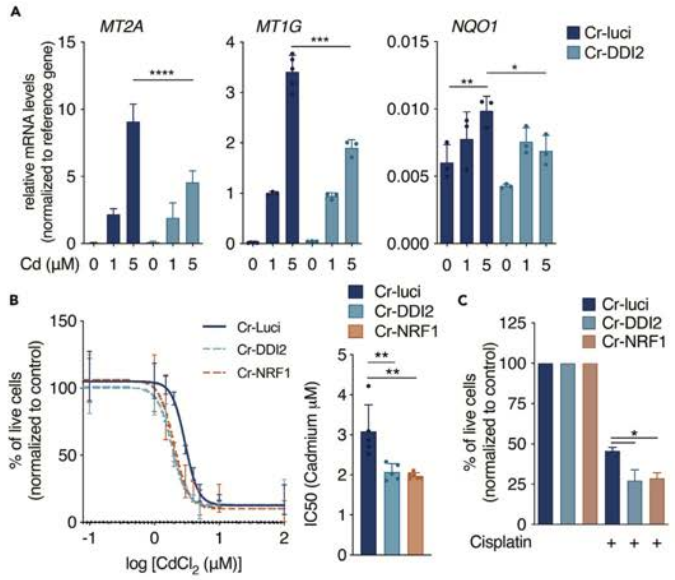

Figure 5. DDI2 promotes cell survival during metal toxicity

(A) Relative mRNA levels of *MT2A*, *MT1G* and *NQO1* in CRISPR KO (Cr)-DDI2 or Cr-luciferase (luci) control HepG2 cells treated with $CdCl_2$ (Cd, as indicated concentrations) for 6 h. Target genes were normalized with *GAPDH* mRNA levels. (n = 3).

(B) Left, Viability of Cr-DDI2 and Cr-luci control HepG2 cells after 48 h treatment with indicated doses of Cd and correspondent IC50 values presented in the bar graph, right (n = 5). Relative viability assessed by 3-(4,5-dimethylthiazol-2-yl)-2,5-dimethyltetrazolium bromide (MTS)/1-methoxyphenazine methosulfate (PMS) assay.

(C) Viability of Cr-DDI2, Cr-NRF1 and Cr-luci control HepG2 cells after 48 h treatment with 500 μM of cisplatin, normalized to non-treated cells (n = 3). p values were calculated using two-tailed unpaired Mann-Whitney t-tests and error bars denote SD. *p<0.05; **p<0.01; ***p<0.001.

MT gene and protein levels increase following the exposure of different metals in both mouse and humans. Recently, it has been suggested that MT promotes chemoresistance during metal-based cancer chemotherapies (Borchert et al., 2020; Rodrigo et al., 2021). Cisplatin is a platinum-based compound, commonly used in chemotherapy treatments alone or in combination with other drugs. To test if the DDI2-NRF1-MT axis promotes cell survival and resistance to cancer chemotherapies, we treated HepG2 cell with cisplatin and evaluated the cell survival. Similar to what we observed in cells treated with Cd (Figure 5B), HepG2 cells lacking DDI2 or NRF1 are more sensitive to cell death following cisplatin treatments compared to WT cells (Figure 5C), further indicating that DDI2 and NRF1 can modulate responses to heavy metal exposure.

DISCUSSION

-This study reports a mouse model to investigate DDI2-associated molecular mechanisms and physiological functions. We used this model to describe the involvement of DDI2 during cell stress response against Cd toxicity. We demonstrated that on Cd exposure in mice, DDI2mediated cleavage and activation of NRF1 and regulated downstream metallothionein (MT) expression in both human and mouse models. Using liver-specific DDI2-KO animals, we found that very few genes were significantly affected by DDI2 deficiency in untreated mice. Unexpectedly, no defects in well-known NRF1 targets such as the proteasome subunits (Koizumi et al., 2016; Lehrbach and Ruvkun, 2016) were identified, except for *Mt1* and *Mt2* expression. These results are consistent with previous reports showing that liver-specific NRF1-KO mice are viable and display reduced expression levels of *Mt1* and *Mt2* (Ohtsuji et al., 2008). These data strongly suggest that DDI2 is upstream of NRF1 signaling pathway in the liver and contributes to *Mt* expression.

Although it has been proposed that both NRF1 and NRF2 share a common target DNA motif, here, we demonstrate that NRF1 controls *Mt* gene expression independently of NRF2. Our observations agree with previous reports showing that both WT and NRF2-KO mice present similar *Mt* expression levels in both Cd-treated and untreated conditions (Chen et al., 2021). However, the activation of MT is not exclusively controlled by the DDI2-NRF1 pathway. *Mt* genes are activated by different response elements, present in the gene promoter, in response to stress stimuli. Previous reports suggest that Cd can displace zinc (Zn) and copper (Cu) from MT conjugates. Consequently, free Zn ions are able to bind and induce the activation of MTF-1 transcriptional factor. Active MTF-1 binds to MRE in the DNA and eventually stimulates the synthesis of *Mt* mRNA (Sabolic et al., 2010). Interestingly, *Mt* null mice are highly sensitive to Cd toxicity (Masters et al., 1994). In comparison, no lethal toxicity was reported in MTF-1-KO mice (Wimmer et al., 2005), and in this study, we did not observe increased lethality in DDI2-KO when treated with 8 mg/kg of Cd. Altogether, *Mt* genes are regulated by distinct mechanisms, including DDI2-NRF1 axis, and are essential to cope with metal toxicity.

The proteasome is a key machinery in eukaryotic cells responsible to cope with cellular toxicity and maintain homeostasis. Importantly, cancer treatments, including proteasome inhibitors, are based on the activation of cell stress to induce apoptosis of targeted tumor cells (Manasanch and Orlowski, 2017). Understanding the molecular mechanisms of cell stress response is crucial to design new therapeutic approaches and to bypass the cancer resistance to treatments. Here, we reported that cellular exposure to metals, as Cd, blocks the proteasome function, increases ubiquitinated proteins, and induces the DDI2-NRF1 stress response pathway to promote the cell survival in hepatocytes. Several studies suggested that metal complexes may regulate proteasome activity (Verani, 2012). However, the molecular mechanisms are largely unknown, these may include the blockade of the UPS by inhibiting de-ubiquitinating enzymes (DUBs) or proteasome assembly chaperones (Chen et al., 2018; Padmanabhan et al., 2016; Xu et al., 2021).

In addition to Cd detoxification, MTs can bind to metal-based drugs, like cisplatin, promoting chemo-resistance in cancer treatments (Borchert et al., 2020; Rodrigo et al., 2021; Si and Lang, 2018). MT expression in tumors is associated with cancer treatment resistance (Si and Lang, 2018) and targeting MT proteins has been suggested to be a powerful tool to boost response rates to metal-based therapies (Borchert et al., 2020). Our data suggest that inhibiting the protease activity of DDI2 could be a suitable therapeutic target to dampen the resistance to metal-based treatments. Nelfinavir is a clinically approved HIV-inhibitor, also described to inhibit DDI2 (Gu et al., 2020). Previous reports demonstrated a beneficial effect of targeting DDI2 using nelfinavir in cancer treatments (Chow et al., 2009) including in Multiple Myeloma (Besse et al., 2018; Driessen et al., 2016; Fassmannova et al., 2020; Gu et al., 2020; Hitz et al., 2019). However, it remains to be evaluated if nelfinavir affects results from inhibition of DDI2-downstream activation of NRF1-MT cellular response.

Altogether, our findings identify heavy metals as activators of the DDI2-NRF1 pathway and downstream MT-chelating proteins. Our results contribute to the understanding of the metal-compounds secretion from the body, as well as the chemotherapy resistance to metal-based treatments.

LIMITATION OF THE STUDY

The contributions of DDI2 during development are still unknown. DDI2-deficient mice die at the mid-gestational stage. Additional studies are necessary to understand the cause of death. Comparing these defects with those observed in NRF1 deficient animals could hint at additional functions for DDI2, possibly independent of NRF1. Although we extrapolate that the phenotypes observed in DDI2 deficiency are mainly a consequence of lack of NRF1 activation, we cannot exclude the contribution of other DDI2 substrates yet to be characterized. For example, NRF3, a close homolog of NRF1, could contribute to DDI2 functions in tissues where it is expressed.

STAR★METHODS

Detailed methods are provided in the online version of this paper and include the following:

- KEY RESOURCES TABLE
- RESOURCE AVAILABILITY
  - Lead contact

SUPPLEMENTAL INFORMATION

Supplemental information can be found online at https://doi.org/10.1016/j.isci.2022.105227.

ACKNOWLEDGMENTS

We thank to Masayuki Yamamoto, Laurie H. Glimcher, Nicolas Fasel, Pascal Schneider and Margot Thome for providing essential material. We thank to the Mouse Facility, Mouse Pathology Facility, Metabolomics Plat-form and Genomics facility of the University of Lausanne for technical assistance. We thank to the members of the Department of Immunobiology for the discussion and helpful input. This work was supported by a grant from the Swiss National Science Foundation (310030_173152) and Human Frontier Science Program CDA-00059.

AUTHOR CONTRIBUTIONS

Conceptualization, F.M; Methodology, S.T.R., A.D.G., and F.M.; Investigation, S.T.R., A.D.G., S. B.; C.C., M.O., K.N., and L.Z.; Writing - Original Draft, S.T.R; Funding Acquisition, F.M.; Supervision, F.M.

DECLARATION OF INTERESTS

The authors declare no competing interests.

INCLUSION AND DIVERSITY

One or more of the authors of this paper self-identifies as a member of the LGBTQIA+ community.

Received: April 20, 2022
Revised: August 9, 2022
Accepted: September 23, 2022
Published: October 21, 2022

REFERENCES

Besse, A., Stolze, S.C., Rasche, L., Weinhold, N., Morgan, G.J., Kraus, M., Bader, J., Overkleeft, H.S., Besse, L., and Driessen, C. (2018). Carfilzomib resistance due to ABCB1/MDR1 overexpression is overcome by nelfinavir and lopinavir in multiple myeloma. Leukemia *32*, 391–401. https://doi.org/10.1038/leu.2017.212.

Borchert, S., Suckrau, P.M., Walter, R.F.H., Wessolly, M., Mairinger, E., Steinborn, J., Hegedus, B., Hager, T., Herold, T., Eberhardt, W.E.E., et al. (2020). Impact of metallothionein-knockdown on cisplatin resistance in malignant pleural mesothelioma. Sci. Rep. *10*, 18677. https://doi.org/10.1038/s41598-020-75807-x.

Chan, J.Y., Kwong, M., Lu, R., Chang, J., Wang, B., Yen, T.S., and Kan, Y.W. (1998). Targeted disruption of the ubiquitous CNC-bZIP transcription factor, Nrf-1, results in anemia and embryonic lethality in mice. EMBO J. *17*, 1779–1787. https://doi.org/10.1093/emboj/17.6.1779.

Chan, K., Lu, R., Chang, J.C., and Kan, Y.W. (1996). NRF2, a member of the NFE2 family of transcription factors, is not essential for murine erythropoiesis, growth, and development. Proc. Natl. Acad. Sci. USA *93*, 13943–13948. https://doi.org/10.1073/pnas.93.24.13943.

Chen, C., Han, X., Wang, G., Liu, D., Bao, L., Jiao, C., Luan, J., Hou, Y., Xu, Y., Wang, H., et al. (2021). Nrf2 deficiency aggravates the kidney injury induced by subacute cadmium exposure in mice. Arch. Toxicol. *95*, 883–893. https://doi.org/10.1007/s00204-020-02964-3.

Chen, J., and Shaikh, Z.A. (2009). Activation of Nrf2 by cadmium and its role in protection against cadmium-induced apoptosis in rat kidney

cells. Toxicol. Appl. Pharmacol. *241*, 81–89. https://doi.org/10.1016/j.taap.2009.07.038.

Chen, L., Ma, L., Bai, Q., Zhu, X., Zhang, J., Wei, Q., Li, D., Gao, C., Li, J., Zhang, Z., et al. (2014). Heavy metal-induced metallothionein expression is regulated by specific protein phosphatase 2A complexes. J. Biol. Chem. *289*, 22413–22426. https://doi.org/10.1074/jbc.M114.548677.

Chen, X., Wu, J., Yang, Q., Zhang, X., Zhang, P., Liao, S., He, Z., Wang, X., Zhao, C., and Liu, J. (2018). Cadmium pyrithione suppresses tumor growth in vitro and in vivo through inhibition of proteasomal deubiquitinase. Biometals *31*, 29–43. https://doi.org/10.1007/s10534-017-0062-6.

Chow, W.A., Jiang, C., and Guan, M. (2009). Anti-HIV drugs for cancer therapeutics: back to the future? Lancet Oncol. *10*, 61–71. https://doi.org/10.1016/S1470-2045(08)70334-6.

Cubillos-Ruiz, J.R., Bettigole, S.E., and Glimcher, L.H. (2017). Tumorigenic and immunosuppressive effects of endoplasmic reticulum stress in cancer. Cell *168*, 692–706. https://doi.org/10.1016/j.cell.2016.12.004.

Driessen, C., Kraus, M., Joerger, M., Rosing, H., Bader, J., Hitz, F., Berset, C., Xyrafas, A., Hawle, H., Berthod, G., et al. (2016). Treatment with the HIV protease inhibitor nelfinavir triggers the unfolded protein response and may overcome proteasome inhibitor resistance of multiple myeloma in combination with bortezomib: a phase I trial (SAKK 65/08). Haematologica *101*, 346–355. https://doi.org/10.3324/haematol.2015.135780.

Fassmannová, D., Sedlák, F., Sedláček, J., Špička, I., and Grantz Šašková, K. (2020). Nelfinavir inhibits the TCF11/nrf1-mediated proteasome recovery pathway in multiple myeloma. Cancers *12*, E1065. https://doi.org/10.3390/cancers12051065.

Figueiredo-Pereira, M.E., Yakushin, S., and Cohen, G. (1997). Accumulation of ubiquitinated proteins in mouse neuronal cells induced by oxidative stress. Mol. Biol. Rep. *24*, 35–38. https://doi.org/10.1023/a:1006848405975.

Gu, Y., Wang, X., Wang, Y., Wang, Y., Li, J., and Yu, F.X. (2020). Nelfinavir inhibits human DDI2 and potentiates cytotoxicity of proteasome inhibitors. Cell. Signal. *75*, 109775. https://doi.org/10.1016/j.cellsig.2020.109775.

Habeebu, S.S., Liu, J., Liu, Y., and Klaassen, C.D. (2000). Metallothionein-null mice are more sensitive than wild-type mice to liver injury induced by repeated exposure to cadmium. Toxicol. Sci. *55*, 223–232. https://doi.org/10.1093/toxsci/55.1.223.

Hitz, F., Kraus, M., Pabst, T., Hess, D., Besse, L., Silzle, T., Novak, U., Seipel, K., Rondeau, S., Stüdeli, S., et al. (2019). Nelfinavir and lenalidomide/dexamethasone in patients with lenalidomide-refractory multiple myeloma. A phase I/II Trial (SAKK 39/10). Blood Cancer J. *9*, 70. https://doi.org/10.1038/s41408-019-0228-2.

Itoh, K., Chiba, T., Takahashi, S., Ishii, T., Igarashi, K., Katoh, Y., Oyake, T., Hayashi, N., Satoh, K., Hatayama, I., et al. (1997). An Nrf2 small Maf heterodimer mediates the induction of phase II detoxifying enzyme genes through antioxidant response elements. Biochem. Biophys. Res. Commun. *236*, 313–322. https://doi.org/10.1006/bbrc.1997.6943.

Jungmann, J., Reins, H.A., Schobert, C., and Jentsch, S. (1993). Resistance to cadmium mediated by ubiquitin-dependent proteolysis. Nature *361*, 369–371. https://doi.org/10.1038/361369a0.

Klaassen, C.D., Liu, J., and Diwan, B.A. (2009). Metallothionein protection of cadmium toxicity. Toxicol. Appl. Pharmacol. *238*, 215–220. https://doi.org/10.1016/j.taap.2009.03.026.

Koizumi, S., Irie, T., Hirayama, S., Sakurai, Y., Yashiroda, H., Naguro, I., Ichijo, H., Hamazaki, J., and Murata, S. (2016). The aspartyl protease DDI2 activates Nrf1 to compensate for proteasome dysfunction. Elife *5*, e18357. https://doi.org/10.7554/eLife.18357.

Kottemann, M.C., Conti, B.A., Lach, F.P., and Smogorzewska, A. (2018). Removal of RTF2 from stalled replisomes promotes maintenance of genome integrity. Mol. Cell *69*, 24–35.e5. https://doi.org/10.1016/j.molcel.2017.11.035.

Lee, C.S., Lee, C., Hu, T., Nguyen, J.M., Zhang, J., Martin, M.V., Vawter, M.P., Huang, E.J., and Chan, J.Y. (2011). Loss of nuclear factor E2-related factor 1 in the brain leads to dysregulation of proteasome gene expression and neurodegeneration. Proc. Natl. Acad. Sci. USA *108*, 8408–8413. https://doi.org/10.1073/pnas.1019209108.

Lehrbach, N.J., and Ruvkun, G. (2016). Proteasome dysfunction triggers activation of SKN-1A/Nrf1 by the aspartic protease DDI-1. Elife *5*. https://doi.org/10.7554/eLife.17721.

Manasanch, E.E., and Orlowski, R.Z. (2017). Proteasome inhibitors in cancer therapy. Nat. Rev. Clin. Oncol. *14*, 417–433. https://doi.org/10.1038/nrclinonc.2016.206.

Masters, B.A., Kelly, E.J., Quaife, C.J., Brinster, R.L., and Palmiter, R.D. (1994). Targeted disruption of metallothionein I and II genes increases sensitivity to cadmium. Proc. Natl. Acad. Sci. USA *91*, 584–588. https://doi.org/10.1073/pnas.91.2.584.

Ohtsuji, M., Katsuoka, F., Kobayashi, A., Aburatani, H., Hayes, J.D., and Yamamoto, M. (2008). Nrf1 and Nrf2 play distinct roles in activation of antioxidant response element-dependent genes. J. Biol. Chem. *283*, 33554–33562. https://doi.org/10.1074/jbc.M804597200.

Op, M., Ribeiro, S.T., Chavarria, C., De Gassart, A., Zaffalon, L., and Martinon, F. (2022). The aspartyl protease DDI2 drives adaptation to proteasome inhibition in multiple myeloma. Cell Death Dis. *13*, 475. https://doi.org/10.1038/s41419-022-04925-3.

Padmanabhan, A., Vuong, S.A.T., and Hochstrasser, M. (2016). Assembly of an evolutionarily conserved alternative proteasome isoform in human cells. Cell Rep. *14*, 2962–2974. https://doi.org/10.1016/j.celrep.2016.02.068.

Perteguer, M.J., Gómez-Puertas, P., Cañavate, C., Dagger, F., Gárate, T., and Valdivieso, E. (2013). Ddi1-like protein from Leishmania major is an active aspartyl proteinase. Cell Stress Chaperones *18*, 171–181. https://doi.org/10.1007/s12192-012-0368-9.

Radhakrishnan, S.K., den Besten, W., and Deshaies, R.J. (2014). p97-dependent retrotranslocation and proteolytic processing govern formation of active Nrf1 upon proteasome inhibition. Elife *3*, e01856. https://doi.org/10.7554/eLife.01856.

Radhakrishnan, S.K., Lee, C.S., Young, P., Beskow, A., Chan, J.Y., and Deshaies, R.J. (2010). Transcription factor Nrf1 mediates the proteasome recovery pathway after proteasome inhibition in mammalian cells. Mol. Cell *38*, 17–28. https://doi.org/10.1016/j.molcel.2010.02.029.

Rodrigo, M.A.M., Michalkova, H., Strmiska, V., Casar, B., Crespo, P., de Los Rios, V., Ignacio Casal, J., Haddad, Y., Guran, R., Eckschlager, T., et al. (2021). Metallothionein-3 promotes cisplatin chemoresistance remodelling in neuroblastoma. Sci. Rep. *11*, 5496. https://doi.org/10.1038/s41598-021-84185-x.

Rousseau, A., and Bertolotti, A. (2018). Regulation of proteasome assembly and activity in health and disease. Nat. Rev. Mol. Cell Biol. *19*, 697–712. https://doi.org/10.1038/s41580-018-0040-z.

Sabolić, I., Breljak, D., Skarica, M., and Herak-Kramberger, C.M. (2010). Role of metallothionein in cadmium traffic and toxicity in kidneys and other mammalian organs. Biometals *23*, 897–926. https://doi.org/10.1007/s10534-010-9351-z.

Serbyn, N., Noireterre, A., Bagdiul, I., Plank, M., Michel, A.H., Loewith, R., Kornmann, B., and Stutz, F. (2020). The aspartic protease Ddi1 contributes to DNA-protein crosslink repair in yeast. Mol. Cell *77*, 1066–1079.e9. https://doi.org/10.1016/j.molcel.2019.12.007.

Si, M., and Lang, J. (2018). The roles of metallothioneins in carcinogenesis. J. Hematol. Oncol. *11*, 107. https://doi.org/10.1186/s13045-018-0645-x.

Siva, M., Haberecht-Müller, S., Prochazkova, M., Prochazka, J., Sedlak, F., Chawengsaksophak, K., Kasparek, P., Sedlacek, R., Konvalinka, J., Krüger, E., and Saskova, K.G. (2020). DDI2 protease activity controls embryonic development and inflammation via TCF11/NRF1. Preprint at bioRxiv. https://doi.org/10.1101/2020.12.16.423023.

Sivá, M., Svoboda, M., Veverka, V., Trempe, J.F., Hofmann, K., Kožíšek, M., Hexnerová, R., Sedlák, F., Belza, J., Brynda, J., et al. (2016). Human DNA-damage-inducible 2 protein is structurally and functionally distinct from its yeast ortholog. Sci. Rep. *6*, 30443. https://doi.org/10.1038/srep30443.

Verani, C.N. (2012). Metal complexes as inhibitors of the 26S proteasome in tumor cells. J. Inorg. Biochem. *106*, 59–67. https://doi.org/10.1016/j.jinorgbio.2011.09.003.

Wang, S., Cheng, H., Wang, L., Zhao, R., and Guan, D. (2020). Overexpression of NRF1-742 or NRF1-772 reduces arsenic-induced cytotoxicity and apoptosis in human HaCaT keratinocytes. Int. J. Mol. Sci. *21*, E2014. https://doi.org/10.3390/ijms21062014.

Wimmer, U., Wang, Y., Georgiev, O., and Schaffner, W. (2005). Two major branches of anti-cadmium defense in the mouse: MTF-1/metallothioneins and glutathione. Nucleic Acids Res. *33*, 5715–5727. https://doi.org/10.1093/nar/gki881.

Xu, D.C., Yang, L., Zhang, P.Q., Yan, D., Xue, Q., Huang, Q.T., Li, X.F., Hao, Y.L., Tang, D.L., Ping Dou, Q., et al. (2022). Pharmacological characterization of a novel metal-based proteasome inhibitor Na-AuPT for cancer treatment. Acta Pharmacol. Sin. *43*, 2128–2138. https://doi.org/10.1038/s41401-021-00816-z.

Yeh, Y.H., Tsai, C.C., Chen, T.W., Lee, C.H., Chang, W.J., Hsieh, M.Y., and Li, T.K. (2022). Activation of multiple proteolysis systems contributes to acute cadmium cytotoxicity. Mol. Cell. Biochem. *477*, 927–937. https://doi.org/10.1007/s11010-021-04298-9.

Yu, X., Sidhu, J.S., Hong, S., Robinson, J.F., Ponce, R.A., and Faustman, E.M. (2011). Cadmium induced p53-dependent activation of stress signaling, accumulation of ubiquitinated proteins, and apoptosis in mouse embryonic fibroblast cells. Toxicol. Sci. *120*, 403–412. https://doi.org/10.1093/toxsci/kfr010.

Zhang, Y., Lucocq, J.M., Yamamoto, M., and Hayes, J.D. (2007). The NHB1 (N-terminal homology box 1) sequence in transcription factor Nrf1 is required to anchor it to the endoplasmic reticulum and also to enable its asparagine-glycosylation. Biochem. J. *408*, 161–172. https://doi.org/10.1042/BJ20070761.

Zhang, Z., Bi, C., Fan, Y., Zhang, N., Deshmukh, R., Yan, X., Lv, X., Zhang, P., Zhang, X., and Dou, Q.P. (2015). L-Ornithine Schiff base-copper and -cadmium complexes as new proteasome inhibitors and apoptosis inducers in human cancer cells. J. Biol. Inorg. Chem. *20*, 109–121. https://doi.org/10.1007/s00775-014-1219-1.

Zhao, R., Hou, Y., Xue, P., Woods, C.G., Fu, J., Feng, B., Guan, D., Sun, G., Chan, J.Y., Waalkes, M.P., et al. (2011). Long isoforms of NRF1 contribute to arsenic-induced antioxidant response in human keratinocytes. Environ. Health Perspect. *119*, 56–62. https://doi.org/10.1289/ehp.1002304.

CellPress
OPEN ACCESS

iScience
Article

STAR★METHODS

KEY RESOURCES TABLE

REAGENT or RESOURCE	SOURCE	IDENTIFIER
Antibodies		
anti-DDI2	This study	N/A
anti-DDI2	Abcam	ab197081
anti-NRF1	Cell signaling	8052
anti-NRF2	Cell signaling	12721, RRID: AB_2715528
anti-Tubulin	Adipogen	AG-27B-0005-C100, RRID: AB_2490494
anti-MT	Enzo Life Sciences	ADI-SPA-550-D, RRID: AB_2039383
anti-ubiquitin	Cell signaling	3936, RRID: AB_331292
anti-K48	Abcam	EP8589
anti-PSMB8	Cell signaling	13726, RRID: AB_2798304
anti-PSMB5	Cell signaling	12919, RRID: AB_2798061
Chemicals, peptides, and recombinant proteins		
Bortezomib	LC-Laboratories	B-1408
Carfilzomib	LC-Laboratories	C-3022
H_2O_2	Sigma-Aldrich	216763-100ML
$CdCl_2$	Sigma-Aldrich	202908-10G
$NaAsO_2$	Sigma-Aldrich	35000-1L-R
$K_2Cr_2O_7$	Sigma-Aldrich	207802-100g
$ZnSO_4$	Sigma-Aldrich	83265
tBHQ	Sigma-Aldrich	112941-5g
NaF	Sigma-Aldrich	201154
Na4P2O7	Sigma-Aldrich	P8010
MG132	Sigma-Aldrich	c2211-5mg
Suc-LLVY-AMC	Enzo Life Sciences	BML-P802-0005
Z-ARR-AMC	Calbiochem	CAS 90468-18-1
Z-LLE-AMC	Adipogen	CAS 348086-666-8
AMC	Biovision	K245-100-4
Purified human proteasome complexes	Bio-Techne	E−365-025
Critical commercial assays		
RNeasy mini kit	QIAGEN	74104
2X Reverse Transcription master mix	Applied Biosystems	4368814
KAPA HiFi HotStart PCR Kit	KapaBiosystems	KK2502
Pierce BCA Protein assay	Thermo Fisher Scientific	23227
TBARS kit	Abnova	KA4409
Catalase activity	Biovision	K773
SOD activity	Biovision	K335
MTS assay	Promega	G1111
Dual-Luciferase Assay System	Promega	E1910
Deposited data		
RNA-seq data	Gene Expression Omnibus	GSE198150
Raw data for immunoblots	Mendeley	https://doi.org/10.17632/9krjdj44p5.1

(Continued on next page)

Continued

REAGENT or RESOURCE	SOURCE	IDENTIFIER
Experimental models: Cell lines		
HepG2	Pascal Schneider, University of Lausanne	N/A
Experimental models: Organisms/strains		
$DDI2^{flox/flox}$	This study	N/A
$DDI2^{flox/flox}Alb^{Cre+}$	This study	N/A
$DDI2^{KO}$	This study	N/A
$NRF2^{lacZ/lacZ}$	Prof. M. Yamamoto Tohoku University Graduate School of Medicine, Japan	N/A
$DDI2^{flox/flox}Alb^{Cre-}$; $NRF2^{lacZ/lacZ}$	This study	N/A
Oligonucleotides		
RT-PCR *ACTIN*: fwd 5′-TACCACCA TGTACCCAGGCA-3′ rev 5′-CTCAGGA GGAGCAATGATCTTGAT-3′	This study	N/A
RT-PCR *GAPDH*: fwd 5′-CGCTC TCTGCTCCTCCTG-3′, rev 5′-CGAT GGTGTCTGAGCGAT-3′	This study	N/A
RT-PCR *Mt1*: fwd 5′-ATGGAC CCCAACTGCTCCT-3′, rev 5′-AC AGCCCTGGGCACATTT-3′	This study	N/A
RT-PCR *Mt2*: fwd 5′-CCGATCTC TCGTCGATCTTCAACC-3′, rev 5′-CA GGAGCAGCAGCTTTTCTTGCAG-3′	This study	N/A
RT-PCR *NFE2L1*: fwd 5′-TGGAACAGC AGTGGCAAGATCTCA-3′, rev 5′-GGCA CTGTACAGGATTTCACTTGC-3′	This study	N/A
RT-PCR *NFE2L2*: fwd 5′-TTCCCGG TCACATCGAGAG-3′, rev 5′-TCC TGTTGCATACCGTCTAAATC-3′	This study	N/A
RT-PCR *MT2A*: fwd 5′-CTCTTC AGCTCGCCATGGAT-3′, rev 5′-TG GAAGTCGCGTTCTTTACA-3′	This study	N/A
RT-PCR *MT1G*: fwd 5′-TTGCAA TGGACCCCAACT-3′, rev 5′-TC CTGGATTTTACGGGTCAC-3′	This study	N/A
RT-PCR *NQO1*: fwd 5′-CAGCT CACCGAGAGCCTAGT-3′, rev 5′-AG TGCTCTTCTGCCGACCAT-3′	This study	N/A
RT-PCR *PSMA4* (human): fwd 5′- CCC TTTGGTGTTTTGCT-3′, rev 5′ – GCT GCAGCGCTATTATTTCC-3′	This study	N/A
RT-PCR *Psma4* (mouse): fwd 5′ – AAAAG TGGAAATCGCCACAC-3′, rev 5′ – TTT CTTTCTTCTCCCGCTCA-3′	This study	N/A
SgLuci fwd 5′-CACCGCTTCGAAA TGTCCGTTCGGT-3′, rev 5′- AAAC ACCGAACGGACATTTCGAAGC-3′	(Op et al., 2022)	N/A
SgDDI2 fwd 5′- CACCGGCTCGAAG TCGGCGTCGAC-3′, rev 5′- AAACG GTCGACGCCGACTTCGAGCC-3′	(Op et al., 2022)	N/A

(*Continued on next page*)

Continued

REAGENT or RESOURCE	SOURCE	IDENTIFIER
SgNRF1 fwd 5′- CACCGCTTTCT CGCACCCCGTTGTC-3′, rev 5′- AAA CGACAACGGGGTGCGAGAAAGC-3′	(Op et al., 2022)	N/A
Recombinant DNA		
LentiCRISPR-v2 vector	Addgene	52961
MT-Firefly-luciferase reporter	Prof. M. Yamamoto Tohoku University Graduate School of Medicine, Japan	(Ohtsuji et al., 2008)
Software and Algorithms		
R bioconductor package "limma"	Bioconductor	R version 3.1.1, limma version 3.20.8

RESOURCE AVAILABILITY

Lead contact

Any additional information or inquiries regarding code availability or resources should be directed to Fabio Martinon (Fabio.Martinon@unil.ch).

Materials availability

Request for generated mice models and constructs should be directed to Fabio Martinon (Fabio.Martinon@unil.ch).

Data and code availability

The data presented in this publication have been deposited in NCBI's Gene Expression Omnibus and are accessible through GEO Series accession number: GSE198150.

Raw data for immunoblots were deposited on Mendeley Data: https://doi.org/10.17632/9krjdj44p5.1

This paper article not report original code. Any additional information required to reanalyze the data reported in this article is available from the lead contact on request.

EXPERIMENTAL MODEL AND SUBJECT DETAILS

Cell culture and reagents

The human hepatocellular carcinoma HepG2 cell line (originating from a hepatocellular carcinoma of a 15-year-old, white male with liver cancer) was provided from Pascal Schneider (University of Lausanne), and maintained in Dulbecco's modified Eagle's medium (DMEM) supplemented with 10% (v/v) fetal bovine serum, 1x non-essential amino acids solution, and cultured in a 37°C incubator with 5% CO_2. Bortezomib and carfilzomib were purchased from LC-Laboratories (Woburn, MA, USA), cisplatin, $CdCl_2$, $ZnSO_4$, tBHQ, $K_2Cr_2O_7$, $NaAsO_2$ and H_2O_2 from Sigma-Aldrich (St. Louis, MO, USA).

Animal models

Animal experiments were performed in accordance with the Swiss animal welfare law and were approved by the local authorities and the animal ethics committee (license numbers: 2390.1; 2390.1a; 2390x2). Both male and female mice, within 6–12 weeks old, were randomly assigned to each experimental condition.

$DDI2^{flox/flox}Alb^{Cre+}$ (DDI2-KO) mouse model was generated by microinjection of C57BL/6N-Atm1Brd blastocysts with mouse embryonic stem (ES) cells containing the L1L2_Bact_P cassette ($Ddi2^{tm1a(EUCOMM)Hmgu}$, MGI ID: 4842030) inserted at position GRCm38:Chr4:141,410,874-141450730, following standard methodology. DDI2 full KO mouse was generated by blastocyst microinjection of ES cells containing the pGT1Lxf gene-trap vector (BayGenomics, CA, USA) targeting the *Ddi2* gene (GRCm39:Chr4:141,435,521-141435739). B6J.129P2-Nfe2l2^{tmLacz} (NRF2-KO) mouse were obtained from Prof. M. Yamamoto (Tohoku University Graduate School of Medicine, Japan) (Itoh et al., 1997). DDI2-NRF2 double KO animals and littermate controls were generated by breeding heterozygous DDI2-KO and NRF2-KO mice ($DDI2^{flox/flox}Alb^{Cre+}$; $NRF2^{wt/lacZ}$ x $DDI2^{flox/flox}Alb^{Cre-}$; $NRF2^{lacZ/lacZ}$) (d-KO). Animal genotyping by PCR was done

before and after each experiment. All mouse experiments were performed using littermate controls. Both male and female mice were randomly assigned to each experimental condition.

The following oligos were used for genotyping. CRE alleles: CRE frw 5′-AACATGCTTCATCGTCGG-3′ CRE rev 5′-TTCGGATCATCAGCTACACC-3′; Positive band: ~350 bp. DDI2 flox alleles: frw 5′-GTAACGCCTGG GTCAGGATT-3′ and rev 5′-CCCACAGCCAAGTAAGGAGA-3′; on a 1.5% Gel, WT allele: 188 bp, *LoxP* allele: 268 bp. DDI2 KO alleles: frw 5′-GACAGTATCGGCCTCAGGAAGATCG-3′, and rev 5′-TGACTTAGAC AGACACTGAG-3′; on a 1.5%, WT band: ~ 0.5Kb, DDI2 KO band: ~1.1Kb.

METHOD DETAILS

RNA sequencing

Following total RNA was extracted using RNeasy mini kit (QIAGEN, Hilden, Germany) high-throughput sequencing was performed at the Lausanne Genomics Technologies Facility (University of Lausanne) with Illumina HiSeq 2500 (San Diego, CA, USA) using TruSeq SBS Kit v3 reagents. For the RNA-seq analysis, we used a moderated t-test from the R bioconductor package "limma" (R version 3.1.1, limma version 3.20.8). The data discussed in this publication have been deposited in NCBI's Gene Expression Omnibus and are accessible through GEO Series accession numberGSE198150.

Quantitative real-time PCR

Total RNA was isolated from the same number of cells or similar tissue weight between experimental conditions. RNA was isolated with Trizol (Invitrogen, Waltham, MA, USA) and cDNA was synthesized from 2 µg of RNA using 2X Reverse Transcription master mix (Applied Biosystems, Waltham, MA, USA) following the manufacture's protocol. The cDNA was quantified by real-time PCR with KAPA HiFi HotStart PCR Kit (Kapa Biosystems, Wilmington, MA, USA) using the LightCycler 480 System (Roche, Basel, Switzerland). Primer sequences used were as follows: *ACTIN*: fwd 5′-TACCACCATGTACCCAGGCA-3′, rev 5′-CTCAGGAGG AGCAATGATCTTGAT-3′; *GAPDH*: fwd 5′-CGCTCTCTGCTCCTCCTG-3′, rev 5′-CGATGGTGTCTGAGCG AT-3′; *Mt1*: fwd 5′-ATGGACCCCAACTGCTCCT-3′, rev 5′-ACAGCCCTGGGCACATTT-3′; *Mt2*: fwd 5′-CC GATCTCTCGTCGATCTTCAACC-3′, rev 5′-CAGGAGCAGCAGCTTTTCTTGCAG-3′; *NFE2L1*: fwd 5′-TGG AACAGCAGTGGCAAGATCTCA-3′, rev 5′-GGCACTGTACAGGATTTCACTTGC-3′; *NFE2L2*: fwd 5′-TTCC CGGTCACATCGAGAG-3′, rev 5′-TCCTGTTGCATACCGTCTAAATC-3′; *MT2A*: fwd 5′-CTCTTCAGCTCG CCATGGAT-3′, rev 5′-TGGAAGTCGCGTTCTTTACA-3′; *MT1G*: fwd 5′-TTGCAATGGACCCCAACT-3′, rev 5′-TCCTGGATTTTACGGGTCAC-3′; *NQO1*: fwd 5′-CAGCTCACCGAGAGCCTAGT-3′, rev 5′-AGTGCT CTTCTGCCGACCAT-3′.

Immunoblotting

Cells and tissue protein extracts were prepared with ice-cold RIPA buffer (50 mM NaCl, 50 mM Tris pH 7.4, 1 mM EDTA, 0.1% SDS, 1% NP-40, 1% sodium deoxycholate) supplemented with protease inhibitor cocktail (Roche, Basel, Switzerland), 10 mM Na3VO4, 50 mM NaF, 10 mM Na4P2O7, and 5 µM MG132 (Sigma-Aldrich, St. Louis, MO, USA). Liver tissue was dissociated for 5 min using the Qiagen TissueLyser II (Hilden, Germany). Total protein was quantified by Pierce BCA Protein assay (Thermo Fisher Scientific, Waltham, MA, USA), denaturated and equal amounts were loaded in SDS-PAGE. The following antibodies were used for immunoblot analysis: anti-DDI2 (from our lab, produced from human DDI2 immunized-rabbit serum using HiTrap NHS activated HP columns, GE Healthcare, Chicago, IL, USA), anti-NRF1 (8052) and anti-NRF2 (12,721) from Cell Signaling (Danvers, MA, USA), anti-Tubulin (AG-27B-0005-C100) from AdipoGen (Epalinges, Switzerland), anti-MT (ADI-SPA-550-D) from Enzo Life Sciences (Farmingdale, NY, UA).

Plasmid construction and cell line generation

Gene knockout (KO) cell lines were generated by viral transfection of LentiCRISPR-v2 vector (Addgene reference: 52,961) containing the target single guide RNA (sgRNA) sequence as described in (Op et al., 2022). The sgRNA sequence of the Luciferase gene was used as control and denominated as Cr-luci cell line. KO cell lines were selected with 1.5 µg/mL of puromycin (Sigma-Aldrich, St. Louis, MO, USA) for 15 days.

Immunohistochemistry

Hematoxylin–eosin (H&E) staining of the liver was performed by the Mouse Pathology Facility (University of Lausanne) according to standard protocols. Briefly, paraffin-embedded liver slides, with 3 µm thick, were

treated with Tris-EDTA (pH 9) in a pressure cooker for 2 min. The staining was performed with anti-MT (1/100 in PBS 0.1% BSA, 60 min), Dako EnVision+, and HRP anti-mouse antibody (30 min). The slides were reveled with DAB and counterstain with Harris hematoxylin following standard procedures.

Proteasome activity assay

Two million cells were lysed in 300 µL proteasome lysis buffer (50 mM HEPES pH 7.8, 10 mM NaCl, 1.5 mM $MgCl_2$, 1 mM EDTA, 1 mM EGTA, 250 mM sucrose and 5 mM DTT in PBS without Ca^{2+} or Mg^{2+}). Cell lysates were sonicated 3 s using the microtip output set on ~3 and centrifuged at 16,000 RCF for 10 min at 4°C. The total proteins were quantified from the supernatant. Equal amounts of total protein were diluted in proteasome lysis buffer supplemented with 2 mM ATP (Sigma-Aldrich, St. Louis, MO, USA) and incubated with 100 µM of proteasome substrate reporters. The following chymotrypsin-, trypsin- and caspase-like substrate reporters were used: Suc-LLVY-AMC from Enzo Life Sciences (#BML-P802-0005, Farmingdale, NY, USA); Z-ARR-AMC from Calbiochem (#CAS 90468-18-1, San Diego, CA, USA); and Z-LLE-AMC from AdipoGen (#CAS 348086-666-8, Epalinges, Switzerland). Fluorescence, $A_{360}ex/A_{460}em$, was measured during 60 min at 37°C with SpectraMax i3 (San Jose, CA, USA). AMC (#K245-100-4, BioVision Milpitas, CA, USA) was used as technical positive control. Purified human proteasome complexes (#E−365-025, Bio-Techne, MN, USA) were used for the cell-free proteasome activity assays.

Enzymatic assays

Freshly isolated liver tissue was analyzed following the manufacturer's instructions to quantify the TBARS levels (from 25 mg of tissue, #KA4409, Abnova, Taipei, Taiwan), Catalase activity (from 100 mg of tissue, #K773, BioVision, Milpitas, CA, USA), and SOD activity (from 50 mg of tissue, #K335, BioVision, Milpitas, CA, USA). Blood was collected from the left ventricle and serum was analyzed for ALT, AST and LDH levels using Cobas C111 (Roche, Basel, Switzerland) according to the manufacturer's instructions.

Cytotoxic assay

Cell viability was evaluated by using a 3-(4,5-dimethylthiazol-2-yl)-5-(3-carboxymethoxyphenyl)-2-(4-sulfonphenyl)-2H-tetrazolium (MTS) assay (Promega, Madison, WI, USA) and calculated as the percentage of vehicle control cells. Dose-response curves were plotted using a four-parameter logistic equation. Graphs and IC50 values (the 50% maximal inhibitory concentration) were obtained using GraphPad Prism 9.0 (GraphPad, San Diego, CA, USA).

Luciferase assay

For each condition, one million cells were transfected with 0.9 µg MT-Firefly-luciferase reporter plasmid (Ohtsuji et al., 2008) provided by Masayuki Yamamoto (Tohoku University Graduate School of Medicine); 0.1 µg Renilla plasmid was used as the internal control. Dual-Luciferase Assay System (Promega, Madison, MI, USA) was performed 48 h after transfection, according to the manufacturer's instructions. Specific Firefly luciferase activity was calculated from light intensity measurements and normalized against Renilla luciferase activity as internal control.

QUANTIFICATION AND STATISTICAL ANALYSIS

Representative results from at least three independent experiments were shown. Statistical comparisons were made as described in the Figure legends with GraphPad Prism. The significance of the difference was set at p values <0.05. * denotes $p<0.05$; ** $p<0.01$; *** $p<0.001$. n indicates the number of independent experiment, except in Figures 2A, 2D, and S5 where it indicates number of animals per group and Figure S1, where N indicates total number of animals.

iScience, Volume *25*

Supplemental information

The protease DDI2 regulates NRF1 activation in response to cadmium toxicity

Sérgio T. Ribeiro, Aude de Gassart, Sarah Bettigole, Lea Zaffalon, Claire Chavarria, Melanie Op, Kalvin Nugraha, and Fabio Martinon

Supplemental figures

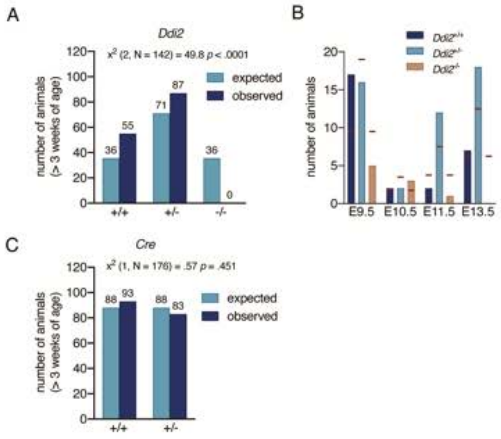

Figure S1. Observed progeny of DDI2 deficient mice, related to Figure 1A

Analysis of all progeny derived from mating heterozygous Ddi2+/- mice, with more than 3 weeks of age (A) or during embryonic development (B). Analysis of all progeny derived from mating Ddi2flox/floxAlbCre-/- and Ddi2flox/floxAlbCre+/- mice, with more than 3 weeks of age (C).

Number of animals per group indicated above the bars, red horizontal lines indicates the number of expected animals. χ2-test analysis are represented.

A

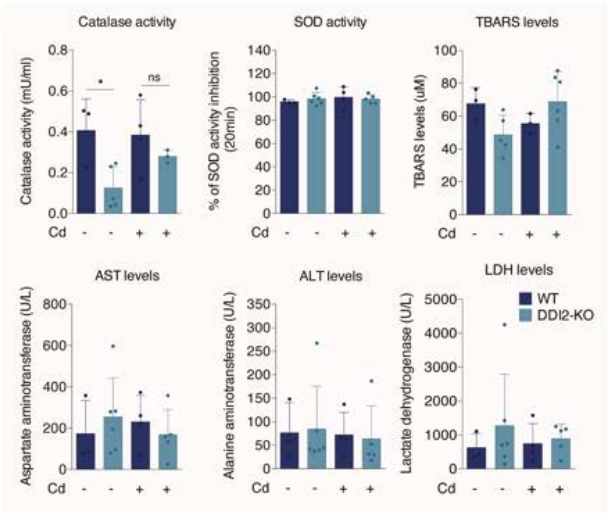

B

Gene Ontology: Biological Process				
#term ID	term description	genes mapped	enrichment score	false discovery rate
GO:0071280	Cellular response to copper ion	4	3.88964	0.0077
GO:0055086	Nucleobase-containing small molecule metabolic proces	53	0.460364	0.0077
GO:0019637	Organophosphate metabolic process	74	0.408501	0.0026
GO:0008610	Lipid biosynthetic process	43	0.404631	0.0076
GO:1901135	Carbohydrate derivative metabolic process	77	0.375283	0.0068
GO:0044281	Small molecule metabolic process	165	0.332546	8.58e-05
GO:1901566	Organonitrogen compound biosynthetic process	130	0.328815	0.0018
GO:0045944	Positive regulation of transcription by rna polymerase ii	102	0.300128	0.0077
GO:0055114	Oxidation-reduction process	130	0.287102	0.00070
GO:0006357	Regulation of transcription by rna polymerase ii	172	0.231131	0.0072

Gene Ontology: Molecular Function				
#term ID	term description	genes mapped	enrichment score	false discovery rate
GO:0003677	DNA binding	162	0.280794	0.00026
GO:0140110	Transcription regulator activity	115	0.262335	0.0058

Figure S2. Impact of DDI2 on liver physiology and gene expression, related to Figure 1B

(**A**) Catalase and superoxide dismutase (SOD) activities and thiobarbituric acid reactive substance (TBARS) levels measured form liver samples; Aspartate aminotransferase (AST), alanine aminotransferase (ALT) and lactate dehydrogenase (LDH) levels measured from serum of wild-type (WT) and liver-specific DDI2-knockout (KO) animals, after 16 h of intraperitoneal injection of PBS or 8 mg/kg of $CdCl_2$ (Cd). Each dot represents a single animal. *p*-values were calculated using two-tailed unpaired Mann-Whitney t-tests and error bars denote standard deviation (SD). *$p<0.05$. (**B**) Gene ontology (GO) analysis of biological process and molecular function generated with RNA-seq data (Figure 1). Functional enrichment analysis obtained with the online software: STING database version 11.5

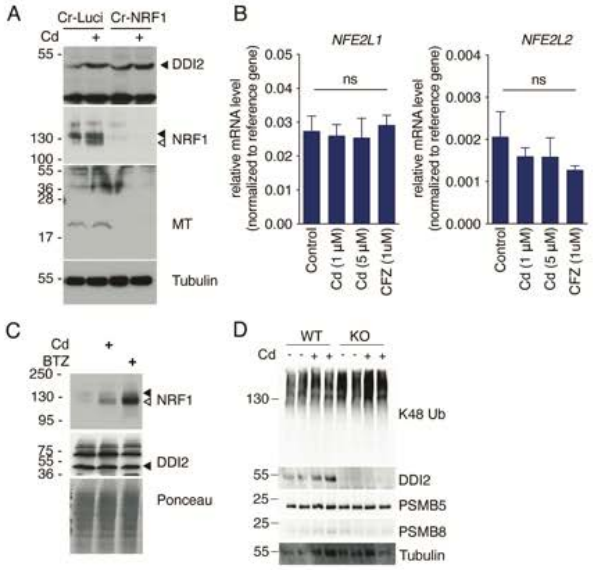

Figure S3 Cadmium promotes NRF1 proteolytic maturation, related to Figure 3

(**A**) Immunoblotting showing the relative protein levels of DDI2, NRF1, ponceau staining, of HepG2 cells treated with cadmium (Cd, 5 µM) or bortezomib (BTZ, 10 nM) for 6 hours (representative of n = 2). (**B**) Relative mRNA levels of NRF1 and NRF2 genes (*NFE2L1* and *NFE2L2*, respectively) normalized with *GAPDH* mRNA levels, from HepG2 cells treated 6 hours with indicated concentrations of cadmium (Cd) or carfizomib (CFZ). (**C**) Immunoblotting showing the relative protein levels of DDI2, NRF1, MT, and Tubulin, of CRISPR KO (Cr)-NRF1 or Cr-luciferase (luci) HepG2 cells treated with or without cadmium (Cd, 5 µM) for 6 hours (representative of n = 2). (**D**) Immunoblotting from liver samples of DDI2-KO (KO) and wild-type (WT) mice after 16 h of intraperitoneal injection of PBS or 8 mg/kg of CdCl2 (Cd) showing the relative protein levels of Ubiquitin-K48, DDI2, PSMB5, PSMB6 and Tubulin as loading control. Each line represents one animal and the protein molecular weights in KDa are indicated. ◀ indicates the full-length protein, ◁ indicates the cleaved protein. Samples were analyzed by two-tailed unpaired Mann-Whitney t-tests and error bars denote standard deviation (SD), ns: not significant.

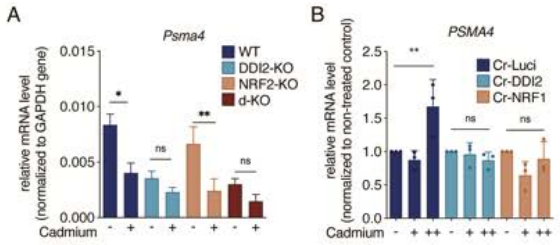

Figure S4. Impact of Cadmium on proteasome subunit expression, related to Figure 4

Relative mRNA levels of *PSMA4* from both mouse models (**A**) or HepG2 cells (**B**). (**A**) liver samples of DDI2-KO (KO), NRF2-KO, double-DDI2-NRF2-KO (d-KO) and wild-type (WT) collected from mice after 16 h of intraperitoneal injection of PBS (-) or 8 mg/kg of $CdCl_2$ (+). (**B**) CRISPR KO (Cr)-DDI2, Cr-NRF1 or Cr-luciferase (Cr-luci) control HepG2 cells treated with $CdCl_2$ (-: 0 µg; +: 1µM, ++: 5 µM) for 6 h. Target genes were normalized with *GAPDH* mRNA levels. (n = 3).

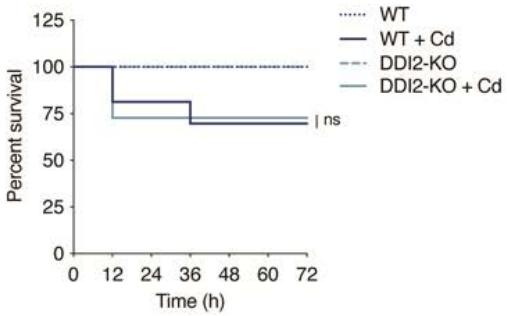

Figure S5. Viability of mice treated with Cadmium, related to figure 5

Percent of survival of DDI2-KO (KO) and wild-type (WT) mice treated with a single dose of cadmium 8 mg/kg (Cd) (n = 15 and 9, respectively) or PBS (n = 12 per group). Survival plots were constructed using Prism software (GraphPad Software Inc., version 9.1.2) with corresponding evaluation using two-sample log-rank statistical analysis (equivalent to Mantel–Haenszel test, two-tailed analysis), ns: not significant.